KTH ROYAL INSTITUTE
OF TECHNOLOGY

Targeting Arsenic-Safe Aquifers in Regions with High Arsenic Groundwater and its Worldwide Implications (TASA)

PROSUN BHATTACHARYA, ROGER THUNVIK,
GUNNAR JACKS, MATTIAS VON BRÖMSSEN

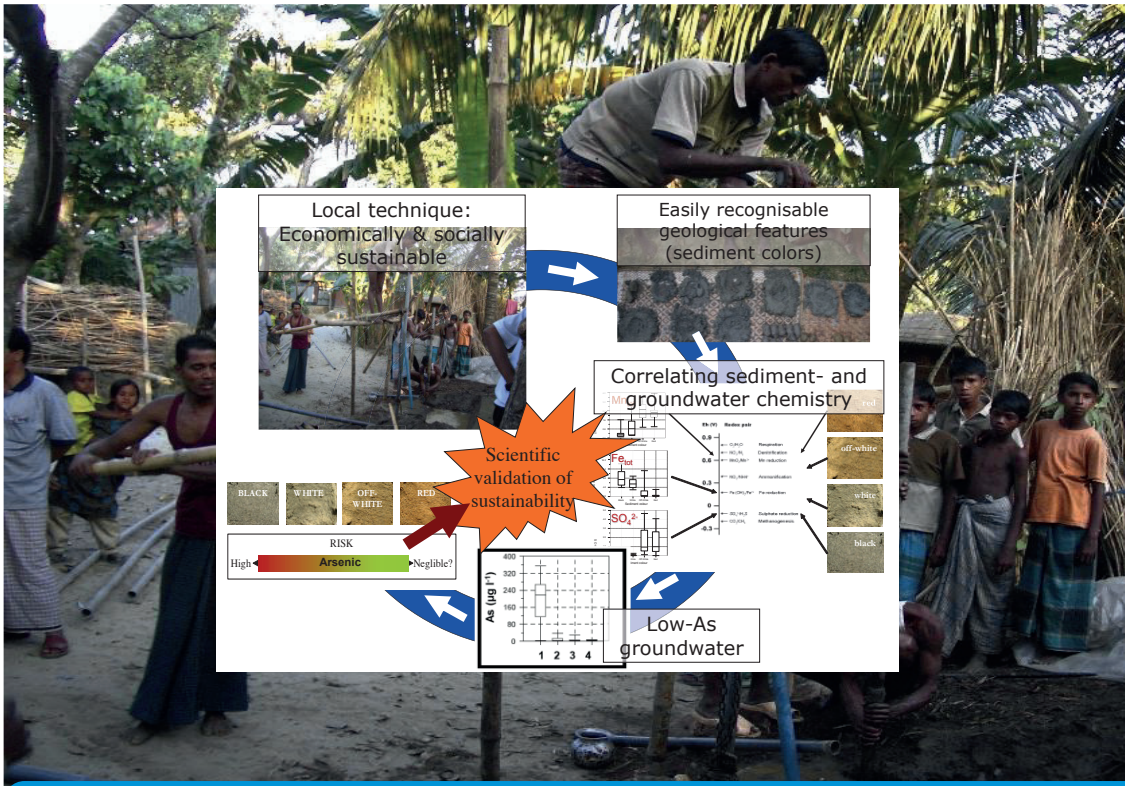

IN COOPERATION WITH:

RAMBØLL

FUNDED BY
MISTRA
The Swedish Foundation for
Strategic Environmental Research

KTH ROYAL INSTITUTE OF TECHNOLOGY
DEPARTMENT OF SUSTAINABLE DEVELOPMENT,
ENVIRONMENTAL SCIENCE AND ENGINEERING

FUNDED BY
MISTRA
The Swedish Foundation for Strategic Environmental Research

TARGETING ARSENIC-SAFE AQUIFERS IN REGIONS WITH HIGH ARSENIC GROUNDWATER AND ITS WORLDWIDE IMPLICATIONS (TASA)

Project Report

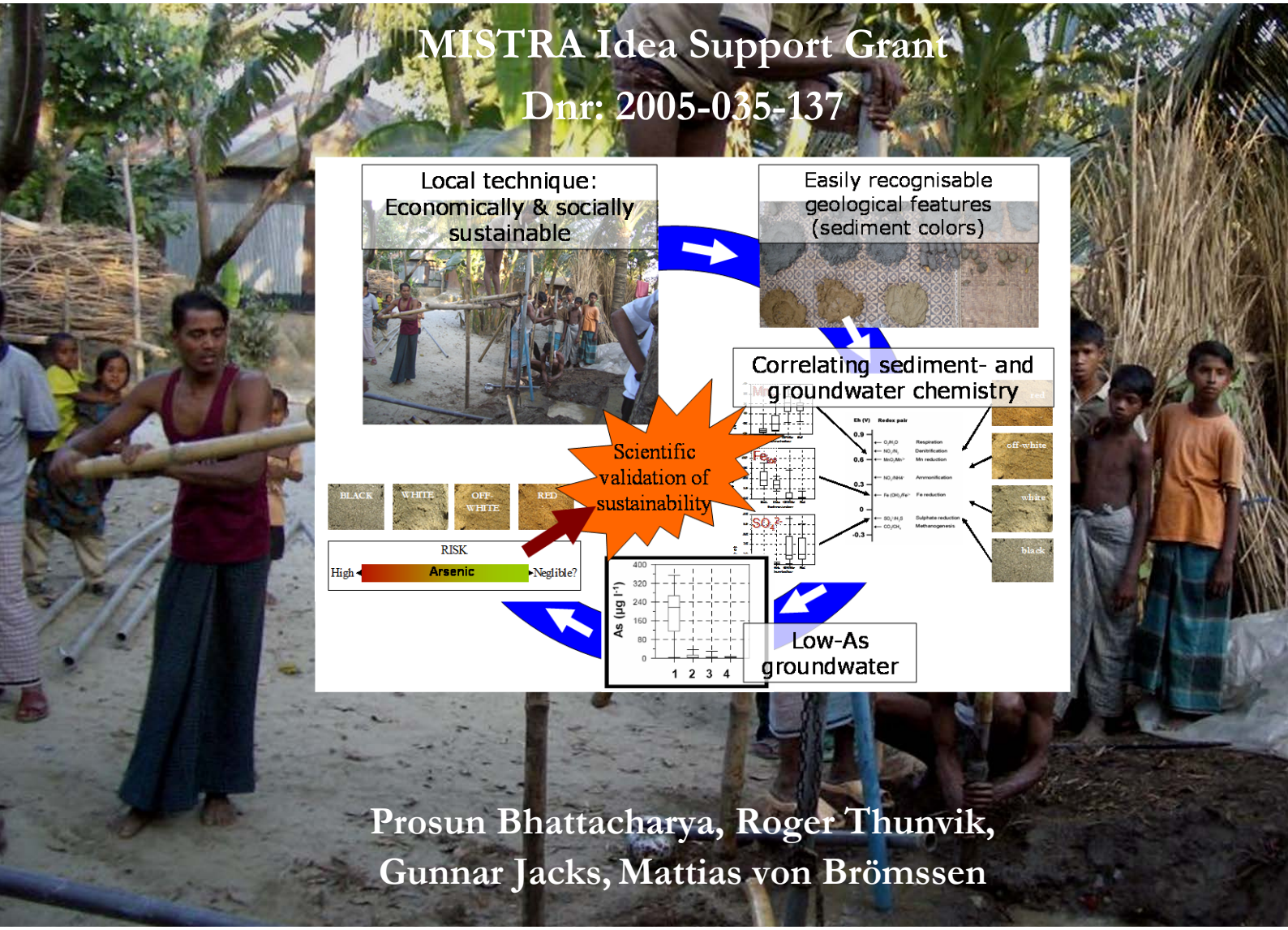

Prosun Bhattacharya, Roger Thunvik,
Gunnar Jacks, Mattias von Brömssen

Stockholm, Sweden
June 2015

Cover Illustrations:

Conceptual framework for targeting safe aquifers by local drillers for tubewell installation. © Project Consortium TASA

Background photograph showing the installation of tubewells by the local drillers. © Mattias von Brömssen 2004-2012

TARGETING ARSENIC-SAFE AQUIFERS IN REGIONS WITH HIGH ARSENIC GROUNDWATER AND ITS WORLDWIDE IMPLICATIONS (TASA)

PROJECT REPORT

MISTRA Idea Support Grant (Dnr: 2005-035-137)

Prosun Bhattacharya, Roger Thunvik, Gunnar Jacks
KTH-International Groundwater Arsenic Research Group
Department of Sustainable Development, Environmental Sciences and Engineering
KTH Royal Institute of Technology
SE-100 44 STOCKHOLM, Sweden

Mattias von Brömssen
Department of Soil and Water Environment
Ramböll Sweden AB
Box 4205
SE-102 65 Stockholm, Sweden.

Other Participants:

K.R. Gunaratna (KTH, Sweden), Kazi Matin Ahmed, M. Aziz Hasan (Dhaka University, Bangladesh), M. Jakariya (NGO Forum for Public Health, Dhaka, Bangladesh), Ashis Biswas (University of Kalyani, West Bengal, India and KTH, Sweden), Jochen Bundschuh (National Cheng Kung University, Tainan, Taiwan) & Ondra Sracek (Palack'y University, Olomouc, Czech Republic)

Disclaimer: This report is compiled from a number of publications authored by MISTRA project consortium members between the years 2007 through 2014. The entire data set belongs to the KTH-International Groundwater Arsenic Research Group at the KTH Royal Institute of Technology, Stockholm, Sweden.

Cite this Report as:

Bhattacharya, P., Thunvik, R., Jacks, G. and von Brömssen, M. (2015) Targeting Arsenic-Safe Aquifers in Regions with High Arsenic Groundwater and its Worldwide Implications (TASA). Project Report, MISTRA Idea Support Grant (Dnr: 2005-035-137). TRITA LWR Report 2015:01, 100p.

TRITA-LWR.REPORT 2015:01
ISSN 1650-8610
ISBN 978-91-7595-461-5

FOREWORD

This MISTRA project report covers a crucial period of the work on the growing concerns on the occurrence of arsenic in groundwater used for drinking and its public health consequences. It includes especially the discovery of the Bangladeshi local drillers´ strategy to find low iron groundwater by assessing the colour of the sediments. With the link between mobilization of arsenic along with iron which was published by our team 1997 this gave an immediate hint on means of predicting arsenic low groundwater during well construction. The strategy was discovered by our team when we were advising a M.Sc. thesis project. The "sediment colour strategy" led to the idea that safe water access can be facilitated through the involvement of the local drillers, if targeting safe arsenic aquifers could be conceptualized. Therefore, the effort of our team has been to develop a strategy to be used for the installation of safe wells, optimised on the basis of increased local hydrogeological knowledge and the demand for safe water among the underserved segments of the society. The insight gained indicates that the strategy of finding low arsenic aquifers is sustainable. The methods used comprised of groundwater and sediment sampling, detailed chemical analysis of water, sediment extractions, mineralogical investigations and hydrogeochemical- and groundwater flow modelling. The results based on the studies in Matlab, was also replicated through similar studies in the Chakdaha Block in the state of West Bengal, India where identical set of grey sand and brown sand aquifers were identified with similar characteristics with similar hydrochemical characteristics of aquifers and the approach for finding arsenic safe drinking water sources through the initiatives of the local drillers.

Prof. Em. Gunnar Jacks
Stockholm, Sweden
June 2015

ACKNOWLEDGEMENTS

We would like to express our thanks to The Swedish Foundation for Strategic Environmental Research (MISTRA) for providing the Idea Support Grant for the Project "Targeting arsenic-safe aquifers in regions with high arsenic groundwater and its worldwide implications (TASA)" to the KTH-International Groundwater Arsenic Research Group, Department of Sustainable Development, Environmental Science and Engineering (SEED), formerly Department of Land and Water Resources Engineering (LWR) at KTH Royal Institute of Technology, between 2007 to 2010.

We are grateful to the entire faculty, staff at the LWR and SEED, KTH for the administrative and various academic and technical support. project. We are thankful to Ann Fylkner, Monica Löwen and Bertil Nilsson for their cooperation and assistance in the laboratory analyses. We deeply appreciate the assistance from Magnus Mörth of Department of Geology and Geochemistry, Stockholm University for providing us the laboratory facilities for ICP analyses.

The project team would like to express our gratitude to the collaborative partner organization, Ramböll Sweden AB for their support during the activities of this project. We would like to thank Lars Markussen, Ramböll Denmark, Dr. Clifford Voss, United States Geological Survey, and Sven Jonasson, Geologic in Göteborg AB for discussions on groundwater flow modelling.

We acknowledge all the help we have received from Department of Geology, Dhaka University, and the local drillers especially Omar Faruq, Malek and their team for their untiring support for the drilling operations, people of Matlab for generosity with making their properties available for research activities during the project activities. We would also like to thank Biswajit Chakraborty for his untiring help with the groundwater level monitoring exercise during the study.

We would also acknowledge the support from all the graduate students Lisa Lundell, Linda Jonsson (LWR, KTH, Department of Geosciences, Uppsala University), M. Moklesh Rahman, M. Rajib Hassan Mozumder (LWR-KTH and Department of Geology, Dhaka University), Annelie Bivén, Sara Häller, and Pavan Kumar Pasupuleti (LWR-KTH) and our PhD graduates M. Jakariya (Bangladesh Rural Advancement Committee (BRAC) and NGO Forum for Public Health (formerly NGO Forum for Water Supply and Sanitation) and M. Aziz Hasan (LWR, KTH and Department of Geology, Dhaka University) for their active involvement and contributions to the study. Dr. Anisur Rahman at ICCDR,B-Matlab is specially acknowledged for facilitating the access at the ICDDR,B guesthouse in Matab field area.

We also acknowledge Professor Debashis Chatterjee at the University of Kalyani for his valuable support for the replication studies on the TASA concept in West Bengal, India. We are thankful to P. K. Das (Bapi), N. Bhabani (Probhu), R. Das (Bapi) and S. Karmakar (Bablu) and his drilling team, who were always ready to work at the field even at very short notice.

We are grateful to all our international colleagues working in cooperation with the KTH-International Groundwater Research Group for all fruitful discussions on our research outcomes and common research issues related to arsenic contamination in groundwater sources.

Prosun Bhattacharya, Roger Thunvik, Gunnar Jacks, Mattias von Brömssen
Stockholm, Sweden
June 2015

TABLE OF CONTENT

EXECUTIVE SUMMARY

Naturally occurring arsenic (As) in Holocene aquifers in Bangladesh have undermined a long success of supplying the population with safe drinking water. Arsenic is mobilized in reducing environments through reductive dissolution of Fe(III)-oxyhydroxides. Several studies have shown that many of the tested mitigation options have not been well accepted by the people. Instead, local drillers target presumed safe groundwater on the basis of the colour of the sediments. The overall objective of the study has thus been focussed on assessing the potential for local drillers to target As safe groundwater. The specific objectives have been to validate the correlation between aquifer sediment colours and groundwater chemical composition, characterize aqueous and solid phase geochemistry and dynamics of As mobility and to assess the risk for cross-contamination of As between aquifers in Matlab Upazila in southeastern Bangladesh. In Matlab, drillings to a depth of 60 m revealed two distinct hydrostratigraphic units, a strongly reducing aquifer unit with black to grey sediments overlying a patchy sequence of weathered and oxidised white, yellowish-grey to reddish-brown sediment. The aquifers are separated by an impervious clay unit. The reducing aquifer is characterized by high concentrations of dissolved As, DOC, Fe and PO_4^{3-} tot. On the other hand, the off-white and red sediments contain relatively higher concentrations of Mn and SO_4^{2-} and low As. Groundwater chemistry correlates well with the colours of the aquifer sediments. Geochemical investigations indicate that secondary mineral phases control dissolved concentrations of Mn, Fe and PO_4^{3-} tot. Dissolved As is influenced by the amount of *Hfo*, pH and PO_4^{3-} tot as a competing ion. Laboratory studies suggest that oxidised sediments have a higher capacity to absorb As. Monitoring of hydraulic heads and groundwater modelling illustrate a complex aquifer system with three aquifers to a depth of 250 m. Groundwater modelling studies illustrate two groundwater flow-systems: i) a deeper regional predominantly horizontal flow system, and ii) a number of shallow local flow systems. It was confirmed that groundwater irrigation, locally, affects the hydraulic heads at deeper depths. The aquifer system is however fully recharged during the monsoon. Groundwater abstraction for drinking water purposes in rural areas poses little threat for cross-contamination. Installing irrigation- or high capacity drinking water supply wells at deeper depths is however strongly discouraged and assessing sustainability of targeted low-As aquifers remain a main concern.

Delineation of safe aquifer(s) that can be targeted by cheap drilling technology for tubewell (TW) installation becomes highly imperative to ensure access to safe and sustainable drinking water sources for the As-affected population in Bengal Basin. In order to replicate the salient outcomes of the Matlab study results, an investigation was carried out in Chakdaha Block of Nadia district, West Bengal, India covering an area of ~100 km^2 to investigate the potentiality of brown sand aquifers (BSA) as a safe drinking water source which is currently being practiced in the area for safe tubewell installation. The results revealed salient hydrogeochemical contrasts within the sedimentary sequence designated as shallow grey sand aquifers (GSA) and the brown sand aquifers (BSA) within shallow depth (< 70 m). These two sand groups with all possible variability in the colour shades were analogous to the reducing and the

oxidized sequences as delineated aquifers based on the sediment color as perceived by the local driller in Matlab. Although the major ion compositions indicated close similarity, the redox conditions were markedly different in groundwater abstracted from the two group of aquifers. The redox condition in the BSA is delineated to be Mn oxy-hydroxide reducing, not sufficiently lowered for As mobilization into groundwater. In contrast, lower Eh in groundwater of GSA, along with the enrichments of NH_4^+, PO_4^{3-}, Fe and As reflect reductive dissolution of Fe-oxyhydroxide coupled to microbially mediated oxidation of organic matter as the prevailing redox process causing As mobilization into groundwater of this aquifer type. In some segments of GSA in the Chakadaha region, there were indications of very low redox status, reached to the stage of SO_4^{2-} reduction, which might sequester dissolved As from groundwater by co-precipitation with authigenic pyrite. The groundwater of the BSA had consistently low concentration of As with concomitant elevated concentration of Mn.

The outcomes of the TASA project has thus established a scientific knowledge linking relationship between the colour of aquifer sediments, redox-conditions and hydrogeochemical parameters that provides unique opportunity for the local drillers in rural communities to target As-safe aquifers for well installations in Bangladesh. The red/brown sand aquifers are the prime targets for As-safe drinking water well installations and the concept could be used to target aquifers in similar environments in other areas with similar hydrogeological setting. However, the results also reveal that groundwater abstracted from most low As red/brown sand aquifers are often characterized by elevated concentration of Mn which warrants rigorous assessment of attendant health risk for Mn prior to considering mass scale exploitation of these aquifers from the perspectives of the drinking water safety plan and ensuring sustainability in drinking water supply especially in rural areas.

Key words: Arsenic, drinking water supply, geochemistry, hydrogeology, modelling, groundwater, sediment color, safe aquifers, sustainability.

1. INTRODUCTION

Access to safe drinking water is a basic human right and an important component for effective public health protection. Natural arsenic (As) have been reported in groundwater from several parts of the world (Bhattacharya et al. 2002a,b, Smedley and Kinniburgh 2002; Nriagu et al. 2007), and currently incidences are being reported from 70 countries across the globe (Ravenscroft et al. 2009). The most critical incidences of high As groundwater exists in e.g. Bangladesh, the states of West-Bengal, Uttar Pradesh, Bihar, Jharkhand and Assam in India, the Chaco-Pampean Plain in Argentina, Huhott Alluvial Basin, Inner Mongolia in China, Bolivian Highlands in Bolivia, Taiwan, Hungary, Mexico, USA, Pakistan, Nepal, Thailand, Cambodia, Greece, Sweden, Finland, Denmark and Germany (**Figure 1**).

Groundwater environments governing mobilization of geogenic As can be broadly categorized in three groups (Smedley and Kinniburgh 2002; Sracek et al. 2001, 2004a): i) strongly reducing aquifers, ii) high alkaline- and pH in mostly oxidising aquifers, and iii) aquifers containing elevated amounts of arsenopyrite and other sulphides. From a human health perspective, high As aquifers related to strongly reducing conditions pose most serious problems because of its wide geographical coverage especially in countries like Bangladesh, India, Pakistan, Vietnam and Cambodia (Bhattacharya et al. 1997, 2001, 2002b, Ravenscroft et al. 2001, 2005, Smedley and Kinniburgh 2002, 2006a, Nickson et al. 2005, Berg et al. 2007) and also the Great Alluvial Basin in Hungary Romania and Slovenia (Varsanayi et al. 1991, 2006, Lindberg et al. 2005, Petrusivski et al. 2007).

Arsenic is also commonly encountered in oxidizing aquifers with high alkalinity and pH in the Chaco-Pampean region of Argentina affecting at least 1.2 million people (about 3 % of total population) are exposed to elevated As concentrations mobilized primarily from volcanic ash, interbedded or dispersed within sediments (Bundschuh et al. 2004, Bhattacharya et al. 2006b, Nicolli et al 2010, 2012). In mineralized areas, As may be mobilized due to the oxidation of the sulphides minerals from ore bodies and black schists especially in Sweden and Finland, containing pyrite and arsenopyrite (Welch and Stollenwerk 2003, Jacks et al. 2013).

The magnitude of the problem is however, severe in the Bengal Delta Plain of Bangladesh and in the adjoining state of West Bengal, India where it has emerged as one of the greatest environmental health disaster of this century. Approximately, a population of 70 million in this region are exposed to elevated concentration of As in drinking from groundwater sources.

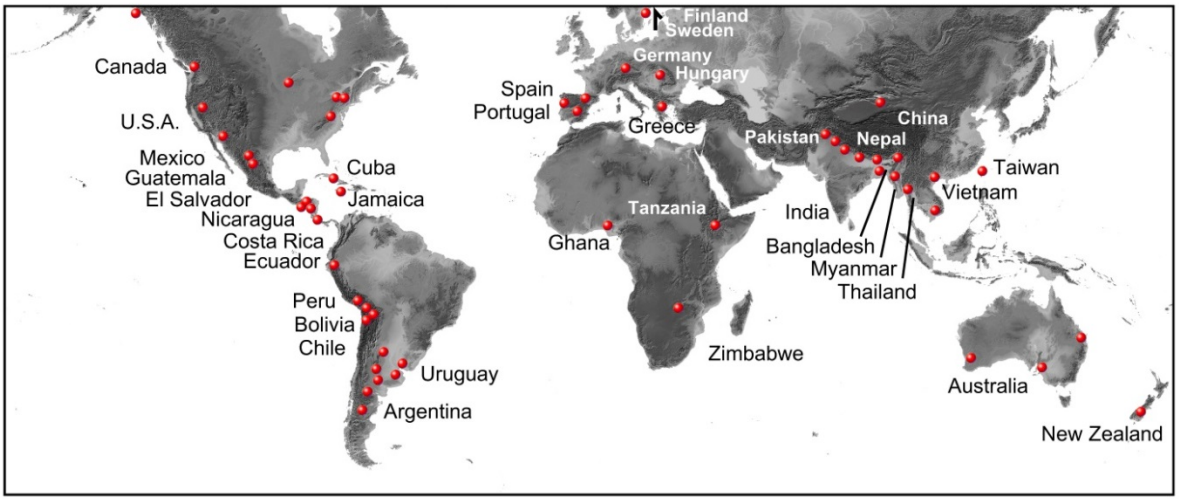

Figure 1. Occurrences of arsenic in groundwater across the world (modified from Nriagu et al. 2007)

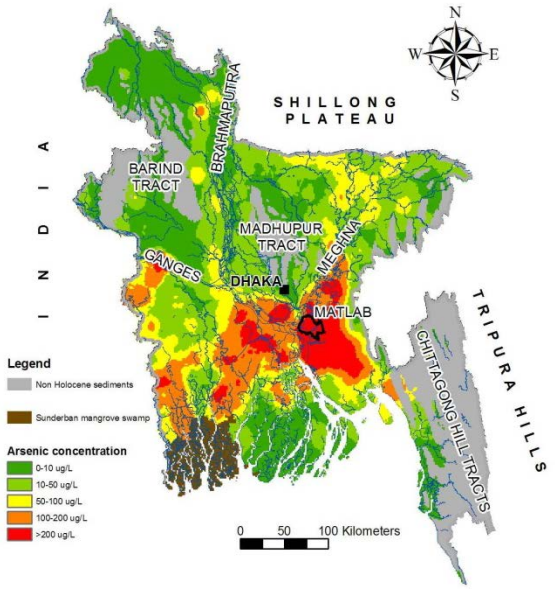

Figure 2. Map of Bangladesh showing the great rivers of Ganges, Brahmaputra and Meghna, the location of Matlab and the distribution of As in groundwater, (based on data from BGS and DPHE 2001).

The widespread occurrence of natural As in groundwater in Bangladesh and its magnitude of exposure have drastically reduced the safe water access across the country. Despite several efforts, there has been very limited success in mitigation since the discovery of As in the country in 1993; still tens of millions of people are exposed to levels above the Bangladesh drinking water standard (BDWS; 50 µg/L) which is even 5 times higher than WHO drinking water guideline (10 µg/L, **Figure 2**).

The toxic effect of long-term exposure to As, a well known carcinogen, can extend from pigment changes and hard patches on the skin to gangrene and lung, kidney and bladder cancer, and those drinking water with As in excess concentrations are obviously considered at risk. The magnitude of the continuation of this human tragedy will depend on the rate at which mitigation programs are implemented and now, the main challenge is to develop a sustainable and cost-efficient mitigation option that will be adopted by the people for scaling up safe water access.

1.1. Chronic arsenic exposure

Drinking groundwater, consumption of food-crops cultivated using groundwater irrigated with groundwater with elevated As concentrations are the main exposure pathways in Bangladesh (Polya et al. 2009). Chronic As poisoning results from ingestion of elevated levels of As over a long period of time (UN 2001, Kapaj et al. 2006). The consequences of chronic As exposure are dependent on the susceptibility, the dose and the time course of exposure (Kapaj et al. 2006). The effects include different forms of skin disorders related to skin pigmentation such as leucomelanosis, melanosis, keratosis, skin cancer, lung cancer, cancer of the kidney and bladder, and can lead to gangrene. Estimation of annual excess deaths is in the order of thousands and disability-adjusted life years (DALY) of the order of hundreds of thousands (Polya et al. 2009) in Bangladesh.

1.2. Societal needs and cross-cutting issues

Water plays a pivotal role in human well-being and in economic development. Because of the need of water in domestic use (drinking and cooking) and in food production (primarily for irrigation), conflict over water and the effects of gender influenced decisions about water may have far-reaching consequences on human well-being, economic growth, and social change. Water handling in Bangladesh, as in the case of other developing countries, is generally the task of women and in general their opinions on the safe drinking water supplies therefore need to be integrated during the installation of new hand tube wells (HTW).

The impacts of As poisoning in the society is reflected in several ways by socio-economic status and gender. While close proximity of the households with safe water access points simplify the task of women for water handling, the easy access to water through family hand tubewells (HTWs) are also crucial in maintaining a healthy drinking water supply, beside promoting the custom of hand-washing after toilet use and before food preparation. The proximity of the safe HTWs also are important in close vicinity of the school to protect the health of the children. The sensitivity to As poisoning is

also related to economic status of the individuals which in turn affect the nutritional status as well as affordability to secure access to safe water. Higher cost involvement in installing As-safe deep wells causes the poor communities vulnerable to As poisoning. The poorer sections of the society consume more water (hence exposed to more As) as they work harder. The worse nutritional status of poor households, and particularly the women of those households, may mean that As contamination has more severe physiological consequences for them.

1.3. Lessons learnt from previous mitigation activities

Different options have been implemented including household and community As-removal filters (ARF), rainwater harvesters (RWH), pond sand filters (PSF), dug wells (DW), hand tubewells (HTW) at targeted depths and deep tube wells (DTW) usually installed at depths of 200-250 m. These options have been assessed on several criteria, such as community acceptability, technical viability and their socio-economic implications.

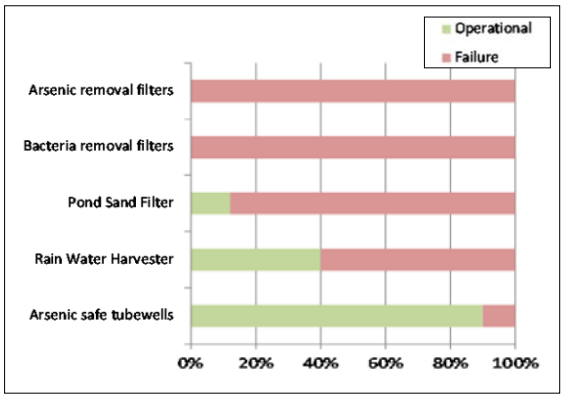

Figure 3. Performance analysis of the different options adopted for arsenic mitigation in Bangladesh.

It has been found that community acceptance of many of the options is low as people do not find them as convenient as the tubewells (Hoque et al. 2004, APSU 2005, Jakariya et al. 2005, 2007, Johnston et al. 2010, Biswas et al. 2014a,b). The concept of drinking water from tubewells is well rooted in the daily life of the people in Bangladesh. Women in the rural areas of Bangladesh are severely burdened in spite of the provision of HTWs located at short distance. Any additional task, for instance the handling of filters on the household basis, is thus likely to be difficult to handle by the rural population on a long term basis. This may be one reason for the failure of several of the alternative options to As safe water that have been provided in Bangladesh during the past two decades (**Figure 3**).

All the safe water options have their own strengths and limitations but none is as easy as fetching water directly from tubewells. Pre-Holocene aquifers usually at depths >100 m are generally known to have low concentrations of dissolved As (BGS and DPHE 2001) and offer a possible alternative source of As-safe drinking water.

However, drilling to depths more than 100 m is costly as it involves mechanised technique as compared to the locally available hand-percussion technique and may therefore not always be readily available and affordable. Though most options were not accepted many villagers realized the urgency for drinking safe water and thus two practices emerged based on the community's own initiative (van Geen et al. 2003, Jakariaya et al. 2005): i) the preferred use of As safe hand tubewells that were painted green after examination by field personal, and ii) reinstalling tubewells to a presumed safe depth based on local drillers knowledge of the colour of the sediments and As occurrence.

2. RATIONALE

Although significant progress has been made to understand the source and distribution of As in the respective aquifers, and its mobilization in groundwater, there has been limited success in transferring this knowledge towards large-scale and substantial mitigation efforts to reduce As exposure from drinking water sources in Bangladesh. Since, tubewells have emerged as a community acceptable option as As-safe drinking water supply over major part of the country.

Based on the long term research mostly carried out between 1998-2005 on prevailing aquifer conditions, at country- wide as well as local scales, the scientific community has been able to delineate the principle mechanisms of genesis and mobilization of As in groundwater (Mukherjee and Bhattacharya 2001, Ahmed et al. 2004, Akai et al. 2004, BGS 2001, Bhattacharya et al. 1997, 2001, 2002a,b, Bundschuh et al. 2004, Harvey et al. 2002, McArthur et al. 2004, Nickson et al. 1998, Smedley and Kinniburgh 2002, van Geen et al. 2003, Zheng et al. 2005). However, in many of these regions the distribution of As is extremely heterogeneous, both laterally as well as vertically and As-safe and unsafe tubewells have been encountered in close vicinity at places located <25 m from each other.

On the basis of the geological settings, the prevailing aquifer conditions and the theories of mobilization many of the As-safe tubewells should in fact have high concentrations of As. Consequently, the "patchy distribution" has often been explained in terms of "local variations in sedimentary characteristics as well as hydrogeological and hydrogeochemical conditions" in different aquifers in affected areas (BGS 2001, Bhattacharya et al. 2002a, Bhattacharya et al. 2002c, McArthur et al. 2004, Smedley et al., 2002, 2005; Bundschuh et al. 2004; Bhattacharya et al., 2006). It is also important to emphasize that all these studies have primarily illustrated the major mechanisms of As mobilization, but explanation for the As-safe tubewells have been insufficient. **Figure 4** illustrates the depth-wise distribution of As in Bangladesh aquifers. The mechanism of enhanced mobilization of As triggered by reductive dissolution of Fe-oxyhydroxides in the Holocene aquifers is a plausible explanation for the set of groundwater samples in area marked A, while within area B the geological model with older and oxidized Pleistocene aquifers with low inherent As concentrations seems applicable. However, for the As-safe tubewells within area C ($n_C \approx 50\%$), a reappraisal of the geological and hydrogeological model and/or mobilization theory needs to be readdressed.

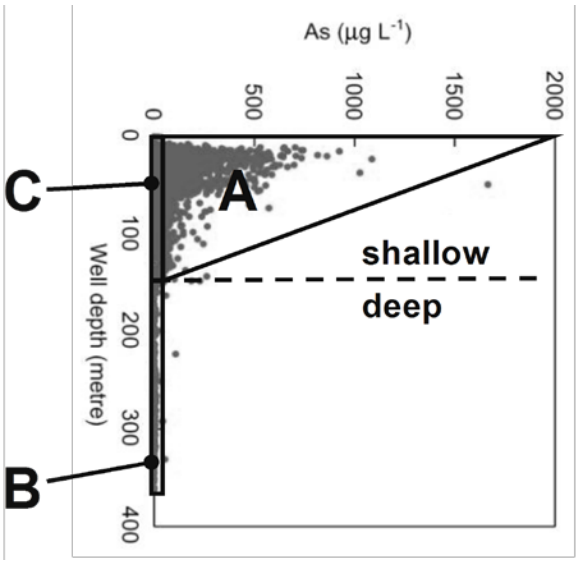

Figure 4. Depth wise distribution of As in hand tubewells for Bangladesh (BGS and DPHE 2001). Within area A and B the prevailing mobilization theory is valid. However, for the tubewells at shallow depth with low As (C) which includes 54% of the samples the explanation of the low As concentrations are poorly described.

Detailed aquifer and groundwater characteristics have been refined in many of the recent studies in Bangladesh (von Brömssen et al. 2007, Harvey et al. 2002, McArthur et al. 2004, van Geen et al. 2004, Ahmed et al. 2004) which indicate the plausible explanations for the spatial distribution of As in the aquifers with depth. In these studies the groundwater chemical composition has been correlated to specific aquifer sand characteristics.

The MISTRA project was conceived to develop a systematic approach to target safe drinking water in communities exposed to elevated As at a low cost. The project also aimed to provide the local drillers in the rural communities with specific knowledge to improve their indigenous skills to target safe aquifers for tubewell installation.

3. Research Objectives

Keeping in mind the number of exposed people and the low rate of outcomes of the mitigation programmes driven by government and donor organisation for As mitigation, it is obvious that there is an

urgent need for the people themselves to find practical mitigation options. Thus the overall objective of the present research has been to develop a concept for local drillers to target As-safe aquifers in regions with high As groundwater of geogenic origin. This could be a sustainable option for safe drinking water in many regions in the world with groundwater containing geogenic As exceeding the WHO permissible drinking water limit.

4. Project Area and Hydrogeological Setting

4.1. The Project Area

The investigations were done in Matlab, in Chandpur district in southeastern Bangladesh, situated at the distance of about 60 km south-east of Dhaka on the eastern side of the great river Meghna. Matlab is one of worst affected areas of the country and a considerable part form part of the low-lying Meghna floodplain (**Figure 5**).

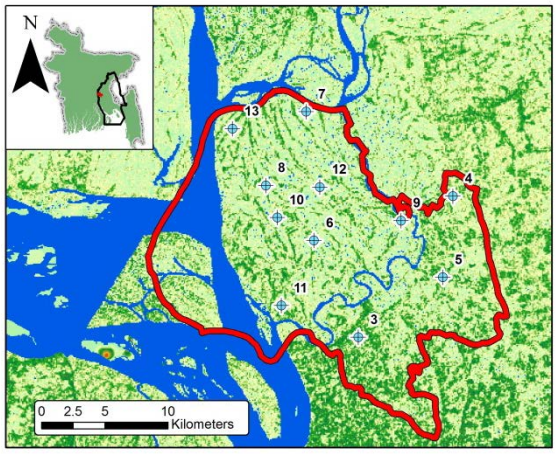

Figure 5. Map showing the location of piezometer nests, the red line shows the boundary of Matlab.

4.2. Geological Setting

The Bengal basin represents one of the largest delta systems of the world. Three mighty rivers, the Ganges, Brahmaputra and Meghna carry enormous load of sediments into the basin (Hasan et al. 2007). The basin is classified into three distinctive terrains:

i) The Tertiary hill ranges occur in the east, southeast and north-northeast and primarily comprises lithologic succession represented by sandstone, shale and limestone (BGS and DPHE 2001). The hills have been formed due to the collision of the Indian shield at the Indo-Burma boundary forming the Indo-Burman fold belt.

ii) The Pleistocene Barind and Madhupur Terraces in the central north and Holocene plains are found as a thin sediment veneer in large part of the basin. These terraces represent uplifted blocks of fluvial deposits and comprise include clay, silt, sand and pebbles of Pleistocene age, exposed to weathering during the latest period of glaciation, and the aquifer sediments are red-, brown- and yellowish in colour. Groundwater in the Pliestocene terraces has been found to be low in dissolved As groundwater , and

iii) The Holocene sedimentary sequences include piedmont deposits occurring mostly in the northern Bangladesh, floodplain and other inter-fluvial/overbank deposits of the Ganges–Brahmaputra–Tista–Meghna river system, in the delta plains of the Ganges-Brahmaputra-Meghna system, and in the coastal plains and active sub-basins including large inland lakes or "haors and bil" (Ahmed 2005). During the late Holocene time, as marine transgressions were waning, marshy or swampy lowlands developed in several parts of the Basin giving rise to peat deposits and sediments rich in organic matter. The Holocene flood plains are characterized by meandering rivers, natural levees and back swamps. The upper part of the Holocene sequence includes the flood plains, fine-grained and/or muddy deposits, down to approximately 10 to 20 m (Umitsu 1987, 1993, Goodbred et al. 2003). Below the floodplains are channel deposits including coarser sediments such as sand and gravel. The Holocene sequence extends down to the depth of approximately 100 m. The deepest Holocene deposits are found at the Meghna River. Goodbred et al. (2003)

identified oxidized surfaces that may coincide with oxidized low-As aquifers (von Brömssen et al. 2007) at a depth of 80 m between Comilla and Meghna and at shallow depths (<20 m) between Comilla and Dhaka. The floodplain is covered by non-calcareous grey to dark grey flood plain soil (Brammer 1996). A thick sequence of the Quaternary sediment constitutes the substratum of the study area. The topmost Holocene sequence is composed of alluvial sand, silt and clay with marsh clay. The location of the Meghna river channel has been relatively constant over the last 18 ka (Umitsu 1993). It can be assumed that the present location of the Meghna coincide with the location of Palaeo-Meghna river channel dating back to 120 ka BP (BGS and DPHE 2001). Thus it can be assumed that the sedim ents near and below the present river channel are relatively coarse with high permeability. This has also been observed in borelogs collected by DPHE/DFID/JICA (2006).

4.3. Precipitation and Climate

Bangladesh has a typical South-Asian tropical monsoon climate with considerable variation in rainfall over the year. Most parts of Bangladesh, including Matlab, receive precipitation more than 1 500 mm annually, however, in the hilly areas of north eastern Sylhet, the annual precipitation is as high as 5 000 mm. Approximately 90 % of the rainfall occurs during the monsoon season, between May and October. The monsoon period is followed by a moderately warm winter and spring between November and February and a hot and humid period between March and May. Temperature varies from approximately 10 to 36°C (Rahman and Ravenscroft 2003, Hasan et al. 2009). Evapotranspiration in the region (data for Dhaka) is 1 602 mm/yr and varies from 89 to 188 mm/month peaking in April and May (BGS and DPHE 2001; **Figure 6**). As a result of the heavy monsoon, the low-lying landscapes in extended parts of Bangladesh are flooded each year due to the increased volume of water in the great rivers of Ganges, Brahmaputra and Meghna flowing from the upper reaches of the Himalayas. The average fluctuation of the water level in the Meghna river at Matlab is approximately 4 m.

4.4. Hydrogeological Setting

The aquifer system of the Bengal basin is one of the most productive in the world. The alluvial Holocene aquifers of the delta plain are prolific and found within very shallow depths. Groundwater levels in the Holocene aquifers lies very close to the surface and the fluctuations in groundwater levels follow the annual rainfall pattern.

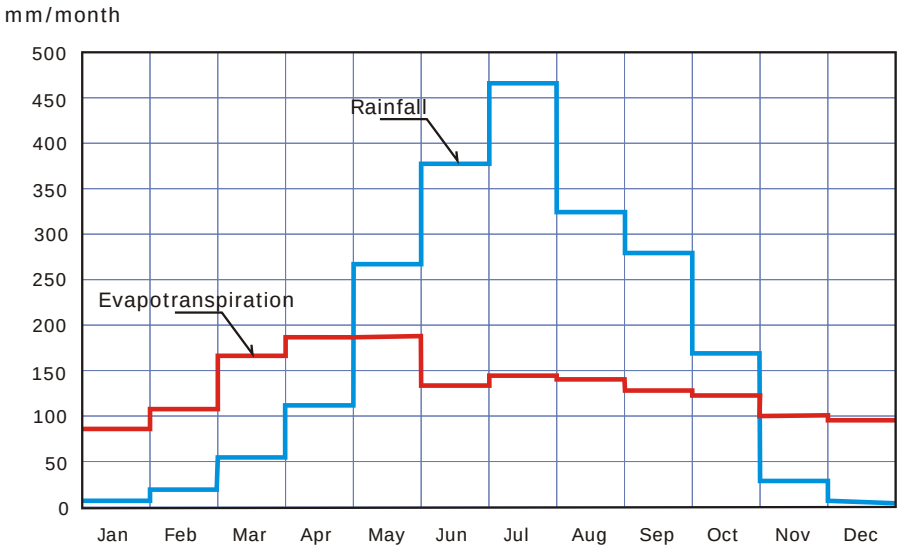

Figure 6. Average long term monthly rainfall and evapotranspiration for Dhaka City between 1953 and 1977 (modified from BGS and DPHE 2001).

Locally, groundwater level fluctuations are affected by groundwater abstraction although in most places the system is fully recharged after monsoonal precipitation. Amplitudes of natural groundwater level fluctuations are in the order of 2-5 m over the year. As Bangladesh experiences a tropical monsoon climate with heavy rainfall during June to October, the groundwater levels start to increase during May/June and decreases in September/October. The groundwater levels are lowest during the end of April to early May (BGS and DPHE 2000, Hasan et al. 2007).

A number of attempts have been made to describe the aquifer distribution (UNDP 1982, EPC/MMP 1991, BGS and DPHE 2001, DPHE/DFID/JICA 2006, Mukherjee et al. 2007, 2008) and most of the aquifer models were established on the basis of the lithological units. For instance, EPC/MMP (1991) had developed a four-layer model taking into account the vertical head differences for the assessment of water balance. The alluvial aquifers of Bangladesh are mostly semi-confined to confined in nature. Most aquifer tests have been analysed by classical methods based on tests with partial penetration of the aquifers and transmissivity, hydraulic conductivity and storage coefficients have been determined from a large number of pumping tests (BGS and DPHE 2000).

Three groundwater flow systems have been identified in Bangladesh (Ravenscroft 2001):

i) *a local system,* down to 10 m, this system is a product of local topography such as levees, local hills, terraces, haors and bils and rivers,

ii) *an intermediate flow system* with flow path down to a couple of 100 m driven by the larger terraces, major rivers etc. and

iii) *a basin-scale flow system,* down to a depth of several 1,000 m. This system would include the entire Bengal basin with its borders in the Tertiary Hills towards east, the Indian shield towards west, the Shillong plateau to the north and the Bay of Bengal in the south.

Groundwater flow patterns have been affected because of heavy abstraction of groundwater for irrigation and drinking water purposes (Michael and Voss 2009a, b). Domestic drinking water wells in rural areas of Bangladesh are generally small diameter hand-pump wells. These hand-pump wells can easily be installed to a depth up to 100 m depending on local geological conditions. Based on population and per capita use, groundwater abstraction for domestic usage can be calculated. Approximately 50 l/day/person is used for domestic purposes in Bangladesh, in some areas of rural Bangladesh as much as 30 mm/yr can be abstracted for domestic purposes (Michael and Voss 2008). However groundwater abstraction for irrigation purposes is about an order of magnitude more in rural areas and in some areas more than 600 mm/yr is used. Today, the abstraction of groundwater for irrigation and drinking purposes, construction of water channels and embankments and road construction etc. have substantially changed the natural surface water and groundwater flow pattern.

5. Work Components

Combinations of different approaches were followed to assess the hydrogeological criteria for delineation of low As groundwater in the aquifer system for further development by local and rural people in southeastern-Bangladesh. Focus was laid on delineation of As safe aquifers by linking recognizable geological features to typical groundwater compositions through field-work in close collaboration with the local drillers. The methods used comprised of groundwater and sediment sampling, detailed chemical analysis of water, sediment extractions, mineralogical investigations and hydrogeochemical- and groundwater modelling (von Brömssen et al. 2008, Hasan et al. 2009, Robinson et al. 2011, Jakariya 2007, von Brömssen et al. 2012, von Brömssen et al. 2014, Mukherjee et al. 2008).

5.1. Hydrogeological investigations

A comprehensive hydrogeological investigation was carried out to understand the prevailing hydrological and biogeo-

chemical processes responsible for mobilization and immobilization of As for identifying the safe aquifers, their sustainability and the risk for cross-contamination.

5.1.1. Groundwater flow and hydraulics

Multilevel piezometer nests (n=10) and pumping wells (n=5) were installed for determination of the groundwater level fluctuation, monitoring and sampling for groundwater chemistry and performing pumping tests. Hydraulic heads were monitored on weekly basis between May 2009 and October 2010 from ten piezometer nests and the data were used. to prepare hydrographs at varying depth of the aquifer system and to investigate the vertical gradients within the aquifer system. The information is important for investigating the hydraulic properties of the aquifers in order to assess the risk for cross-contamination induced from e.g. irrigation-wells that have much higher flow than drinking water tubewells. A conventional hydraulic test was done in January 2008 in order to determine hydraulic properties of the shallow aquifers including the vertical and horizontal hydraulic conductivity.

The computer code MODFLOW was used to generate a three-dimensional finite difference groundwater model to study the groundwater flow of the aquifer system. The flow chart followed for the groundwater modelling exercise is presented in **Figure 7**. A regional steady state- and transient flow model was constructed. The models were run for both undisturbed and disturbed conditions including abstraction of groundwater for irrigation purposes. The steady state model was calibrated to match ^{14}C dating while the transient models were calibrated to match measured hydraulic heads in the piezometer nests. Abstraction from irrigation wells were introduced into the model, based on an existing survey in the area.

The hydrostratigraphy was delineated through analysis of the drilling logs from the piezometer installations and ^{14}C analysis (incl. ^{13}C) was used for estimation of groundwater age in the study area.

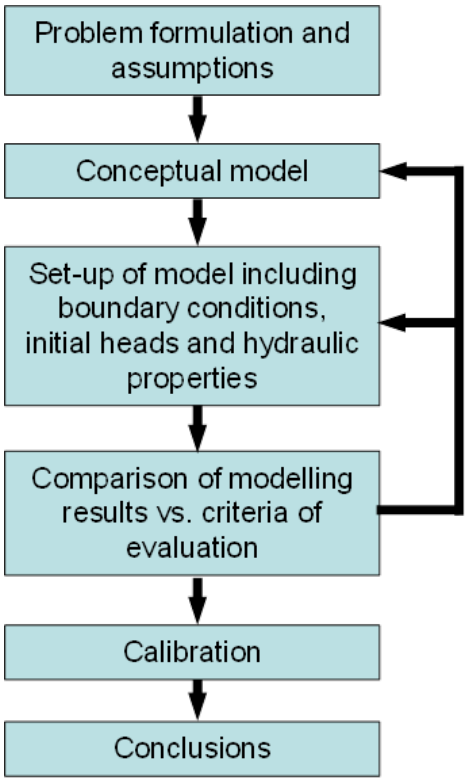

Figure 7. The flow chart followed for groundwater modelling.

5.1.2. Groundwater sampling and analyses

Groundwater sampling were carried out from the existing wells and the piezometer nests installed in Matlab following the procedure described by Bhattacharya et al. (2002b). Field parameters such as pH, redox potential (Eh), temperature, and electrical conductivity (EC) were measured in the field in a flow-through cell. The pH and Eh were measured using an EcoScan pH 6 meter. Samples collected for analyses included: a) filtered aliquot (using Sartorius 0.20 µm online filters) for major anion determination; b) aliquot filtered and acidified with suprapure HNO_3 (14 M) for the cations and other trace element determination including As (Bhattacharya et al. 2002b). Arsenic speciation was performed with Disposable Cartridges® (MetalSoft Center, PA) in the field (Meng et al. 2001) which adsorb As(V), but allows As(III) to pass through.

Major anions, F^-, Cl^-, and SO_4^{2-} were analyzed in filtered unacidified water samples, with a DionexDX-120 ion chromatograph with an IonPac As14 column. NO_3-N, PO_4-P and NH_4-N were analyzed with a Tecator Aquatec 5400 spectrophotometer. The major cations (Ca, Mg, Na and K) and minor and trace elements (Fe, Mn, As) were analyzed by inductively coupled plasma (ICP) emission spectrometry (Varian Vista-PRO Simultaneous ICP-OES) at Stockholm University. Dissolved organic carbon (DOC) in the water samples was determined on a Shimadzu 5000 TOC analyser with a detection limit of 0.5 mg/L and precision of ±10% at the detection limit.

5.1.3. Sediment sampling and characterization

Three boreholes were drilled using hand percussion technique (Rahman and Ravescroft 2003) at different sites within the study area to confirm the driller's perception of the sediment colour and the lithology of the aquifer sediments. Washed sediment samples were collected for every 3.0 m, or more often if characteristics of the sediment changed (**Figure 8**). Washed sediments were collected in a bucket and allowed to settle before being transferred on a bamboo carpet (**Figure 7**). Later, the excess water from the sediment samples were allowed to drain (but not dry), before putting them into plastic bags.

Each of the sediment samples were described on the basis of texture and colour by the local driller in field and later visual inspection of the sediments was carried out and compared with the Munsell standard soil colour chart for colour classification. For proper characterisation of sediment geochemistry on undisturbed sediments, core drillings were done. The sites were chosen in order to get as diversified, with respect to texture and colour characteristics, sediments as possible. The core drilling in Matlab reached a depth of 63 m (200 ft) and was performed with a combination of a hammer technique and a donkey pump. Samples were taken every 1.5 m (5 ft) down to the depth of 30 m and between 30 and 60 m at an interval of 0.6 m (2 ft). The reason for short sampling interval below 30 m was to target and collect as much oxidized sediments (whitish to reddish in colour) as possible as the blackish reducing sediments have been studied more thoroughly by earlier studies.

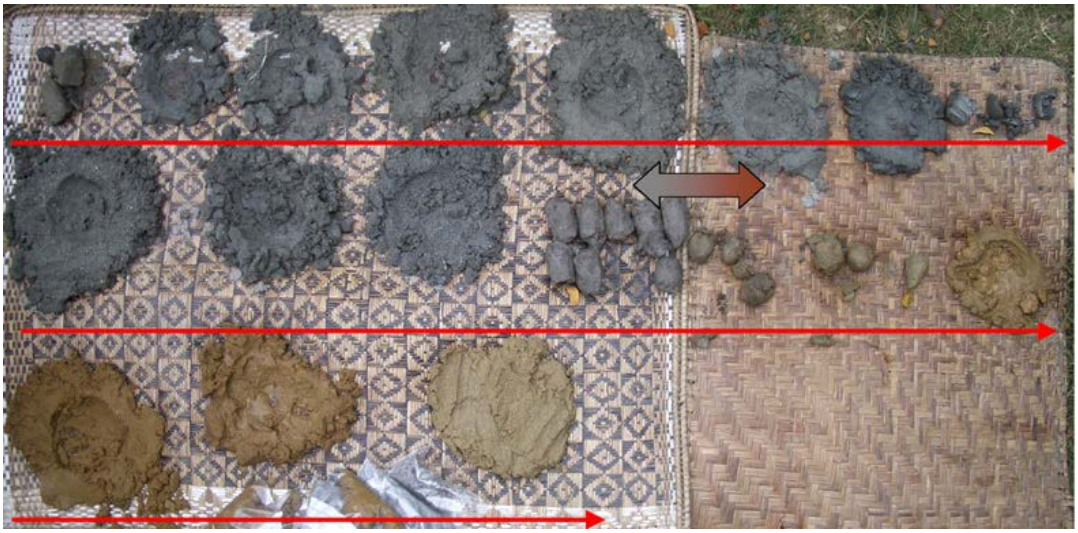

Figure 8. Sequence of washed sediments collected at the interval of 3.0 m (10 ft) from the boreholes using hand percussion technique by the local drillers. The arrow represents the transition of the black (reduced) sediments with the underlying white, off-white and the reddish (oxidized) sediments.

The core-samples were splited vertically for lithological and mineralogical studies as well as sequential extraction. At that time, a coal-like vegetation remains were collected and sent for dating through ^{14}C analysis. The ^{14}C analysis was performed at the Radiocarbon Dating Laboratory in Lund using Single Stage Accelerator Mass Spectrometry (SSAMS).

Ten samples representing the depth of the drilling and range of sediment colours as perceived by the local tubewell drillers were selected for mineralogical studies and geochemical characterization of solid phase (**Figure 9**). Selected sediment samples were analyzed under the stereomicroscope in order to identify the bulk minerals responsible for the colour of the sediments.

5.1.3.1 Mineralogical studies

Mineralogical studies included i) X-ray diffraction (XRD) for targeting oxide, hydroxide, sulphide, sulfate and carbonate minerals, and ii) scanning electron microscopy (SEM) with energy dispersive X-ray spectrometer (EDS) for characterisation of coatings on detrital grains and authigenic mineral phases.

5.1.3.2 Major element geochemistry

X-ray fluorescence (XRF) analysis of the bulk major element composition of sediments was carried out at the Institute of Chemical Technology in Prague, Czech Republic.

5.1.3.3 Sequential extractions

Sequential extraction was carried out to quantify the amount of reactive components such as Fe and Mn in the sediments and their relationship with As (Table 1). Ten selected core sediment samples were sequentially leached using:

i) *Fraction 1*: deionized water (DIW) for quantification of the water soluble fraction of As and other trace elements,

ii) *Fraction 2*: 0.01M $NaHCO_3$ for the release of elements under high pH conditions,

iii) *Fraction 3*: 1M Na-acetate ($C_2H_3NaO_2$, NaAc) for elements bound to carbonate and phosphate phases (Dodd et al. 2000, Ahmed et al. 2004),

iv) *Fraction 4*: 0.2M oxalate ($NH_4C_2O_4$, oxalate) to quantify Fe, Al, and Mn

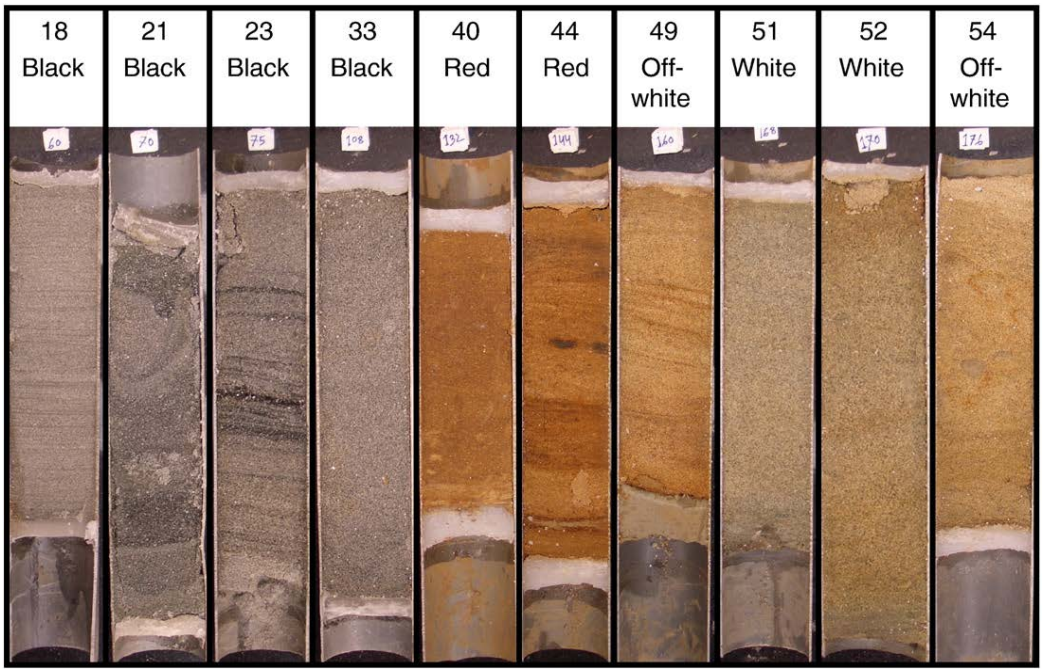

Figure 9. Ten sediment core samples used for mineralogical and geochemical studies. The cores are designated by depth (in meter). The color descriptions correspond to the colors identified by local drillers (see von Brömssen et al. 2007, 2008).

Table 1. Operationally defined steps for sequential extraction of the sediment core-samples from Matlab (von Brömssen et al. 2008)

Fraction	Extractant	Extracting condition	SSR	Wash step
1	DIW	2 h shaking, 20 °C, pH adjusted to 6.95 with NaOH	1:25	25 mL DIW
2	0.01 M $NaHCO_3$ (pH 8.65) 2 h shaking	2 h shaking, 20 °C	1:25	25 mL DIW
3	1 M Na-acetate ($C_2H_3NaO_2$)	3 h shaking, 20 °C , pH adjusted to 5,0 with acetic acid ($C_2H_4O_2$)	1:50	25 mL DIW
4	0.2 M Ammonium oxalate ($NH_4C_2O_4$)	4 h shaking, 20 °C, in the dark	1:25	25 mL DIW
5	0.2 M Ammonium oxalate ($NH_4C_2O_4$ +0.1 M ascorbic acid)	30 min in water bath at 96 °C ± 3 °C in the light	1:25	25 mL 0.2 M oxalate ($NH_4C_2O_4$), 10 min shaking in the dark
6	7 M HNO_3	2 h on sand bed, boiling	1:15	None

bound to amorphous oxides and hydroxides in the sediments,

v) *Fraction 5*: 0.2M oxalate ($NH_4C_2O_4$) + 0.1 M ascorbic acid (oxalate+AA) for amount of Fe, Al and Mn bound to oxides and hydroxides including crystalline phases; and

vi) *Fraction 6*: 7M HNO_3 residual As and other elements associated with the non-silicate minerals (Table 1).

Operationally defined sequential extractions were performed on sediment core-samples, and essentially followed the methods described by Wenzel et al. (2001) and Bhattacharya et al. (2006b) and were performed through extraction of 1 g air-dried homogenized sediment sample in a 50 mL centrifuge tube. Between each step, the sediment was washed. The extracts were preserved by acidification with 0.5 mL ultrapure 14 M HNO_3/100 mL. Blanks were used in each step so that impurities could be subtracted from the extractants. The extracts were analyzed by Varian Vista-PRO Simultaneous Inductively Coupled Plasma Optical Emission Spectroscopy (ICP-OES) at Stockholm University.

5.2. Adsorption studies

Adsorption dynamics of oxidized sediments from Matlab were investigated by extractions, batch isotherm experiments and column experiments. Three sediment samples were chosen with distinct oxidized character from locations below the clay aquitard for the experiments. The samples 1 and 3 were collected from borehole A at depths of 48.8 m and 53.3 m respectively, while the sample 2 was collected from borehole B at a depth of 51.8 m (**Figures 9, 10**).

5.2.1. Selective extractions

For quantifying the elements, including Fe, Mn and Al, present as amorphous oxides and hydroxides, the sediment samples were extracted with 0.2 M oxalate ($NH_4C_2O_4$) at pH 3.25. Each sediment sample were also extracted with 7 M HNO_3 were also conducted to quantify the amounts of As and other elements associated with the non-silicate minerals (i.e., including crystalline phases). Duplicates were performed for each sample. The procedure for these extractions is detailed in Bivén and Häller (2007).

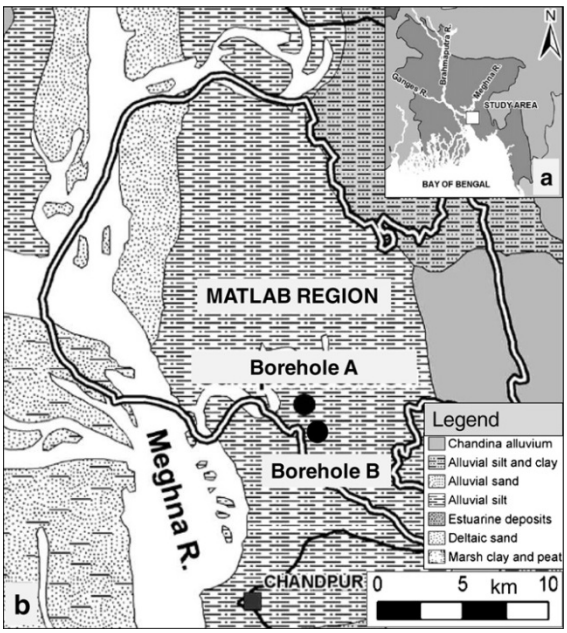

Figure 10. a) Map of Matlab Region in southeastern Bangladesh, b) location of borehole sites A and B (Robinson et al. 2011).

5.2.2. Batch adsorption experiments

Batch adsorption isotherm tests were conducted using the three sediment samples. For each sample, 2 g of drained sediment was mixed with 30 mL 0.01 M $NaNO_3$ in centrifuge tubes. Sodium hydroxide (NaOH) and HNO_3 were added to adjust the pH to 7. Distilled water with 7 different concentrations of As(V) ranging from 0.2 to 100 mg/L (prepared from K_2HAsO_4) were added to each sediment sample, giving 21 filled centrifuge tubes. The tubes were placed in a vertical rotating shaker for 2 weeks and then the samples were centrifuged and filtered. Considering the thermodynamic stability of As and Fe in the oxidized sediments, As(V) was used for the batch tests because it was considered to be the predominant sediment-bound As species in the oxidized aquifers. In most of the groundwater samples abstracted from the oxidized aquifers, the concentration of dissolved As was very low with no detectable As(III) (von Brömssen et al. 2007, see also Table 2).

5.2.3. Column experiments

Column experiments were conducted to examine the influence of DOC on the adsorption capacity of the oxidized sediments. Six columns, each with a diameter of 2 cm and height of 10 cm, were filled with 45 g of oxidized sediments. Two identical columns for each of the three oxidized sediment samples were set up for this study. Synthetic water sample prepared by mixing distilled water with NaCl, $NaHCO_3$ and $NaAs(III)O_2$, was leached through the columns. The concentrations of As, Na, Cl and alkalinity in the influent water correspond to their average concentrations measured in groundwater from tubewells in the reduced sediments in Matlab Region in November 2006 (Table 2). Data from this sampling event was used as a bench mark because this corresponds to the period of sediment sampling (Häller and Bivén, 2007). Arsenic(III) was used in the influent water as it is the major As redox species in the groundwaters abstracted from reduced aquifers in Bangladesh in general and also in the Matlab study region (Table 2). In general, this is considered to represent water that infiltrates into the oxidized aquifers (Ahmed et al. 2004). In the replicate columns, 0.2 wt% lactose was added to the influent solution to stimulate the reductive dissolution of Fe(III) and Mn(IV) oxides. Prior to the addition of the chemicals the influent water was purged with N_2 to remove any dissolved oxygen. The flow rate through the columns was adjusted to 2 mL/day and the experiments were run for 13 weeks. Major anions, cations and trace elements in the influent and effluent solutions were determined once a week throughout the experimental period and the amount of adsorbed As was determined as the difference between the influent and effluent As concentrations.

5.3. Geochemical modelling

The geochemical modelling codes PHREEQC, version 2.14.2 (Parkhurst and Appelo 1999) and Visual MINTEQ version 2.53 (Gustafsson 2011, Dzombak and Morel 1990, Allison et al. 1991) were used for:

- Calculation of saturation indices with an aim to determine aqueous speciation in groundwater samples and identifying the possible mineral phases controlling the solubility of various chemical species based on groundwater chemical data; composition;
- Simulation of adsorbed and dissolved As for prevailing conditions with the objective to understand the pattern of As adsorption and mobilization in aquifers; and
- Simulation of the adsorption of As on oxidized sediments, as surface complexation reactions on generic hydrous ferric oxides, in order to investigate the dynamics of As adsorption the oxidized sediments

5.3.1. Aqueous speciation modelling

The thermodynamic relationships between aquifer solid phases and the species in solution were established through the degree of saturation with respect to mineral phases.

Table 2. Typical water quality parameters measured in groundwater from the oxidized and the reduced aquifers in the Matlab study area (KTH-International Groundwater Arsenic Research Group groundwater monitoring data between 2004-2008)

Sample ID	Sediment colour	Sampling Date	Depth m	pH	Temp °C	HCO_3 mg/L	Cl mg/L	NO_3-N mg/L	PO_4-P mg/L	Na mg/L	K mg/L	Mg mg/L	Ca mg/L	Total As µg/L	As(III) µg/L	Total Fe mg/L	Total Mn mg/L	DOC mg/L	Si mg/L
OXIDIZED SEDIMENT																			
A	Off-white	11-May-04	57.9	6.12	26.8	107	255	0.20	210	75.9	4.2	25.8	53.8	<DL	<DL	0.13	2.53	0.53	53.0
		30-jan-05		6.27	26.2	106	233	0.85	169	88.1	3.8	23.9	57.1	<DL	<DL	0.28	2.59	0.91	48.8
		29-nov-06		6.40	25.8	234	234	0.43	156	82.3	3.4	24.9	58.8	16	nd	0.32	2.62	0.80	34.8
		18-jan-08		6.34	25.6	233	245	<DL	87	91.1	3.9	33.2	57.0	<DL	<DL	0.26	2.54	4.92	43.2
		17-mar-09		6.50	26.1	125	267	1.23	57	77.0	2.0	24.4	62.2	<DL	9	0.40	1.51	1.29	18.9
B	Yellow	11-May-04	57.9	6.39	26.6	136	149	0.23	349	54.3	3.4	20.8	43.1	<DL	<DL	0.32	1.99	1.01	43.7
		30-jan-05		6.59	25.6	154	179	0.20	71	59.9	2.4	20.2	53.9	<DL	<DL	0.79	2.04	0.36	39.9
		28-nov-06		6.60	25.0	147	147	0.23	61	54.7	2.3	21.4	56.7	13	nd	0.81	2.04	1.35	29.8
		18-jan-08		6.76	24.8	320	152	0.01	102	53.7	2.5	26.3	50.8	<DL	<DL	0.72	2.12	1.82	37.7
16	Red	27-May-04	61.0	6.17	26.7	96	206	0.49	293	62.4	3.6	24.4	53.0	<DL	<DL	0.46	3.19	1.41	49.1
		30-jan-05		6.14	26.1	117	232	0.30	166	67.2	3.2	22.3	62.5	<DL	<DL	0.37	3.16	0.56	44.5
		29-nov-06		6.40	25.8	187	187	0.65	123	60.7	2.9	22.6	57.5	11	nd	0.70	3.14	0.78	32.3
		18-jan-08		6.47	23.5	256	189	<DL	150	59.6	3.3	28.1	60.4	6	<DL	1.00	3.27	1.68	43.8
		02-apr-09		7.10	27.0	116	185	0.39	54	68.3	2.7	25.4	65.6	<DL	8	0.71	4.30	2.19	26.4
		15-mar-09		6.40	26.3	163	246	1.05	64	79.1	3.3	25.7	55.6	<DL	7	0.51	2.78	1.42	22.9
19	Off-white	29-apr-04	59.4	6.20	26.5	112	234	1.00	135	78.8	3.6	26.5	53.2	<DL	<DL	0.20	3.58	0.54	50.2
		30-jan-05		6.29	26.2	116	285	0.39	101	80.8	3.1	23.0	57.9	<DL	<DL	0.21	3.53	0.65	43.2
		29-nov-06		6.50	26.2	216	216	1.12	77	76.2	2.9	25.1	60.6	8.20		0.17	3.61	0.67	32.1
20	Off-white	29-apr-04	59.4	6.19	26.7	107	186	0.54	334	58.4	3.7	22.4	49.7	<DL	<DL	0.41	2.90	0.47	54.7
		30-jan-05		6.32	26.3	87	283	0.27	199	78.6	3.3	21.6	56.8	<DL	<DL	0.27	3.01	0.53	43.7
		29-nov-06		6.30	25.0	216	216	0.82	199	75.2	3.0	24.1	60.0	7	nd	0.43	3.21	0.86	32.7
		18-jan-08		6.45	25.3	224	230	<DL	177	81.8	3.5	31.9	60.5	6	<DL	0.25	3.15	2.73	41.1
		16-mar-09		6.50	26.2	139	232	0.95	79	81.8	2.9	26.0	68.5	<DL	8	0.23	4.31	1.74	26.6
		06-apr-09		7.00	26.7	105	214	0.74	35	70.3	2.7	24.8	57.0	11	7	0.25	3.78	1.20	21.2
22	Off-white	29-apr-04	59.4	6.55	26.9	164	138	5.01	526	67.1	3.0	19.4	37.8	<DL	9.63	3.81	1.74	1.18	39.8
		30-jan-05		6.68	26.5	164	170	0.18	509	72.2	2.9	19.1	40.7	<DL	<DL	4.85	1.60	0.40	35.9
		28-nov-06		6.40	24.9	201	201	1.14	67	80.1	2.6	25.2	50.7	<DL	nd	0.28	2.50	1.39	29.2
		18-jan-08		6.66	25.3	263	197	<DL	75	87.1	2.8	32.5	42.5	<DL	<DL	0.35	2.33	1.56	33.6
		11-mar-09		6.60	27.0	136	129	0.60	17	49.4	2.1	20.0	41.7	<DL	6.63	3.95	2.24	1.43	19.7
26	Red	29-apr-04	53.3	6.19	26.5	113	169	0.51	392	55.2	3.3	21.1	45.5	<DL	<DL	0.24	2.34	1.00	53.6
		30-jan-05		6.30	26.1	112	210	0.20	234	58.6	3.1	19.6	48.8	<DL	<DL	0.27	2.35	0.60	48.9
		28-nov-06		6.40	22.6	167	167	0.94	242	54.7	3.0	21.5	55.0	6	nd	0.42	2.40	0.97	35.0
		18-jan-08		6.59	26.2	265	170	<DL	209	60.0	3.1	27.9	51.1	<DL	<DL	0.42	2.32	2.11	41.9
32	Red	30-apr-04	64.0	6.38	26.8	140	150	1.01	212	59.5	3.4	19.0	39.6	<DL	<DL	0.37	3.96	1.18	46.3
		30-jan-05		6.40	26.3	174	196	0.22	88	63.4	3.1	19.1	49.6	<DL	<DL	0.37	3.68	0.73	41.0
		28-nov-06		6.50	25.1	156	156	0.52	80	60.5	2.8	20.2	50.4	10	nd	0.47	3.81	0.79	31.5
		18-jan-08		6.72	25.9	299	154	<DL	82	66.7	3.1	26.0	48.7	<DL	<DL	0.36	3.50	2.72	37.9
		12-mar-09		6.5	27.0	125	104	0.42	82	52.9	2.6	22.0	47.3	<DL	12.35	0.56	2.61	1.14	23.2
35	Off-white	30-apr-04	79.3	6.33	26.8	118	199	0.39	199	68.6	3.9	24.1	47.7	<DL	<DL	0.33	2.57	0.93	55.8
		30-jan-05		6.31	26.2	128	268	0.30	115	74.4	3.6	22.7	54.9	<DL	<DL	0.29	2.67	0.32	50.0
		28-nov-06		6.60	29.1	196	196	0.60	113	67.4	3.2	23.4	58.7	<DL	nd	0.45	2.69	0.80	36.0
		18-jan-08		6.68	25.8	364	204	<DL	96	75.6	3.7	32.9	72.6	<DL	<DL	0.40	2.72	0.85	46.6
		14-mar-09		7.00	26.8	455	309	1.23	46	75.5	3.0	26.6	64.2	<DL	<DL	0.31	3.71	1.25	30.7
43	White	3-May-04	59.4	6.55	26.8	206	292	0.89	1583	137.4	3.7	33.7	62.1	12	12	8.90	0.25	0.87	42.0
		30-jan-05		6.51	26.6	174	397	0.40	1508	144.4	3.4	28.5	69.6	17	14	8.61	0.26	0.99	37.7
		19-jan-08		6.79	25.1	288	288	0.00	1223	130.3	3.6	37.7	69.2	21	<DL	9.83	0.25	0.99	35.6
44	White	3-May-04	57.9	6.77	26.8	415	272	1.22	3933	202.1	4.7	34.0	62.8	37	35.78	7.06	0.22	1.95	39.0
		30-jan-05		6.73	26.5	402	368	1.15	3941	223.8	4.4	29.4	72.0	43	44.72	7.06	0.24	2.66	36.4
		29-nov-06		6.70	27.1	264	264	0.54	3671	205.1	3.8	29.2	68.3	64	nd	6.97	0.25	2.09	26.7
		19-jan-08		6.84	24.8	501	276	0.24	3163	192.4	4.5	36.3	67.5	52	10	6.92	0.27	3.20	33.8
		05-apr-09		7.50	26.6	410	277	<DL	3803	210.1	3.5	32.2	80.2	42	36	8.23	0.28	3.02	21.3
51	Off-white	30-apr-04	57.9	6.66	26.7	355	530	0.98	555	374.7	4.1	28.7	57.1	<DL	<DL	0.14	1.93	0.65	32.2
		30-jan-05		6.62	26.5	350	720	2.51	370	385.7	3.6	25.3	62.0	<DL	<DL	0.13	1.91	0.81	28.8
		30-nov-06		6.70	25.2	518	518	1.65	405	357.3	3.3	25.8	62.7	<DL	<DL	0.29	1.93	0.89	23.0
		19-jan-08		6.71	22.9	840	424	<DL	310	382.5	3.6	33.4	60.3	<DL	25	0.16	1.76	2.35	26.6
		05-apr-09		6	26.3	306	601	2.79	1026	263.8	3.1	30.8	72.2	44	43	0.13	1.94	2.03	16.6
58	Off-white	1-May-04	57.9	6.66	26.8	319	648	1.51	1583	406.4	4.9	40.4	77.7	22	19	2.06	1.76	0.68	30.9
		30-jan-05		6.69	26.3	292	893	0.47	1305	432.6	4.3	32.2	89.9	27	25	2.05	1.78	1.27	27.6
		29-nov-06		6.70	24.4	603	603	0.00	1417	388.0	3.7	33.6	79.7	35	nd	2.47	1.741	0.83	22.3
		19-jan-08		6.87	24.3	760	638	0.00	1299	362.0	4.5	41.3	79.8	34	9	2.74	1.76	3.42	27.0
		04-apr-09		7.40	27.0	353	256	0.94	1440	344.0	3.3	36.9	90.9	44	34	2.62	2.18	1.62	16.8
63	Red	1-May-04	68.6	6.51	26.6	166	433	1.23	222	208.5	6.1	42.2	79.0	<DL	<DL	0.34	2.16	1.00	35.6
		30-jan-05		6.50	26.1	166	674	0.66	156	221.7	5.4	34.7	93.4	<DL	<DL	0.43	2.21	0.68	32.1
		28-nov-06		6.60	24.9	493	493	<DL	147	209.4	4.8	37.2	92.0	7	<DL	0.81	2.36	1.94	24.7
		19-jan-08		6.62	24.9	407	521	0.54	128	237.7	6.0	52.7	93.8	<DL	<DL	0.81	2.37	2.98	31.0
		06-apr-09		6.6	26.7	187	47	1.75	96	232.9	4.9	46.6	119.4	10	10	0.81	3.32	1.65	20.8
REDUCED SEDIMENT																			
25	Black	30-apr-04	24.4	6.81	26.1	307	83	0.62	7282	102.3	6.2	17.0	36.1	241	241	6.77	0.14	3.79	43.1
		30-jan-05		7.00	25.8	305	110	0.46	7552	104.9	5.7	17.1	40.6	260	nd	6.92	0.14	4.67	39.8
		28-nov-06		7.00	25.5	294	94	0.58	6789	95.0	5.0	19.1	50.9	383	380	7.54	0.16	5.37	29.8
		18-jan-08		6.85	23.0	663	86	0.12	6960	89.4	5.8	22.3	42.8	323	109	7.04	0.18	4.01	37.4
37	Black	1-May-04	39.6	6.58	26.8	189	356	1.00	3642	189.0	5.3	25.3	51.4	23	19	9.18	0.28	1.05	52.3
		30-jan-05		6.62	26.3	193	433	0.54	3442	195.6	4.8	23.6	58.4	25	23	9.09	0.29	1.24	46.1
		28-nov-06		6.70	25.3	297	297	0.77	3465	170.7	4.4	25.9	67.7	39	39	9.61	0.31	1.57	33.8
		18-jan-08		6.58	25.9	261	158	<DL	3137	155.0	3.2	25.4	49.2	<DL	<DL	9.00	0.25	2.30	41.9
53	Black	1-May-04	16.8	6.65	26.7	202	13	0.17	5657	8.2	3.6	11.5	45.1	148	144	11.5	0.63	3.29	55.2
		30-jan-05		6.72	26.4	185	15	0.10	5867	8.0	3.2	11.0	45.5	163	160	11.9	0.60	3.17	47.9
54	Black	1-May-04	25.9	6.62	26.6	409	16	0.24	7297	35.4	6.4	36.4	91.9	274	259	6.98	0.10	4.11	48.4
		30-jan-05		6.73	26.3	441	10	0.10	6841	25.1	5.7	30.9	145.6	312	306	8.76	0.29	4.39	40.4
		30-nov-06		6.80	24.0	430	20	<DL	6078	32.3	5.0	31.9	90.4	408	nd	6.79	0.10	3.99	31.7
		19-jan-08		6.85	24.8	487	151	0.10	5097	28.8	4.4	41.8	89.8	349	326	7.51	0.08	4.78	21.0
57	Black	1-May-04	25.9	6.67	26.5	499	12	0.20	7610	22.3	6.3	36.1	119.6	245	239	7.84	304	5.02	44.6
		30-jan-05		6.75	26.2	405	10	0.10	6895	22.4	5.4	28.7	137.4	259	235	7.47	300	4.59	39.1
		30-nov-06		6.80	25.4	445	8	<DL	6253	19.2	4.8	30.2	110.6	339	nd	7.42	319	4.09	29.7
		19-jan-08		6.88	23.9	450	8	0.60	6341	22.8	5.2	39.6	109.7	252	90	6.58	305	5.63	35.5

Saturation index (SI) is defined as:

$$SI = \log\left(IAP/K_{sp}\right) \quad \text{..... (eqn. 1)}$$

where IAP is the ion activity product and K_{sp} is the solubility product for a mineral at a given temperature. When SI=0 (IAP=K_{sp}) the solution is at thermodynamic equilibrium with respect to a specific mineral and when SI>0 the water is supersaturated with respect to a mineral and vice versa. Calculation of SI was done to identify possible sinks and sources of dissolved elements and for further interpretation of possible reactions controlling the aqueous chemistry (Sracek et al. 2004a,b).

Saturation indices were calculated using PHREEQC version 2.14.2 (Parkhurst and Appelo, 1999) with the WATEQ4F thermodynamic database. Eh values measured in field and corrected with respect to standard hydrogen electrode (SHE) were used for speciation of redox couples. The model calculated the activities of different species of each element and then using these activities saturation indices were calculated. Since the measured redox potential (Eh) is a

Table 3. Reactions and thermodynamic constants for PHREEQC surface complexation model with strong (Hfo_s) and weak (Hfo_w) adsorption sites.

Adsorption reaction	Log K	Reference
$Hfo\_sOH + H^+ = Hfo\_sOH^{2+}$	7.29	Allison et al. (1990)
$Hfo\_wOH + H^+ = Hfo\_wOH^{2+}$	7.29	
$Hfo\_sOH = Hfo\_sO^- + H^+$	-8.93	
$Hfo\_wOH = Hfo\_wO^- + H^+$	-8.93	
Arsenite		
$Hfo\_sOH + H_3AsO_3 = Hfo\_sH_2AsO_3 + H_2O$	5.41	Allison et al. (1990)
$Hfo\_wOH + H_3AsO_3 = Hfo\_wH_2AsO_3 + H_2O$	5.41	
Arsenate		
$Hfo\_sOH + H_3AsO_4 = Hfo\_sH_2AsO_4 + H_2O$	8.61	Allison et al. (1990)
$Hfo\_wOH + H_3AsO_4 = Hfo\_wH_2AsO_4 + H_2O$	8.61	
$Hfo\_sOH + H_3AsO_4 = Hfo\_sHAsO_4^- + H_2O + H^+$	2.81	
$Hfo\_wOH + H_3AsO_4 = Hfo\_wHAsO_4^- + H_2O + H^+$	2.81	
$Hfo\_sOH + H_3AsO_4 = Hfo\_sOHAsO_4^{-3} + 3H^+$	-10.12	
$Hfo\_wOH + H_3AsO_4 = Hfo\_wOHAsO_4^{-3} + 3H^+$	-10.12	
Phosphate		
$Hfo\_sOH + PO_4^{-3} + 3H^+ = Hfo\_sH_2PO_4 + H_2O$	31.29	Allison et al. (1990)
$Hfo\_wOH + PO_4^{-3} + 3H^+ = Hfo\_wH_2PO_4 + H_2O$	31.29	
$Hfo\_sOH + PO_4^{-3} + 2H^+ = Hfo\_sHPO_4^- + H_2O$	25.39	
$Hfo\_wOH + PO_4^{-3} + 2H^+ = Hfo\_wHPO_4^- + H_2O$	25.39	
$Hfo\_sOH + PO_4^{-3} + H^+ = Hfo\_sPO_4^{-2} + H_2O$	17.72	
$Hfo\_wOH + PO_4^{-3} + H^+ = Hfo\_wPO_4^{-2} + H_2O$	17.72	
Carbonate		
$Hfo\_wOH + CO_3^{-2} + H^+ = Hfo\_wCO^{3-} + H_2O$	12.56	van Geen et al. (2004)
$Hfo\_wOH + CO_3^{-2} + 2H^+ = Hfo\_wHCO_3 + H_2O$	20.62	
Silica		
$Hfo\_sOH + H_4SiO_4 = Hfo\_sH_3SiO_4 + H_2O$	4.28	Swedlund and Webster (1999)
$Hfo\_wOH + H_4SiO_4 = Hfo\_wH_3SiO_4 + H_2O$	4.28	
$Hfo\_sOH + H_4SiO_4 = Hfo\_sH_2SiO_4^- + H_2O + H^+$	-3.22	
$Hfo\_wOH + H_4SiO_4 = Hfo\_wH2SiO_4^- + H_2O + H^+$	-3.22	
$Hfo\_sOH + H_4SiO_4 = Hfo\_sHSiO_4^{-2} + H_2O + 2H^+$	-11.69	
$Hfo\_wOH + H_4SiO_4 = Hfo\_wHSiO_4^{-2} + H_2O + 2H^+$	-11.69	
Calcium		
$Hfo\_sOH + Ca^{+2} = Hfo\_sOHCa^{+2}$	4.97	Allison et al. (1990)
$Hfo\_wOH + Ca^{+2} = Hfo\_wOCa^+ + H^+$	-5.85	

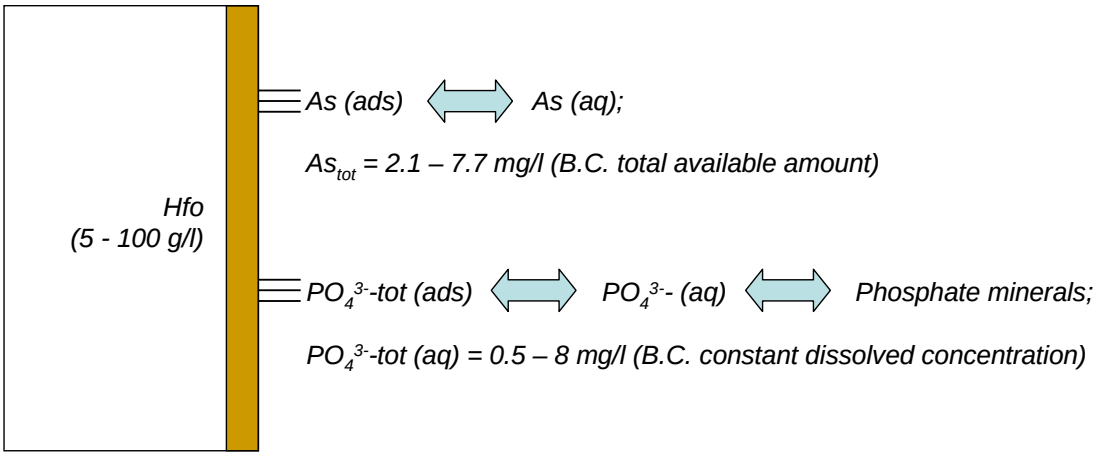

Figure 11. Conceptual model for simulation of As adsorption in aquifers

proxy for redox condition for modelling valid only under redox equilibrium conditions, a sensitivity analysis was done to evaluate the impact of Eh on the resulting SI values by altering Eh in the model.

5.3.2. Simulation of As adsorption characteristics of aquifer sediments

The adsorption of As on the oxidized sediments was simulated as surface complexation reactions on generic hydrous ferric oxides (*Hfo*) surfaces using the Diffuse Layer Model (Dzombak and Morel (1990). The modelling was conducted using the geochemical modeling code PHREEQC (Parkhurst and Appelo 1999). The Minteq.v4 database (Allison et al. 1990) was adopted and modified as required. Using the surface complexation approach the adsorption of different species to *Hfo* are described by equilibrium mass action equations. The Dzombak and Morel (1990) model includes both strong and weak binding sites on *Hfo*. The surface reactions considered and thermodynamic constants used are provided in Table 3.

Arsenic adsorption chatacteristics under prevailing aquifer conditions were simulated as surface complexation reactions on hydrous ferric oxides (*Hfo*) with the Diffuse Layer Model (DLM) (Dzombak and Morel 1990, Allison et al. 1991). The simulations comprised of a batch system of *Hfo*, adsorbed and dissolved As(III)-tot and dissolved PO_4^{3-}-tot as described by **Figure 11**. The adsorption of As was assumed to be controlled by pH, *Hfo* content, species of As (AsIII or AsV) and presence of PO_4^{3-}-tot as competing ion (Smedley and Kinniburgh 2002, Sracek et al. 2004a,b, Gustafsson and Bhattacharya 2007).

The system hydrous ferric oxides, adsorbed and dissolved AsIII and PO_4^{3-} were simulated and compared with analytical data. Default parameter based on Dzombak and Morel (1990) was used for specific surface area for *Hfo* (600 m^2/g). Input data for the modelling, were based partly on the groundwater chemistry data as well as the solid phase extractions (Table 4). The amounts of *Hfo* and As were calculated based on oxalate extractions data for Fe and As respectively (Fe_{ox}, As_{ox}) and the L/S ratio of alluvial aquifer properties. Dissolved As concentration was added to As_{ox} amount giving total available As in the system. A constant concentration of dissolved PO_4^{3-}-tot was used as boundary condition simulating phosphate mineral phases in equilibrium with the groundwater described below. This assumption was based on the findings from speciation modelling showing phosphate mineral phases in equilibrium with the groundwater.

Table 4 Analytical data used for adsorption simulations using Visual MINTEQ v. 2.53 and diffusive layer model by Dzombak and Morel (1990)

Analytical data	Unit	Min	Max	Corresponding input data for simulation
Fe_{ox}	mg/kg	700	15000	Hfo
As	µg/L	1	350	As (dissolved)
PO_4^{3-}	mg/L	0.5	8	PO43- (dissolved)
As_{ox}	mg/kg	0.5	1.5	As (assumed to be adsorbed)
Input data for simulation				**Boundary condition**
Hfo	g/L	5	100	Total amount (adsorbed+dissolved)
PO_4^{3-}	mg/L	0.5	8.0	Fixed dissolved concentration
pH		6.3	7.1	Fixed
T	°C	25	25	Fixed
As	mg/L	2.1	7.77	Total amount (adsorbed+dissolved)
L/S ratio in aquifer volume			0.238	Used for unit conversion for the model

5.4. Geomicrobiology

Transformation of As by microorganisms has important environmental implications because As(V) and As(III) have different sorption properties. Primarily studies have mostly focused on sites contaminated by mining, pesticides or other related anthropogenic activities, and they all demonstrate enhanced microbial mobilization on short time scales. The importance of various microbial processes in the dynamics of As underscore the need for our continued inquiry regarding As transformations. Microbial processes in the sediment-groundwater interface and their impact on As mobilization has not been investigated in these areas and perhaps provide new insights to the validations on the sustainability of the targeted safe aquifers.

Microbial processes associated with organic matter degradation have important environmental implications on redox transformations of As in groundwater environment. In order to ensure the sustainability of the As-safe aquifers, investigations on enhanced mobilization of As in the sediments representing typical aquifer sediments, e.g. the color groups. So far the study has focused on isolation of microbial populations in sediments and their role in microbial transformation of As is being investigated.

5.4.1. Sediment sampling

Undisturbed core samples were collected by a modified split spoon method upto a depth of 60 m. Core samples were collected in 0.3 m plastic tubes with 5 cm diameter. The drilling was performed with a combination of a hammer technique and a donkey pump. Core samples were taken every 1.5 m down to the depth of 30 m and between 30 and 60 m core samples were taken every 0.6 m. The core samples were sealed in both ends with wax during sampling. Later, the core-samples were split and one half was used for microbiological studies, and the other half was preserved for mineralogical and sediment geochemical studies.

5.4.2. Isolation and characterization of microbiota

The splitted samples from the tubes were placed in small vials under anaerobic conditions. The sample was weighed and added known amount of sterile distilled water to suspend and made serial dilutions with sterile water and placed on nutrient Agar plates and incubated at room temperature, 30°C and 37°C for few days under both aerobic and anaerobic con-ditions. The colonies were separated and isolated un-til to pure colonies were observed. The isolated col-onies of microorganisms were grown on MacConkey agar, EMB agar for biochemical characterization (Gunaratna et al. 2010).

The isolated colonies were grown overnight in Nutrient Broth at respective temperatures. The DNA was extracted using Qiagen DNA isolation kit. The DNA template was used to amplify the 16SrRNA gene using PCR method. The universal forward and reverse primers were used in the PCR reaction. The reaction conditions were 98°C for 30 sec; 98°C for 10 sec, 55°C for 30 sec, 72°C for 30 sec under 30 cycles and final extension at 72°C for 10 min. The reaction product was analyzed by running electrophoresis on 1% agarose gel. The product was then analyzed for sequencing and the sequence was later compared in NCBI data base using Blast search.

5.5. Conceptualisation

The practice of installation of safe tubewells with local technique has already reached the affluent class of rural population. In order to develop and intensify this practice we are proposing a strategy for the local drillers to target safe aquifers in regions with high As groundwater.

In order to identify safe aquifers, their sustainability and the risk for cross-contamination etc., a hydrogeological investigation including prevailing biogeochemical processes responsible for mobilization and immobilization of As has been discussed in the light of the various outcomes and results of this research project.

6. Results and Discussion

6.1. Hydrogeological field investigations

6.1.1. Aquifer delineation based on borelogs

A 3-D subsurface aquifer model was developed using the program Rockworks (v. 2004). Based on the generalized description of the sediments, three aquifers denoted as Aquifer 1, Aquifer 2 and Aquifer 3 were delineated (**Figure 12**). The three aquifers are separated by two dominantly silty clay aquitards (Aquitard 1 and Aquitard 2), identified and described by Mozumder (2011) and Mozumder et al. (2011). The subsurface sequence of the study area has been divided into six hydrostratigraphic units. In most cases, the lower two units are missing within the explored depth. The so-called "oxidized aquifer" (von Brömssen et al. 2007) occurs as Aquifer 1 and/or in the upper reaches of Aquifer 2. Aquifer 1 composed predominately of fine sand and ranges with thickness between 25 and 60 m. The aquitard delineating the two Aquifers 1 and 2 is significant from a hydraulic point of view and dominated by silty clay and sandy clay units with thickness varying between between 3 and 59 m. This. The aquitard has been encountered at depths varying between 39 and 70 m as revealed by the drilling logs prepared during piezometer installation at different sites (**Figure 13**).

6.1.2. Estimation of groundwater abstraction in Matlab

The total groundwater abstraction rate for Matlab (both North and South) was estimated to 176 mm/yr. The survey of irrigation wells revealed that the maximum abstraction amounts to 143 mm/yr (81%) from shallow depths (<50 m), 25 mm/yr (14%) from depths between 50–75 m and only 8 mm/yr (5%) from depths below 75 m. The entire irrigation season is between November to June with the maximum abstraction for irrigation from January to April. In Matlab the present groundwater abstraction is slightly less than in other parts of the country, 200 mm/yr has been assumed for Bangladesh on average (Michael and Voss, 2008). If all irrigation water were to be tapped from the deep low-As aquifers, the risk of cross contamination from shallow high-As aquifers would increase significantly. However, the adsorption of As must be considered as well because this process would slow the transport of As significantly (Stollenwerk et al. 2007, von Brömssen et al. 2008, Robinson et al. 2011). Irrigation wells are not evenly distributed in the area, they are rather installed in clusters. Thus, the effect from pumping will differ locally within Matlab Upazila.

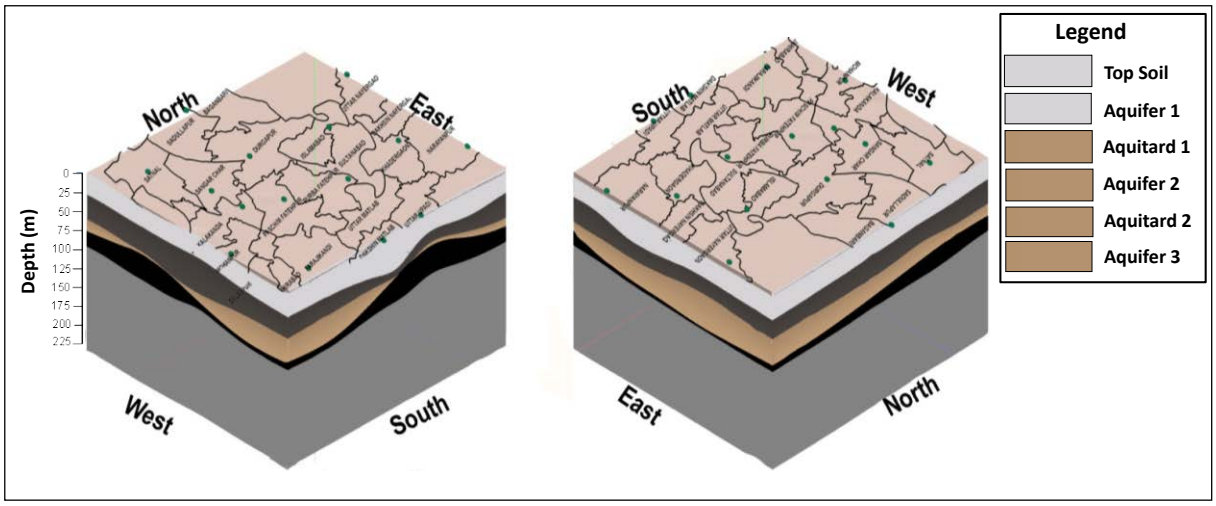

Figure 12. Geometry of the three aquifer units generated by Rockworks using the borelogs constructed from piezometer borings (von Brömssen et al. 2014).

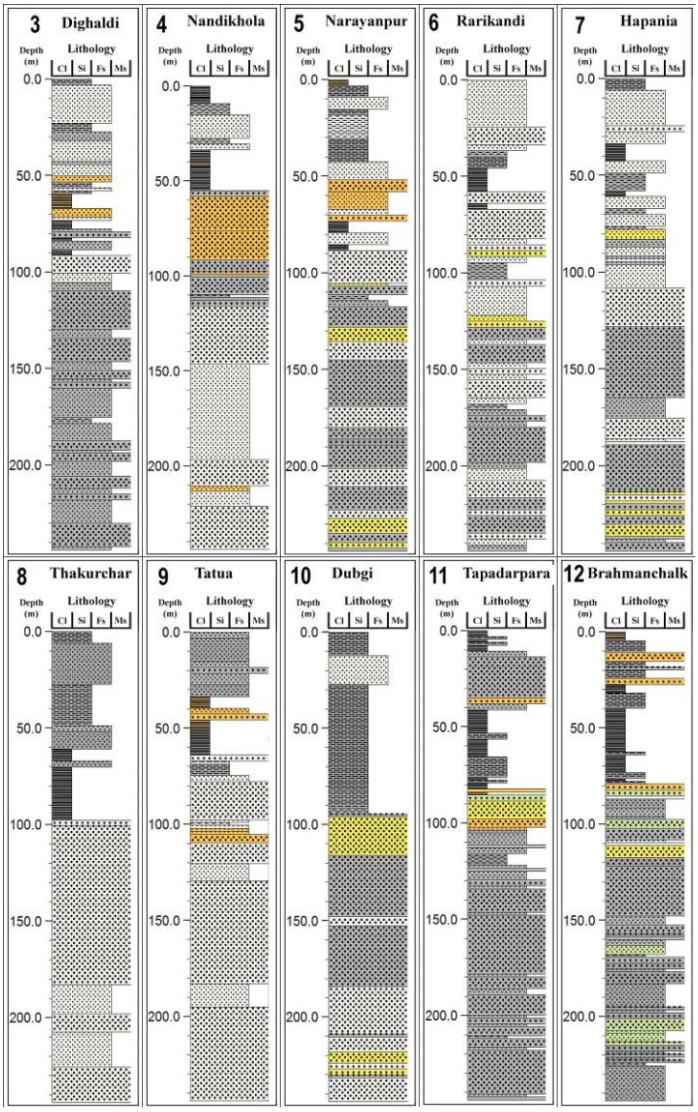

Figure 13. Aquifer delineation from borelog data from the piezometer installation sites.

6.1.3. Hyraullic head monitoring results

The hydrographs produced from the monitoring data are shown in **Figure 14**.

6.1.3.1 Measured vertical hydraulic gradient

A vertical downward gradient was apparent in all piezometer nests. The annual average for all nests, as measured between the top- and the lowest piezometer, is 0.006, while the maximum value is 0.029 (Nest 7). In four of the nine piezometric nests (nests 6, 7, 9, 11), an upward gradient is observed during the winter period (November to January). The observed downward gradient is consistent with the modelling results (see later). The region acts as a recharge area rather than a discharge area, although Matlab lies adjacent to the Meghna River.

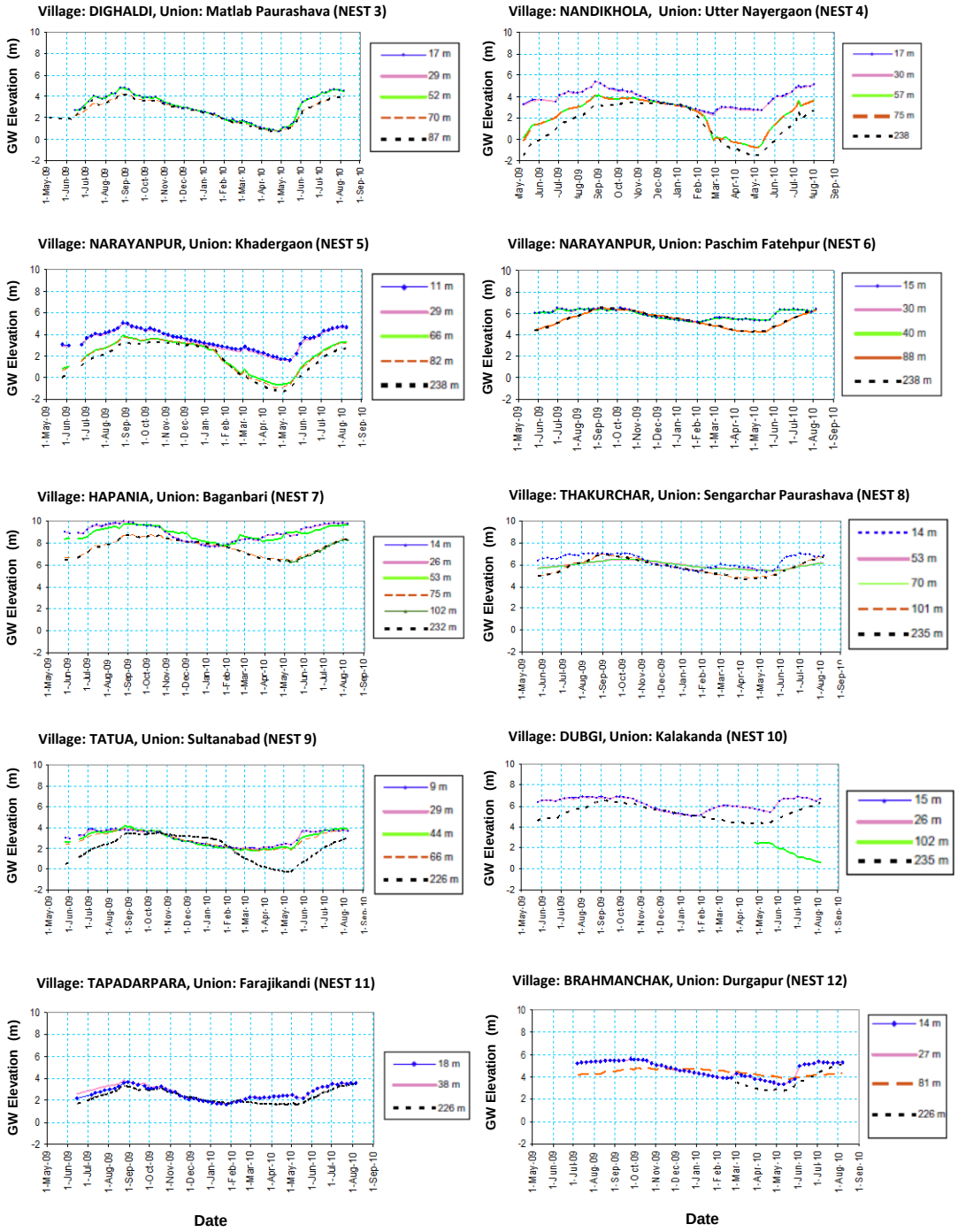

Figure 14. Groundwater elevation observed in 10 piezometer nests.

6.1.3.2 Amplitude of hydrographs

The amplitude of the hydraulic heads as observed in the piezometers varies between 1.0 and 5.1 m. The highest amplitudes are observed in the deeper piezometers of nest 4 and 5 where the number of irrigation wells was high. Although groundwater abstraction increases the stress imposed on the aquifers, the system is recharged during the monsoon rains, and fully recharged after the monsoon period.

6.1.3.3 Seasonal variation

The hydraulic heads in the shallow piezometers peak during August to September following the beginning of the monsoon period and the lowest hydraulic heads are observed during the dry–irrigation season between January and May. The shallow part of the groundwater reservoir seems to be recharged rather quickly compared to the deeper part of the reservoir, since the deeper piezometers in many cases (especially nests 4, 6, 7, 9, 10) have their lowest hydraulic heads 2–4 months later. The relatively higher amplitude of the groundwater level fluctuations in the deeper piezometers is puzzling, but it may be the result of the combination of the water level fluctuations in Meghna and hydraulic properties of the deep aquifers.

6.1.3.4. Trends shown by the hydrographs in the hydrostratigrahic units

The hydrographs show differential behaviour of shallow and of deeper piezometers, indicating the presence of two or three separate aquifer units depending on location, i.e. a shallow, an intermediate and a deep aquifer. Using hydraulic pressure heads to delineate of aquifers indicates the presence of the following:

- Aquifer 1 extends down to a depth of approximately 50 m b.g.l.
- Aquifer 2 located between 50–100 m b.g.l.
- Aquifer 3 located from approximately 100 to at least 250 m b.g.l.

Aquifers 2 and 3 seem to behave similarly and the distinction is not clear. Thus, an aquitard between these aquifers may be discontinuous or thin as observed in the generalized hydrostratigraphic cross section along N-S in both North Matlab and South Matlab (**Figure 15**).

6.1.3.5. Hydraulic heads below mean sea level

In nests 4, 5 and 9, the hydraulic heads measured in the deep and intermediate deep piezometers are below the mean sea level during the end of the heavy irrigation period from March to May.

This can be a consequence of pumping only. However, most irrigation water is abstracted from relatively shallow depth. Thus, the lower hydraulic head in the deeper piezometers are caused by an unknown abstraction point or a combination of the identified localirrigation and differences in aquifer properties at depth.

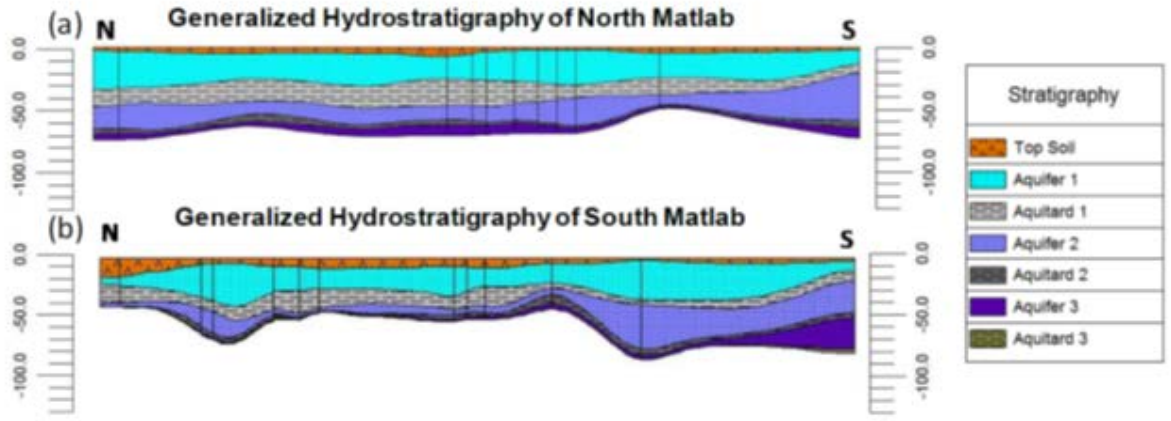

Figure 15. Generalized hydrostratigraphic cross section along N-S in (a) North Matlab and (b) South Matlab.

6.1.4. Hydraulic testing

The pumping test was carried out in January 2008 in the middle of the dry season using and irrigation well for abstraction of groundwater. For the test, 9 piezometers were installed at varying depths (23–88 m) and distances between 2 and 36 m from the pumping well, and pumping test was carried out for a period of 23½ hours at the rate of 65 m^3/hour (Table 5),. Groundwater levels were monitored in the pumping well and piezometers prior, during and after the pumping period. The piezometers were installed in two perpendicular lines with the origin at the irrigation well (**Figure 16**).

The water levels were also monitored in two nearby private wells located at a distance of 128 and 94 m from the irrigation well at similar depths. The irrigation well had not been in prior use during the season. The water levels were monitored automatically with loggers in two piezometers as well as manually, twice a minute initially. During the installation of the piezometers, with the hand percussion method, washed sediment samples were collected at intervals of 1.5 m for the reconstruction of the lithological succession at the pumping test site (**Figure 17**).

Drawdown was obvious in all piezometers although the drawdown in piezometer 1:285 (88 m) was small (only a few centimetres). The drawdown in the piezometer closest to the pumping well was only 0.52 m which indicates that this piezometer was installed in silty to clayey sediments with little hydraulic response. The maximum drawdown during the pumping test for each of the piezometers, and the distance to the pumping wells are listed in Table 5 and plotted in **Figure 18**.

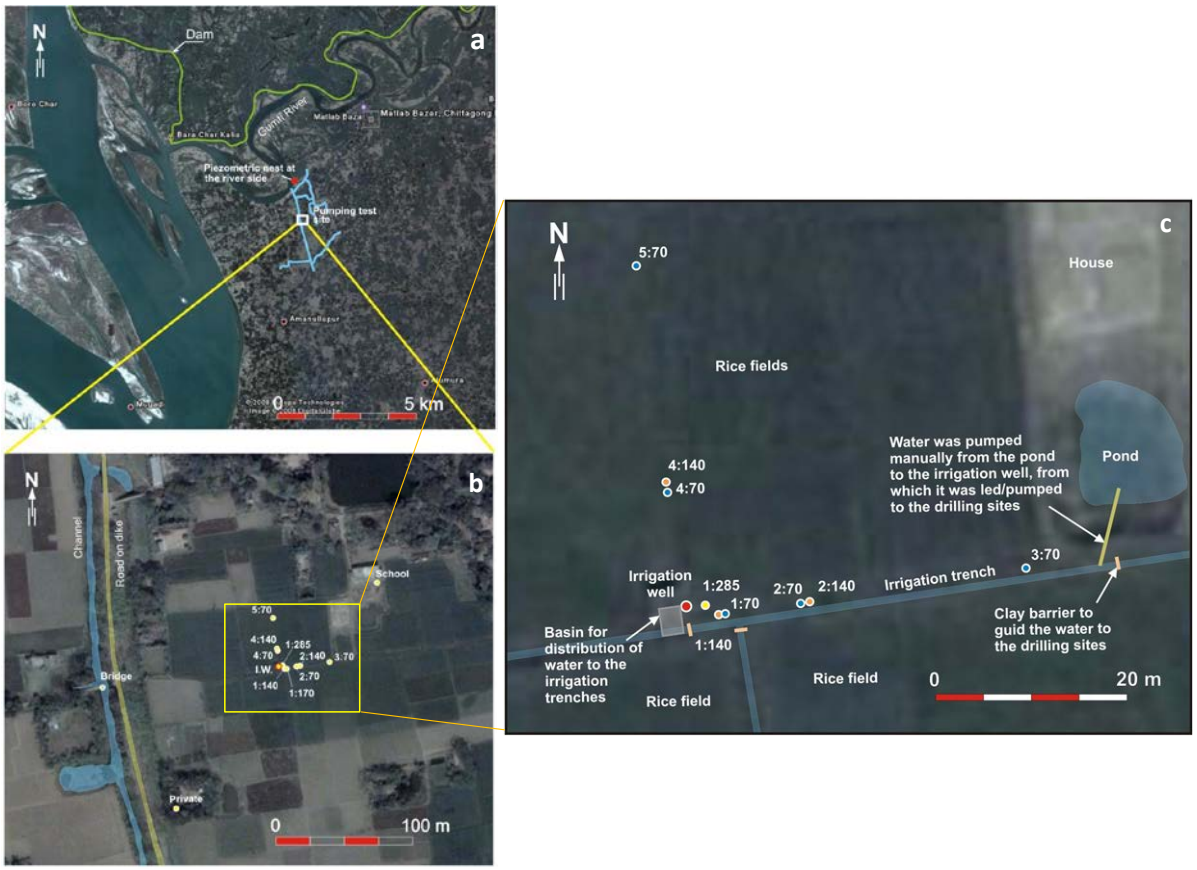

Figure 16. Location of the hydraulic test site: a) in regional scale with rivers Meghna and Gumti, b) piezometers used for pumping test, c) detail of the field and wells. The numbers indicate piezometer site ID and depth in ft, i.e. 2:70 indicate site 2 and depth of the screen at 70 ft.

Table 5. Depth of the nine piezometers installed for pumping tests and maximum drawdown during the pumping test observed in installed piezometers and wells NABO 1 (School) and NABO 2 (Private).

Piezometer ID	Coordinates (degree)		Depth (m)	Distance from pumping well (m)	Maximum drawdown (m)
1:285	N 23.31365	E 90.68735	88.4	2.0	0.02
1:140	N 23.31364	E 90.68737	42.7	3.5	0.19
1:70	N 23.31364	E 90.68738	21.3	4.3	0.52
2:70	N 23.31366	E 90.68745	21.3	12.0	2.06
4:70	N 23.31376	E 90.68731	21.3	12.0	2.07
2:140	N 23.31366	E 90.68746	42.7	13.1	0.19
4:140	N 23.31377	E 90.68731	42.7	13.2	0.09
5:70	N 23.31397	E 90.68729	21.3	35.9	1.33
3:70	N 23.31368	E 90.68768	21.3	36.0	1.48
NABO 1/School	N 23.31420	E 90.68727	29.0	127.5	0.35
NABO 2/Private	N 23.31273	E 90.68725	17.4	93.6	0.27
Irrigation Well	N 23.31365	E 90.68726	21.3	0.0	-

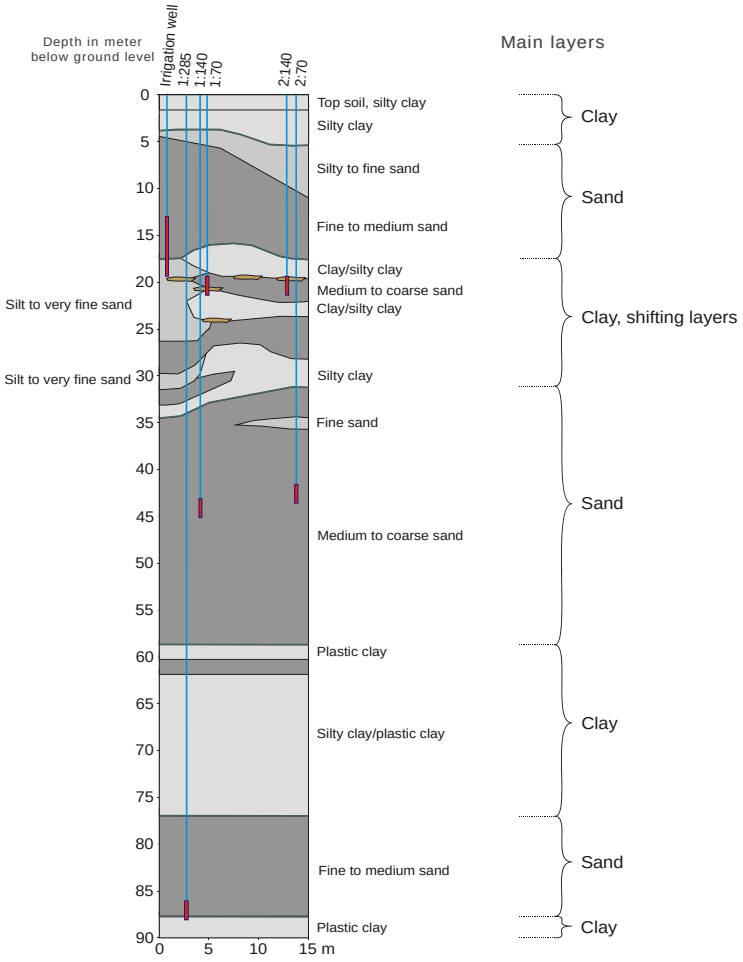

Figure 17. Litholog based on sediment samples recovered during the installation of the piezometers.

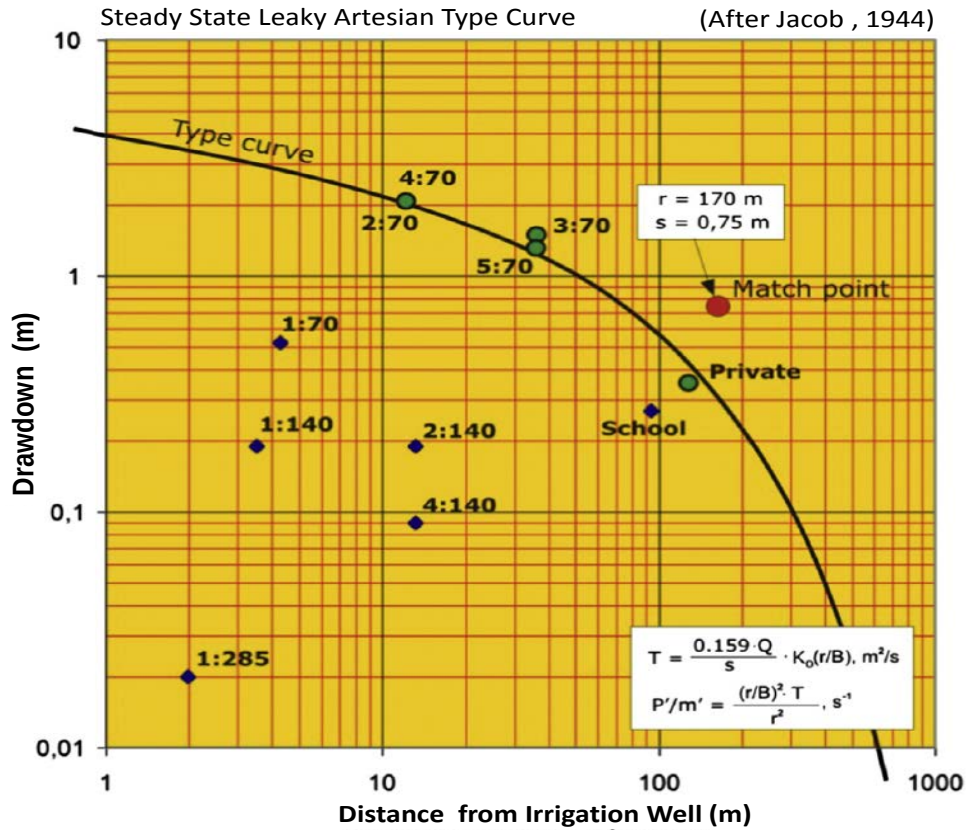

Figure 18. Maximum drawdown during the pumping test versus the distance from the pumped wells plotted in log–log scale. The match point has been chosen so that $K_o(r/B)=1$ and r/B is 1.

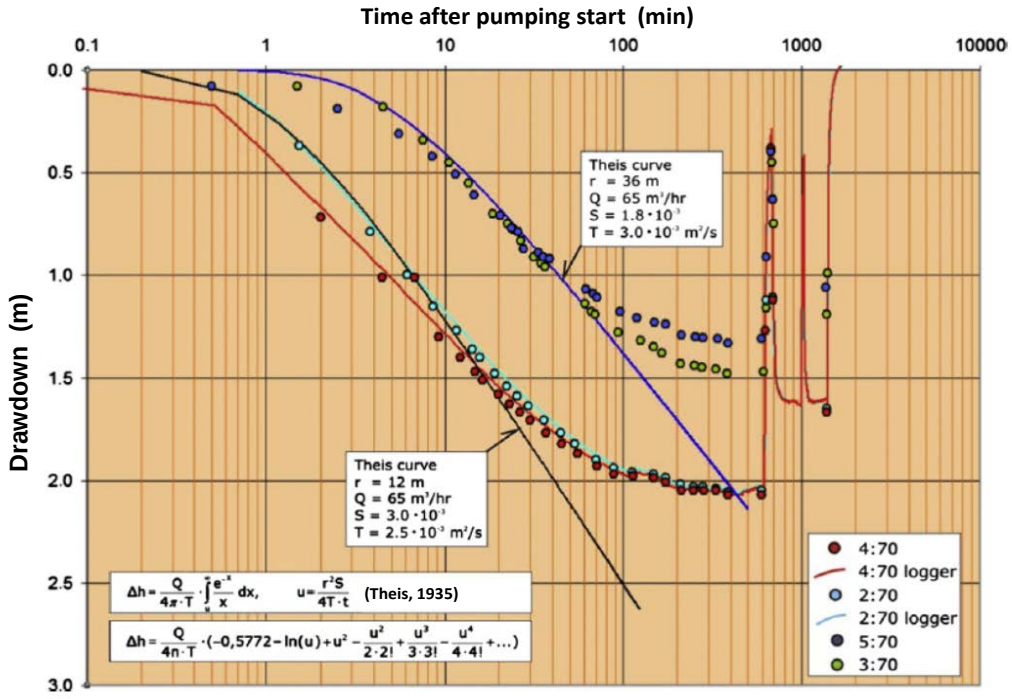

Figure.19. Semi-log plot and interpretation of drawdown versus time for the piezometers 4:70, 2:70, 5:70 and 3:70 screened at the depth 21 m (70 ft) below ground level. Piezometer 4:70 and 2:70 are located at the same distance, 12 m, from the pumping well and piezometer 3:70 and 5:70 both located 36 m from the pumping well.

Table 6. Estimated transmissivity, T, and storage coefficient, S, based on semi-log plot.

Piezometer	T 10^{-3} m^2/s	S (10^{-4})
2:70	***2.5***	***30***
3:70	***3.0***	***18***
4:70	***2.5***	***30***
5:70	***3.0***	***18***

The drawdown observed in the piezometers 2:70, 3:70, 4:70 and 5:70, and the private wells (NABO 1 and NABO 2) indicated responses similar to the pumping well and relatively homogenous hydrostratigraphic unit. The transmissivity (T) and the leakage coefficient (P´/m´) are estimated as 3.8 x 10^{-3} m^2/s and 1.3 x 10^{-7} 1/s, respectively. Based on drillings at the site, it can be assumed that the thickness of the aquifer is approximately 20 m, and that it is separated from the reservoir at 42 m depth by a 10 m thick layer with a lower vertical hydraulic conductivity. Based on this assumption, the average horizontal permeability (K_h) of the aquifer is 2 x 10^{-4} m/s and the vertical permeability (K_v) of the layer separating the two aquifer is 1.3 x 10^{-6} m/s.

The evaluation of the results focuses primarily on the drawdowns measured in the piezometers 2:70, 3:70, 4:70 and 5:70. Semi log plots and interpretations of drawdown versus time for the piezometers 2:70, 3:70, 4:70 and 5:70 are presented in **Figure 18** and the calculated hydraulic parameters are listed in Table 6 and the corresponding log–log plots are shown in **Figure 19**.

6.1.5. Groundwater flow modelling

6.1.6.1. Regional groundwater model

A generic three-dimensional finite-difference groundwater model MODFLOW (Visual Modflow v. 4.1) was used to study the aquifer system. Both regional steady state models and transient flow models covering the eastern part of Bangladesh, from the Tripura Hills to the river Meghna, were developed. Models were realized for natural/undisturbed conditions, i.e. no groundwater abstraction from wells, as well as for the present conditions with high groundwater abstraction for irrigation purposes. The regional transient models were calibrated to match monitored groundwater level fluctuations, while the steady state models were calibrated to match groundwater ages based on ^{14}C dating (von Brömssen 2012, von Brömssen et al. 2014).

6.1.6.2 Model area and boundary conditions

The modelled area extends from the Bay of Bengal in the south to the low-lying bils and haors of the Sylhet region in the north, and from the Meghna River in the west to the Tripura Tertiary Hills in the east. The model setting consists of 138 rows, 93 columns and 20 layers to a depth of 1000 m. The lower boundary was assumed to be flat, due to lack of available data. However, groundwater flow interactions at depth were assumed to be negligible. All 601 irrigation wells that were identified at Matlab were introduced into the models as specific well points. One irrigation well per km^2, matching the average distribution and abstraction rate found in Matlab, was introduced for the area outside Matlab into the model. The boundary conditions have been set based on the criteria given in Table 7. Boundaries were set beyond the maximum propagation of pumping in Matlab. At north and east there were no-flow boundaries, in the south sea-level represented constant head boundary, and in the west constant head was also applied, corresponding to the levels in Meghna and Gumti rivers. The surface water level data (**Figure 20**) from stations of Meghna around the study area, obtained from Bangladesh Water Development Board (BWDB) were used in the model.

6.1.6.3. Parameterisation

In order to idealise and simplify the complexity of the aquifer system, the system was assumed to be anisotropic with horizontal hydraulic conductivity higher

Table 7. Boundary conditions of the regional model outer limits.

Boundary	Boundary condition	Selection criteria
South	Constant head at sea-level.	It is assumed that Bay of Bengal is a hydraulic boundary with a constant head at 0 m.a.s.l.
East	No-flow boundary	Tripura Hills is a watershed towards east.
West	Constant head at Meghna surface to appr. 140 m b.s.l. at Matlab with greater depth towards south and lesser towards north. R. Gumti, surrounding parts of Matlab is included as constant head down to 16 m b.s.l. Constant heads has been varied according to surface level measurements.	It is assumed that the great river Meghna and the lesser river Gumti is a hydraulic boundary.
North	No-flow boundary	The groundwater flow is assumed to follow the northern boundary in east-west direction and thus little flow would cross the northern boundary.
Lower	No-flow	At 1000 m depth groundwater flow would be small.
Upper	Drain at 0.1 m below surface. Recharge	As excess water reaches the surface it is removed from the model simulating surface overflow. For the transient model recharge was calculated as P-ET (≥ 0) and applied on a monthly basis following data presented in Figure 1.
Irrigation wells	Pumping wells	It was assumed that irrigation stand for most of the groundwater abstraction and thus only the surveyed irrigation wells were included in the model.

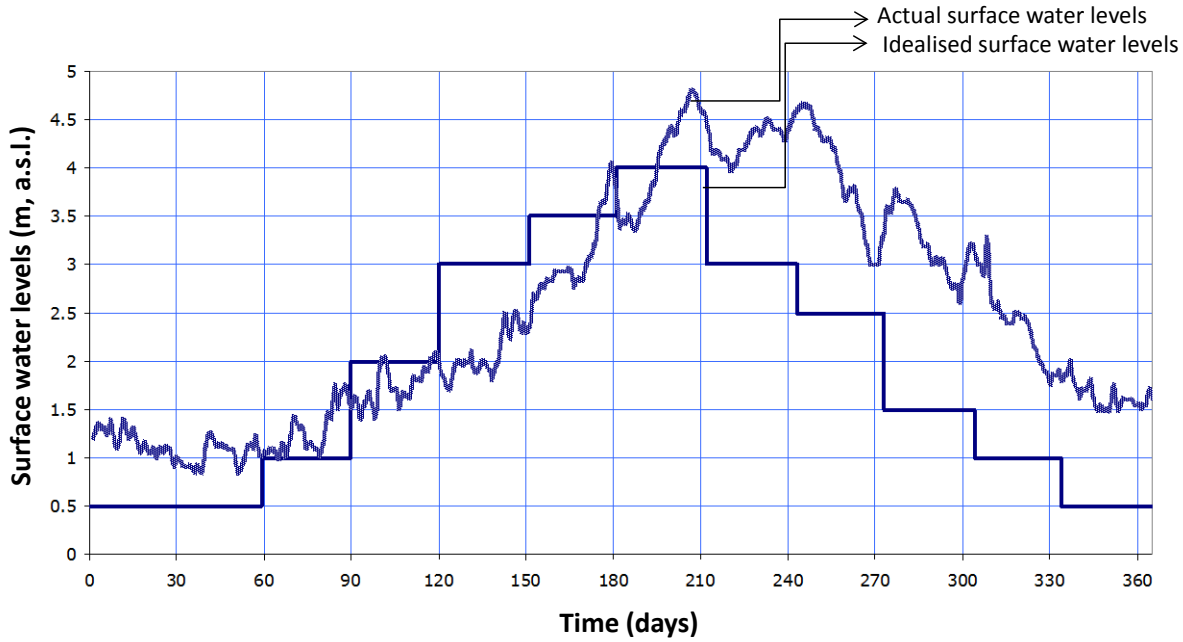

Figure 20. Idealized surface water levels (m) introduced as constant head in the model and actual surface water levels at Matlab (Meghna) for 2005.

than vertical conductivity. This assumption is reasonable considering the sediment characteristics of the Bengal basin comprising fining upward cycles of sediments in these settings (Michael and Voss 2008). Two major approaches with subsequent modifications were used: i) *an anisotropic model* assuming homogeneous conditions from surface level down to the bottom of the modelling domain (1000 m

Table 8. Input data for parameter estimation (PEST) module.

Parameter	Initial value	Min	Max
Horizontal hydraulic conductivity (K_x)	10^{-4} m/s	10^{-5} m/s	10^{-3} m/s
Horizontal hydraulic conductivity (K_x)	10^{-4} m/s	10^{-5} m/s	10^{-3} m/s
Vertical hydraulic conductivity (K_z)	10^{-7} m/s	10^{-8} m/s	10^{-5} m/s
Specific storage (S_s)	10^{-5} 1/m	10^{-6} 1/m	10^{-3} 1/m
Specific yield (S_y)	0.2	0.05	0.2

b.s.l.) where vertical hydraulic conductivity (K_v)<<horizontal hydraulic conductivity (K_h), and ii) *an anisotropic model* including generic aquitards identified through exploratory drillings and aquifer delineation as well as a third aquitard identified and described by DPHE/DFID/JICA (2006).

The hydraulic properties varied for both modelling approaches (i.e. anisotropic homogeneous and generic aquifer/aquitard model). The variations of the properties of the model for the Holocene and Pleistocene aquifers of Bangladesh were based on results based on the:

- present pumping test data,
- data from the steady-state regional modelling of the Bengal Basin (Michael and Voss 2009a,b), and
- aquifer parameter data (BGS and DPHE, 2001)

The horizontal and vertical hydraulic conductivity values were varied between 10^{-3} and 10^{-6} m/s and 10^{-6} and 10^{-9} m/s respectively. The hydraulic conductivity of the aquitard, included in the models, was varied between 10^{-9} and 10^{-7} m/s. The storage properties were varied for the calibration of the transient models only. The specific yield (S_y) was varied between 0.1 and 0.2. The total porosity (n) was set to 0.3 and the effective porosity (n_e) was varied between 0.15 and 0.3. A reasonable storativity (S) of approximately 10^{-4}–10^{-3} (BGS and DPHE, 2001) results in specific storage (Ss) for the aquifers varying from 10^{-4} to10^{-6} 1/m, as S = b x S_s, depending on the thickness of aquifer (*b*).

For the transient model, the recharge was calculated as the difference between the rainfall and evapotranspiration (ET). During the dry period from November to April, no rain was applied in the model and the applied recharge varied from 0 mm/month to a maximum 300 mm/month (in July). For the steady state model the recharge was set to 700 mm/yr.

6.1.6.4. Calibration

The steady state model was calibrated to match the interpreted groundwater ^{14}C ages using the MODPATH backtracking flow module. The procedure, as described by Michael and Voss (2008) was applied. The transient models were calibrated to match the measured hydraulic head fluctuations in the installed piezometer nests. The transient model was then realized for five years to generate a stable model. In cases, when the model was not stabilized within five years, it was executed again, using input from the previous run. The amplitude and timing of groundwater levels fluctuations could be calibrated fairly well with a generic approach, i.e. the model could simulate the behaviour of the system, and the amplitudes of the hydraulic heads in simulations correlated with measured hydraulic heads. However, as local hydrogeological properties could not be reproduced exactly in the model, a correlation between specific piezometer nests was difficult to achieve.

6.1.6.5 Simulation of pumping test with a groundwater model

Visual Modflow Pro (version 4.1) was used for simulating the pumping test. Only saturated flow was simulated. The model was set up for transient conditions

describing the pumping test. An area of 1000 x 1000 m surrounding the pumping well was modelled to simulate the pumping test and the base of the modelling domain was set to 250 m below the ground surface. The flow domain was discretized into 35 rows, 42 columns and 17 layers.

It was assumed that the system is homogeneous and anisotropic with a higher horizontal hydraulic conductivity than that of the vertical hydraulic conductivity except, for the upper most layer, which was assumed to be silty clay with a low hydraulic conductivity ($K = 10^{-8}$ m/s). The initial heads were set to 2 m b.g.l (-2 m), using only relative levels and drawdowns obtained in the modelling. No recharge was applied to the groundwater model, since the model only describes the situation during the pumping test. Constant heads or no-flow boundaries were used as boundary conditions for the exterior boundary of the modelled domain and no flow boundary conditions were applied to the bottom boundary.

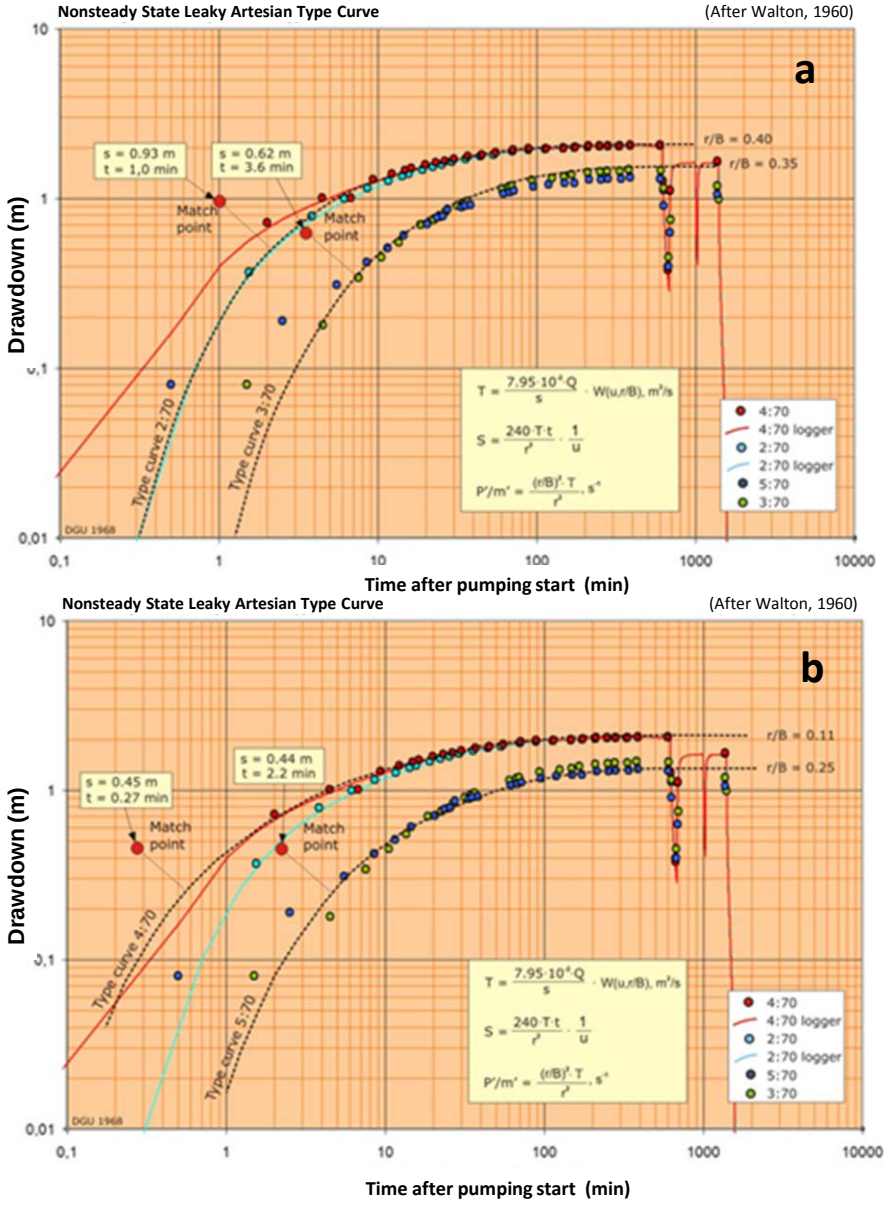

Figure 21. Log–log plot and interpretation of drawdown versus time for the piezometers 2:70 and 3:70 screened at the depth of 20 m (70 ft) below ground level and located on a an east–west line.

General aquifer properties for the shallow aquifers in the flood plains of the Bengal Basin given by BGS and DPHE (2001) were used as initial values for the calibration. The model was calibrated to match the measured drawdown in the piezometers during the pumping test. The parameter estimation module (PEST) was used to calibrate the model (von Brömssen et al. 2014).

The data used for the optimisation and the calibrated values of hydraulic conductivities of the aquifer match the previous studies results, i.e. the hydraulic conductivities are within the same order of magnitude (Table 8). The PEST module used to calibrate the model also revealed acceptable results (Table 6), except for piezometer 1:70 that appears to be installed in silty and clayey sediments and/or was not working properly as it does not response accordingly. Measured and simulated drawdowns for selected piezometers are shown in **Figure 21**.

A number of pumping tests would have been ideally performed to ascertain the representativity of the pumping test for Matlab, however the results correlates with literature findings (BGS and DPHE 2001) The test however amply demonstrates the distinct hydraulic properties in terms of horizontal and vertical conductivity for the aquifer system (see Table 6).

6.1.6. Groundwater flow models

6.1.7.1. Steady state flow model

In order to reproduce regional groundwater flow pattern, hydraulic conductivity (K_h and K_v) were varied during modelling. Backward particle tracking was used for the calibration of the groundwater travel times versus estimated groundwater ages (Table 9). Particles were released from the study area at depth corresponding to the corrected ^{14}C groundwater dating, representing the boundary between different flow systems (Michael and Voss 2008).

Groundwater age estimates through anisotropic homogeneous modelling approach were younger than the ^{14}C dating, of groundwater in the aquifer depths up to 75 m for all models. Using a ratio K_h/K_v > 1000 in the model, for depths of 200 m and beyond, the simulated groundwater ages were found to be unreasonably old (>50 k yr) and thus did not comply with the ages estimated by Aggarwal et al. (2000) and Hoque (2010). This also assumes that the groundwater travelling distances needs to be considerably long, all the way to the eastern boundary of the model as well as the prevalence of a long regional flow system at very shallow depth, i.e. 30 m and below.

Based on the aquifer delineation, a four layer model was also developed. This modelling approach improved the calibration of estimated groundwater ages. The accuracy of the model improved, when aquitards with hydraulic conductivity ranges 10^{-8} – 10^{-9} m/s were considered. **Figure 22** illustrates the differences in regional groundwater flow patterns between the homogeneous anisotropic model and the four layer aquifer/aquitard model.

The sensitivity of the model to hydraulic properties of shallower domain as well as low hydraulic conductivity of the Tertiary Hill terrain was tested and evaluated. Simulated groundwater ages at Matlab were not sensitive to these changes and the calibration did not change. The groundwater simulations clearly identified two flow-systems, a regional horizontal flow system with recharge areas at the Tripura Hills and local flow systems driven by local topography. The local flow systems reach a depth of approximately 30 m b.g.l. in Matlab, based on the calibrated steady state modelling results.

In Matlab, very few deep (>100m) irrigation- and production wells are installed and the vertical gradient observed in most piezometer nests out of the irrigation period is likely to reflect natural groundwater flow conditions. The vertical hydraulic gradient of 0.01 based on the observed field measurements is also consistent with the models developed for the study area.

The local recharge zones result in elevated hydraulic heads compared to the heads of the regional flow. Even though

Table 9. Model types, hydraulic conductivity (K_h and K_v) and simulated groundwater ages used for developing groundwater steady state models.

Model	Type	Aquifer K_h (m/s)	K_v (m/s)	Aquitard K (m/s)	Hills K[1] (m/s)	Simulated groundwater ages
A	Anisotropic homogeneous	10^{-4}	10^{-6}	-	-	Young
B	Anisotropic homogeneous	10^{-4}	$5x10^{-7}$	-	-	Young
C	Anisotropic homogeneous	10^{-4}	10^{-7}	-	-	Young
D	Anisotropic homogeneous	10^{-4}	$2x10^{-8}$	-	-	Young down to 100 m depth
E	Anisotropic homogeneous	10^{-4}	10^{-9}	-	-	Reasonable, old at depth
F	Anisotropic homogeneous	$5x10^{-5}$	10^{-6}	-	-	Young
G	Anisotropic homogeneous	$5x10^{-5}$	$5x10^{-7}$	-	-	Young
H	Anisotropic homogeneous	$5x10^{-5}$	10^{-7}	-	-	Young, gives unreasonable (>50 kyr) old GW in neighbouring areas
I	Anisotropic homogeneous	$5x10^{-5}$	$2x10^{-8}$	-	-	Young, gives unreasonable (>50 kyr) old GW in neighbouring areas
J	Anisotropic homogeneous	$5x10^{-5}$	10^{-9}	-	-	Could not be calibrated well
K	4 aquifer/aquitard model	10^{-4}	10^{-5}	10^{-9}	-	Ok
L	4 aquifer/aquitard model	10^{-4}	10^{-6}	10^{-8}	-	Young down to 100 m depth
M	4 aquifer/aquitard model	10^{-4}	10^{-6}	$5x10^{-9}$	-	Young down to 100 m depth
N	4 aquifer/aquitard model	$5x10^{-5}$	10^{-6}	$5x10^{-9}$	-	Young down to 100 m depth although reasonable ages
O[1)]	4 aquifer/aquitard model	10^{-4}	10^{-5}	10^{-9}	10^{-8}	Ok
P[1)]	4 aquifer/aquitard model	10^{-4}	10^{-6}	10^{-8}	10^{-8}	Young although simulated groundwater ages are reasonable
Q[1)]	4 aquifer/aquitard model	10^{-4}	10^{-6}	$5x10^{-9}$	10^{-8}	Young although simulated groundwater ages are reasonable
R[1)]	4 aquifer/aquitard model	$5x10^{-5}$	10^{-6}	$5x10^{-9}$	10^{-8}	Young although simulated groundwater ages are reasonable
S[1)]	4 aquifer/aquitard model	10^{-4}	10^{-6}	10^{-8}	10^{-8}	Young although simulated groundwater ages are reasonable
T[1)]	4 aquifer/aquitard model	10^{-4}	$5x10^{-7}$	10^{-8}	10^{-8}	Young although simulated groundwater ages are reasonable
U[1)]	4 aquifer/aquitard model	10^{-4}	10^{-7}	10^{-8}	10^{-8}	Young although simulated groundwater ages are reasonable
V[1)]	4 aquifer/aquitard model	10^{-4}	$2x10^{-8}$	10^{-8}	10^{-8}	Young although simulated groundwater ages are reasonable

[1] Lower hydraulic conductivity applied for hilly areas.

the vertical gradient is present in Matlab, cross-contamination is likely to be limited (von Brömssen et al. 2007, 2008) or restricted to certain areas with many irrigation wells and the absence of aquitards. Introducing groundwater abstraction (pumping wells) into the model substantially changes the local flow patterns, especially around the irrigation pumping well clusters.

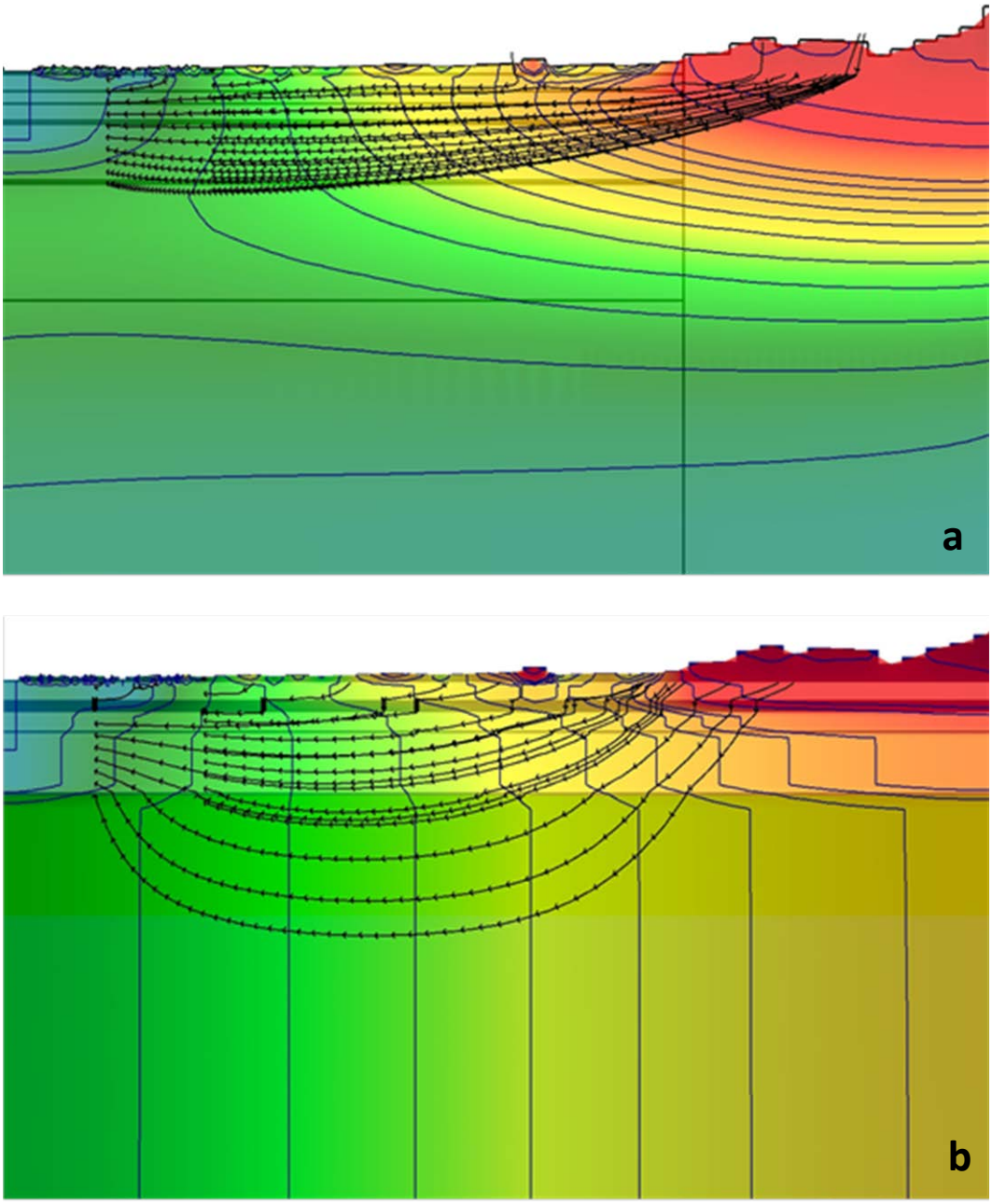

Figure 22. a) Cross-section of the homogeneous anisotropic model; and b) Cross-section of the 4 aquifer/aquitard model. Cross-sections are from west to east across the study area. Time marks of the backward particle tracking are set to 1000 yr. Blue lines indicate the piezometric heads.

6.1.7.2. Transient flow model

The transient flow model was calibrated to match observed behaviour of the hydrographs presented earlier in **Figure 14**. The present study did not allow calibration of measured hydraulic heads from all piezometers with simulated heads in one single model because of the lack of specific hydrogeological information. The transient model was updated continuously and new conceptual models were developed based on the two steady state flow models.

Altogether 51 scenarios were run using the using the following four major conceptual model approaches (Table 10). These were grouped as:

Table 10. Transient flow models conceptualized on the basis of different considerations

		Aquifer 1			Aquifer 2			Aquifer 3			Aquifer 4			Aquitard			Topsoil (if not aquitard)		
File	Type	Kh	Kv	Ss	Kh	Kv	Ss	Kh	Kv	Ss	Kh	Kv	Ss	Kh	Kv	Ss	Kh	Kv	Ss
		(m/s)	(m/s)	(1/m)	(m/s)	(m/s)	(1/m)	(m/s)	(m/s)	(1/m)	(m/s)	(m/s)	(1/m)	(m/s)	(m/s)	(1/m)	(m/s)	(m/s)	(1/m)
T_009b	Homogeneous anisotropic	1.E-04	1.E-08	1.E-05	N/A	N/A	N/A	N/A	N/A	N/A	N/A	N/A	N/A	N/A	N/A	N/A	-	-	-
T_009c	Homogeneous anisotropic	1.E-04	1.E-06	1.E-05	N/A	N/A	N/A	N/A	N/A	N/A	N/A	N/A	N/A	N/A	N/A	N/A	-	-	-
T_009h	Homogeneous anisotropic	1.E-04	1.E-07	1.E-05	N/A	N/A	N/A	N/A	N/A	N/A	N/A	N/A	N/A	N/A	N/A	N/A	-	-	-
T_010c	Homogeneous anisotropic	1.E-04	1.E-08	1.E-04	N/A	N/A	N/A	N/A	N/A	N/A	N/A	N/A	N/A	N/A	N/A	N/A	-	-	-
T_010d	Homogeneous anisotropic	1.E-04	1.E-07	1.E-04	N/A	N/A	N/A	N/A	N/A	N/A	N/A	N/A	N/A	N/A	N/A	N/A	-	-	-
T_012m	Homogeneous anisotropic	1.E-05	1.E-08	1.E-04	-	-	-	-	-	-	-	-	-	-	-	-	-	-	-
T_10e	4 aquifer/aquitard model	1.E-04	1.E-06	1.E-05	1.E-04	1.E-06	1.E-05	1.E-04	1.E-06	1.E-05	1.E-04	1.E-06	1.E-05	2.E-08	2.E-08	1.E-05	-	-	-
T_10f	4 aquifer/aquitard model	1.E-04	1.E-06	1.E-05	1.E-05	1.E-06	1.E-05	1.E-05	1.E-06	1.E-05	1.E-05	1.E-06	1.E-05	2.E-08	2.E-08	1.E-05	-	-	-
T_10g	4 aquifer/aquitard model	1.E-04	1.E-06	1.E-03	1.E-04	1.E-06	1.E-04	1.E-04	1.E-06	1.E-04	1.E-04	1.E-06	1.E-04	2.E-08	2.E-08	1.E-04	-	-	-
T_012b	4 aquifer/aquitard model	1.E-04	1.E-06	1.E-03	1.E-04	1.E-06	1.E-03	1.E-04	1.E-06	1.E-03	1.E-04	1.E-06	1.E-05	1.E-08	1.E-08	1.E-03	-	-	-
T_012c	4 aquifer/aquitard model	1.E-04	1.E-06	1.E-03	1.E-04	1.E-06	1.E-03	1.E-04	1.E-06	1.E-03	1.E-04	1.E-06	1.E-03	1.E-08	1.E-08	1.E-03	-	-	-
T_012d	4 aquifer/aquitard model	1.E-04	1.E-06	1.E-05	1.E-04	1.E-06	1.E-05	1.E-04	1.E-06	1.E-05	1.E-05	1.E-08	1.E-05	1.E-08	1.E-08	1.E-05	-	-	-
T_012e	4 aquifer/aquitard model	1.E-04	1.E-06	1.E-05	1.E-04	1.E-06	1.E-05	1.E-04	1.E-06	1.E-05	1.E-05	1.E-06	1.E-05	1.E-08	1.E-08	1.E-05	-	-	-
T_012q	4 aquifer/aquitard model	5.E-05	1.E-06	1.E-05	5.E-05	1.E-06	1.E-05	5.E-05	1.E-06	1.E-05	1.E-05	1.E-08	1.E-05	5.E-08	5.E-08	1.E-05	-	-	-
T_010i	4 aquifer/aquitard model	1.E-04	1.E-05	1.E-04	1.E-04	1.E-05	1.E-04	1.E-04	1.E-05	1.E-04	1.E-04	1.E-05	1.E-05	1.E-09	1.E-09	1.E-05	-	-	-
T_10h	4 aquifer/aquitard model no Meghna	1.E-04	1.E-06	1.E-04	1.E-04	1.E-06	1.E-04	1.E-04	1.E-06	1.E-05	1.E-04	1.E-06	1.E-05	2.E-08	2.E-08	1.E-04	-	-	-
T_012f	2 layer model (1+2;3+4)	1.E-04	1.E-06	1.E-04	1.E-04	1.E-06	1.E-04	-	-	-	1.E-05	1.E-08	1.E-04	1.E-04	1.E-06	1.E-04	-	-	-
T_012h	2 layer model (1+2;3+4)	1.E-04	1.E-06	1.E-04	1.E-04	1.E-06	1.E-04	-	-	-	1.E-05	1.E-08	1.E-04	1.E-04	1.E-06	1.E-04	-	-	-
T_012i	2 layer model (1+2;3+4)	1.E-04	1.E-08	1.E-04	1.E-04	1.E-08	1.E-04	-	-	-	1.E-06	1.E-08	1.E-04	1.E-04	1.E-08	1.E-04	-	-	-
T_012j	2 layer model (1+2;3+4)	1.E-04	1.E-08	1.E-04	1.E-04	1.E-08	1.E-04	-	-	-	1.E-06	1.E-08	1.E-05	1.E-04	1.E-08	1.E-04	-	-	-
T_012k	2 layer model (1+2;3+4)	1.E-05	1.E-08	1.E-04	1.E-05	1.E-08	1.E-04	-	-	-	1.E-06	1.E-08	1.E-05	1.E-05	1.E-08	1.E-04	-	-	-
T_012l	2 layer model (1+2;3+4)	1.E-04	1.E-08	1.E-04	1.E-04	1.E-08	1.E-04	-	-	-	1.E-06	1.E-09	1.E-05	1.E-05	1.E-08	1.E-04	-	-	-
T_012n	2 layer model (1+2;3+4)	1.E-04	1.E-06	1.E-04	1.E-04	1.E-06	1.E-04	-	-	-	1.E-06	1.E-08	1.E-04	1.E-04	1.E-06	1.E-04	-	-	-
T_012o	2 layer model (1+2;3+4)	1.E-05	1.E-07	1.E-04	1.E-05	1.E-07	1.E-04	-	-	-	1.E-06	1.E-08	1.E-05	1.E-05	1.E-07	1.E-04	-	-	-
T_012g	3 aquifer model (1; 2; 3+4)	1.E-04	1.E-08	1.E-04	1.E-04	1.E-08	1.E-04	-	-	-	1.E-04	1.E-06	1.E-04	1.E-04	1.E-08	1.E-04	-	-	-
T_012p	3 aquifer model (1; 2; 3+4)	1.E-04	1.E-05	1.E-04	1.E-04	1.E-05	1.E-04	-	-	-	1.E-04	1.E-05	1.E-05	1.E-09	1.E-09	1.E-04	-	-	-
T_010k	3 aquifer model (1; 2; 3+4)	1.E-04	1.E-06	1.E-04	1.E-04	1.E-06	1.E-04	1.E-05	1.E-05	1.E-05	1.E-05	1.E-05	1.E-05	5.E-09	5.E-09	1.E-04	-	-	-
T_010l	3 aquifer model (1; 2; 3+4)	1.E-04	1.E-06	1.E-04	1.E-04	1.E-06	1.E-04	1.E-05	1.E-05	1.E-05	1.E-05	1.E-05	1.E-05	5.E-09	5.E-09	1.E-04	-	-	-
T_010m	3 aquifer model (1; 2; 3+4)	1.E-04	1.E-06	1.E-04	1.E-04	1.E-06	1.E-04	1.E-05	1.E-05	1.E-05	1.E-05	1.E-05	1.E-05	5.E-09	5.E-09	1.E-04	1.E-07	1.E-07	1.E-04
T_010n	3 aquifer model (1; 2; 3+4)	1.E-04	1.E-06	1.E-04	1.E-04	1.E-06	1.E-04	1.E-05	1.E-05	1.E-05	1.E-05	1.E-05	1.E-05	5.E-09	5.E-09	1.E-04	1.E-08	1.E-08	1.E-04
T_010o	3 aquifer model (1; 2; 3+4)	1.E-04	1.E-06	1.E-04	1.E-04	1.E-06	1.E-04	1.E-05	1.E-06	1.E-05	1.E-05	1.E-06	1.E-05	5.E-09	5.E-09	1.E-04	1.E-08	1.E-08	1.E-04
T_010p	3 aquifer model (1; 2; 3+4)	1.E-04	1.E-06	1.E-04	1.E-06	1.E-06	1.E-05	1.E-06	1.E-06	1.E-05	1.E-06	1.E-06	1.E-05	5.E-09	5.E-09	1.E-04	1.E-08	1.E-08	1.E-04
T_010q	3 aquifer model (1; 2; 3+4)	1.E-04	1.E-06	1.E-04	1.E-06	1.E-06	1.E-05	1.E-06	1.E-06	1.E-05	1.E-06	1.E-06	1.E-05	5.E-09	5.E-09	1.E-04	1.E-08	1.E-08	1.E-04
T_010r	3 aquifer model (1; 2; 3+4)	1.E-04	1.E-06	1.E-04	1.E-06	1.E-06	1.E-06	1.E-06	1.E-06	1.E-06	1.E-06	1.E-06	1.E-06	5.E-09	5.E-09	1.E-04	1.E-08	1.E-08	1.E-06
T_010s	3 aquifer model (1; 2; 3+4)	1.E-05	1.E-05	5.E-05	1.E-05	1.E-05	1.E-05	1.E-05	1.E-05	1.E-05	1.E-05	1.E-05	1.E-05	5.E-09	5.E-09	1.E-04	1.E-08	1.E-08	1.E-05
T_010t	3 aquifer model (1; 2; 3+4)	1.E-04	1.E-06	1.E-04	1.E-06	1.E-06	1.E-05	1.E-06	1.E-06	1.E-05	1.E-06	1.E-06	1.E-05	5.E-09	5.E-09	1.E-04	1.E-08	1.E-08	1.E-04
T_010u	3 aquifer model (1; 2; 3+4)	1.E-04	1.E-06	1.E-04	1.E-06	1.E-06	1.E-05	1.E-06	1.E-06	1.E-05	1.E-06	1.E-06	1.E-05	5.E-09	5.E-09	1.E-04	1.E-08	1.E-08	1.E-04
T_010v	3 aquifer model (1; 2; 3+4)	1.E-05	1.E-05	1.E-04	5.E-04	5.E-04	1.E-05	1.E-04	1.E-04	5.E-06	1.E-04	1.E-04	5.E-06	2.E-08	2.E-08	5.E-06	1.E-07	1.E-07	5.E-06
T_020a	3 aquifer model (1; 2; 3+4)	1.E-05	1.E-05	1.E-04	5.E-04	5.E-04	1.E-05	1.E-04	1.E-04	5.E-06	1.E-04	1.E-04	5.E-06	2.E-08	2.E-08	5.E-06	1.E-07	1.E-07	5.E-06
T_020b	3 aquifer model (1; 2; 3+4)	1.E-05	1.E-05	1.E-04	1.E-04	1.E-04	1.E-05	1.E-04	1.E-04	5.E-06	1.E-04	1.E-04	5.E-06	2.E-08	2.E-08	5.E-06	1.E-05	1.E-05	5.E-06
T_020c	3 aquifer model (1; 2; 3+4)	1.E-04	1.E-06	1.E-04	1.E-04	1.E-04	1.E-05	1.E-04	1.E-04	5.E-06	1.E-04	1.E-04	5.E-06	2.E-08	2.E-08	5.E-06	1.E-07	1.E-07	1.E-04
T_020d	3 aquifer model (1; 2; 3+4)	5.E-04	1.E-06	1.E-04	1.E-04	1.E-04	1.E-05	1.E-04	1.E-04	5.E-06	1.E-04	1.E-04	5.E-06	2.E-08	2.E-08	5.E-06	5.E-04	1.E-06	1.E-04
T_020e	3 aquifer model (1; 2; 3+4)	5.E-04	1.E-06	1.E-04	1.E-06	1.E-06	1.E-05	1.E-04	1.E-04	5.E-06	1.E-04	1.E-04	5.E-06	2.E-08	2.E-08	5.E-06	5.E-04	1.E-06	1.E-04
T_020f	3 aquifer model (1; 2; 3+4)	1.E-04	1.E-06	1.E-04	1.E-05	1.E-05	1.E-05	1.E-05	1.E-05	5.E-06	1.E-05	1.E-05	5.E-06	2.E-08	2.E-08	5.E-06	1.E-04	1.E-06	1.E-04
T_020g	3 aquifer model (1; 2; 3+4)	1.E-04	1.E-06	5.E-05	1.E-05	1.E-07	8.E-06	1.E-05	1.E-05	5.E-06	1.E-05	1.E-05	1.E-06	2.E-08	2.E-08	5.E-06	1.E-07	1.E-07	5.E-05
T_020h	3 aquifer model (1; 2; 3+4)	1.E-04	1.E-06	1.E-04	1.E-05	1.E-07	8.E-06	8.E-06	1.E-05	5.E-06	5.E-06	1.E-05	1.E-06	1.E-07	1.E-07	5.E-06	1.E-07	1.E-07	5.E-05
T_20i	3 aquifer model (1; 2; 3+4)	1.E-04	1.E-06	1.E-04	1.E-05	1.E-07	8.E-06	5.E-06	5.E-07	5.E-06	5.E-06	5.E-07	5.E-06	5.E-08	5.E-08	5.E-06	1.E-07	1.E-07	5.E-05
T_20j	3 aquifer model (1; 2; 3+4)	1.E-04	1.E-06	1.E-04	1.E-06	1.E-07	8.E-06	5.E-06	5.E-07	5.E-06	5.E-06	5.E-07	5.E-06	5.E-08	5.E-08	5.E-06	1.E-07	1.E-07	5.E-05
T_20k	3 aquifer model (1; 2; 3+4)	1.E-04	1.E-06	1.E-04	1.E-06	1.E-07	5.E-06	5.E-06	5.E-07	1.E-06	5.E-06	5.E-07	1.E-06	5.E-08	5.E-08	5.E-06	1.E-07	1.E-07	5.E-05
T_20l	3 aquifer model (1; 2; 3+4)	1.E-04	1.E-06	1.E-04	1.E-06	1.E-08	5.E-05	1.E-05	1.E-06	1.E-05	1.E-05	1.E-06	1.E-05	2.E-08	2.E-08	1.E-05	1.E-06	1.E-06	1.E-04
T_20m	3 aquifer model (1; 2; 3+4)	1.E-04	1.E-06	1.E-04	1.E-06	1.E-08	5.E-05	1.E-05	1.E-06	1.E-06	1.E-05	1.E-06	1.E-06	2.E-08	2.E-08	1.E-05	1.E-06	1.E-06	1.E-04

- homogeneous anisotropic model (the same as for steady state flow model),
- 4 aquifers/aquitard model (the same as for steady state flow model),

- 3 aquifers/aquitard model (in which aquifers 3 and 4 from ii were merged together and treated as one unit). The reason for merging aquifers 3 and 4 was to increase the stress on the deeper aquifer, i.e. piezometers at >200 m depth, to attempt to reproduce field observations that otherwise was difficult to simulate,
- 2 layer model (with no aquitards in between the layers, aquifers 1 and 2 were merged to one unit and aquifers 3 and 4 were merged to another unit. The reason for merging aquifer 3 and 4 was again to increase the stress on the deeper aquifer).

The evaluation criteria used for the calibration of the model and the refining the conceptual models were based on behaviour of hydrographs, in particular:

- Amplitude and seasonal fluctuation of hydraulic heads: The amplitude and the seasonal patterns of the simulated hydraulic heads were compared with the monitoring data. Since a system with three distinct aquifers could be identified through the monitoring programme, special emphasis was laid on understanding the variability of the hydraulic heads with depth of the piezometers .
- Vertical gradient: As a vertical downward gradientwas identified through the monitoring programme, one important evaluation criteria was that the model should reproduce this behaviour
- Pumping effect: Models simulating drawdown due to groundwater abstraction from irrigation wells met the evaluation criteria.
- Aquifer delineation: Hydrographs from the piezometers at varying depths in the 10 nests indicate a multi-aquifer/ layered system was used as an evaluation criterion..

The amplitude and groundwater level fluctuations could be calibrated fairly well, and thus the simulated hydraulic head as modelled correlated in general with measured hydraulic heads (**Figure 23**). However, it was not possible to develop a model that could meet all the criteria for the

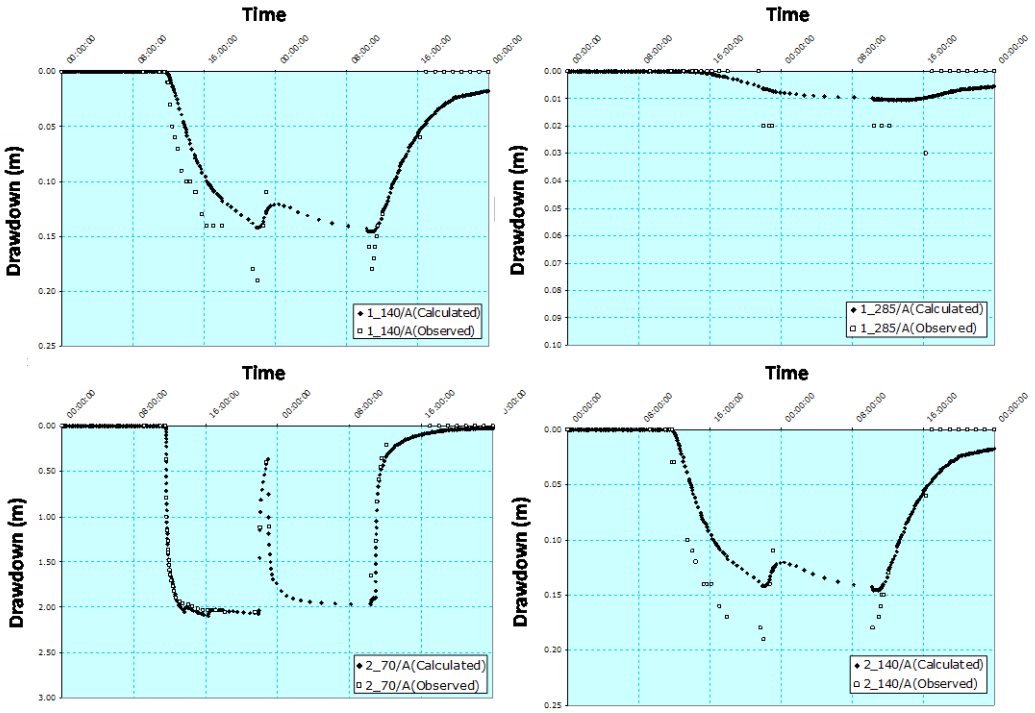

Figure 23. The amplitude and the seasonal patterns of the simulated hydraulic heads in the piezometers compared with the observed data.

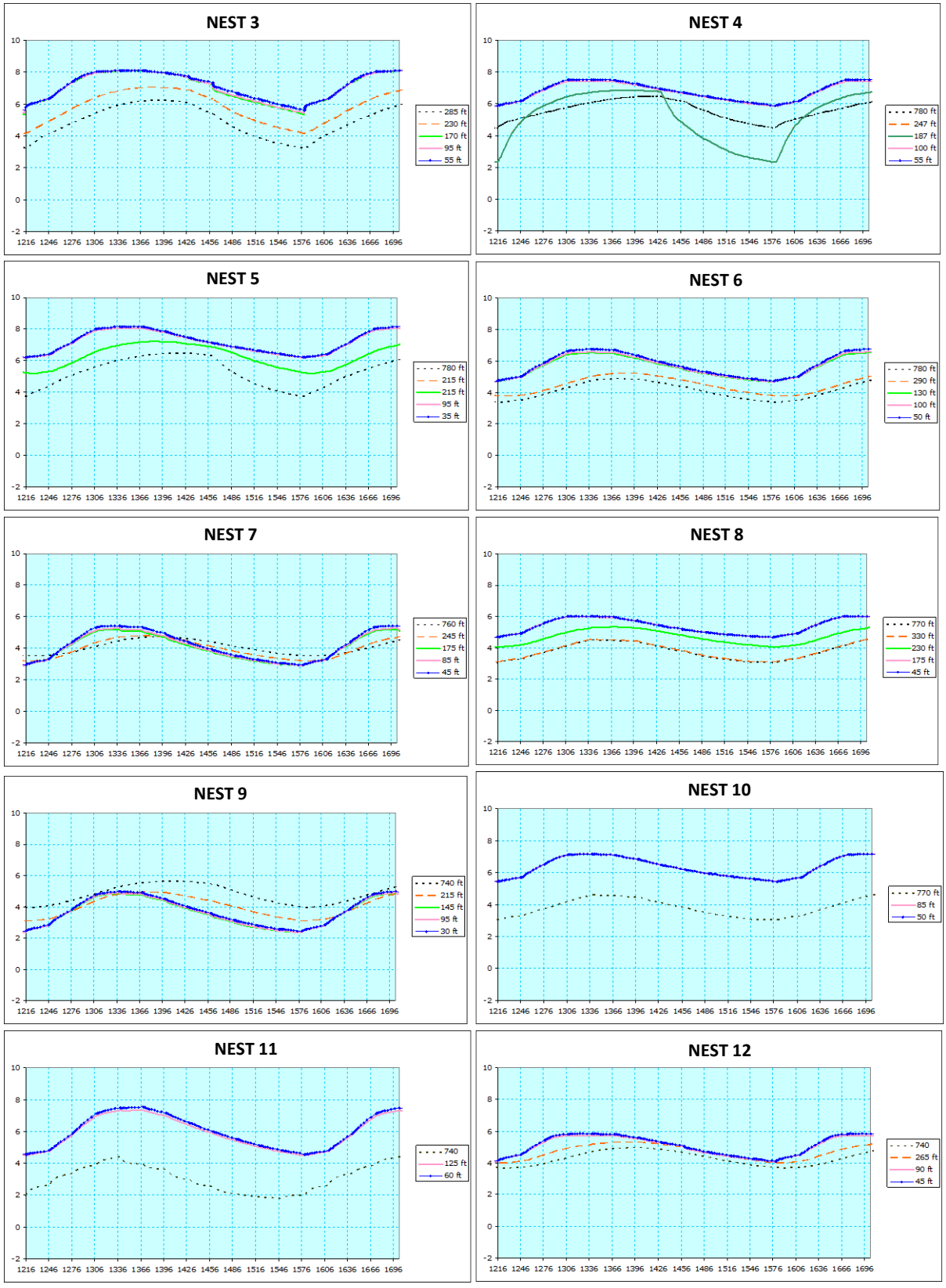

Figure 24. Simulated hydraulic heads of a 3 aquifer/aquitard model

evaluation of entire Matlab study area, and at the same time, to match all hydrographs from each piezometer nests.

6.1.7.3. Homogeneous anisotropic model.

The homogeneous anisotropic model did not meet the evaluation criteria well and this modelling approach could not reproduce the vertical downward gradient identified in the hydrographs. Although the homogeneous anisotropic models with a low (100) K_h/K_v ratio could meet the evaluation criteria for amplitudes at shallow and deep depths, this set-up could not be calibrated for the steady state scenario. Here simulated heads over depth were close at respective locations, as seen in hydrographs, and the vertical gradients were reasonable, however the aquifer delineation could not be observed and pumping effects were absent even though S_s was low (10^{-5} 1/m). When the K_h/K_v ratio increased (1000–10,000) pumping effects could be seen at shallow depths and thus the amplitudes and vertical gradients could not meet the evaluation criteria. The homogeneous anisotropic models could not meet the evaluation criteria of pumping effects on the deep aquifer (at depth of approximately 200 m, piezometer 5). For homogeneous anisotropic models with $S_s = 10^{-4}$ 1/m, deep aquifers head pressure fluctuations were almost absent.

6.1.7.4. 3- and 4-aquifer/aquitard model

The conceptual models with 3 or 4 aquifers separated by aquitards met the evaluation criteria better and could simulate the hydrographs satisfactory, consistent with the findings based on the results of steady state modelling (**Figure 24**). In order to improve the modelling result, the Ss value was decreased at depth in order to simulate the pumping effect in the deep aquifer (aquifer 3 and 4 in the model). Models, where the aquifers 2, 3 and 4, respectively, had an S_s value of 10^{-5} 1/m or even lower simulated the pumping effect better. For the shallow aquifer an S_s value of 10^{-4} 1/m seems reasonable. The three aquifer/aquitard model (merging the aquifers 3 and 4) met the evaluation criteria better.

6.1.7. Suggested model and aquifer characteristics.

The modelling results thus indicated that it was possible to simulate the pumping effect at shallow depth in a satisfactory way, while the abstraction is negligible at depth >200 m b.s.l. where the deep piezometers are installed. The amplitude and pattern of the hydrographs obtained from piezometers installed at depths between 50 or 100 m b.s.l. down to a depth of 200 m b.s.l. coincided with the simulated results.

In order to simulate this, the unit between 100 and 200 m b.s.l. needed to be rather uniform with a very thin or no aquitard included in the model. Thus a 3 aquifer model generally met the evaluation criteria better than a 4 aquifer model. Although it was possible to simulate the impact of groundwater abstraction at all depths, we did not succeed to simulate a drawdown at 200 m depth that coincided with the drawdown observed at 100 m. The pumping effect could be simulated, but in these models the effect was greatest at the depth were most irrigation wells was installed. Hydraulic heads below 0 m a.s.l. were also difficult to simulate with reasonable parametrization. The nests where simulated drawdowns were largest coincided with the areas with high density of irrigation wells (nest 3, 4, 5, 9 and 12), which were also the nests where largest impacts from irrigation abstraction had been observed.

The models that best meet the evaluation criteria results in a high yield 3 (or 4) aquifer/aquitard model are separated by two or three aquitards and decreasing S_s and K with depth (Table 11). The suggested model properties are in good agreement with those of the steady state model.

Table 11. Calibrated parameter values for 3 (or 4) aquifer/aquitard model

Parameter	Calibrated value
Horizontal hydraulic conductivity (K_x)	2.25×10^{-4} m/s
Horizontal hydraulic conductivity (K_x)	10^{-4} m/s
Vertical hydraulic conductivity (K_z)	1.30×10^{-6} m/s
Specific storage (S_s)	7.75×10^{-6} 1/m
Specific yield (S_y)	0.2

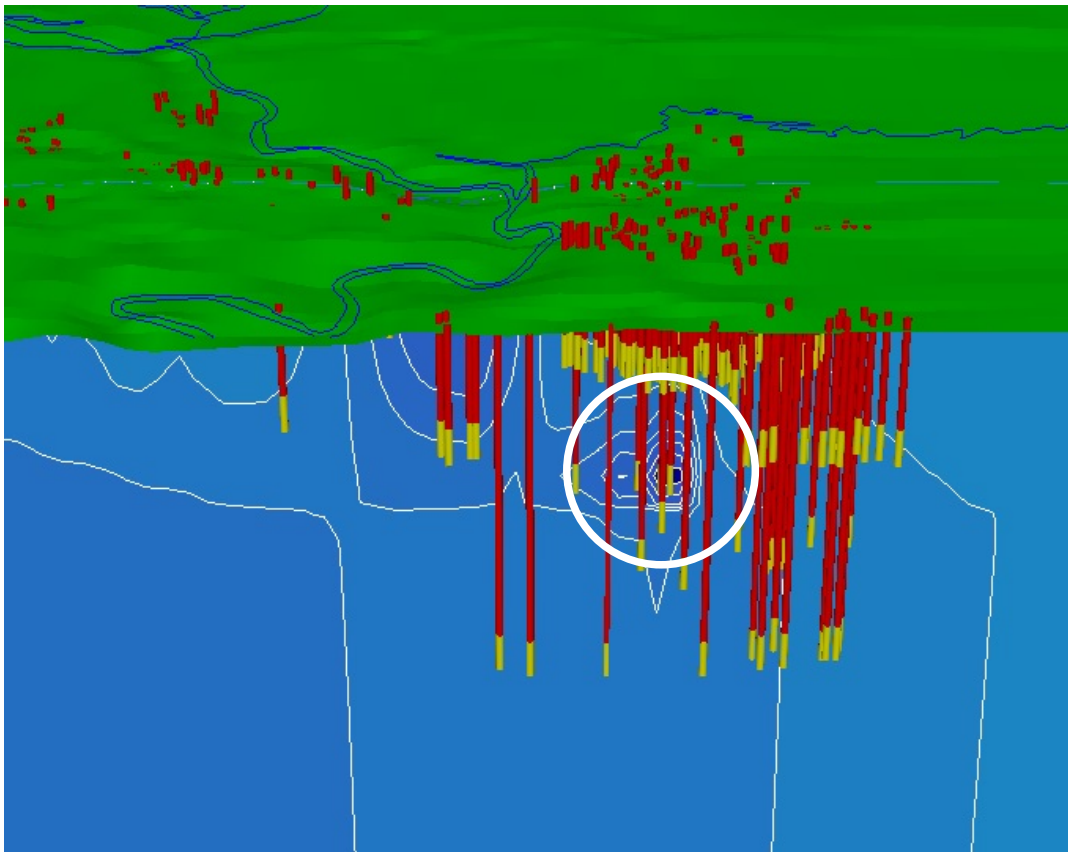

Figure 25. The observed impact of cluster of irrigation wells on hydraulic head distribution for aquifer unit 2. The irrigation wells are indicated as red and yellow staples where the yellow parts represent the abstraction point of the wells. The white circle spots the point of a heavy abstraction due to the cluster of irrigation wells.

The groundwater flow models clearly support the Conceptual Model of the smaller and locally abundant flow-systems driven by local topography for the shallow and to some extent the intermediate aquifer. These local flows-systems are more obvious during the monsoon period, as recharge raises the groundwater levels and thus amplifies the locally developed flow-cells at shallow depths (**Figure 24**).

Flooding of the lowlands gives the system a more regional flow pattern as compared to modelling without flooding. The model used does not take into account the surface water levels and thus results in more distinct local flow-patterns. The resulting vertical hydraulic conductivity would probably be higher than the value used in the models, if flooding were modelled. Deep unidentified aquitards and the lower boundary of the model (set to -1000 m in the model) play an important role, as the specific storage is connected with the thickness of the aquifer. In the model, this is accounted for by varying the S_s value. Typically a thicker model with lower S_s value would behave similarly to a thinner model with proportionally higher Ss value (see **Figure 25 and 26**). Generally a lower S_s value ($<10^{-5}$ 1/m) was, with the exception of the shallow aquifer is needed in order to simulate the amplitudes observed at deep piezometer hydrographs (Table 12).

Table 12. Aquifer properties based on results from the transient flow model.

	Depth m b.g.l.	K_h m/s	K_v m/s	S_s 1/m
Aquifer 1	0-50	$10^{-5} - 10^{-4}$	$10^{-6} - 10^{-4}$	$5\times10^{-4} - 5\times10^{-3}$
Aquifer 2	75-100	$10^{-6} - 10^{-5}$	$10^{-6} - 10^{-5}$	$10^{-5} - 10^{-4}$
Aquifer 3	100->	$10^{-6} - 10^{-5}$	$10^{-6} - 10^{-5}$	$10^{-6} - 5\times10^{-6}$

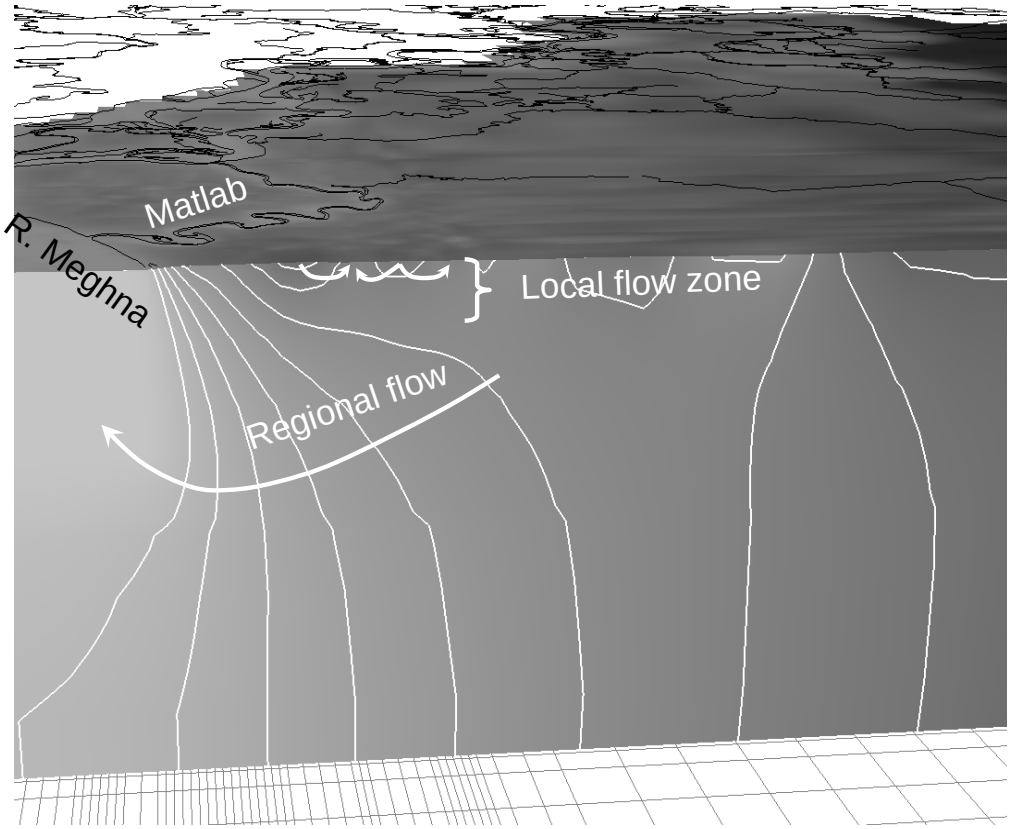

Figure 26. Simulation results illustrating the two flow system in Matlab region.

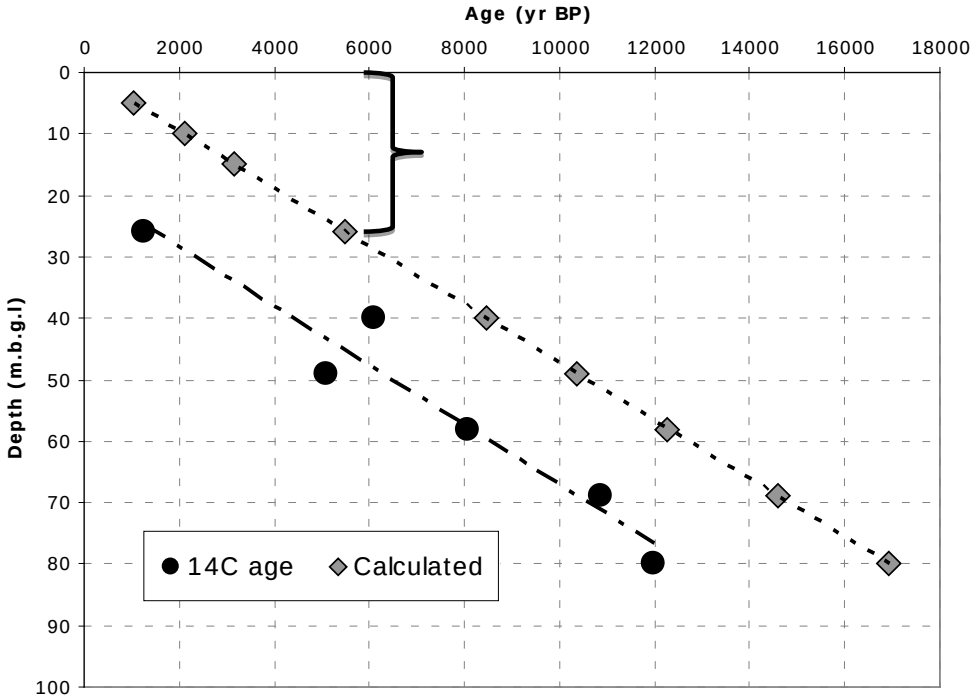

Figure 27. Groundwater ^{14}C age and calculated age based on downward vertical flow assuming a natural vertical gradient (1%) and K_v 1.5 x 10^{-8} m/s.

The fluctuation of the water level in Meghna to some extent controls the results of the simulated hydraulic heads. This was validated by removing the fluctuation of Meghna in some of the models and also through comparison of the amplitudes of

hydraulic heads at depth. In models where the hydrographs at depth were flat, the corresponding field data from deep piezometer in nest 11 showed fluctuating water levels due to its close proximity to Meghna.

6.1.8. Linking the modelling results with groundwater age

The ^{14}C-activity in the groundwater samples varied from 23 to 86 pMC (percent modern carbon), d^{13}C values ranged between -19.6‰ and -13.1‰. The corrected groundwater age is linearly correlated with the depth of tube wells and the groundwater samples were old; ages 1250–11 960 yr indicate restricted groundwater flow at depth below 30 m. The estimated groundwater ages at the depth of 40 m (6100 yr) coincided with the estimated age of sediments at the depth of 36 m in the area (8000 yr; von Brömssen et al. 2008). The groundwater ages also coincide with the findings of Aggarwal et al. (2000) and Hoque (2010) (**Figure 27** and Table 12).

Table 13. ^{14}C-activity and δ^{13}C values for tubewells samples

Tubewell No	Depth m	^{14}C-activity pMC	δ^{13}C ‰	Estimated age yr
54	26	85.89 ± 0.45	-17.6	1 250 ± 65
37	40	47.23 ± 0.30	-17.3	6 100± 65
32	49	53.26 ± 0.34	-13.1	5 095 ± 65
58	58	36.80 ± 0.28	-17.6	8 065 ± 65
63	69	28.98 ± 0.25	-19.6	10 865 ± 80
35	80	22.67 ± 0.23	-12.9	11 960 ± 80

When measured and calculated ages are compared, the measured vertical gradient of 0.01 and the vertical hydraulic conductivity (K_v) of 1.5 x 10^{-8} m/s fit the slope of the ^{14}C-age of groundwater with depth (**Figure 27**). If ^{14}C ages are extrapolated young groundwater would be expected at a depth of approximately 25 m b.g.l., which coincides with the depth of the previously described local flow-systems (Table 13).

6.2. Hydrogeochemical characteristics

6.2.1. On-site field parameters

The physico-chemical parameters of the groundwater samples collected from black, white, off-white, and white group of sediments are presented in Table 14. In general, groundwater temperatures are typically within the range of 25.7 to 29.6°C.

Groundwater pH was essentially circum-neutral ranging from 6.32 to 7.84 (**Figure 28a**). Higher pH values are found in samples derived from black sediments containing higher levels of As. This is because the black sediments representing the most reducing environment where H^+ has consumed through the reduction of iron, manganese, and ammonium. The median values of redox potential (Eh) in groundwater derived from black, white, off-white, and red sediments were 211.5, 227, 268, and 274 mV respectively which indicate that the black group of sediments are most reduced, followed by white, off-white, and red sediments (**Figure 28b**). The electrical conductivity (EC) of all water samples reveals high values regardless of corresponding sediment colors. This is may be due to the presence of high Na^+ and Cl^- in groundwater samples. However, the highest median value of 1630 µS/cm observed in samples screened from red sediments (Table 14, **Figure 28c**).

6.2.2. Major ion characteristics

Salient chemical composition of the groundwater screened at four different color groups of the aquifer sediments is summarized in Table 15.

Sodium (Na^+) and Chloride (Cl^-) ion concentrations of the groundwater samples surpassed all major ion concentrations regardless of the depth of sampling (Table 15). Water samples collected from the red (R) sediments show the highest Na+ (median: ≈355 mg/L) and Cl^- (median: ≈463 mg/L) concentrations, followed by Na^+ and Cl^- concentrations observed in water samples screened from off-white (OW), white (W), and Black (B) sediments (**Figure 29a-b**). Because the red and off-white sediments are mostly targeted for groundwater withdrawal from these sediments along with water level decline might result in changed water circulation pattern and induce saline water to move from the surrounding clay/shale layers to

Table 14. Physico-chemical parameters of the groundwater samples collected from black, white, off-white, and red group of sediments

Physico-chemical parameter	sediment colors	Min[m]	Max[m]	Average	Q25	Q50	Q75
Temperature	Black	25.7	29.5	26.95	26.6	26.8	27.275
(°C)	White	26.2	29.1	27.39	26.85	27.2	27.95
	Off-white	26.2	29.4	27.43	26.925	27.25	27.775
	Red	26.2	29.6	27.30	26.6	27.2	27.7
pH	Black	6.32	7.3	6.91	–	–	–
	White	6.34	7.84	6.77	–	–	–
	Off-white	6.35	7.03	6.61	–	–	–
	Red	6.34	7.35	6.69	–	–	–
Eh	Black	147	339	226.67	196.75	211.5	268.25
(mV)	White	168	280	229.11	199	227	267.5
	Off-white	167	342	255.43	228	268	279.75
	Red	191	322	280.32	259	274	311
Electrical Conductivity	Black	300	5330	1201.73	610	960	1400
(µS/cm)	White	260	4170	1423.33	770	1245	1717.5
	Off-white	460	6190	1374.82	805	1025	1705
	Red	500	3810	1667.06	870	1630	2050

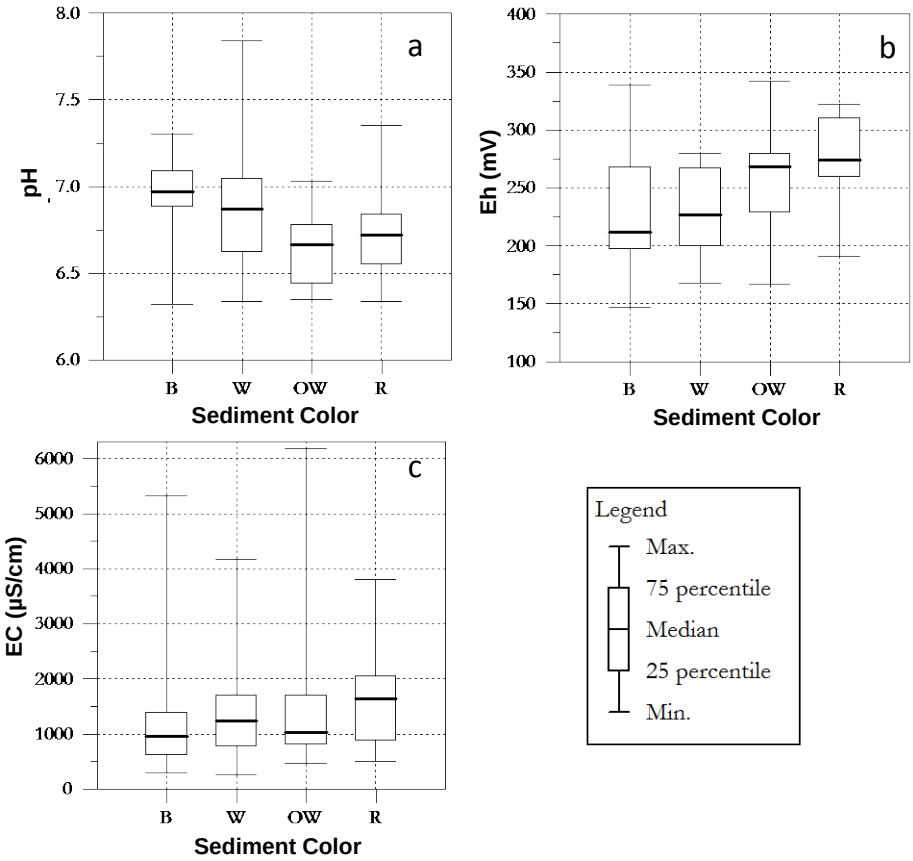

Figure 28. Box and Whiskers plot showing the variability of pH, Eh and SEC in groundwater samples from the fore sediment groups, black (B), white(W), off-white (OW) and red (R).

Table 15 Summary of the major ion composition of groundwater samples with corresponding sediment colors encountered at screen depths

Parameter	Color	Min	Max	Average	Q25	Q50	Q75
As (total)	Black	2.8	968	273	83	252.5	397
(µg/L)	White	8.8	359	68.6	15.2	20.3	51.8
	Off-white	5.0	94	27.2	11.8	17.4	37.9
	Red	2.8	35.5	16.6	12.9	15.1	18.9
Fe (total)	Black	0.22	13.3	5.8	2.86	4.87	8.21
(mg/L)	White	0.11	12.9	3.9	1.86	2.94	5.00
	Off-white	0.07	11.0	3.1	0.21	2.25	3.68
	Red	0.12	14.3	2.1	0.41	0.63	1.79
NH_4^+	Black	0	42.7	5.69	1.55	3.47	6.14
(mg/L)	White	0	8.6	1.86	0.06	0.37	1.94
	Off-white	0	52.3	2.89	0	0	0.43
	Red	0	2.75	0.45	0	0	0.36
PO_4^{3-}	Black	0.05	4.52	1.54	0.65	1.36	1.99
(mg/L)	White	0.04	2.75	0.65	0.14	0.29	0.68
	Off-white	0.03	6.29	0.60	0.04	0.14	0.46
	Red	0.01	1.20	0.18	0.03	0.04	0.11
Mn^{2+}	Black	0.05	2.92	0.73	0.19	0.54	1.04
(mg/L)	White	0.02	1.30	0.29	0.09	0.19	0.28
	Off-white	0.04	3.16	1.32	0.20	1.12	1.88
	Red	0.04	4.82	1.71	0.74	1.54	2.47
NO_3^-	Black	0.05	2.00	0.23	0.05	0.05	0.28
mg/L	White	0.05	0.52	0.072	0.05	0.05	0.03
	Off-white	0.05	0.41	0.032	0.05	0.05	0.05
	Red	0.05	2.083	0.22	0.05	0.05	0.05
DOC	Black	1.42	23.23	7	4.16	5.81	8.04
mg/L	White	1.28	18.78	4.14	2	2.96	3.68
	Off-white	1.20	25.41	3.82	1.33	1.95	4.32
	Red	1.14	39.11	4.04	1.35	1.71	1.92

the sandy sequences resulting an additional increase in salinity.

Water samples collected from the black sediments contain very high bicarbonate (HCO_3^-) concentrations (median: 424 mg/L) (**Figure 29c**) due to the presence of high organic content in the black sediments (eqn. 2). Water samples screened from white, off-white, and red sediments contain significantly low (almost half of that of black) HCO_3^- concentrations (Table 15). High HCO_3^- concentrations in water samples derived from black sediments can also be attributed to carbonate dissolution. Carbonate (CO_3^{2-}) ions produced from calcite/dolomite dissolution associate with available hydrogen ions (H^+) of the anoxic groundwater system to form HCO_3^- (eqn. 3). High HCO_3^- concentrations in the black sediments can also be attributed to sulfate (SO_4^{2-}) reduction (eqn. 4).

$8FeOOH + CH_3COOH + 14H_2CO_3 \rightarrow 8Fe^{2+} + 16HCO_3^- + 12H_2O$ …… (eqn. 2)

$CaCO_3 \rightarrow Ca^{2+} + CO_3^{2-}$ ……....(eqn. 3)

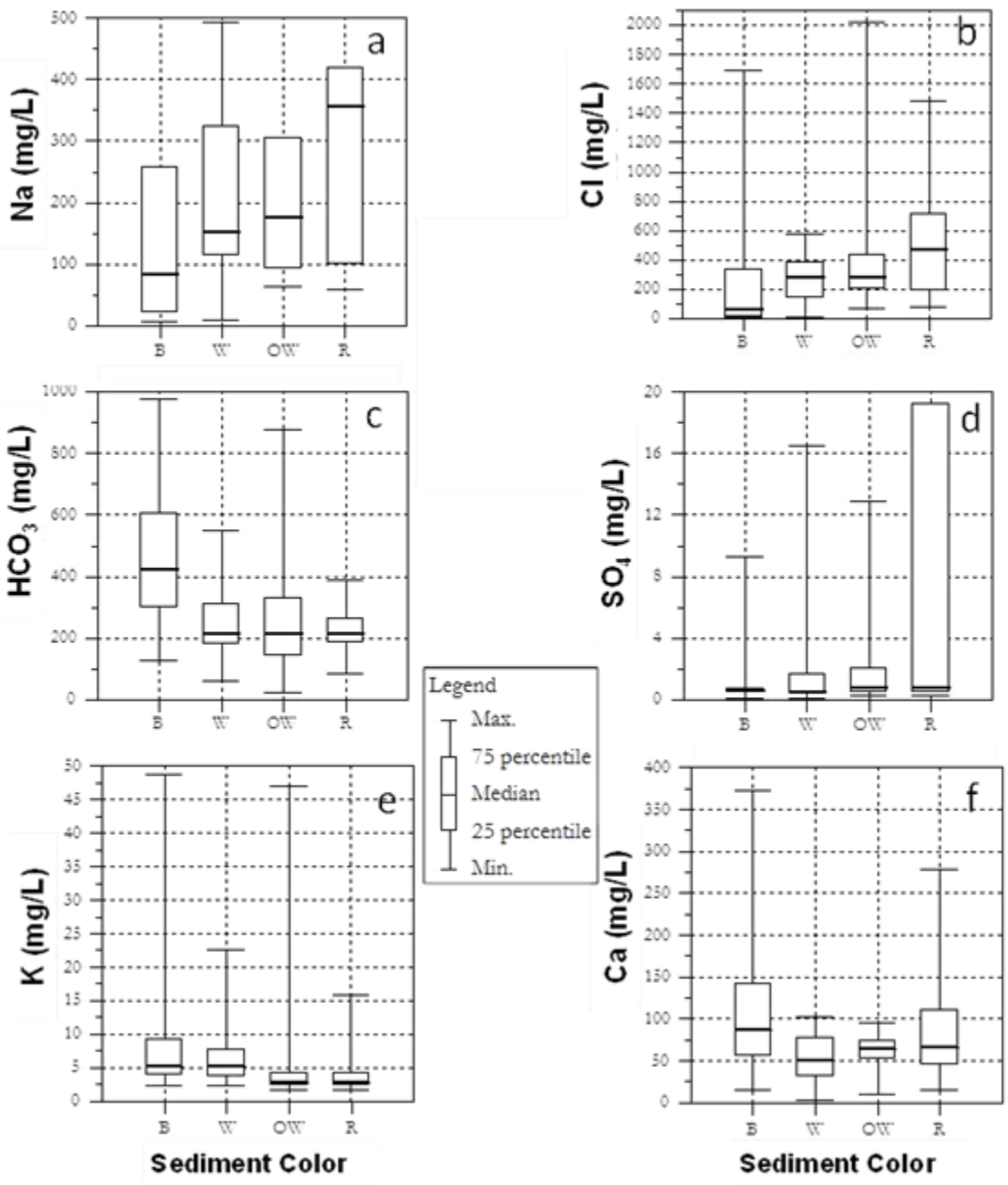

Figure 29. Box and Whiskers plot showing the variability of a) Na^+, b) Cl, c) HCO_3^-, d) SO_4^{2-}, e) K^+, and f) Ca^{2+} in groundwater samples from the four sediment groups, black (B), white(W), off-white (OW) and red (R).

$CH_2O + ½\ SO_4^{2-} \rightarrow ½H_2S + HCO_3^-$ ...(eqn. 4)

In compliance with eqn. 3, comparatively lower levels of SO_4^{2-} can be observed in groundwater samples derived from black and white sediments (median: ≈0.5 mg/L) than that derived from red and off-white sediments with a median value of ≈0.8 mg/L (**Figure 29d**) which validate the existence of a more reducing environment in the black/white sediments than in red/off-white sediments. However, high molar ratio of Cl^-/SO_4^{2-} due to elevated Cl^- concentrations in groundwater also indicates sulfate reduction.

High concentrations (median: 5.26 mg/L; (**Figure 29e**) of potassium (K^+) in the groundwater samples screened from black sediments may be due to the predominance

of clay layers (K-feldspars alters to silica, clay, and K^+ as it interacts with groundwater) within the top 40 to 50 meter of the aquifer sequence. Weathering of biotite can be one of the major sources of not only Fe-oxyhydroxides which play a significant role in the process of As mobilization (Hasan et al. 2009) in the black sediments, but also a source of high K^+ (eqn. 5).

$2KFe_3AlSi_3O_{10}(OH)_2$ (biotite)$+14H^+ + H_2O \rightarrow 2K^+ + 6Fe^{2+} + 4H_4SiO_4^0 + Al_2Si_2O_5(OH)_4$ (kaolinite)……..…(eqn. 5)

Another source of high K^+ in black sediments could be the K^+ assimilated by plants becoming available following the decomposition of plant remains at the end of the growing season (Hem 1985). In the natural recycling that occurs in the croplands at Matlab, this potassium might be leached into the soil by rains during the dormant season or made available by the gradual decay of the organic material. Some leakage of potassium to the shallow ground water could be possible in this way.

Though no significant trend can be observed in Mg^{2+} concentrations (median: ≈25 mg/L) within the groundwater samples collected from the four color-classified sediment groups, Ca^{2+} concentrations in water samples derived from black sediments is significantly higher (median: 87 mg/L) than that in water samples collected from white (median: 49 mg/L), off-white (median: 64 mg/L), or red (median: 66.4 mg/L) sediments (**Figure 29f**). This can be attributed to dissolution of calcite or other carbonate minerals (eqn. 2); which has been identified as one of the sources of high HCO_3^- concentrations in groundwaters abstracted from the black sediments.

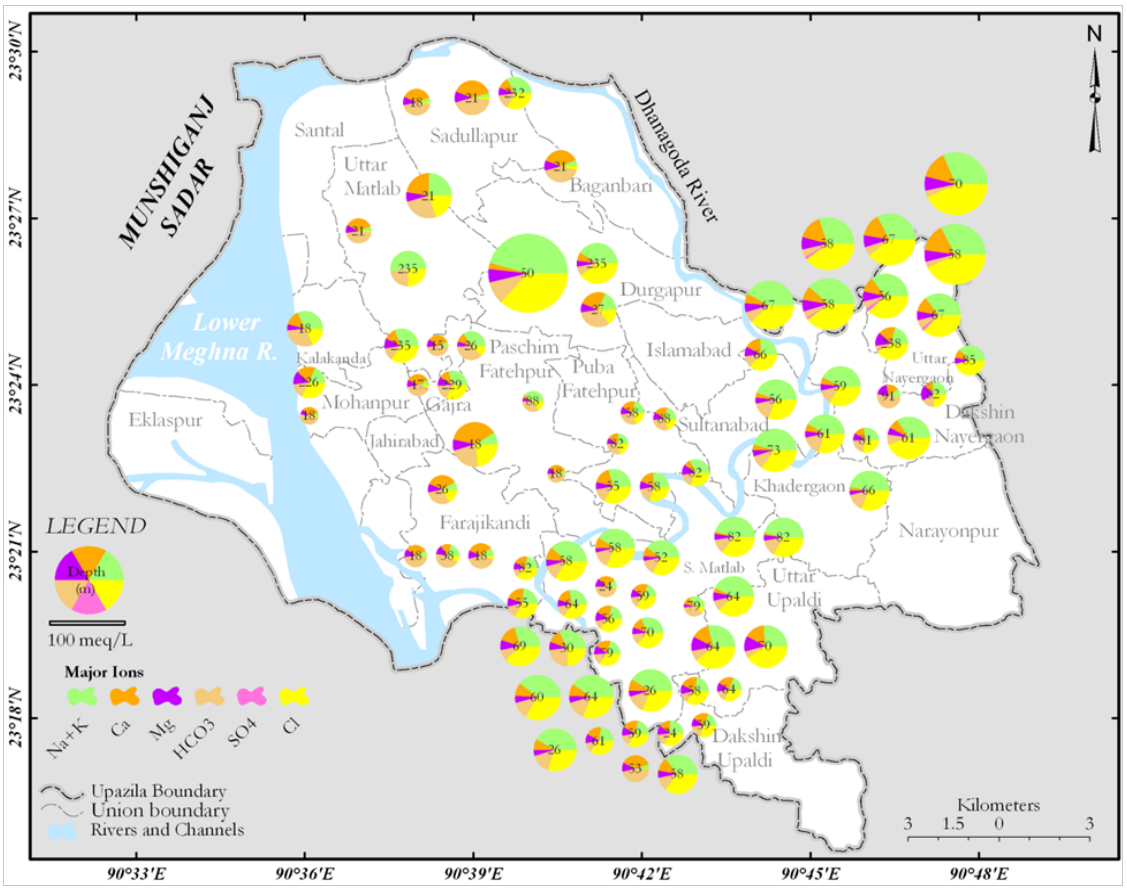

Figure 30. Spatial distribution of major ions in individual groundwater samples collected from the study area represented by circular diagrams. Sampling depth is mentioned at the center of each pie diagram).

The spatial distribution of selected samples within the study area is shown with circular diagrams where sectors within a circle show the fractions of the major ions expressed as milliequivalents per liter (**Figure 30**). Sampling depths are also given in the center of each pie. The maximum and minimum total dissolved ions (TDI) amount to 154.6 and 7.89 meq/L respectively. Comparatively higher TDI has been observed in the southeastern part of the Matlab study area. However, TDI values are not related to depth of sampling.

6.2.3. Hydrochemical facies

The piper tri-linear diagram (**Figure 31a**), indicates that most of the groundwater samples screened from black/white and red/off-white sediments fall in Ca-Mg-HCO_3 or Ca-Na-HCO_3 water-class (zone 1) and in the Na-Ca-Cl or Na-Ca-Cl-HCO_3 or Na-Cl water-type (zone 3 and 5) respectively. However, some of the samples represent Na-HCO_3-Cl facies (zone 6). Thus, mixing of fresh water (Ca-Mg-HCO_3) with saline water (Na-Cl) is more common in the samples collected from red/off-white sediments. The facies assemblage suggests that, at first, ion exchange took place between Mg^{2+} and Na^+ and then Ca^{2+} ions were replaced by Na^+ during the evolution of groundwater along it's flow-path (indicated with an arrow in **Figure 31a**). Similar facies associations can be observed in relation to the color of the sediments from the Schoeller diagram (**Figure 31b**).

We can also predict that G-I samples with the highest Na^+ and Cl^- concentrations derived from red sediments have been mostly targeted by the local drillers to abstract iron (Fe^{2+}) free water and thereby mobilizing retained saline water from nearby impermeable layers to the aquifer, followed by the red/off-white layers from where G-II and G-III groups of water samples were collected (**Figure 31a**).

6.2.4. Redox sensitive elements

The summary of the redox sensitive parameters are summarized in Table 16 and **Figure 32a-f**.

6.2.4.1 Arsenic (As)

Significant variations in As concentrations can be observed within groundwater samples collected from the four groups of sediments (Figure 31a). Median values (Q50) in water-samples derived from the black, white, off-white and red sediments are 252.5 µg/L, 20.3 µg/L, 17.4 µg/L, and 15.1µg/L.

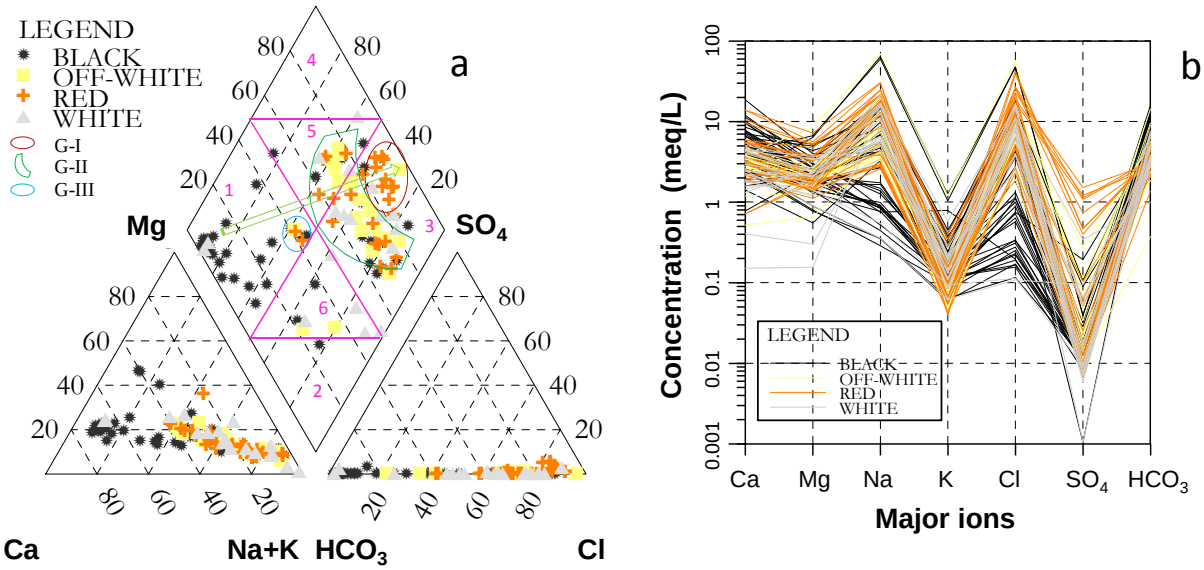

Figure 31. a) Piper tri-linear diagram showing the hydrochemical facies represented by the groundwater samples from the four sediment groups, b) Schoeller diagram representing the water types with corresponding sediment colour group at the well screens.

Table 16. Concentrations of redox-sensitive parameters in groundwater samples collected from the four groups of sediments

Parameter	Color	Min	Max	Average	Q25	Q50	Q75
As (total)	Black	2.8	9679	273	83	252.5	397
(µg/L)	White	8.8	359	68.6	15.2	20.3	51.8
	Off-white	5.0	94	27.2	11.8	17.4	37.9
	Red	2.8	35.5	16.6	12.9	15.1	18.9
Fe (total)	Black	0.22	13.3	5.8	2.86	4.87	8.21
(mg/L)	White	0.11	12.9	3.9	1.86	2.94	5.00
	Off-white	0.07	11.0	3.1	0.21	2.25	3.68
	Red	0.12	14.3	2.1	0.41	0.63	1.79
NH_4^+	Black	0	42.7	5.69	1.55	3.47	6.14
(mg/L)	White	0	8.6	1.86	0.06	0.37	1.94
	Off-white	0	52.3	2.89	0	0	0.43
	Red	0	2.75	0.45	0	0	0.36
PO_4^{3-}	Black	0.05	4.52	1.54	0.65	1.36	1.99
(mg/L)	White	0.04	2.75	0.65	0.14	0.29	0.68
	Off-white	0.03	6.29	0.60	0.04	0.14	0.46
	Red	0.01	1.20	0.18	0.03	0.04	0.11
Mn^{2+}	Black	0.05	2.92	0.73	0.19	0.54	1.04
(mg/L)	White	0.02	1.30	0.29	0.09	0.19	0.28
	Off-white	0.04	3.16	1.32	0.20	1.12	1.88
	Red	0.04	4.82	1.71	0.74	1.54	2.47
NO_3^-	Black	0.05	2.00	0.23	0.05	0.05	0.28
mg/L	White	0.05	0.52	0.072	0.05	0.05	0.03
	Off-white	0.05	0.41	0.032	0.05	0.05	0.05
	Red	0.05	2.083	0.22	0.05	0.05	0.05
DOC	Black	1.42	23.23	7	4.16	5.81	8.04
mg/L	White	1.28	18.78	4.14	2	2.96	3.68
	Off-white	1.20	25.41	3.82	1.33	1.95	4.32
	Red	1.14	39.11	4.04	1.35	1.71	1.92

It has been observed that all the water samples collected from both the black as well as white sediments within a depth of 50 m b.g.l. contain ≥ 50 to > 500 µg/L of As (**Figure 33a**). However, we found only four water samples below Bangladesh Drinking Water Standard (BDWS) of 50 µg/L As which have been screened from wells screened at aquifers with identified off-white (n = 3) and red (n = 1) sediments. Thus, up to a depth of 50 m b.g.l., almost 86% of the groundwater samples are above BDWS for As. The central part of Matlab (e.g. Durgapur, Paschim and Purba Fatehpur, southeast Baganbari and north of Farajikandi) and north-western part (e.g. Santal, Sadullapur, northwest Baganbari) of the study area is severely affected by As concentrations as high as > 500 µg/L (**Figure 33a**).

A completely different scenario can be observed when we consider the groundwater samples collected between 50 and 100 m depths (**Figure 33b**). Most of the water samples (82%) in this case are screened from red, off-white and white sediments contain As concentrations < 50 µg/L. The water samples screened from red (n = 33) and off-white (n = 20) sediments between 50 and 100 m depths suggest that low As aquifers can be encountered at this level. Lower levels of As can be found in most areas of the study area except some portion of Uttar Matlab, Sadullapur, Nayergaon, and Dakhshin Matlab. The **Figure 33b** also implies that it is unlikely to find low As aquifers along the fringes of the lower Meghna floodplain. At depths > 100 m (**Figure 33c**), all the samples fall below BWDS of 50 µg/L As. It is interesting to

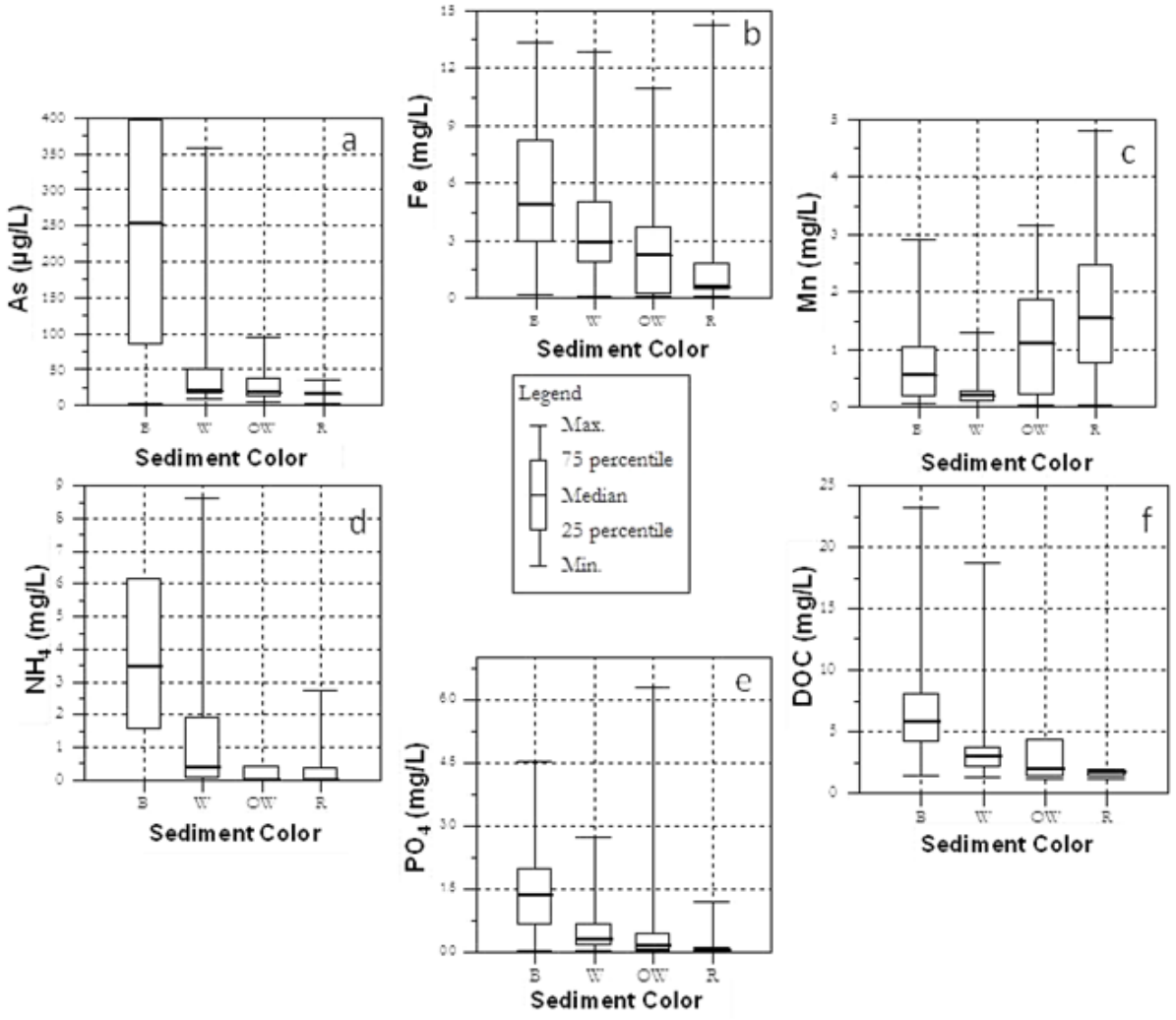

Figure 32. Box and Whiskers plot showing the variability of a) As, b) Fe, c) Mn, d)NH_4^+, e) PO_4^{3-} and f) DOC in groundwater samples from the four sediment groups.

note here that no samples were taken from black or red sediments; in other words, local drillers could hardly encounter red/black sediments aquifers at depths > 100 m b.g.l.

Speciation results show that approximately 90% of the total As in groundwater exists in the form of As (III) in samples collected from black sediments, while this percentage decreases to approximately 50% in white, and 40 – 35% in off-white and red sediments.

6.2.4.2 Iron (Fe) and manganese (Mn)

Significant variations in the concentrations of total iron (Fe_{tot}) and Mn^{2+} can be observed within the water samples derived from the four groups of sediments (Table 16 and **Figure 32b,c**). The median values of Fe_{tot} in groundwater samples screened from black, white, off-white and red sediments are 4.87, 2.93, 2.25 and 0.63 mg/L respectively. Highly reducing condition conducive to iron reduction in the black sediments may be responsible for high Fe concentrations in these sediments (eqn. 1). The spatial distribution of Fe_{tot} concentrations of water samples collected up to 50 meter depth in the study area is presented in **Figure 34a**. It is noteworthy that Fe concentrations in the southeastern half including Matlab South(Dakshin), Uttar Upaldi, Khadergaon,

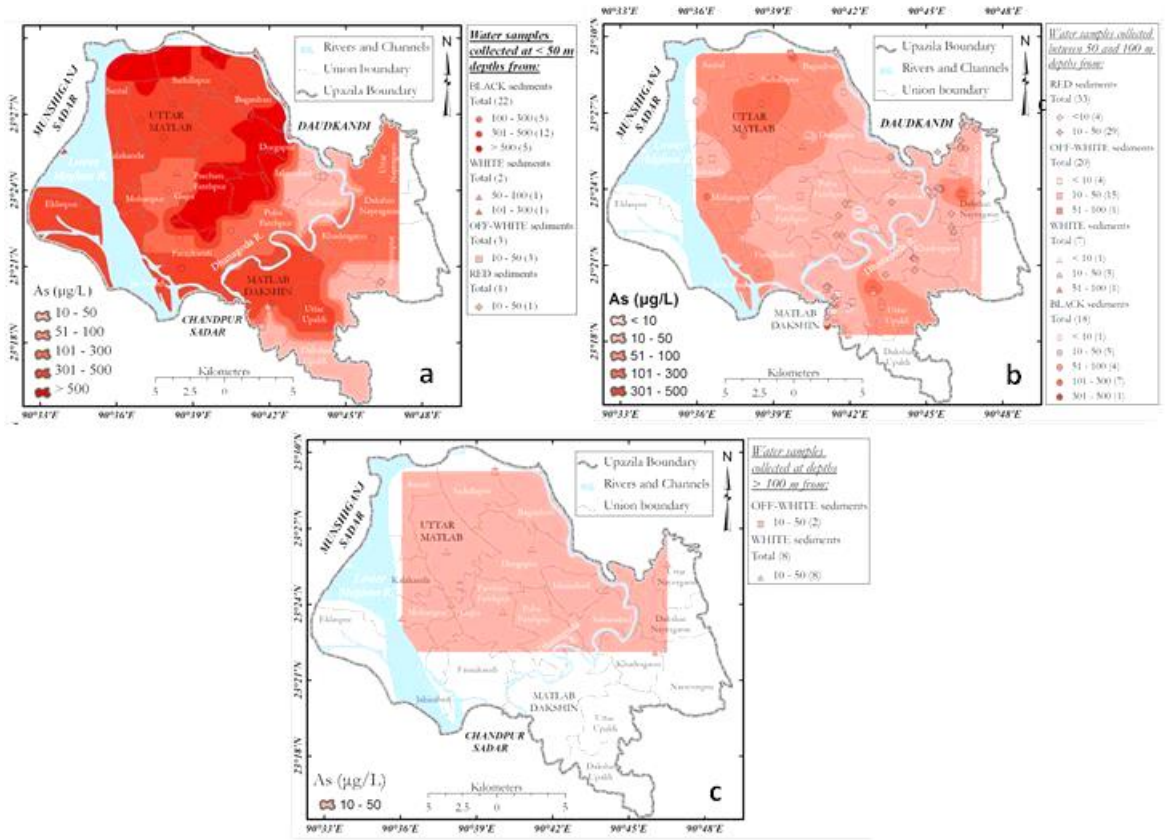

Figure 33. Spatial distribution of As concentrations in groundwater samples collected from well screens placed in black, white, off-white and red sediments at depths: a) < 50 m, b) between 50 and 100 m, and c) > 100 m.

Sultanabad, Uttar Nayergaon, Dakshin Nayergaon, and portions of Purba Fatehpur and Islamabad is lower than that we can observe in the north-western half of the study area. Approximately > 82% of the samples falls above the BWDS standard of 0.3 to 1 mg/L of Fe. In contrast, from the spatial distribution of water samples collected between 50 and 100 m depths indicating a rather lower Fe concentration throughout the study area (**Figure 34c**). This is expected because most of the samples in this zone have been collected from red/off-white sediments. Thus, almost 45% samples falls below BDWS for Fe.

Higher values of Mn^{2+} in water samples screened from red and off-white sediments (median: 1.53 and 1.14 mg/L respectively) than in black and white sediments (median: 0.54 and 0.19 mg/L respectively) suggest an on-going Mn-reduction in the red/off-white sediments (eqn. 6). Here, manganese is redox-buffering the system (i.e. may be Mn^{2+}–MnO_2 buffering the system (i.e. may be Mn^{2+}–MnO_2 pair preventing significant change in Eh) and thus restricting the groundwater system to reach the stage of iron reduction. This is why, iron concentrations are low in the red/off-white sediments.

$$CH_2O + 2\ MnO_2 + 4\ H^+ \rightarrow$$
$$CO_2 + Mn^{2+} + 3\ H_2O \quad \text{..... (eqn. 6)}$$

Spatial distribution of Mn concentrations (**Figure 34b**) for water samples collected up to a depth of 50 m b.g.l. show a mirror image of what can be observed in the case of Fe; i.e. a distinct barrier exists between the north-western half of the study area with relatively low Mn concentrations and the southeastern half with high Mn concentrations. Thus, even within the top 50 m sequence dominated by black facies, marked lateral variation can be observed between the NW and SW halves of the study area. At this level, all the samples exceed the

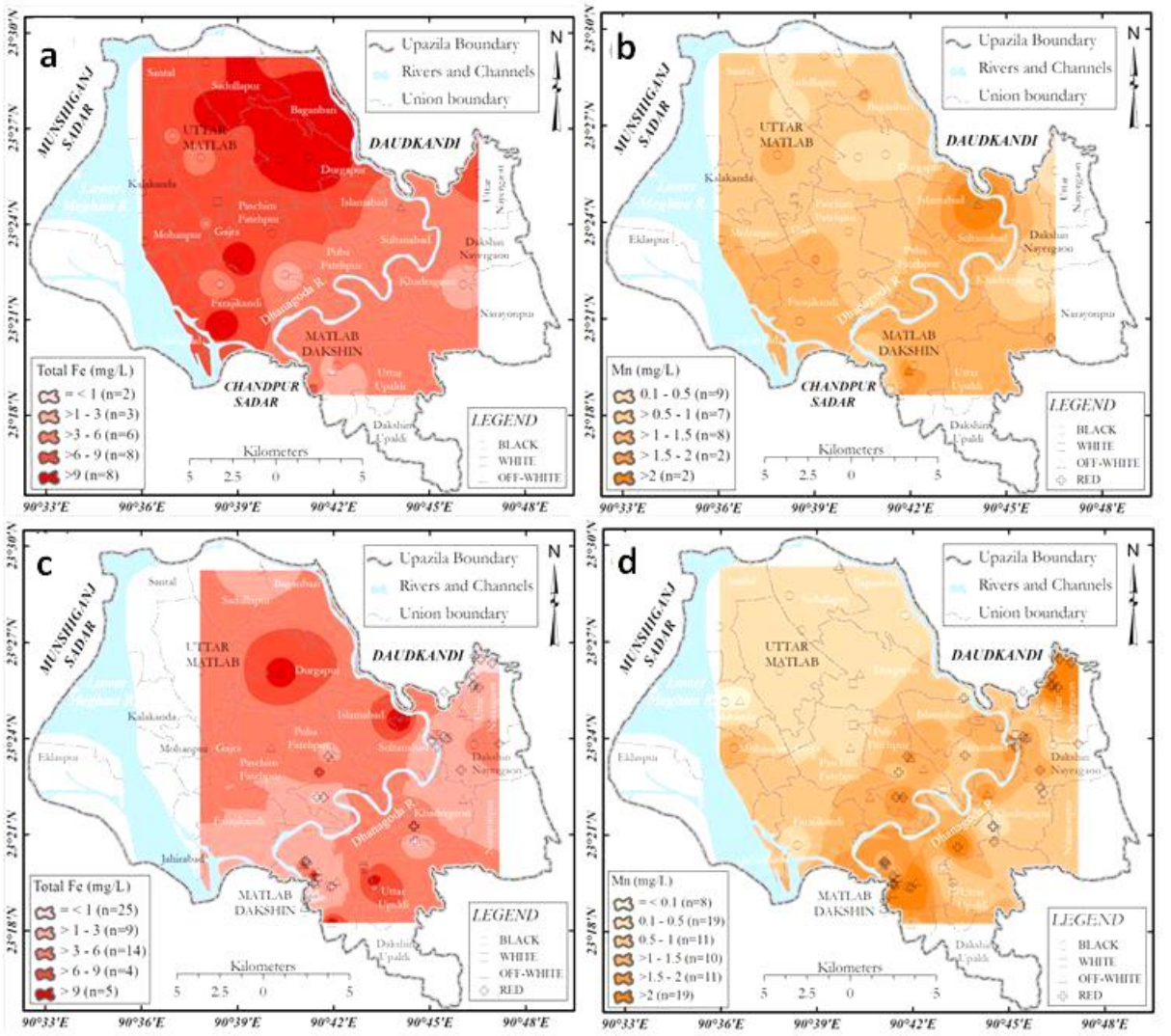

Figure 34. Spatial distribution of Fe and Mn concentrations in groundwater samples collected from wells at depths: a, b) < 50 m, and c, d) between 50 and 100 m depths from black, white, off-white and red sediments.

BDWS of 0.10 mg/L of Mn, although some samples (n=9) were well within the previous WHO guideline of 0.40 mg/L of Mn, about 60% of the total samples exceeded the limit. In depths between 50 m and 100 m, the contrast in Mn concentrations between the NW and SW halves is even more intense (**Figure 34d**). However, in this zone, Mn concentrations in 10% samples are below BDWS limit and in 40% samples below the WHO guideline.

6.2.4.3 Ammonium (NH_4^+), phosphate (PO_4^{3-}) and nitrate (NO_3^-)

Ammonium (NH_4^+) concentrations in groundwater within the four sediment groups also show a wide range of variation (Table 16 and **Figure 32d**). The Q75 concentrations of NH_4^+ in water derived from black, white, off-white and red sediments are 6.14, 1.94, 0.43 and 0.36 mg/L respectively. Black sediment water samples containing such high NH_4^+ values may be due to ammonification (eqn. 7).

$$CH_2O + \tfrac{1}{2}\, NO_3^- + H^+ \rightarrow CO_2 + \tfrac{1}{2}\, NH_4^+ + H_2O \quad \text{…….. (eqn. 7)}$$

Phosphate (PO_4^{3-}) concentrations also vary between the color-classified sediment groups (Table 16 and **Figure 32e**). The median values of PO_4^{3-} in water derived from black, white, off-white and red sediments are 1.35, 0.29, 0.13 and 0.04 mg/L respectively. Higher concentrations of

PO_4^{3-} can be attributed to the precipitation of different mineral phases (e.g. vivianite, $Fe_3(PO_4)_2 .8H_2O$) during the dissolution of Fe-oxy-hydroxides.

Very low nitrate (NO_3^-) concentrations in all the groundwater samples (maximum 2 mg/L) may be due to nitrate reduction through ammonification (eqn. 7) and denitrification processes (eqn. 8) in the redox ladder prior to Fe reduction.

$CH_2O + 4/5\ NO_3^- + 4/5\ H^+ \rightarrow$

$2/5\ N_2 + CO_2 + 7/5\ H_2O$ ……..(eqn. 8)

6.2.4.4 Dissolved organic carbon (DOC)

Groundwater derived from black sediments contain very high DOC concentrations (median: 5.81 mg/L) followed by the white, off-white, and red group of sediments (median values of 2.96, 1.95, and 1.71 mg/L respectively) (Table 16 and **Figure 32f**). High DOC concentrations in the black sediments may be due to the presence of high organic content in these sediments (Nickson et al. 2000, Bhattacharya et al. 2002a, Ahmed et al. 2004, McArthur et al. 2004). It is still unclear whether organic matter (OM) is derived from decomposition of peat layers or from seasonal water-level fluctuations of agricultural and other organic wastes from near-surface environments. However, low organic content in the red and off-white sediments can be attributed to weathering of these sediments and subsequent flushing during Late Pleistocence age.

6.2.5. Relationships between hydrochemical parameters

6.2.5.1 Correlations among the redox drivers

Bicarbonate (HCO_3^-) concentrations in water samples derived from black sediments show strong positive correlation (r_b=0.74) with DOC, while in this case, correlation coefficients for water samples collected from white (r_w =0.11), off-white (r_{ow}=0.17), and red (r_r= – 0.12) sediments are very low or negative (**Figure 35a**). Thus, the process of generation of high DOC due to biodegradation of OM and their microbial oxidation leading to the production of HCO_3^- in aqeous phases. Other redox reactions e.g. iron reduction (eqn. 2), sulfate reduction (eqn. 3) is mainly confined to the recent Holocene black sediments; in other words, the young black sediments are rich in OM (Nickson et al. 2000, Bhattacharya et al. 2002a, Ahmed et al. 2004, McArthur et al. 2004).

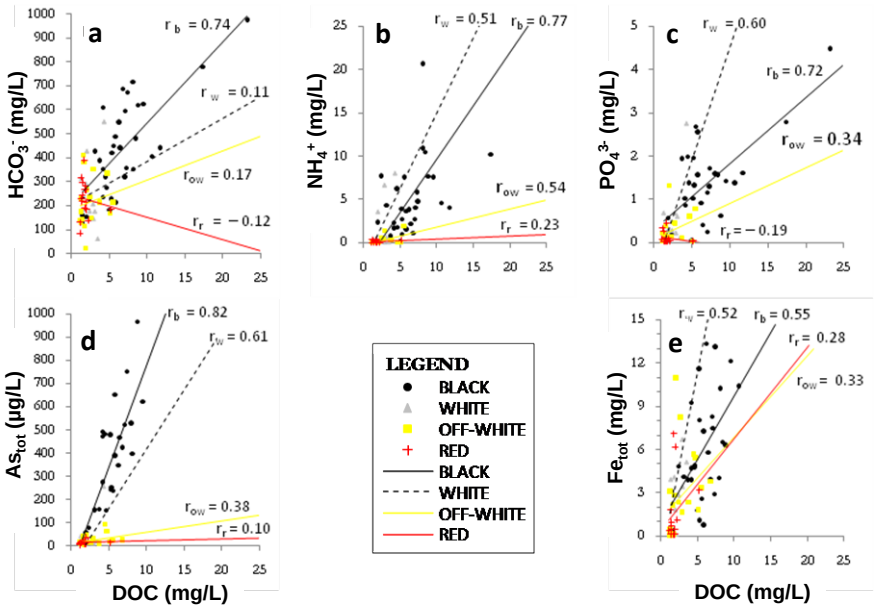

Figure 35. Bivariate plots showing relationship of groundwater DOC in the four sediment colour groups with a) HCO_3^-, b) NH_4^+, c) PO_4^{3-}, d) As_{tot}, and e) Fe_{tot}.

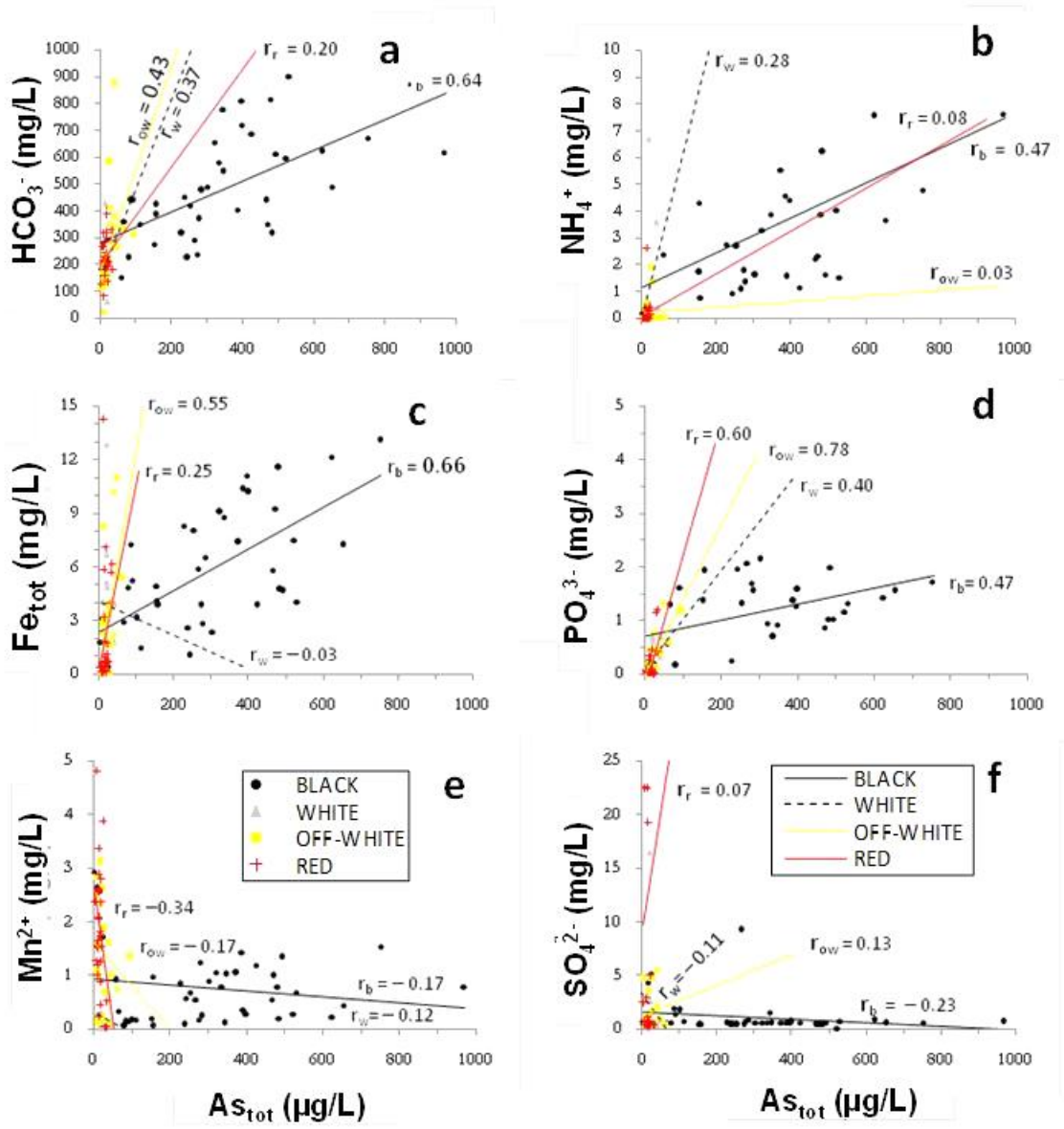

Figure 36. Bivariate plots showing relationship between the As_{tot} concentrations with a) HCO_3^-, b) NH_4^+, c) Fe_{tot}, d) PO_4^{3-}, e) Mn^{2+} and f) SO_4^{2-}.

Likewise, water samples from black sediments display moderate to very strong correlation between DOC and other redox sensitive parameters; e.g. NH_4^+ (r_b= 0.77), PO_4^{3-} (r_b=0.72), As_{tot} (r_b=0.82), and Fe_{tot} (r_b=0.55); which suggests that microbial degradation of OM is the main mechanism behind the release of all these elements in the highly anoxic black sediment environment (**Figure 35b-e**). On the other hand, moderate to negative correlations between DOC and the parameters NH_4^+, PO_4^{3-}, As_{tot}, and Fe_{tot} in white (r_w= 0.51, 0.60, 0.61, and 0.52 respectively), off-white (r_{ow}= 0.54, 0.34, 0.38, and 0.33 respectively) and red (r_r= 0.23, −0.19, 0.10, and 0.28 respectively) sediment water samples suggest that the redox status in white sediments is close to that of black sediment and insignificant OM was preserved in the red and off-white sediments due to weathering of these sediments during the Late Pleistocene time and subsequent flushing.

6.2.5.2 Correlation among the critical redox sensitive parameters

A moderately strong correlation between As_{tot} and HCO_3^- in the black sediment water samples (r_b = 0.64) further validate that highly reducing environment in the black

sediments triggers the release of As (**Figure 35a**) and low As aquifers representing less reducing environments with poor correlation coefficients (r_w= 0.37, r_{ow}=0.43, and r_r=0.20). Similar trend can be observed from the correlation between As_{tot} and NH_4 amongst the color-classified water samples; e.g. r_b = 0.47, r_w= 0.28, r_{ow}=0.03, and r_r=0.08 (**Figure 36b**).

Because water samples from the black sediment show a moderately strong correlation (r_b= 0.66) between Fe_{tot} and As_{tot} (**Figure 36c**), but negative correlation (r_b= – 0.17) between Mn and As (**Figure 36e**); the major mechanism behind As release can be attributed to reductive dissolution of Fe-(oxy)hydroxides (eqn. 1), rather than dissolution of Mn-(oxy)hydroxides. Though water samples derived from white and red sediments exhibit negative (r_r= – 0.03) to poor (r_r= 0.25) correlation between As_{tot} and Fe_{tot}, a moderate correlation (r_{ow}= 0.55) exists in the case of off-white sediment water samples as seen in **Figure 36c**.

The correlation between As_{tot} and PO_4^{3-} (r_b= 0.47, r_w= 0.40) in black and white groups of samples, is rather poor compared to the off-white (r_{ow}= 0.78) and red (r_r= 0.60) groups (**Figure 36d**). Thus, high PO_4^{3-} concentrations in the black sediments is not solely due to the release of PO_4^{3-} during reduction of iron oxy-hydroxides. Use of soil amendments like phosphate fertilizers and other anthropogenic activities can be an additional source of high PO_4^{3-} concentrations in the black group of samples. The Bengal basin sediments are generally sulfur deficient and SO_4^{2-} concentrations are generally low Bhattacharya et al. 1997, 2002b). Negative to poor correlation between As_{tot} and SO_4^{2-} (**Figure 36f**) within all the color-classified samples (r_b = -0.23, r_w= -0.11, r_{ow}= 0.13, and r_r=0.07) suggests that As mobilization can't be ascribed to oxidation of sulfide minerals; e.g. pyrite, arsenopyrite, etc. (Harvey et al. 2005).

6.2.6. Speciation modeling

6.2.6.1 General characteristics

The salient speciation modeling results are presented in **Figure 37**. The major findings from the speciation studies as detailed in Mozumder (2011). are highlighted below:

- For the black group of samples, Saturation Index (SI) ≈ 0 (**Figure 37**) with respect to carbonate phases; e.g. calcite ($CaCO_3$), dolomite [$CaMg(CO_3)_2$], and aragonite ($CaCO_3$) suggests that high HCO_3 concentrations in the black sediments is not only due to carbonate dissolution (eqn 2), but also due to oxidation of OM (Ahmed et al. 2004). However, red, white and off-white groups of samples are under-saturated may be due to less OM content.

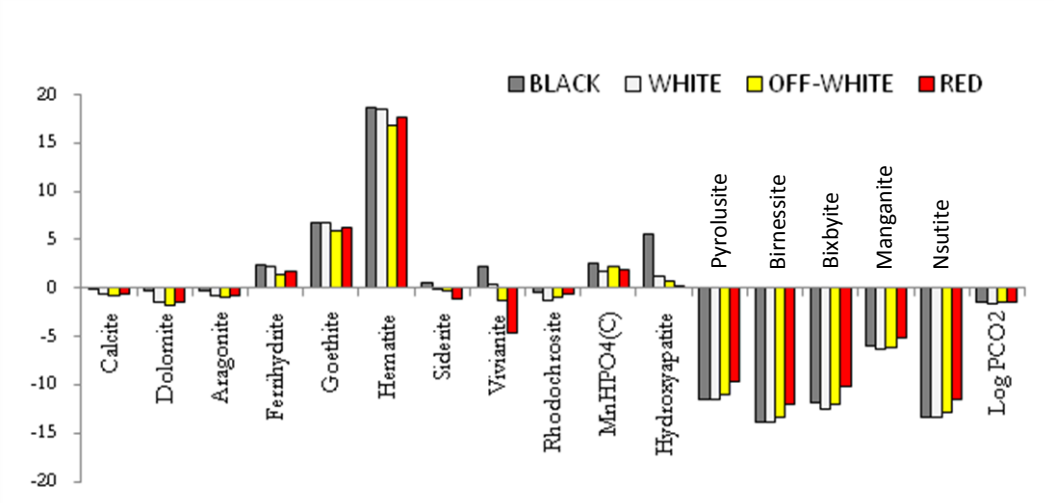

Figure 37. Saturation index (SI) median values for all the four groups of samples.

- For all groups of samples, no noteworthy complexation of Fe with other inorganic anions was detected. Fe^{2+} was found as the major aqueous species of Fe and thus, groundwater is supersaturated with respect to Fe (III) phases like ferrihydrite [$Fe(OH)_3$], goethite (FeOOH), hematite (Fe_2O_3) (**Figure 36**) and magnetite (Fe_3O_4) (not shown); in other words, the environment is conducive to precipitation of Fe(III) minerals.
- The black group of samples are supersaturated with respect to siderite ($FeCO_3$) and vivianite [$Fe_3(PO_4)_2 .8H_2O$], suggesting that precipitation of Fe(II) phases is favorable in black sediments. which is followed by the white (near equilibrium), off-white and red groups (undersaturated) of samples respectively (**Figure 37**)
- No significant variation can be observed in P_{CO2} values within the four groups of samples (**Figure 37**). High P_{CO2} values suggesting generation of CO_2 in redox reactions (eqn 1-7).
- All groups of samples are slightly undersaturated with respect to rhodochrocite ($MnCO_3$) and highly undersaturated with respect to Mn-oxides and hydroxides; e.g. pyrolusite (MnO_2), birnessite (MnO_2), bixbyite (Mn_2O_3), manganite (MnOOH), and nsutite (MnO_2) (**Figure 37**).

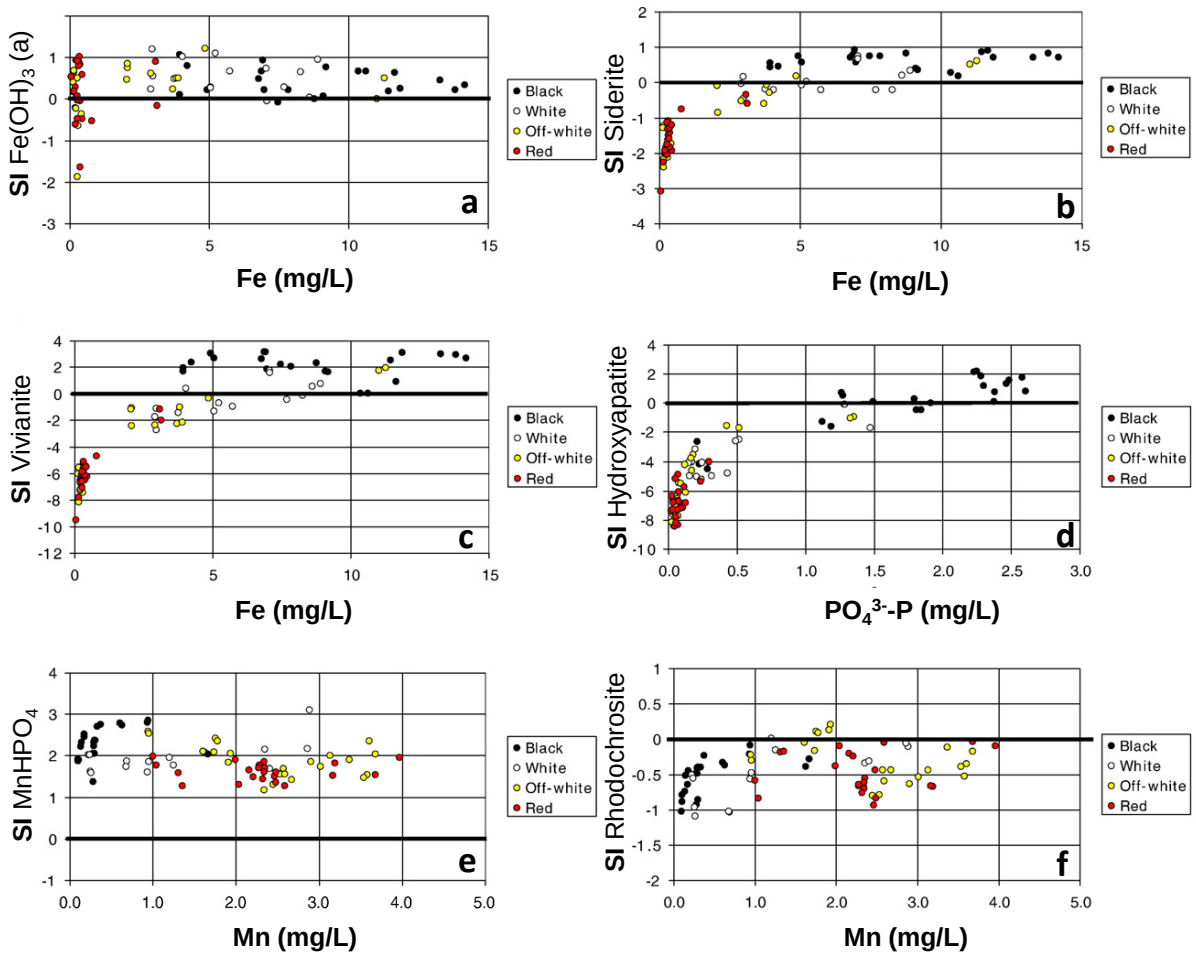

Figure 38. a) Bivariate plots showing the dependency of modelled SI values for a) $Fe(OH)_3$(a) vs Fe, b) siderite vs Fe, c) vivianite vs Fe, d) hydroxyapatite vs PO_4^{3-}, e) $MnHPO_4$ vs Mn, and f) rhodochrosite vs Mn.

- Precipitation of rhodocrocite might have played a significant role in removal of Mn from the solution (Mukherjee et al. 2008). However, groundwater is supersaturated with respect to the phase $MnHPO_4$ and hydroxyapatite $[Ca_5(PO_4)_3OH]$ in all groups of samples. In the case of hydroxapatite, supersaturation reaches maximum for the black group of samples followed by the white, off-white, and red groups.

6.2.6.2 Sensitivity analyses

The sensitivity analysis of the simulations of SI values shows that mineral phases including Fe(III), e.g. Fe(III)-oxyhydroxides, are sensitive to an alteration of Eh. The other mineral phases discussed in this paper, e.g. siderite and vivianite are not sensitive to the alteration of Eh.

SI calculations reveal that groundwater in both reducing (black samples) and oxidizing aquifers (white, off-white and red sediments) is near saturation with respect to Fe(III)-oxyhydroxides. When performing the sensitivity analysis with lower Eh values, groundwater was unsaturated with respect to Fe(III)-oxyhydroxides. Groundwater in the reducing unit is slightly supersaturated with respect to siderite ($FeCO_3$) and vivianite ($(Fe_3(PO_4)_2 \cdot 8(H_2O))$ (SI_{max}~1 and 3, respectively) but undersaturated in the oxidized unit. SI values for siderite and vivianite correlate well with concentration of dissolved Fe.

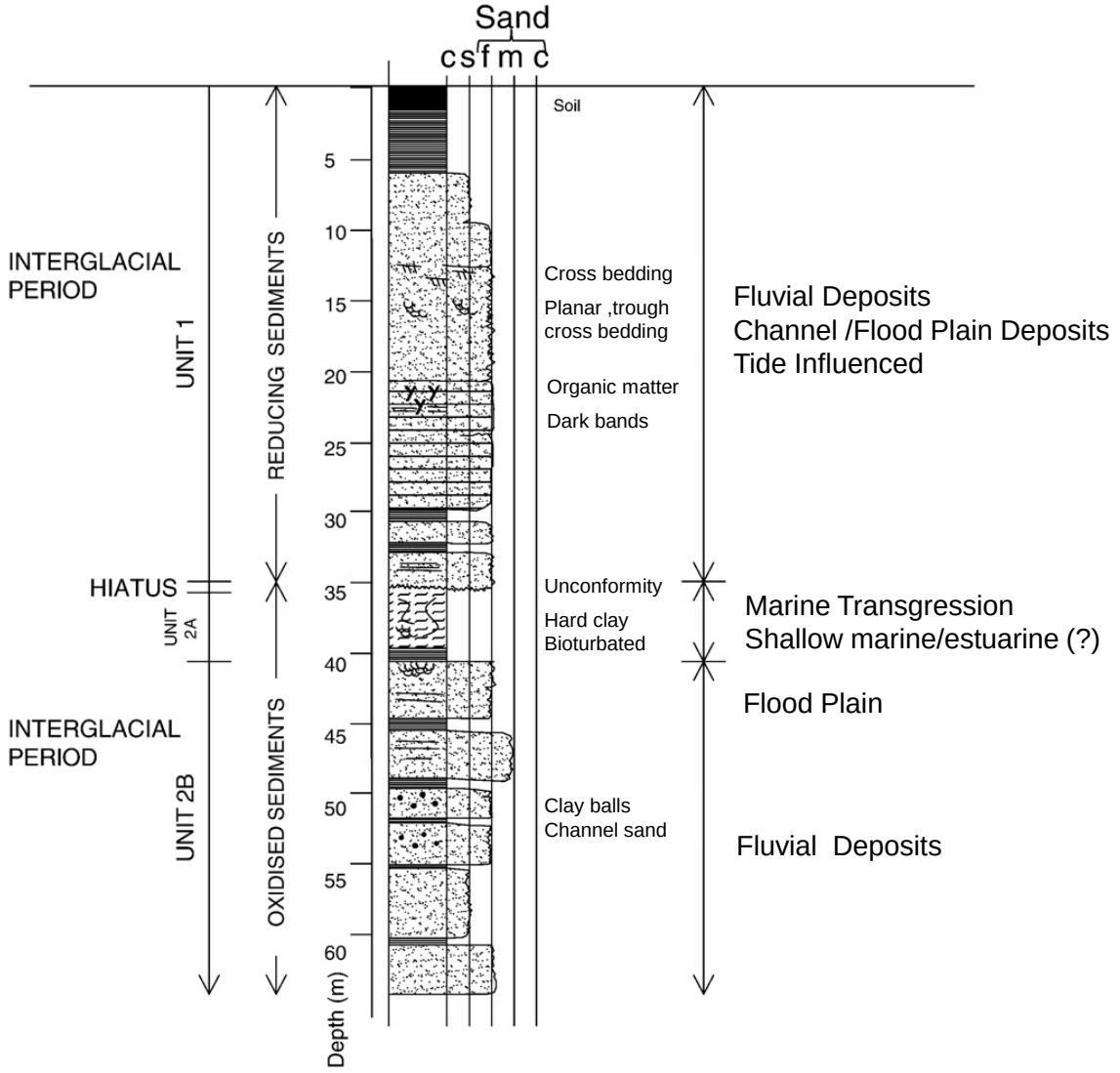

Figure 39. Lithological log with the diagnostic sedimentological characteristics of the aquifer sequence in Matlab study area.

Groundwater in both reduced and the oxidized aquifer units indicated saturation with respect to rhodochrosite ($MnCO_3$) and supersaturated with respect to $MnHPO_4$. Groundwater from the reducing unit is near saturation with respect to hydroxyapatite ($Ca_5(PO_4)_3(OH)$), but it is undersaturated with respect to the mineral phase in the oxidized unit (**Figure 38**).

6.3. Sediment characteristics

6.3.1. Sequence of aquifer sediments

The colour of the sediments from the uppermost sequence is black to greyish while the sediments from the lower sequence are reddish, yellowish to whitish (**Figure 9**). The lithological log prepared from the core samples with the diagnostic sedimentological characteristics of the major units are presented in **Figure 39**.

The uppermost sequence (Unit 1) comprises a partly oxidized topsoil upto a depth 2 m b.g.l. The surface clay is underlain by a dark coloured clay unit ranging with a thickness of 5 m and further by a thick fining upward sequence of sand, silt and clay down to a depth of 35 m below the surface. Cross beddings and trough cross beddings identified in the core samples indicate that the sedimentation occurred in fluvial environment and represented the channel sand facies and tide influenced flood plain environment (**Figure 39**).

This uppermost sequence is of Holocene age and has not undergone any extensive weathering or oxidation and represents reducing aquifer conditions. Biotite and other dark coloured ferromagnesian and opaque minerals are responsible for the dark colours. These minerals are found in bands and together with organic matters at depths of 15–20 m.

The two major sand units are separated by 5 m thick bioturbated hard clay represented as Unit 2A (**Figure 39**). This hard clay is grey in colour and indicate shallow marine depositional environment. ^{14}C-analysis on the plant matter (root) incorporated in the clay (**Figure 40**), indicated an age of ca. 8 ka BP which suggest that the marine transgression took place around that time which is consistent with other published studies (Goodbred et al. 2003). During 7-9.8 ka BP, a basin wide bioturbated sediments are reported in the Bengal basin. An unconformity has been identified between the shale and the uppermost reduced sequence confirming that the underlying sediments were eroded and exposed to weathering and oxidation. Thus, the two major units correspond to two interglacial periods. However, no dating could be done for the underlying sequence due to the lack of organic matter.

Figure 40. Close-up view of bioturbated clay at depth of 36 m, the circle mark the plant material for ^{14}C-dating.

Investigations of the core samples derived from the lower oxidized unit (**Figure 39**, Unit 2B) show that these sediments were also exposed to weathering and oxidation. They have lower abundance of biotite. Fe(III)-oxyhydroxides coatings on quartz, feldspars and other mineral grains impart reddish colour to the sediments. This unit was also deposited in a fluvial and flood plain environment and is represented by fining upward sequences of sand, silt and clay. Clay balls incorporated in the sand (from core 54, **Figure 9**) indicate that these sediments were deposited in river channels.

6.3.2. Mineralogical characteristics

6.3.2.1 XRD studies on aquifer sediments

XRD analysis shows that the mineralogy of the sands is dominated by quartz, K-feldspar

Table 17. Mineralogical composition of sediment samples investigated from the sediment cores

Depth (m)	Unit*	Colour	Mineralogical composition					
18	1	Black	Quartz					
21	1	Black	Quartz	Anortite	Albite	Orthoclase	Magnetite	Biotite	Ferrohornblend
23	1	Black	Quartz	Anortite	Albite	Orthoclase	Rutile	Biotite	Ferrohornblend
33	1	Black	Quartz	Anortite	Albite	Orthoclase			
40	2B	Red	Quartz	Anortite	Albite	Orthoclase	Rutile		
44	2B	Red	Quartz	Rutile					
49	2B	Off-white	Quartz	Anortite	Albite	Orthoclase	Magnetite		
51	2B	White	Quartz	Rutile					
52	2B	White	Quartz						
54	2B	Off-white	Quartz						

Main phase	
Minor phase	
Accessories	

* The number of Unit refer to the position of the sediment samples in the lithological log in **Figure 38.**

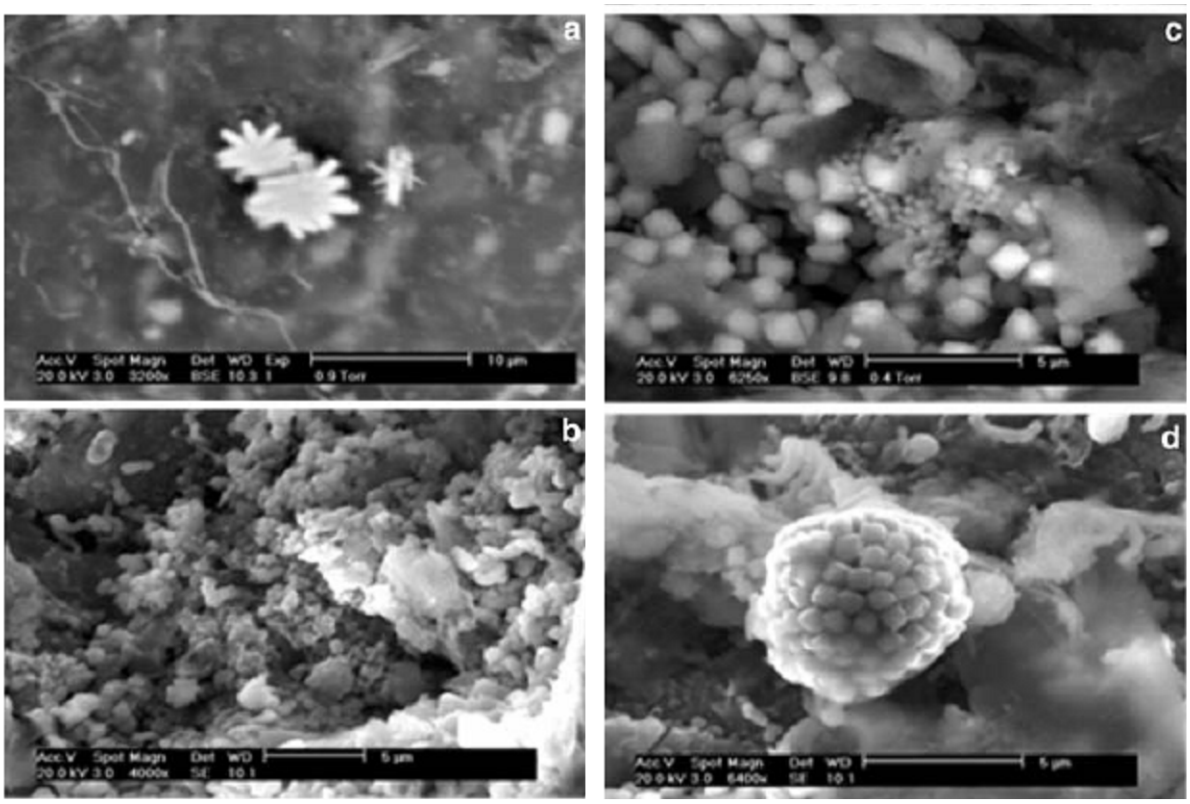

Figure 41. SEM images showing: a) iron oxide (goethite, FeOOH) on biotite grain in the yellowish grey surface sediments, b) amorphous iron oxide with traces of As on a biotite grain in the grey mica-rich reduced sediments, c) octahedral authigenic pyrite; and d) framboidal pyrite on the mica flakes within the reduced sediments.

(orthoclase) and plagioclase (anorthite and albite) with a substantial content of biotite and ferro-hornblende in the reducing Holocene sediments. Heavy minerals such as and ferro-hornblende in the reducing Holocene sediments. Heavy minerals such as magnetite and rutile were also identified in this sequence (Table 17). Biotite identified at the depth of 21 and 23 m corresponds to the dark bands found in the core samples (**Figure 38**). The weathered and oxidized sediments in the lower part of the sequence

contains relatively lower quantities of feldspars. In this sequence neither biotite nor ferro-hornblende were identified, however both rutile and magnetite were found.

6.3.2.2 SEM studies on reduced aquifer sediments

Scanning electron microscopic studies revealed the presence of acicular iron oxide, most likely goethite (FeOOH), as overgrowths on biotite grain from the upper surficial sediments (**Figure 41a**). Amorphous iron oxide were common on biotite flakes within the grey to dark grey organic matter and mica-rich sediments in the reduced sediments within depths of 20 m (**Figure 41b**). Authigenic growths of octrahedral and framboidal pyrite (FeS_2) were observed on the biotite flakes in the reduced aquifer sediments within depths of 20 m (**Figure 41c,d**) which indicates sulphate reduction under strong reducing conditions in the aquifer which is consistent with the groundwater chemical data presented above.

6.3.3. Sediment geochemistry

6.3.3.1 Major element chemistry

Major element chemistry of the selected sediments from the oxidized and the reduced units from Matlab is presented in **Figure 42**. The results indicate that Al is the most abundant element followed by Fe, Ti, and Mn, respectively.

The average value for Fe (recalculated as Fe_2O_3) is approximately 65 times higher than Mn content (MnO) in both reducing and oxidised sediments. Relatively higher contents of Fe_2O_3 and MnO coincide with the reducing sediments, particularly the dark banded core samples at the depth of 21m and 23m, and the red samples from the depth of 40 and 44 m.

The samples from the oxidized sequence were characterized by low contents of CaO, MgO and P_2O_5. The red oxidized sediments from a depth of 44 m reveal distinctively lower content of Na_2O, MgO and CaO. The SiO_2 content is relatively lower in the reducing sequence, ranging from 63 to 82 wt. %.

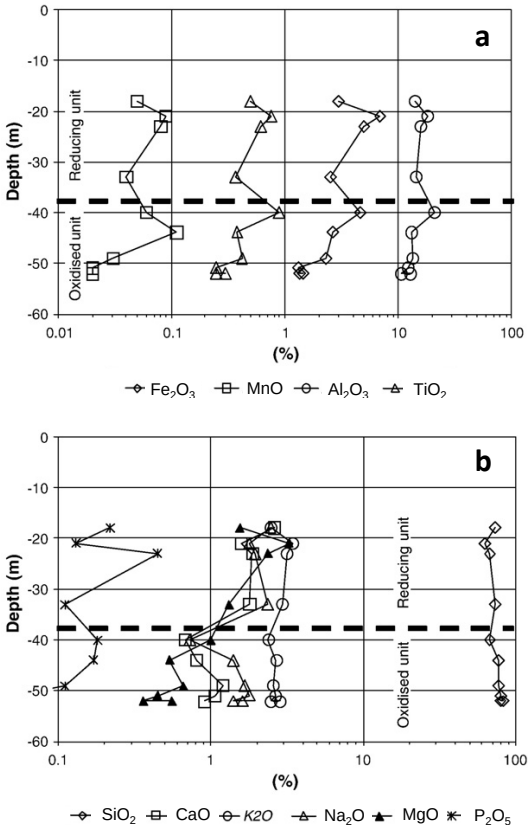

Figure 42. Major element composition (calculated as oxide wt.%) of the sediments from the oxidized and reduced sedimentary units based on the XRF analyses. a) Fe, Mn, Al and Ti, b) Si, Ca, K, Na, Mg and P.

6.3.3.2. Sequential extractions

The total extractable As concentration in Matlab sediments indicated considerable variation in different sediments, both in the reduced and the oxidized units. In general, total As concentration were found to be less than 1.5 mg/kg except for the reduced sediments encountered at depth of 21 m where 3.5 mg/kg was extracted (**Figure 43a**). The total extractable Fe and Mn were generally high in the reduced units.

The fractions of DIW- and $NaHCO_3$-extractable As, Fe and Mn were conspicuously low and below the limits of instrumental detection in all the sediments. The highest fractions of As_{NaAc}, As_{Ox} and As_{Ox+AA} were found in the reducing sediment at 21 m with corresponding high NaAc, oxalate and oxalate+AA extractable

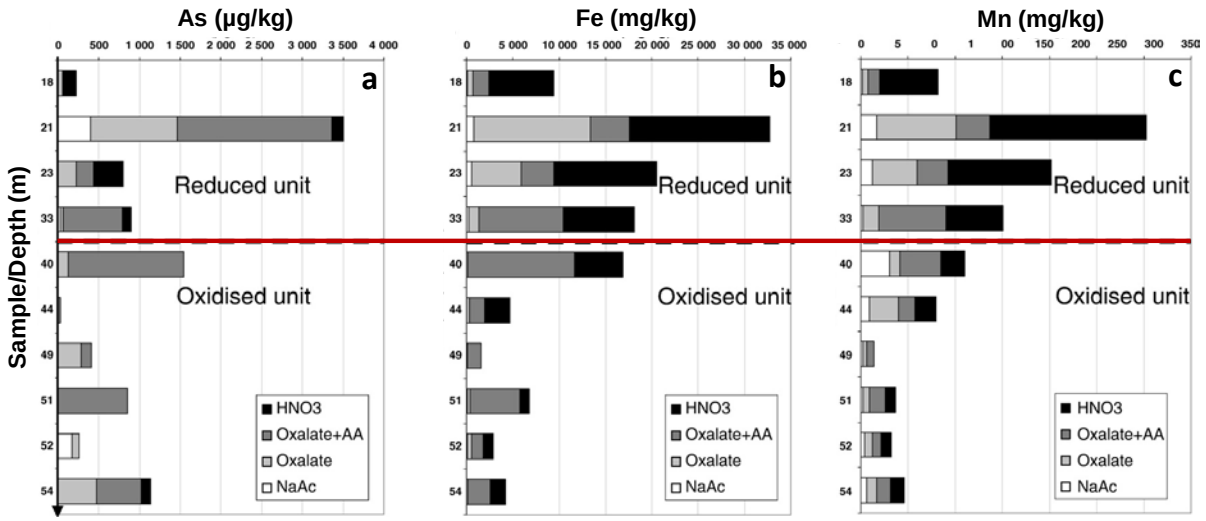

Figure 43. Histograms showing the solid phase associations of As, Fe and Mn in the 10 sediment core samples from Matlab, extracted sequentially by DIW, $NaHCO_3$, Na-acetate, oxalate, oxalate+ascorbic acid and 7 M HNO_3 (as the residual fraction)the distribution of of extractable phases of As, Fe and Mn. Note: DIW and $NaHCO_3$ fractions are not shown as those concentrations were conspicuously low and below the limits of instrumental detection.

fractions of Fe and Mn (**Figure 43a-c**). The highest content of As (1900 µg/kg) was found in the Ox_{AA}-fraction of reducing sample 21 and As_{OxAA} fraction holds most of the As in 50% of the samples.

It is also intriguing that the sediments from a depth of 40 m identified as the oxidized unit reveal significant contents of oxalate and oxalate+AA extractable fractions of As (fractions 4 and 5) and corresponding high oxalate-AA extractable and residual fractions Fe (Fe_{ox+AA} and Fe_{HNO3}) as well as significant proportions of oxalate, oxalate-AA and residual extractable fractions of Mn (Mn_{ox}, Mn_{Ox+AA} and Mn_{HNO3}) (**Figure 43a-c**). Ther proportion of As_{ox} is almost correlated with the oxalate extractable fraction of Mn in the sediments at this depth. Additionally, the sediment also indicates the possible presence of acetate extractable Mn which is partly contributed due to the dissolution of rhodochrosite in the solid phases. The As The extractable fraction 4 (As_{Ox}) and fraction 5 (As_{Ox+AA}) seem to be bound to the crystalline Fe(III)-oxyhydroxide phases as indicated by the content of Fe_{Ox+AA}.

In general, Fe_{Ox} and Mn_{Ox} were positively correlated in sediments of both groups, and exhibit stronger correlation for the reduced sediments (R^2=0.81) as compared to the oxidized sediments (R^2=0.66) (**Figure 44a**). Fe_{Ox}/Mn_{Ox} ratio also varied distinctly among the group of reducing sediments (mean Fe_{Ox}/Mn_{Ox}=107$\pm$24) and oxidized sediments (mean Fe_{Ox}/Mn_{Ox}=35$\pm$19). A very strong correlation is also noted amongst As_{Ox} and Fe_{Ox} (R^2=0.95) for the reduced group of sediments (**Figure 44d**).

The total extractable concentrations of Fe (Fe_{total}) and Mn (Mn_{total}) added from all fractions were generally high in the reducing sequence as compared to the oxidized sediments represented by the white, off-white and red sediments. The maximum concentrations of Fe_{total} and Mn_{total} were 32800 and 300 mg/kg respectively, with respective minimum concentrations of 1580 and 14 mg/kg. The total sequentially extractable concentrations Fe_{total} and Mn_{total} indicated a strong correlation (R^2=0.98) (**Figure 44b**) and similar Fe_{total}/Mn_{total} ratios (mean Fe_{total}/Mn_{total}=112$\pm$35) among all the samples. It is also interesting to note that Fe_{Ox+AA}/Fe_{Ox} ratio is consistently lower for

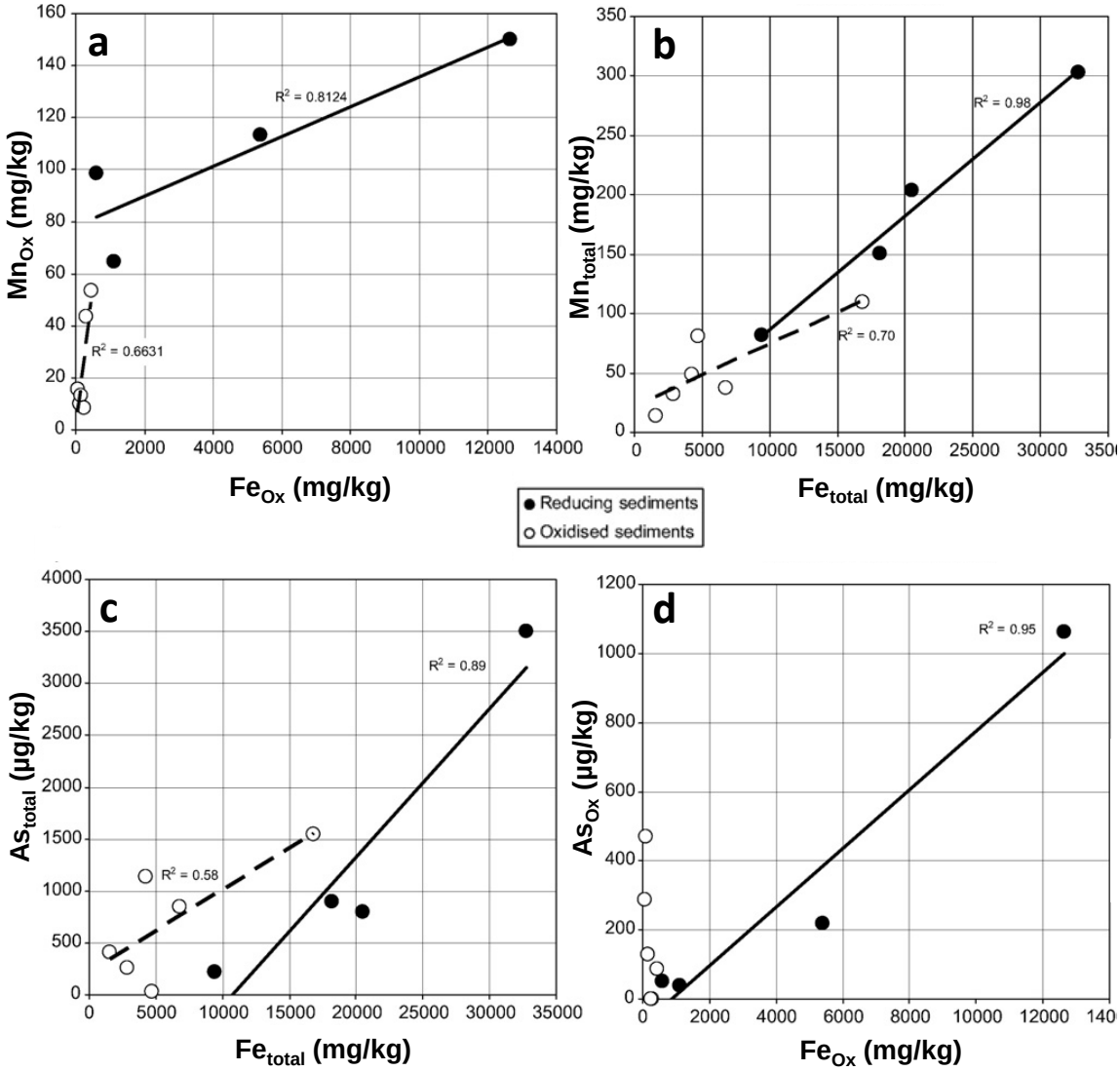

Figure 44. Bivariate plots of fractions extracted during sequential extraction of the reduced and oxidized groups of sediments from Matlab. a) Mn_{Ox} vs Fe_{Ox}, b) Mn_{total} vs Fe_{total}, c) As_{total} vs Fe_{total}, d) As_{Ox} vs Fe_{Ox}.

the reducing sediments (average Fe_{Ox+AA}/Fe_{Ox}=3) as compared to the oxidized counterparts with average Fe_{Ox+AA}/Fe_{Ox}=26). In the oxidised unit Fe_{Ox} is much lower than in the reducing unit, varying by a factor of 10 to 20. While performing the sequential extraction, it was noted that the colour of the red sediments changed from red to whitish during the Ox+AA extraction step.

The blank concentration for respective fractions of Fe and Mn relative to the extraction concentration was 2% and 1% respectively with standard deviation of 6% and 1% respectively, while those for As the standard deviations were higher due to the lower concentrations of the extractable As in the sediments.

6.3.2.3. Surface complexation modelling

The surface complexation modelling of As(III) adsorption in the reducing aquifer unit suggests that adsorption of As(III) is mainly controlled by the amount of *Hfo* in solid phase. pH is considered to be of less importance within the pH-interval found in the aquifer units of the study area. Inclusion of PO_4^{3-}-tot as competing ion in the system during simulations resulted in reasonable concentrations of dissolved and adsorbed As(III). If PO_4^{3-}-tot is excluded, all As(III)

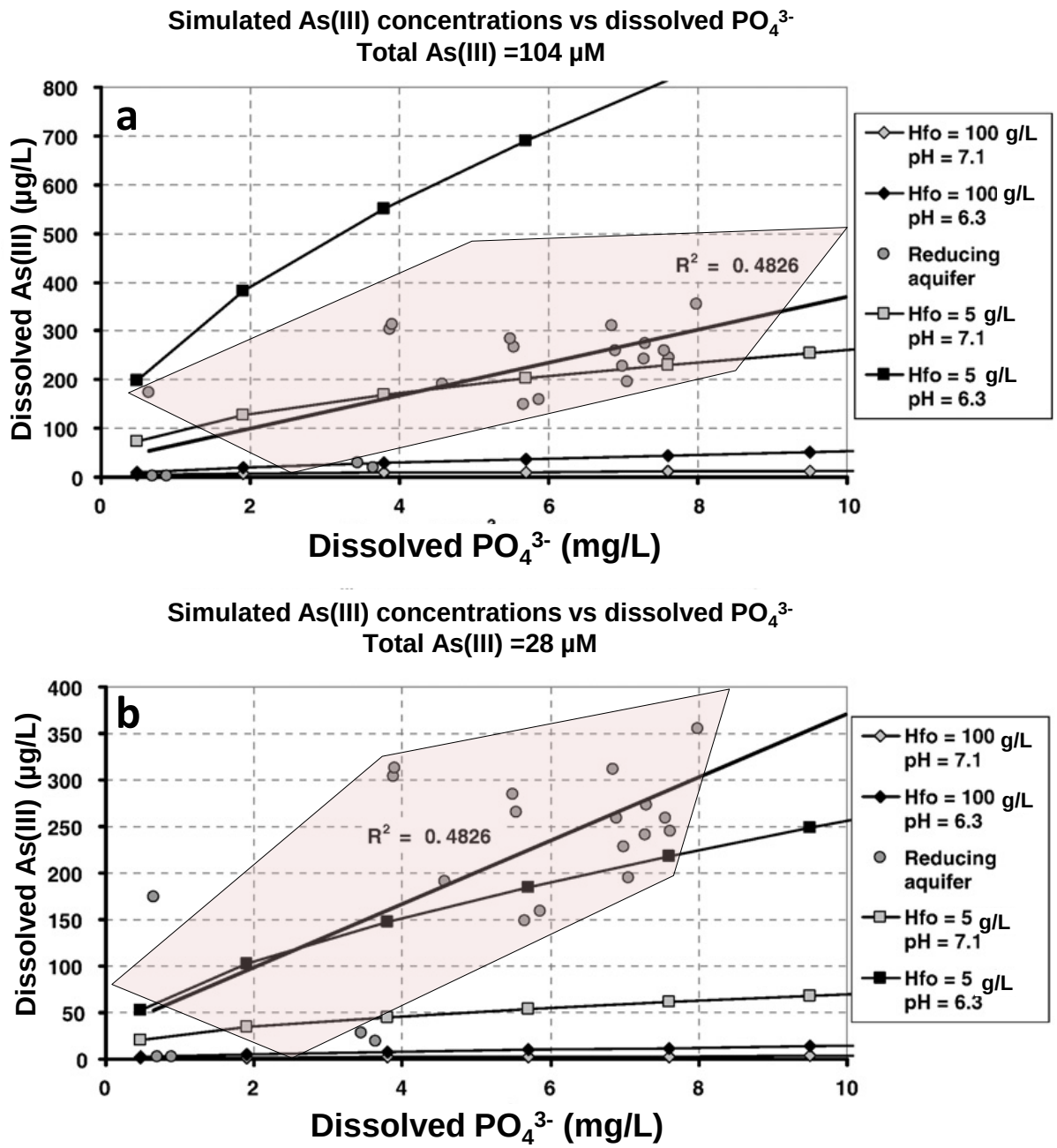

Figure 45. Simulation of adsorbed and dissolved As^{III} for the system with hydrous ferric oxides (Hfo), As^{III} and PO_4^{3-} using the Diffuse Layer Model. a) results based on maximum amount of As (as As(III)) in the sediments (104 µM), and b) with minimum amount of As (as As(III)) in the sediments (28 µM). The shaded polygon demarcates the fields of actual concentrations encountered in the reducing aquifers.

were readily found to be adsorbed onto the *Hfo*. The modelling results suggest that PO_4^{3-} is a minor species, and under the prevailing aquifer conditions $H_2PO_4^-$ represents the major aqueous specie of P with an activity higher than HPO_4^{2-} by a factor of 2 to 4. **Figure 45** presents the simulated dissolved concentrations of As(III) and PO_4^{3-}-tot concentrations, and an overlay of the plots of the actual groundwater concentrations in the reducing aquifers (grey filled circles) and demarcated

Table 18. Results of extraction treatments of the three oxidized sediment samples.

Sample	Oxalate extraction			HNO_3 extraction		
	As (mg/kg)	Fe (mg/kg)	Mn (mg/kg)	As (mg/kg)	Fe (mg/kg)	Mn (mg/kg)
#1	< 1.3	134.4	9.6	2.1	6940	116
#2	< 1.3	118.8	31.2	1.3	5300	153
#3	< 1.3	93.6	4.8	2.4	5070	73

by the shaded polygons (**Figure 45a,b**). The plots also show a positive correlation between As and PO_4^{3-}-tot with a R^2 value of 0.48 observed for the groundwater samples within the reduced aquifer units.

Modelling surface complexation of As(III) onto *Hfos* in the high As- and reducing aquifer unit thus suggests that As(III) adsorption was mainly controlled by the amount of *Hfo* in solid phase. The results also emphasize that a competing ion was needed to obtain high dissolved As concentrations as compared to cases where no competing ion was added, all As was adsorbed onto the *Hfo*. Thus dissolved concentrations of PO_4^{3-}-tot is of importance for the high dissolved concentrations of As, as commonly encountered under field conditions.

6.4. Arsenic adsorption dynamics

6.4.1. Extraction data

Oxalate and HNO_3 extractions performed on the three oxidized sediment samples (Samples #1, #2 and #3) indicate that the content of As associated with the solid phase is relatively low. The As content was measured to be <1.3 mg/kg and between 1.3 and 2.4 mg/kg by the oxalate and HNO_3 extractions, respectively (Table 18).

Table 19. Input parameters for surface complexation model (Dzombak and Morel 1990) implemented in PHREEQC (Parkhurst and Appelo 1999).

Parameters	Sample #1	Sample #2	Sample #3	Comments
Input data for simulations of aquifer conditions (using 2006 field water chemistry and Feox)				
Hfo (g/L)	0.9	0.79	0.66	Calculated from oxalate extraction.
Weak sites (sites/L)	2×10^{-3}	1.8×10^{-4}	1.4×10^{-3}	Used Dzombak and Morel (1990) site density of 0.2 sites/mol Hfo and molecular weight Hfo = 88.8 g/mol.
Strong sites (sites/L)	5×10^{-5}	4.5×10^{-5}	3.5×10^{-5}	Used Dzombak and Morel (1990) site density of 0.005 sites/mol Hfo. and molecular weight Hfo = 88.8 g/mol.
L/S (L/kg)	0.238	0.238	0.238	To convert between aquifer and experiment conditions. Based on porosity = 0.3 and bulk sediment density = 1.8 kg/L
Input data for simulations of experimental adsorption isotherms				
Hfo (g/L)	0.18	0.16	0.15	Calibrated to match adsorption isotherms.
Weak sites (sites/L)	4×10^{-4}	3.6×10^{-4}	3.4×10^{-4}	Used Dzombak and Morel site density (1990).
Strong sites (sites/L)	1×10^{-5}	9×10^{-6}	8.5×10^{-6}	Used Dzombak and Morel site density (1990).
L/S (L/kg)	15	15	15	To convert between aquifer and batch experiment conditions.

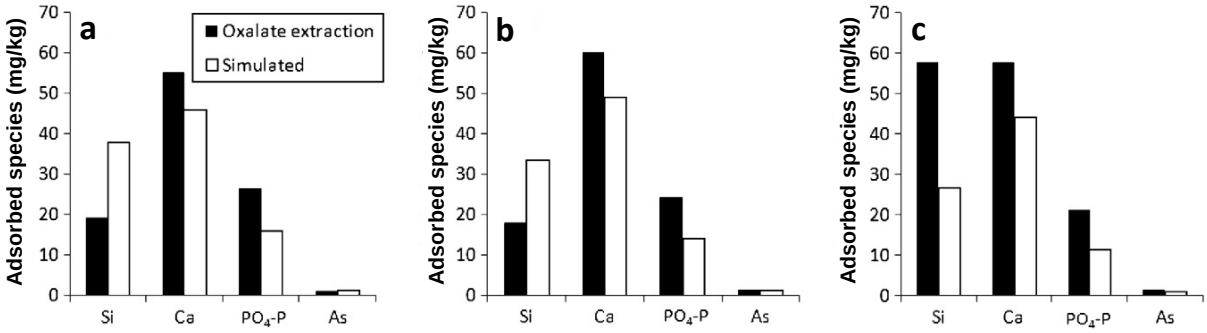

Figure 46. Distribution of adsorbed species based on oxalate extraction data and simulated using PHREEQC surface complexation model (Table 3) in: a) Sample #1, b) Sample #2, and c) Sample #3.

The oxalate extractions indicate that the content of Fe associated with the amorphous fraction (Fe_{ox}) is between 94 and 134 mg/kg, and that associated with the crystalline fraction is considerably higher (5070–6940 mg/kg). This result is in agreement with the sequential extraction results presented above, that the fractions of amorphous Fe and Mn phases are low compared to the crystalline fractions for the oxidized sediments (see Section 6.3.3.2 above and von Brömssen et al. 2008). Based on the observations on the changes in sediment colour during extractions, it was concluded that the reddish colour of the oxidized sediment is primarily associated with the crystalline minerals (von Brömssen et al. 2008). The surface composition of the oxidized sediments was simulated in PHREEQC using the mean water chemistry data for November 2006 from tubewells installed in the oxidized sediments (see Table 2). The *Hfo* mass and surface site concentrations were derived from Fe_{ox} (Table 19). The model gives a good match between the predicted concentration of adsorbed species and those extracted from the amorphous minerals (**Figure 46**).

The adsorption of As relative to other ions that compete for adsorption sites is also consistent. For all samples the quantity of adsorbed As is predicted to be ~1 mg/kg. The model assumes As(V) as the only species and the relative quantity of adsorbed As predicted is similar regardless of whether As(III) or As(V) is considered. The discrepancy between the simulated and measured surface composition may be attributed to varying water chemistry at the specific location from where the sediment was collected and/or influence of other amorphous adsorbent phases including Al(III) and Mn(IV) oxides which are not considered in the model. The reasonable match between the experimental and simulated data suggests that the competitive adsorption of As with Ca, Si, CO_3^{2-} and PO_4^{3-} ions is well represented by the surface reactions and parameter values adopted (see Table 1). Calculated saturation indices indicate that the groundwater in the oxidizing sediments is supersaturated with respect to Fe(III) and Al(III) oxide minerals including ferrihydrite ($Fe(OH)_3$), geothite (FeOOH), magnetite (Fe_3O_4) and gibbsite ($Al(OH)_3$). This suggests potential for the precipitation of these minerals and therefore increased availability of adsorption sites. The groundwater is also slightly supersaturated with respect to $MnHPO_4$ (SI = 1.72). von Brömssen et al. (2008) suggest that the solubility of $MnHPO_4$ may control the availability of dissolved PO_4^{3-} that competes with As for adsorption sites

6.4.2. Adsorption isotherms

The sustainability of targeting the oxidized sediments as a source of As-safe drinking water is influenced by the capacity of these sediments to attenuate As in groundwater that may flow in from As-rich reduced aquifer sediments. The pattern of adsorption characteristics were understood by batch tests and adsorption isotherms were prepared for the three oxidized sediment samples by combining the sediments with

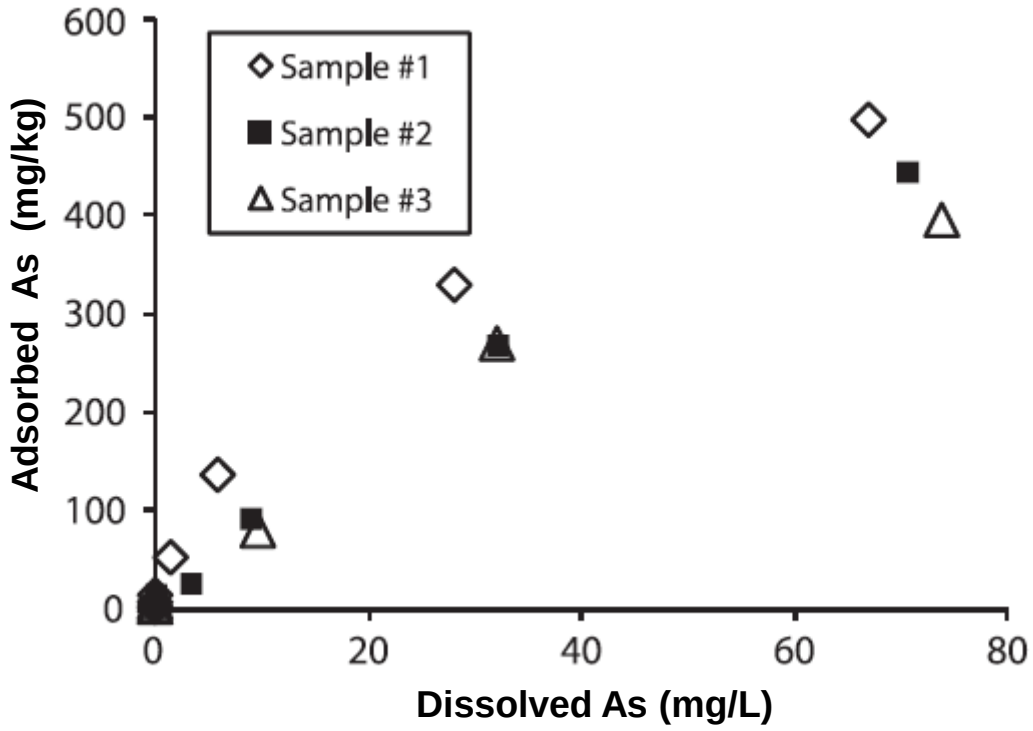

Figure 47. Measured As adsorption isotherms for Sample #1 (◇), Sample #2 (■), and Sample #3 (△).

As(V) solutions with low (0.2 - 1 mg/L) and high (5 - 100 mg/L) concentrations. The amount of adsorbed As(V) was quantified as the difference between the initial and final dissolved As(V). For all experiments with the low As(V) solutions more than 95% of the initial As(V) was adsorbed. Experiments conducted with high As(V) solutions produced similar isotherms for the three sediment samples (**Figure 47**).

The results indicate that the oxidized sediments have a high capacity to adsorb As(V) (>400–500 mg/kg). The sediments continued to adsorb As(V) even for the highest As(V) solutions, suggesting that the adsorption sites were not yet saturated. Although the experiments were performed only for As(V), aqueous As(III) if present in water flowing into the oxidized sediments, would give similar results the adsorption behaviour of As(III) and As(V) onto Fe(III) oxide minerals is similar at pH 6.5–8 (Dixit and Hering 2003). While the adsorption of As(V) to amorphous Fe(III) oxide minerals is higher than As(III) at low pH (below 5–6), the adsorption of As (III) is greater at a pH higher than 7–8 (Dixit and Hering 2003; Manning and Goldberg 1997, Goldberg 2002). Therefore, at the near-neutral groundwater pH conditions, the oxidized sediments is also expected to have significant capacity to adsorb aqueous As(III). For confirmation it is recommended that the adsorption isotherms for As(III) also be investigated in future studies.

Simulation of the adsorption isotherm experiments with the surface complexation model gave a poor match with the observed data. For all sediment samples, the model under-predicts the adsorption of As (V). For the maximum As(V) solution used, 100 mg/L, the model under-predicts the amount of adsorbed As by a factor of 12–14. The model adopted accounted only for adsorption to amorphous Fe(III) oxides (*Hfo*) and does not consider adsorption sites on Al(III) and Mn(IV) oxides, crystalline Fe(III) oxides nor clay minerals.

The poor match indicates that the number of active adsorption sites is greater than that associated with the amorphous Fe(III) oxides and these other minerals may

play an important role in the adsorption dynamics. The HNO3 extractions show that there is a much higher abundance of crystalline compared with amorphous Fe(III) oxides in the sediment (i.e., Fe_{Ox} = 0.09 - 0.13 g/kg compared to Fe_{HNO3} = 5.1 - 6.9 g/kg). Although the specific surface area and adsorption site density of crystalline Fe(III) oxides is typically lower than for amorphous Fe(III) oxides, this higher abundance may account for the significant number of adsorption sites associated with the crystalline minerals. The model developed has adopted the *Hfo* surface area and density of weak and strong adsorption sites recommended by Dzombak and Morel (1990). However, these characteristics could be site specific and may vary for the sediments on a spatial scale. It is therefore recommended that more detailed sediment characterization should be carried out in future including estimation of mineral surface areas and adsorption site density for assessing adsorption behaviour.

6.4.3. Column breakthrough study

The column experiments further illustrate the high capacity of the oxidized sediments to adsorb As (**Figure 48**). Over the 13 week period experimental runs, 90–99% of the influent As adsorbed to the sediments. The concentration of As in the influent water was approximately 1900 µg/L, and throughout the experiment the effluent As concentration ranged from 20–200 µg/L (**Figure 48a**).

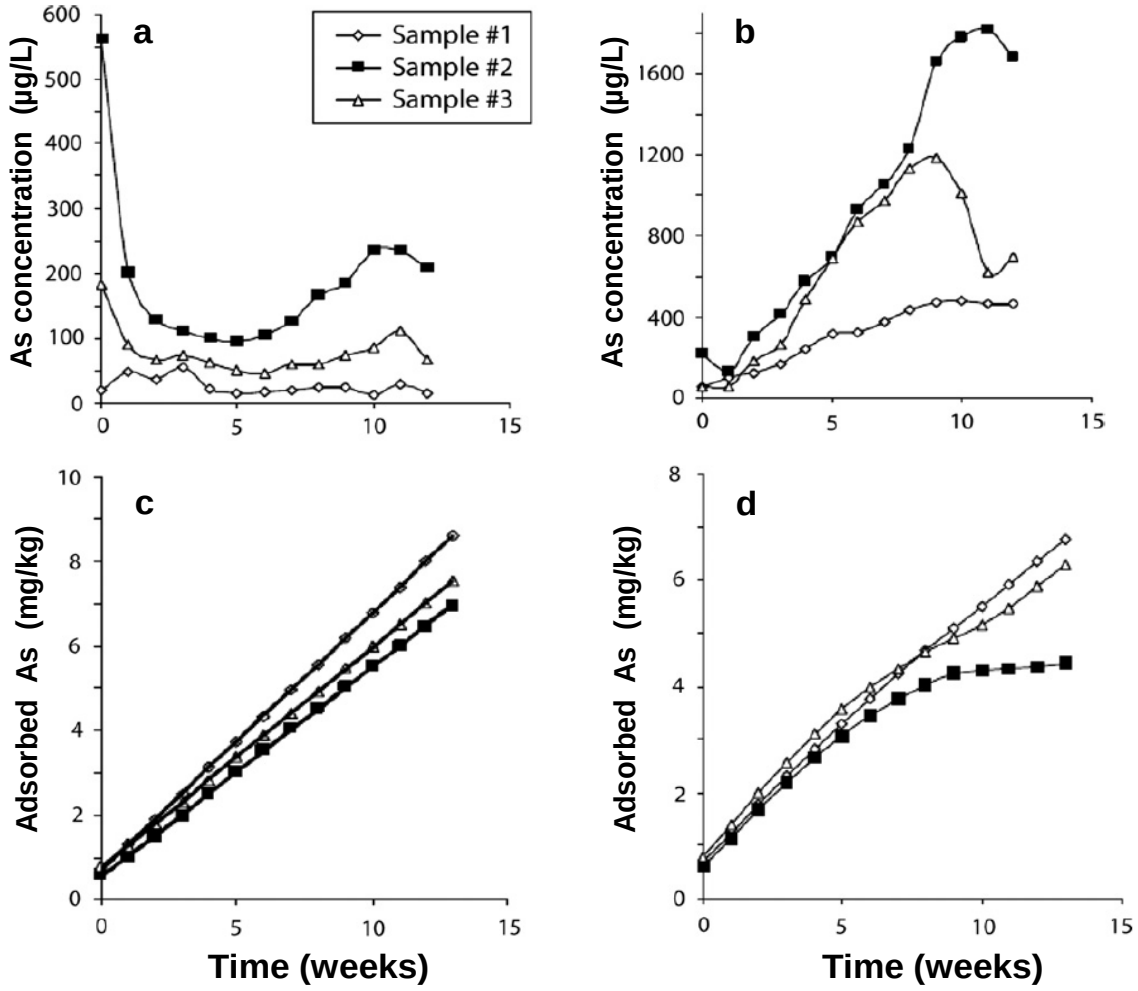

Figure 48. Plots showing the concentrations of As in the effluents and the calculated amount of As adsorbed to the oxidized sediment in the columns without lactose (a,c) as well with added lactose (b,d) over a 13 week experimental period.

The calculated adsorption of As with time is linear suggesting that the adsorption sites were not close to saturation (**Figure 48c**). The presence of As in the effluent despite the continued availability of adsorption sites may be associated with flow short-circuiting combined with kinetic constraints on the adsorption process The addition of lactose to the replicate columns demonstrates that the availability of an electron donor decreases the capacity of the oxidized sediments to adsorb As (**Figure 48b**). All sediment samples showed a lower adsorption capacity when lactose was present with the adsorption sites for Sample #2 reaching saturation after 9 weeks (**Figure 48d**).

The corresponding plots for the concentration of Fe, Mn, Ca and Si in the effluents from the columns with and without lactose additions are presented in **Figure 49a-d**. High dissolved Fe and Mn concentrations in the effluent indicate that the observed decrease in the adsorption capacity of the sediments was due to the reductive dissolution of Fe(III) and Mn(IV) oxides (**Figure 49a,b**).

In the columns with added lactose, the effluent concentrations of Fe and Mn were more than three orders of magnitude higher than for the columns without added lactose (**Figure 49a,b**). The maximum concentrations of Fe and Mn in Sample #2 indicate that the reductive dissolution of the oxide minerals was highest in this column. This corresponds with the saturation of adsorption sites observed for this column

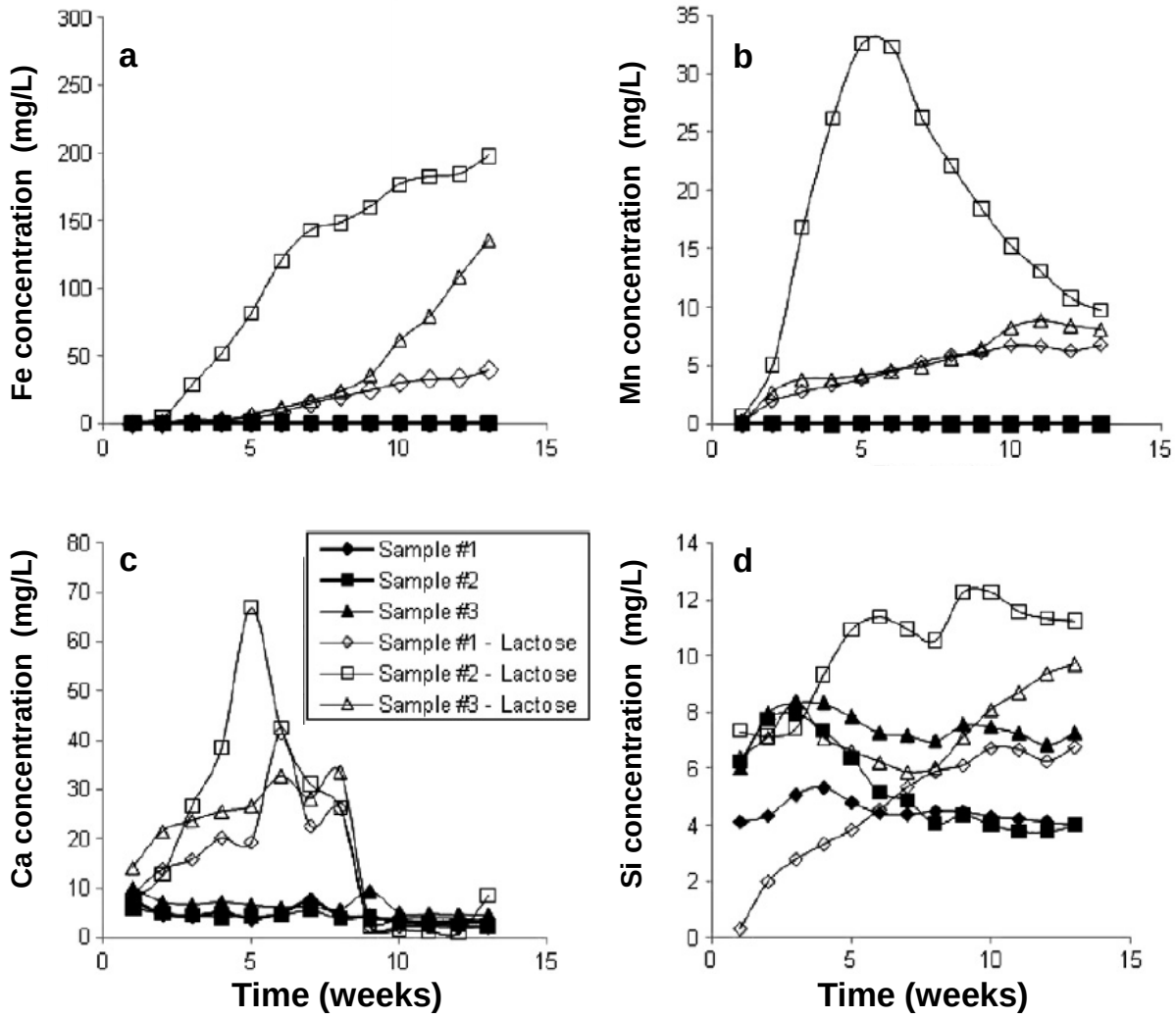

Figure 49. Plots showing the concentrations of a) Fe, b) Mn, c) Ca, and d) Si in the effluents from the columns over a 13 week experimental period.

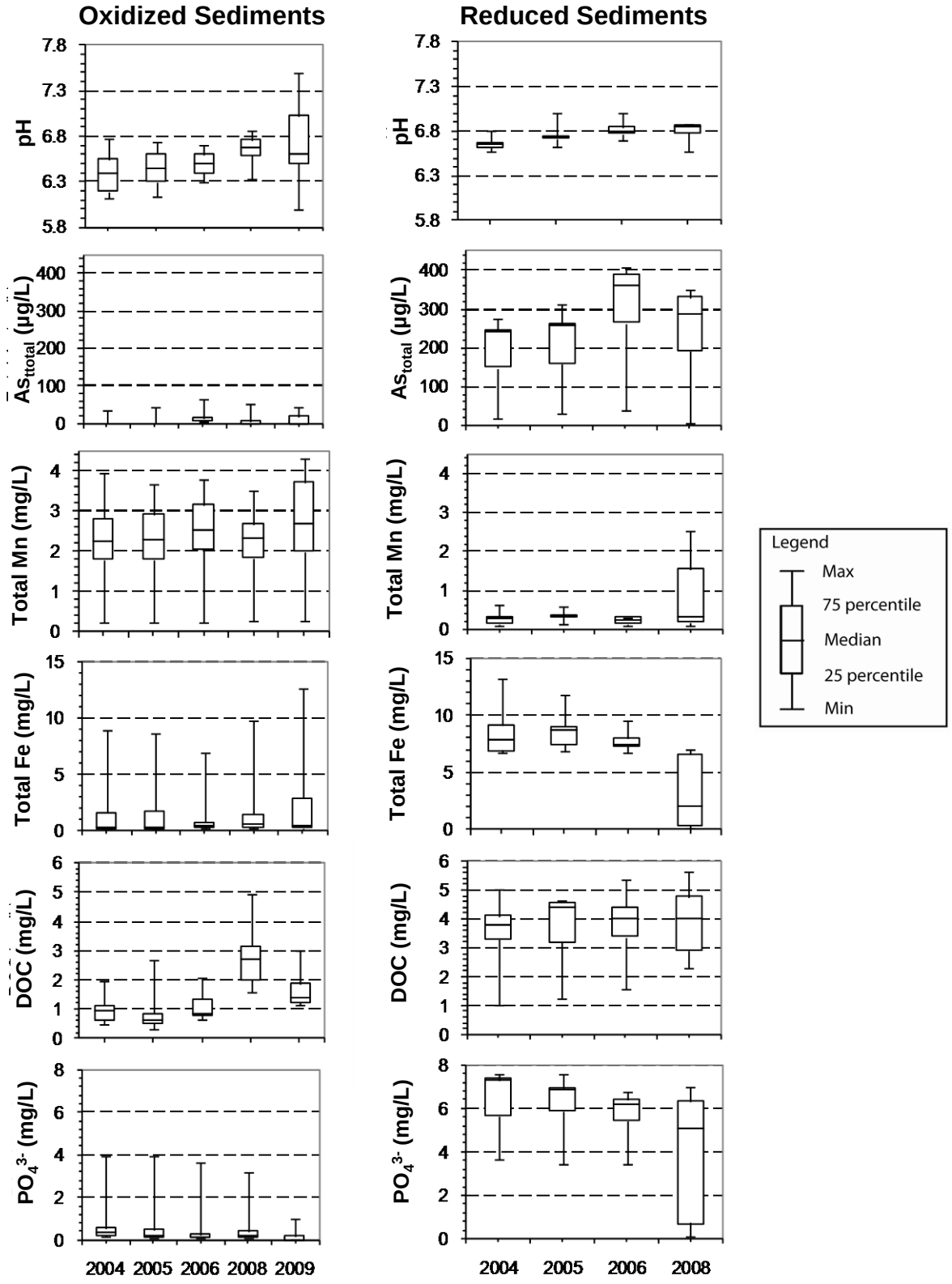

Figure 50. Box plots showing the temporal variations in major water chemistry parameters (pH, total As, total Mn, total Fe, DOC and PO_4^{3-}) in the oxidized sediments (left) and reduced sediments (right). Each tube-well water sample was classified as from oxidized or reduced sediment based on the sediment colour at the screened depth (see Table 3).

(see **Figure 49b**). The effluent concentrations of Ca and Si were also greater for the columns with lactose added, particularly for Sample #2. This suggests that these ions were released as Mn(IV) and Fe(III) oxides were reduced (**Figure 49c,d**). Reductive dissolution of Mn(IV) oxides should occur in preference to Fe(III) oxides in the sequence of redox reactions (Bhattacharya et al. 2002a, Appelo and Postma, 2005).

While the effluent concentrations indicate that this did occur for Sample #2, these reactions and the microbially mediated biogeochemical processes were perhaps common for all columns. The rates of reaction are however affected by the complex consortia of reducing microbes in the sediment as well as the relative stability of the specific Fe(III) and Mn(IV) oxide specie present. Although the reduction of Fe(III) and Mn(IV) oxides adds alkalinity (HCO_3^-) to the solution, the oxidation of lactose adds acidity (H^+). This leads to the effluent pH dropping to around 5 as compared to near-neutral for columns without lactose addition. While decreasing pH has been shown to reduce the adsorption of As(III) to Fe(III) oxides (Dixit and Hering, 2003, 2006), the effluent pH decrease does not account for the significant reduction in the observed adsorption capacity of the sediments.

6.4.4. Linking adsorption dynamics of arsenic with aquifer environments

Analysis of the tube-well water demonstrated that DOC concentrations are higher in the reduced sediments compared to the oxidized sediments (**Figure 50,** see also **Figure 32**). Infiltrating surface waters would also typically also have a much higher organic content (Harvey et al. 2006). As a result, these experiments show that if groundwater from reduced sediments, or alternatively surface waters, flows into the oxidized sediments, increased DOC availability will enhance the reductive dissolution of oxide minerals triggering the mobilization of As (Bhattacharya et al. 2002b, 2006a). The type and reactivity of C used in this column study is different to the complex organic matter that exists in natural aquifer systems. In natural aquifers the reductive dissolution of Fe(III) and Mn(IV) oxides by DOC will be strongly controlled by kinetics of the microbial processes. These kinetics and the type and reactivity of the organic matter available in the sediments needs to be further investigated to more accurately predict: i) the capacity of the oxidized sediments to attenuate dissolved As in the infiltrating water and, ii) the potential for the dissolution of Fe(III) and Mn(IV) oxides and subsequent release of sediment-bound As, in cases of cross-contamination.

Table 20. Distribution of microbial population in the sediments

Depth (m)	Sediment Color	Gram stain	Growth in As-media	Microbial species
12.7	Black	-ve	+ve	*Acinetobacter* spp.
25.4	Black	-ve	+ve	*Rhodococcus* spp.
25.4	Black	-ve	-ve	*Pseudomonas* spp.
25.4	Black	-ve	+ve	*Acinetobacter* spp.
25.4	Black	+ve	-ve	*Bacillus* spp.
42.4	Off-white/red	+ve	+ve	*Arthrobacter* spp.
45.9	Off-white/red	-ve	+ve	*Burkholderia* spp.
51.0	Off-white/red	+ve	+ve	*Exiguobacterium* spp.

6.5. Microbial characterization

6.5.1. Characterization of microorganisms

The colonies grown on Nutrient agar plates were analyzed for biochemical characterization. The colonies were grown on MacConkey agar and EMB agar media. The isolated colonies were mainly gram negative, facultative aerobes, rod shaped, oxidase negative and catalase positive. Most of the isolated colonies were grown in the presence of As. Some of the microbial isolates are *Pseudomonas* spp., *Acine-tobacter* spp., *Rhodococcus* spp., *Bacillus* spp., *Arthrobacter* spp., *Exiguobacterium* spp., *Burcholderia* spp. The gram negative organisms are in the upper sediments except *Bacillus* spp. (Table 20). Similar microbial species were identified and reported by Cai et al. (2009) from different As-contaminated sediments. Moreover, they have reported the presence of As resistant genes in the identified species.

In the lower sediments we found most of the gram positive organisms below 25.4 m. On the other hand in 45.9 m sediments gram negative organisms were dominant. There could be a difference in the sediment properties or other chemical redox cycling might be influencing the difference in the microbial distribution. Islam et al. (2005), reported microbial reduction of Fe (III) leading to the formation of different Fe (II) bearing minerals such as siderite, vivianite and magnetite which could be accompanied by the removal of As in solution. Further study is needed to characterize the microbial distribution immediately after the sample collection.

6.5.2. Potential relevance

The microbiological studies reveal presence of a variety of microbial species in the shallow Holocene aquifers of Matlab Upazila. Microbial distribution varies in the sediments with aquifer depths. Further work is required for understanding their role in the stability of the Fe- and Mn-oxyhyroxides and other biogeochemical interactions in the sediments, identification of the As-resistant genes and the specific role of the microbial population for bioremediation for compliance with the drinking water quality in accordance with the Water Safety Plan.

7. CONCEPT FOR TARGETING SAFE AQUIFER IN HIGH ARSENIC REGIONS

Although tubewell technology was introduced by governmental, non-governmental and international donor agencies, an estimated more than 10 million tubewells in Bangladesh and nearly 90% of these wells are installed privately by local drillers. In general, exploitation groundwater will increase for drinking purposes both in rural areas of Bangladesh as the practice of using tubewells is deep-rooted in the rural peoples' mind, and if local drillers could target safe aquifers, it would be a very viable option for As mitigation. The awareness of local drillers on elevated Fe and As concentrations in tubewell water at shallow depths have made them change their practice of tubewell installation. Using the visual colour attribute of the shallow sediments (<100 m) and content of dissolved iron, generally associated with high As concentrations, the local drillers presently install community tubewells at depths targeting red/brownish and/or off-white sediments (**Figure 51**).

Figure 51. Community initiative of the local driller for targeting safe sediments for tubewell installation in Bangladesh – the emergence of the "sediment colour concept".

The practice of installation of safe tubewells with local technique has already reached the affluent class of rural population. In order to develop and intensify this practice we are proposing a

strategy for the local drillers to target safe aquifers in regions with high As groundwater.

In order to identify safe aquifers and their sustainability and the risk for cross-contamination, comprehensive hydrogeological investigation, and sediment characteristics, prevailing biogeochemical processes responsible for mobilization and immobilization of As has been discussed in the light of the various outcomes and results of the research project TASA.

7.1. Perception of sediment color by local drillers

The boreholes drilled in Matlab using the traditional hand percussion technique (hand-flapping) confirmed the drillers' perception of the texture and colour of the sediments as well as identification of two separate lithological units. The local driller describe the aquifers in the region to comprise layers of black to grey sediments overlying a sequence of sediments with yellowish-grey to reddish-brown colour. A clay layer at depth between approximately 30-40 m demarcates these to aquifer units. A comparison between the drillers perception of the sediments and the Munsel colour code resulted in the four major colour groups; black, white, off-white and red as shown in **Figure 52**. Beside these four colours, the local drillers mention yellow, blue and green sediment, although the two later were uncommon according to them. Many drillers are not only aware of the As problem but they also target certain sediment for avoiding high Fe, which can be identified in field, and As based on the sediment colour. In an interview of 10 drillers Jonsson and Lundell (2004) found a consensus among the drillers that the black sediments were unsafe with respect to As while the other sediment colours were safe.

Undoubtedly ground-water exploitation will increase for drinking purposes both in rural and urban areas of Bangladesh and if local drillers could target safe aquifers, it would be a very viable option for As mitigation as the practice of using tubewells is deep-rooted in the rural peoples' mind. The awareness of local drillers on elevated Fe and As concentrations in tubewell water at shallow depth.

7.2. Relation between sediment colours and groundwater chemistry

Groundwater abstracted from the black sediments of the shallow Holocene aquifer is characterized by high concentrations of Fe, As, PO_4^{3-}-tot, NH_4^+, DOC and low SO_4^{2-}, whereas the oxidized low-As aquifers are characterized by high Mn, low NH_4^+ , DOC, Fe, and PO_4^{3-}-tot. Reductive dissolution of Fe (III)-oxyhydroxides in the reduced black to grey sediments mobilizes As in ground-

Drillers description and colour class	Black	White	Off-white	Red/Yellow
Munsell description	Olive black ↔ Dark greyish yellow	Grey ↔ Yellowish grey	Dark greyish yellow ↔ Olive yellow	Yellowish brown ↔ Reddish brown
Munsell code	5Y 3/1 ↔ 2.5 5/2	5Y 4/1 ↔ 2.5Y 5/3	2.5Y 4/2 ↔ 5Y 6/3	2.5Y 5/4 ↔ 5YR 3/4

Figure 52. Representative photographs of the field moist aquifer sediments and their colour described by local drillers as black, white, off-white and red and their Munsell colour cdescription and Munsell code representing each group.

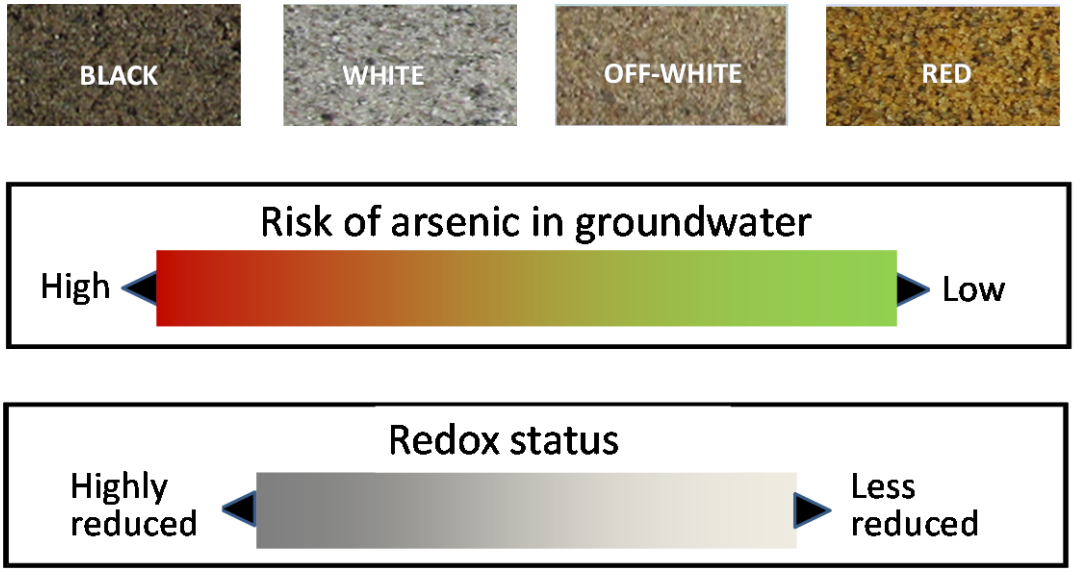

Figure 53. Conceptualization of the scenarios for the risk of arsenic in groundwater and the redox status of the aquifers based on the local drillers perception of sediment colours.

water. However, the present study also reveals high PO_4^{3-}-tot concentrations seems also to be an competing ion for adsorption sites thus facilitate the process of As mobilization.

Groundwater chemical composition correlated well with the colour of the aquifer sediments. Generally the groundwater is anoxic but redox conditions in the shallow aquifers (down to 100 m b.g.l.) follows a trend from very reducing conditions for black (as described by the drillers) sediments with increasing redox potential in sequence through white, off-white to red sediments. The scenarios for the risk of As in groundwater and the redox status of the aquifers based on the local drillers perception of sediment colours is conceptualized in **Figure 53**. Furthermore, the heterogenic distribution of elevated concentration of As has also been explained through the observed relationship between aqueous and solid phase geochemistry of the sediments in the study area.

The oxalate extractions showed that the Fe_{Ox}/Mn_{Ox}-ratio for the reducing black-greyish sediments were distinctively higher than for the oxidized unit. This demonstrates that amorphous Fe(III)-oxyhydroxides are more inclined to weathering and reduction than amorphous Mn oxides and hydroxides. Geochemical modelling revealed that Fe, Mn and PO_4^{3-} are influenced by formation of secondary minerals in addition to redox processes.

Elevated concentrations of dissolved Fe and Mn is prone to be generated through reductive dissolution of solid oxide- and hydroxide phases of Fe(III) and Mn(IV). High dissolved concentrations of both these elements would be expected in groundwater from the reducing aquifer unit as redox-conditions are sufficiently low and distinctively higher contents of amorphous Fe and Mn (Fe_{Ox} and Mn_{Ox}) are found in the reduced unit. However, dissolved Fe is higher in groundwater of the reduced unit while Mn concentration is relatively higher in the oxidized unit even though groundwater redox conditions and extractions of amorphous phases of Fe and Mn (Fe_{Ox}, Mn_{Ox}) suggests otherwise. Using geochemical models demonstrated that secondary phases e.g. rhodochrosite, siderite, vivianite, and possibly $MnHPO_4$, hydroxyapatite and Fe(III)-oxyhydroxides control the concentrations of these elements as well as PO_4^{3-}-tot in the aquifers. A

plausible behavior of Fe, Mn, As, PO_4^{3-}-tot, pH and HCO_3^- and their interactions at the solid-aqueous phase interface within the sediments could be explained through the results of geochemical modelling. Geochemical modelling based on experimental data demonstrated that the mobility of As is largely influenced by *Hfo*, pH and competing ions. In addition to reductive dissolution of Fe(III)-oxyhydroxides it is expected that relatively high PO_4^{3-}-tot concentrations compete for adsorption sites is stimulating As mobilization.

Decomposition of organic matter induce reductive dissolution of Fe(III)-oxyhydroxides and mobilization of As into the groundwater. Active reduction in the grey to dark grey aquifer is also indicated by the depletion of dissolved SO_4^{2-} and formation of authigenic pyrite. In the yellowish grey oxidized topsoil dominance of crystalline iron oxides and hydroxides like magnetite, hematite and goethite. Weathering of biotite seems to plays a crucial role for generation of Fe(III)-oxyhydroxide. The presence of amorphous Fe(III)-oxyhydroxides in the mica rich dark grey reduced sediment, mostly as grain coatings were revealed by SEM and XRD studies.

7.3. Adsorption dynamics of arsenic in oxidized sediments

Laboratory investigations on As adsorption dynamics demonstrates that the oxidized sediments have a high capacity to absorb As. For batch isotherm experiments As(V) was used because sampling of tube-wells indicate this is the dominant aqueous redox species in the oxidized sediments. It is suggested that the adsorption of As(III) is examined as well. Simulations of the experimental isotherms underpredict the adsorption capacity. This may indicate that that crystalline Fe(III) oxides, Mn(IV) oxides, Al(III) oxides and clay minerals may also contribute to the adsorption capacity of the sediment.

Column experiments on oxidized sediments with As(III) and lactose added to the influent water showed that the adsorption capacity may be reduced by high levels of DOC or other electron donors. The column experiments demonstrated that the decreased adsorption capacity was due to the reductive dissolution of Fe(III)-oxyhydroxides and Mn(IV)-oxides due to the microbial interactions induced by the addition of lactose. However, in natural aquifers with present DOC the reactions are expected to be much slower as DOC is a much more complex and may be refractive in character. The complex processes of adsorption however need further investigations on mineralogy, laboratory experiments together with geochemical modelling for accurate site specific prediction of the fate and dynamics of As in aquifers with high influx of DOC in groundwater.

7.4. Risks for cross-contamination between aquifers

7.4.1. Risks from hydrological perspectives and groundwater flow modelling

The groundwater models developed proved to be useful as a tool for enhancing the understating of the groundwater flow system when combined with field observations of seasonal hydraulic head monitoring in piezometer nests and ^{14}C analysis with subsequent dating of groundwater.

Hydrogeological field investigations and groundwater flow modelling demonstrated that Matlab acts essentially as a recharge area even though the area is adjacent to river Meghna. The groundwater simulations could identify at least two flow-systems; i) a deeper regional horizontal flow system with recharge areas at the Tripura Hills in the east and ii) small local flow systems driven by local topography and with local groundwater recharge. The local flow systems reach a depth of approximately 30 m b.g.l. in Matlab for calibrated groundwater models and is consistent with analyzed ^{14}C ages that indicate that young groundwater should be expected down to a depth of approximately 25 m b.g.l. while being older below (>1,000 yr). This demonstrates that the groundwater flow at depth (below local flow

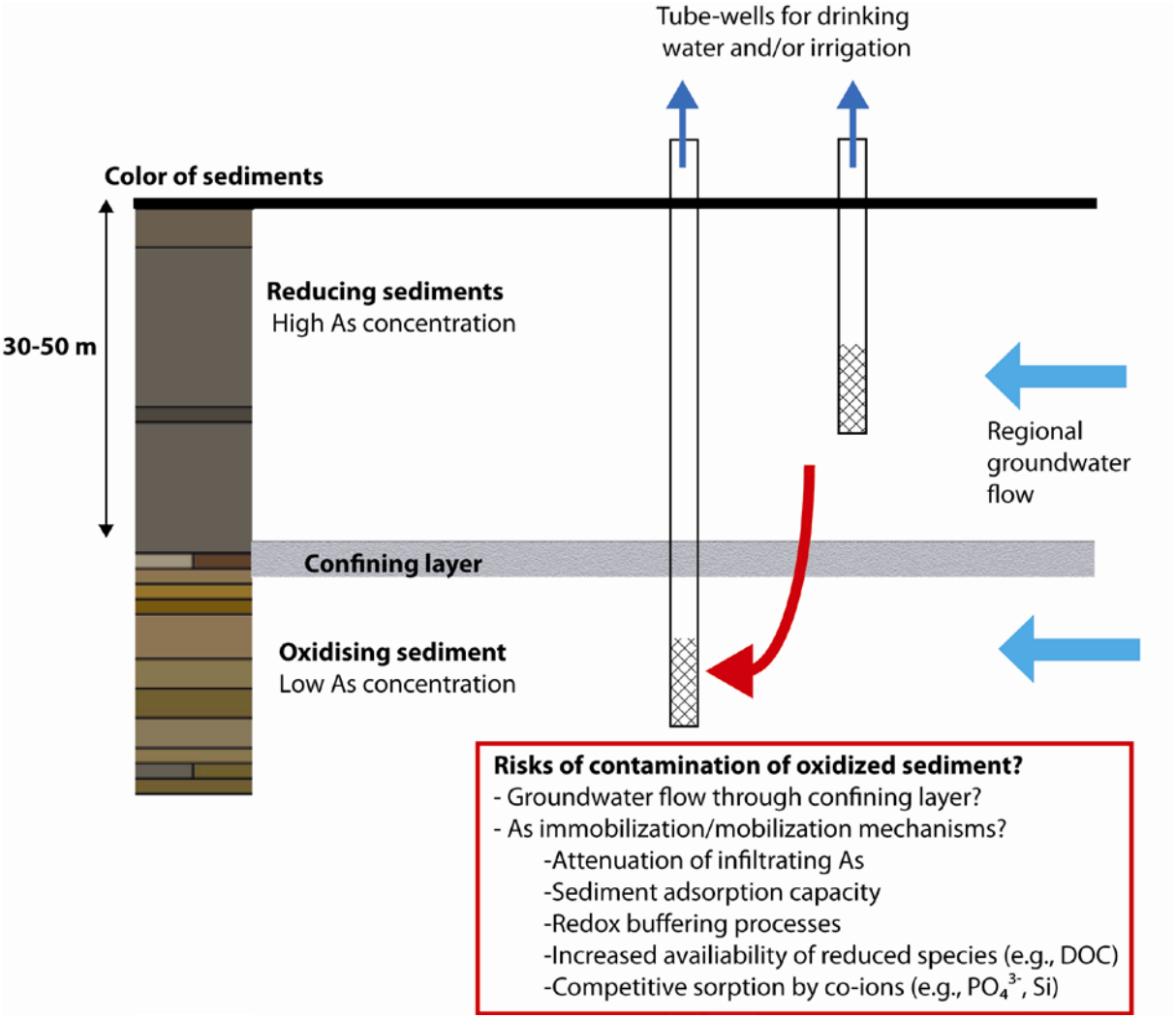

Figure 54. Conceptualized risk scenario for contamination of the oxidized aquifers in Matlab, southeastern Bangladesh.

system) for a natural and undisturbed system is very slow.

It has been estimated that about 85% of the groundwater abstraction is for the purpose of irrigation to support agricultural productivity especially for the cultivation of rice (Abedin et al. 2002, Halder et al. 2012). Irrigation pumps placed in clusters have implications on local flow dynamics and risk for cross-contamination. Although the aquifer system was fully recharged during and after the monsoon season, the effects of pumping during irrigation season were observed in the measured groundwater levels in piezometer nests. The observed downward vertical gradient in piezometer nests were consistent with modelling results. As deep irrigation wells are rarely installed, the vertical gradient appears to be controlled by the hydraulic characteristics of the aquifers. However the model demonstrated that the local flow patterns as well as induces substantial vertical flow due to continuous abstraction from the clusters of irrigation wells. The vertical flow and risk for cross-contamination will be concurrent to the abstraction rate. The cause of hydraulic head of certain deep piezometers being below the mean sea water level during the end of the heavy irrigation period are still unanswered but can only be a result of groundwater abstraction. In Matlab, a high yield three aquifer model to a depth of 250 m b.g.l. best fit field-observations.

7.4.2. Risks of cross-contamination of the oxidized aquifers based on adsorption modelling

The results through our studies as well as a series of other studies have shown that redox conditions and dissolved As concentration are related to the colour of the aquifer sediments (Bhattacharya et al. 2010, Bundschuh et al. 2010, Jonsson and Lundell 2004, von Brömssen et al. 2007, 2008). Overlying black–gray aquifer sediments tend to be reducing with high dissolved As levels. Off-white, yellowish and reddish sediments are oxidized at shallow depths (<100 m) with low risk of elevated As concentrations. However, there is concern that tube-wells installed in As-safe sediments may become enriched in As over time. Water abstraction from the As-safe sediments may induce flow of reduced groundwater from surrounding sediments with high As concentration or surface water that is rich in electron donors such as DOC to the As-safe aquifer zones (Polya and Charlet 2009) to the safe aquifer zones as conceptualized in **Figure 54**).

While the oxidized sediments may initially have a high capacity to adsorb As, this capacity may be reduced by the increased availability of electron donors that stimulate the reduction of Fe(III) and Mn(IV) oxides (Bhattacharya et al. 2009, Sharif et al. 2008, Stollenwerk et al. 2007). The reduction of these minerals may lead to the transfer of sediment-bound As to the groundwater. An increased availability of ions that compete with As for adsorption sites (e.g., PO_4^{3-}, Si, Ca, HCO_3^-) may also stimulate the release of sediment-bound As (Nath et al. 2009, Polya and Charlet, 2009). Understanding of the adsorption behaviour of the oxidized sediments and their ability to attenuate As if cross contamination occurs is, therefore, needed to evaluate the sustainability of targeting the shallow As-safe sediments. Although prior studies have examined the processes leading to As mobilization in the reduced sediments, there is limited understanding of the adsorption processes in the oxidized sediments.

This study has shown that the oxidized sediments in Matlab Region, have a high capacity to absorb As, although they currently have a relatively low sediment-bound As content (below 2.5 mg/kg). This suggests targeting these sediments for installation of tube-wells may be a simple sustainable solution for delivering safe drinking water to the rural communities in areas where these oxidized sediments exist at shallow depth. The As adsorption processes however are complex and require further investigation to more accurately assess the risks of cross-contamination. This assessment needs to be coupled with rigorous long-term monitoring of the water chemistry in tube-wells installed in the oxidized sediments. Discrepancy in the amount of solid phase Fe estimated from oxalate extractions and calibrated based on measured As(V) adsorption isotherms indicate that a significant portion of the adsorption sites in the oxidized sediments are associated with solid phase crystalline, rather than amorphous, Fe. The good match between the shape of the simulated and experimental adsorption isotherms, and the ability of the model to predict the amounts of As and other adsorbing species bound to the amorphous Fe minerals, indicate that the model and parameter values adopted was able to adequately represent the adsorption behaviour in the oxidized sediments. The capacity of the oxidized sediments to attenuate As may be decreased by high levels of DOC (or other electron donors) in water infiltrating the safe aquifer layers and this may lead to the reductive dissolution of Fe(III) and Mn(IV) oxides and the subsequent release of As. The reactivity and rate of degradation of the DOC present in the aquifer layers at Matlab requires further investigation.

8. TESTING THE IDEA FOR WORLDWIDE IMPLICATION

8.1. Replication study in West Bengal

For the validation of the ongoing indigenous drilling practice by local drillers in other parts of the Bengal Basin, this replication study was carried out in Chakdaha Block of

the Nadia district in West Bengal, India. A number of studies in West Bengal, India (McArthur et al. 2004, 2011, Pal and Mukherjee, 2008, 2009, Biswas et al. 2014a) have attempted to link the color of aquifer sediments with the occurrence of As in groundwater. It has been reported that grey sand aquifers (GSA) are mostly contaminated with dissolved As (>10 µg/L), whereas brown sand aquifers (BSA) may be safe (<10 µg/L). The classification of the aquifers as shallow grey sand aquifers (GSA) and the brown sand aquifers (BSA) within shallow depth (< 70 m) have shown all possible variability in the colour shades and analogous to the reducing and the oxidized sequences as delineated aquifers based on the sediment color as perceived by the local driller in Matlab. (von Brömssen et al. 2007). The BSA sediments analogous to the sequence of oxidized unit with red sand colours within shallow depth in Matlab study area has been suggested to be targeted for safe drinking water supply in Bangladesh (von Brömssen et al. 2007, Bundschuh et al. 2010). However, so far no attempt has been made to validate the redox status of these two aquifers, which could be extremely important for assessing the long term sustainability of BSA for safe drinking water supply.

8.2. Location of the study area

In order to validate the local drillers approach to target safe aquifers based on sediment colour, a detailed hydro-geochemical investigation was carried out to assess the redox status of groundwater abstracted from BSA and GSA aquifers within shallow depth (~70 m) within an area (100 km^2; 23.02–23.14°N, 88.49–88.62°E) is located approximately60 km north of Kolkata city, in the Chakdaha Block of Nadia district, West Bengal. The area is. bounded on the west by river Hooghly (distributaries of river Ganges) and by the river Ichamati to the east (**Figure 55**).

8.3. Groundwater sampling and analysis

Samples of groundwater were collected from 57 wells (35 from GSA and 22 from BSA) from the existing TWs at shallow depth (~70 m, except for 3 wells installed in BSA) close to 29 drilled borehole locations (**Figure 55**). Prior to groundwater sampling the TWs were purged continuously until pH, electrical conductivity (EC) temperature (T) and oxidation reduction potential (ORP, latter corrected with respect to standard hydrogen electrode for Eh) were stabilized. The pH, EC, T, ORP and dissolved oxygen (DO) were measured in a flow cell fitted with electrodes for ORP and DO (Biswas et al. 2012, 2014b) and the alkalinity (HCO_3^-) was measured by titrating with 0.02 N H_2SO_4 on site prior to groundwater sampling. From each TW four sets of groundwater samples were preserved after filtering through 0.45 µm Axiva® membrane filters for Fe(II), DOC, anion, major cation, trace elements and As(III) analyses. As(III) and (V) were separated in the field through a Disposable Cartridge® packed with an ion exchanger, at a flow rate of 5 mL/min (Metal Soft Centre, Highland Park, USA, Meng et al. (2001). The samples for quantification of As(III), major cations and trace elements were acidified with 14N, Suprapur HNO_3 (Merck). In the field all samples were stored in ice box and finally after return to the laboratory, samples were stored in refrigerator at 4°C prior to analyses.

To minimize redox alteration, Fe(II), NH_4^+ and anions were analyzed overnight after sampling following the procedure outlined APHA, 1998 and detailed in Biswas et al. (2012). The analysis of DOC was carried out on a Shimadzu 5000 TOC analyser at the KTH Royal Institute of Technology. Anions and NH_4^+ were analyzed in the same sample by Metrohm Ion Chromatography (model 761 Compact IC) at the University of Kalyani, West Bengal. Major cations and trace elements were analyzed by inductively coupled plasma optical emission spectrometer (ICP-OES, Varian Vista-PRO) at the Stockholm University. Ten percent of the samples (n=6) were randomly analyzed to test the precision of analysis by ICP-OES. For all the elements the precision of the analysis

was >97%. Total As as well as As(III) were also re-analyzed by hydride generation atomic absorption spectrometer (HG-AAS, Varian AA240, detection limit ~1 µg/L) following the procedure described by APHA (1998). The mutual agreement between As concentrations measured by ICP-OES and HG-AAS was >99% (p~0.01).

8.4. Sediment sampling and characterization

Based on drilling of 29 boreholes by locally available hand suction drilling technology The distribution of different aquifers (in terms of aquifer sediment color) within shallow depth of the investigated area (**Figure 55**). Though local drillers are very efficient to classify different colors of the sediment, there is still risk of misidentification (von Brömssen et al. 2007). In order to minimize this risk, aquifers within shallow depth were classified according to two major sediment color categories: viz grey and brown. Soon after their recovery from the borehole, prior to atmospheric oxidation, sediment form each 1.5 m interval was assigned either grey or brown color in the field by looking into the washed sediment in consultation with the local driller.

8.5. Hydrochemical characteristics

The physico-chemical characteristics, major ion composition and the water types of the groundwater samples collected from GSA and BSA are presented in Table 21.

8.5.1. Physicochemical characteristics

In both aquifers groundwater has circum-neutral pH (6.87–7.48) with similar temperature range (26.3–28.2 °C). The ranges of electrical conductivity (BSA: 501–935 µS/cm, median: 663 µS/cm; GSA: 356–1177 µS/cm, median: 715 µS/cm) suggest roughly similar extents of water-sediment interactions in both aquifers.

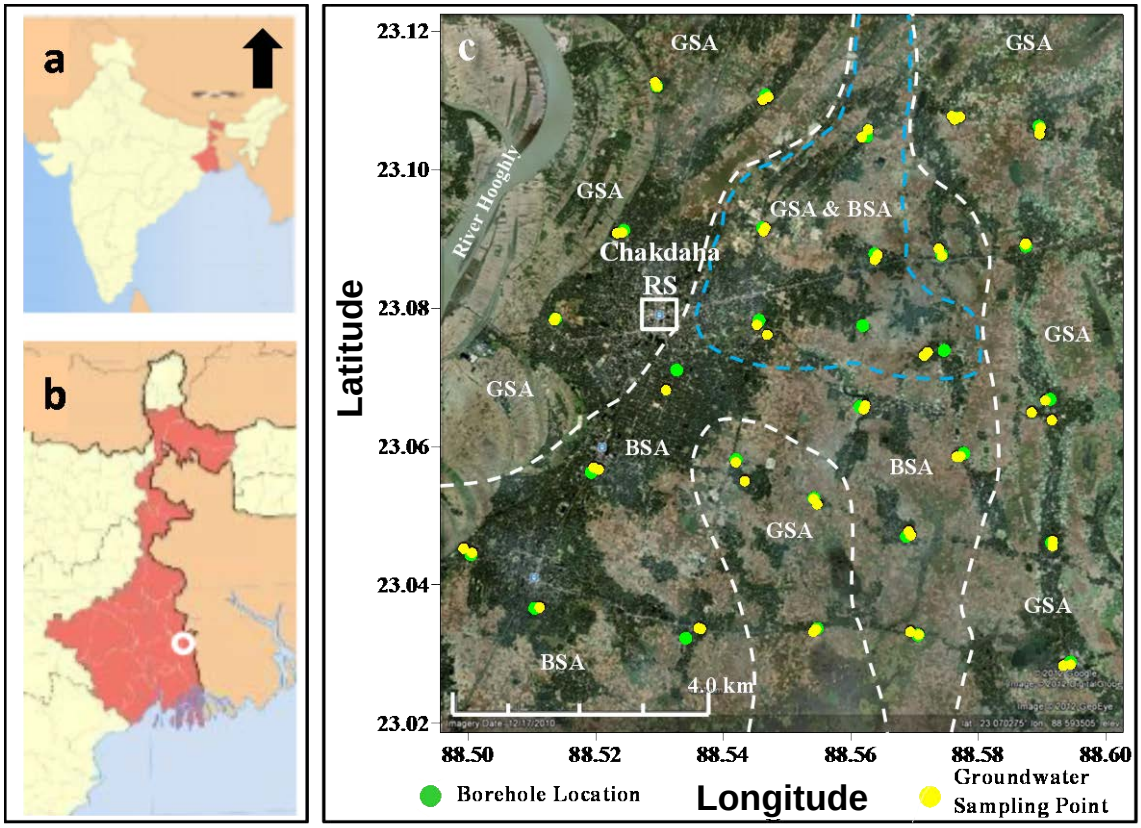

Figure 55. Map of the study area in Chakdaha Block, Nadia District. West Bengal, India (a-c) showing the distribution of GSA and BSA aquifers demarcated by white dashed line. The area with in the blue dashed line represents, where GSA overlies the BSA. The satellite image (c) was acquired from Google Earth 6.0.2.

Table 21. Salient physico-chemical characteristics and major ion compositions of groundwater samples collected from grey sand aquifer (GSA) and brown sand aquifer (BSA) of Chakdaha Block Nadia District, West Bengal, India.

Sample ID	Latitude	Longitude	Depth (m)	pH	Eh (mV)	EC (µS/cm)	T (°C)	HCO_3 (mg/L)	Cl^- (mg/L)	SO_4^{2-} (mg/L)	PO_4^{3-} (mg/L)	Ca^{2+} (mg/L)	Mg^{2+} (mg/L)	Na^+ (mg/L)	K^+ (mg/L)	Water Type
Grey sand aquifers (GSA)																
HG06	23.0336	88.5546	43	7.14	129	659	27.4	400	5.93	0.06	1.58	106	20.0	27.4	2.53	Ca-Mg-HCO_3
HG07	23.0332	88.5541	16	7.06	115	816	26.5	424	46.1	1.91	3.74	112	19.3	49.6	5.17	Ca-Na-HCO_3
HG10	23.0283	88.5933	28	7.11	91.8	775	26.9	466	47.8	0.14	5.83	134	33.4	22.5	6.19	Ca-Mg-HCO_3
HG11	23.0285	88.5945	22	7.16	103	715	27.2	450	17.7	0.13	4.75	125	28.9	16.2	4.42	Ca-Mg-HCO_3
HG12	23.0463	88.5917	19	7.26	133	838	26.3	500	35.6	3.71	4.60	118	31.6	50.7	4.38	Ca-Mg-Na-HCO_3
HG13	23.0456	88.5917	22	7.19	114	887	26.6	514	47.8	4.68	5.78	140	39.5	31.6	3.91	Ca-Mg-HCO_3
HG14	23.0477	88.5691	52	7.39	169	571	27.6	364	4.07	0.06	0.09	86.2	26.6	16.8	3.90	Ca-Mg-HCO_3
HG18	23.0516	88.5547	22	7.24	124	582	27.0	326	24.2	1.20	2.18	81.4	20.4	26.6	1.83	Ca-Mg-HCO_3
HG19	23.0524	88.5542	30	6.96	134	829	27.4	470	40.8	3.16	2.07	132	28.7	32.7	2.58	Ca-Mg-HCO_3
HG20	23.055	88.5434	46	7.17	154	588	27.1	374	3.71	0.08	0.76	91.3	20.2	22.4	2.17	Ca-Mg-HCO_3
HG21	23.0577	88.542	46	7.10	164	685	27.2	400	18.4	0.09	3.22	98.5	29.4	22.7	1.83	Ca-Mg-HCO_3
HG22	23.0776	88.5453	22	7.21	358	687	26.3	378	28.9	9.57	1.30	107	25.2	22.4	2.24	Ca-Mg-HCO_3
HG28	23.0667	88.5905	22	7.05	133	1062	27.4	528	85.8	13.1	4.66	135	34.5	56.8	10.1	Ca-Mg-Na-HCO_3
HG29	23.0638	88.5915	22	7.07	133	672	27.4	370	24.5	0.26	6.75	88.5	17.9	23.6	9.20	Ca-Mg-HCO_3
HG30	23.0649	88.5884	28	7.24	135	658	27.1	370	20.0	1.20	3.71	90.8	23.6	15.2	10.1	Ca-Mg-HCO_3
HG32	23.0731	88.5715	22	7.14	163	691	27.2	420	6.98	0.14	2.27	96.9	26.4	26.7	2.67	Ca-Mg-HCO_3
HG33	23.1053	88.5896	28	7.26	110	607	26.4	350	14.5	BDL	5.33	86.6	24.3	13.7	6.17	Ca-Mg-HCO_3
HG34	23.1051	88.5896	52	7.26	108	633	26.8	380	9.57	0.08	6.12	93.1	25.1	14.5	4.29	Ca-Mg-HCO_3
HG35	23.1061	88.5898	22	7.28	111	813	26.4	460	29.5	0.06	4.33	131	31.4	17.0	7.58	Ca-Mg-HCO_3
HG36	23.0893	88.5875	61	7.17	124	909	27.0	438	82.6	0.41	5.72	130	33.0	28.9	5.91	Ca-Mg-HCO_3-Cl
HG37	23.0892	88.5874	22	7.11	132	978	27.1	490	90.3	0.30	5.07	139	32.5	38.6	4.55	Ca-Mg-HCO_3-Cl
HG38	23.1078	88.5758	46	7.34	222	548	27.1	340	11.3	0.05	1.34	88.2	19.5	10.5	5.35	Ca-Mg-HCO_3
HG39	23.1076	88.5771	34	7.46	173	502	27.2	310	3.01	0.08	1.85	87.6	16.2	6.83	3.06	Ca-Mg-HCO_3
HG40	23.1073	88.5763	40	7.46	193	356	27.5	214	1.26	0.06	2.16	53.6	11.9	6.07	3.64	Ca-Mg-HCO_3
HG44	23.087	88.5638	22	6.87	184	922	27.0	594	4.94	0.37	6.29	112	33.3	50.0	4.16	Ca-Mg-Na-HCO_3
HG46	23.0916	88.5466	25	7.15	175	873	27.4	492	40.8	0.13	5.44	138	34.0	17.5	3.07	Ca-Mg-HCO_3
HG48	23.1047	88.5617	14	7.10	170	839	26.8	506	21.7	0.80	6.18	117	38.7	19.7	4.45	Ca-Mg-HCO_3
HG49	23.1101	88.5462	22	7.42	150	647	26.6	348	21.2	21.1	1.19	104	21.9	18.9	4.20	Ca-Mg-HCO_3
HG50	23.1105	88.5471	22	7.38	175	634	27.2	368	12.1	10.2	1.11	98.0	24.4	14.1	4.91	Ca-Mg-HCO_3
HG51	23.112	88.5296	14	7.27	134	963	27.0	448	94.6	26.2	0.89	152	32.2	29.4	5.99	Ca-Mg-HCO_3-Cl
HG52	23.1126	88.5293	22	7.48	136	654	27.0	392	6.33	8.22	1.34	112	22.1	14.8	4.73	Ca-Mg-HCO_3
HG53	23.0908	88.5233	22	7.07	136	1177	27.6	576	95.8	26.2	3.87	153	50.5	50.7	5.64	Ca-Mg-HCO_3
HG54	23.0909	88.5242	30	7.18	102	960	27.2	498	1.34	26.2	4.92	142	36.4	31.0	4.83	Ca-Mg-HCO_3
HG55	23.0782	88.5134	27	7.20	100	764	27.1	468	3.40	0.05	4.54	108	29.1	21.5	4.71	Ca-Mg-HCO_3
HG56	23.0786	88.5137	30	7.26	100	727	27.3	456	3.15	0.05	3.61	106	27.7	20.3	3.97	Ca-Mg-HCO_3
Min				6.87	91.8	356	26.3	214	1.26	BDL	0.09	53.6	11.9	6.07	1.83	
Median				7.19	134	715	27.1	424	20.0	0.30	3.74	108	27.7	22.4	4.42	
Max				7.48	358	1177	27.6	594	95.8	26.2	6.75	153	50.5	56.8	10.1	
Brown sand aquifers (GSA)																
HG01	23.0446	88.50058	75	7.00	131	704	28.2	414	7.14	6.14	0.26	107	24.9	38.8	4.34	Ca-Mg-Na-HCO_3
HG02	23.0453	88.49925	82	7.21	128	711	28.0	442	5.50	0.52	0.20	94.1	24.8	49.9	4.34	Ca-Mg-Na-HCO_3
HG03	23.0368	88.51119	72	7.11	141	769	27.7	480	6.45	0.32	0.07	118	28.0	39.6	4.75	Ca-Mg-HCO_3
HG04	23.0336	88.53647	50	7.10	208	700	27.7	418	10.1	0.07	0.12	103	25.4	34.6	2.95	Ca-Mg-HCO_3
HG05	23.0338	88.53614	37	7.07	234	746	27.4	452	13.1	0.08	0.19	104	27.5	43.8	2.99	Ca-Mg-Na-HCO_3
HG08	23.0328	88.57067	40	7.02	268	547	27.0	400	7.76	0.07	0.05	103	25.9	26.7	2.30	Ca-Mg-HCO_3
HG09	23.0332	88.56933	46	7.09	244	559	27.6	392	9.09	0.06	BDL*	105	27.2	16.7	2.54	Ca-Mg-HCO_3
HG15	23.0472	88.56939	46	7.25	210	535	27.0	326	3.97	0.18	BDL	80.2	19.6	23.3	2.17	Ca-Mg-HCO_3
HG16	23.0567	88.52044	46	7.18	248	600	27.2	380	6.24	0.11	0.05	95.2	22.7	21.1	2.24	Ca-Mg-HCO_3
HG17	23.0569	88.51964	46	7.13	255	669	27.0	420	11.3	0.52	0.13	102	26.3	24.9	2.11	Ca-Mg-HCO_3
HG23	23.0761	88.54689	52	7.21	251	896	26.8	556	17.6	0.07	0.14	152	29.3	35.1	2.64	Ca-Mg-HCO_3
HG24	23.0654	88.56206	49	7.14	222	601	27.6	378	8.47	0.09	BDL	87.4	24.0	21.6	2.27	Ca-Mg-HCO_3
HG25	23.0659	88.56225	40	7.20	237	586	27.7	360	4.65	0.12	BDL	88.4	23.8	17.5	2.15	Ca-Mg-HCO_3
HG26	23.0585	88.57661	55	7.14	260	722	28.1	440	6.53	0.06	0.49	106	25.7	30.6	2.43	Ca-Mg-HCO_3
HG27	23.0586	88.57719	50	7.19	259	935	27.5	598	6.64	0.09	0.49	149	36.2	37.0	2.58	Ca-Mg-HCO_3
HG31	23.0736	88.57206	46	7.39	315	501	27.3	298	3.35	0.06	0.32	74.6	19.1	16.1	1.68	Ca-Mg-HCO_3
HG41	23.0876	88.57431	46	7.23	262	657	27.3	406	4.58	0.06	0.15	103	21.1	27.7	1.73	Ca-Mg-HCO_3
HG42	23.0886	88.57381	37	7.24	276	653	27.4	410	4.42	0.05	BDL	106	21.2	23.7	1.70	Ca-Mg-HCO_3
HG43	23.0877	88.56419	46	7.20	273	728	27.4	468	3.88	0.13	0.15	103	21.1	45.3	1.56	Ca-Na-Mg-HCO_3
HG45	23.0911	88.54631	46	7.23	271	657	27.6	420	2.68	0.19	BDL	91.6	27.6	29.4	2.34	Ca-Mg-HCO_3
HG47	23.1058	88.56269	52	7.24	284	589	27.8	372	2.98	0.05	0.10	95.5	23.3	12.2	1.58	Ca-Mg-HCO_3
HG57	23.0681	88.53100	34	7.24	174	776	26.7	480	19.7	12.3	0.24	105	44.4	12.7	3.96	Ca-Mg-HCO_3
Min				7.00	128	501	26.7	298	2.68	0.05	BDL	74.6	19.1	12.2	1.56	
Median				7.20	249	663	27.5	416	6.49	0.09	0.12	103	25.2	27.2	2.32	
Max				7.39	315	935	28.2	598	19.7	12.3	0.49	152	44.4	49.9	4.75	

The DO concentration was consistently below detection limit (BDL) in all groundwaters from BSA and GSA. The comparison of observed pe values (calculated from measured Eh), and the pe values calculated from corresponding Fe(III)/Fe(II) and As(V)/As(III) redox couples reveals that the observed pe values for the samples of BSA and GSA fall respectively along the upper and lower end of calculated pe range of the Fe(III)/Fe(II) redox couple (Biswas et al. 2012).

8.5.2. Major ion chemistry and hydrochemical facies

The groundwater in both GSA and BSA aquifers is predominantly of Ca–Mg–HCO_3 type. However, other hydrochemical facies such as Ca-Mg-HCO_3-Cl, Ca-Mg-Na-HCO_3 and Ca-Na-Mg-HCO_3 are also sometimes present due to the local enrichment of particular ion species. Thee major ion concentrations in groundwater in the two GSA and BSA aquifers did not show any significant difference, except for enrichment of K^+ with respective median values of 4.42 mg/L and 2.32 mg/L in GSA and BSA groundwaters. Though in Bangladesh, von Brömssen et al. (2007) have reported the enrichments of HCO_3^- in groundwater of GSA, this study the concentrations are similar in both aquifers (**Figure 56a**).The level of Cl^- in the GSA groundwater was elevated by a factor more than 2.5 with median value of 18.4 mg/L to the median value of 6.49 mg/L in BSA samples. The enrichment of Cl^- in GSA is also consistent with relatively higher EC in this aquifer. The concentration of SO_4^{2-} in GSA varies from below detection levels to 26.2 mg/L and a median value of 0.30mg/L (**Figure 56b**). Strong pungent odor of hydrogen sulphide (H_2S) in few wells from GSA was noticed during sampling. The levels of SO_4^{2-} in the BSA aquifers were consistently low in the range 0.05 to 12.1 mg/L (median: 0.09 mg/L, Table 22) and consistent with the absence of the odor of H_2S noted during sampling of the BSA wells. Although SO_4^{2-} reduction is not entirely responsible for low SO_4^{2-} concentration in groundwater of the study area, the presence of sulphide minerals in the aquifer sediment might also limit initial concentration of SO_4^{2-} in groundwater (Mukherjee and Fryar 2008).

8.5.3. Distribution of redox sensitive species

Data on the distribution of the redox sensitive species and Si in groundwaters from wells screened in from GSA and BSA are presented in Table 22.

8.5.3.1. Arsenic (As)

In nearly 32 (91%) and 19 (54%) (n=35) groundwater samples collected from the GSA wells, As concentration above the WHO safe drinking water guideline value of 10 µg/L and Indian national drinking water standard of 50 µg/L respectively (Figure . 4). The median value (54.3 µg/L) is higher than both WHO guideline and national standard. However, in only 1 of 22 samples collected from BSA, the dissolved As concentration exceeds 10 µg/L (**Figure 56h**).

In GSA, As is predominantly present as As(III) accounting for 75–100% of total As in the water samples (median 95.6%), whereas for samples collected from BSA, when As concentration exceeds instrumental detection limit is mostly present as As(V) (Table 22).

8.5.3.2. Iron (Fe) and manganese (Mn)

Following the same trend the groundwater of GSA is also more enriched with dissolved Fe ranging between 0.82 and 11.3 mg/L (median: 5.31 mg/L) as compared to the BSA wells where the concentration levels in groundwater are distinctly low and vary between 0.24 and 2.87 mg/L an a median value of 0.44 mg/L) (**Figure 56f**). Though, in both aquifers the total Fe (Fe_{tot}) is predominantly present as Fe(II) species in the GSA water samples (range: 84.1-100%, median: 94.5%), in BSA the range is lower (36.6–97.2%, median: 71.2%, see Table 22).

The concentration levels of dissolved Mn in groundwater follows the opposite trends as compared to As and Fe. Out of the 35 samples only 17% (n=6) and 20% (n=7) GSA wells, Mn concentration was found to be above former WHO guideline value of 400 µg/L and Indian national drinking water standard of 300 µg/L respectively. However

Table 22. Distribution of the redox sensitive species and Si in groundwater from wells screened in grey sand aquifer (GSA) and brown sand aquifer (BSA) of Chakdaha Block Nadia District, West Bengal, India.

Sample ID	Latitude	Longitude	Depth (m)	As (µg/L)	As (III) (%)	Fe (mg/L)	Fe (II) (%)	Mn (µg/L)	Al (µg/L)	DOC (mg/L)	NH_4^+ (mg/L)	Si^{4+} (mg/L)
Grey sand aquifers (GSA)												
HG06	23.0336	88.5546	43	53.5	99.3	3.47	91.6	119	17.7	1.55	0.35	14.0
HG07	23.0332	88.5541	16	30.7	98.4	6.81	97.7	113	16.6	3.26	4.30	10.0
HG10	23.0283	88.5933	28	137	99.3	9.19	98.4	231	14.7	3.99	4.43	11.0
HG11	23.0285	88.5945	22	104	91.1	8.30	93.7	156	13.9	2.59	4.04	10.5
HG12	23.0463	88.5917	19	38.1	96.6	4.81	92.9	107	13.2	1.67	2.48	9.65
HG13	23.0456	88.5917	22	49.6	99.6	6.24	97.3	113	12.3	3.00	3.16	10.8
HG14	23.0477	88.5691	52	45.1	96.7	0.82	98.8	123	14.1	1.32	0.43	14.9
HG18	23.0516	88.5547	22	26.9	98.5	1.71	95.3	115	25.7	0.27	1.83	8.42
HG19	23.0524	88.5542	30	46.7	90.8	4.09	84.1	278	30.2	2.43	1.62	9.20
HG20	23.055	88.5434	46	70.3	94.0	2.52	94.8	177	21.7	0.54	0.82	9.90
HG21	23.0577	88.542	46	4.40	75.0	4.57	89.3	124	38.6	0.91	1.78	9.28
HG22	23.0776	88.5453	22	9.16	94.3	2.67	88.4	438	25.3	0.81	0.97	7.78
HG28	23.0667	88.5905	22	67.7	86.0	10.9	100	255	27.6	5.87	3.46	10.3
HG29	23.0638	88.5915	22	83.2	82.0	10.0	100	404	29.2	2.22	6.26	11.2
HG30	23.0649	88.5884	28	54.3	86.4	6.41	94.9	436	21.9	1.40	0.70	8.06
HG32	23.0731	88.5715	22	101	88.6	3.06	91.5	90.8	25.9	7.10	3.20	10.7
HG33	23.1053	88.5896	28	83.4	95.6	5.27	88.8	97.6	24.1	0.39	2.22	10.7
HG34	23.1051	88.5896	52	113	83.6	6.01	95.0	123	23.8	0.34	3.45	11.1
HG35	23.1061	88.5898	22	49.0	86.7	6.00	94.8	203	22.8	1.29	0.94	10.2
HG36	23.0893	88.5875	61	66.0	97.7	6.75	92.3	155	28.5	1.94	3.60	10.8
HG37	23.0892	88.5874	22	56.9	96.8	7.22	99.3	191	22.2	2.06	4.36	10.5
HG38	23.1078	88.5758	46	19.9	96.5	2.92	90.4	295	22.3	BDL	0.99	9.04
HG39	23.1076	88.5771	34	24.3	93.8	2.20	89.5	246	14.4	BDL	BDL	8.17
HG40	23.1073	88.5763	40	29.1	91.1	1.68	84.5	149	23.6	4.61	0.57	8.85
HG44	23.087	88.5638	22	92.5	99.2	5.31	96.2	111	23.2	3.71	6.26	12.4
HG46	23.0916	88.5466	25	71.6	97.3	9.76	99.8	167	21.4	1.91	3.72	11.3
HG48	23.1047	88.5617	14	147	100	6.02	92.9	121	16.4	0.55	5.93	10.2
HG49	23.1101	88.5462	22	16.6	91.0	4.20	91.9	426	26.6	BDL	0.32	6.54
HG50	23.1105	88.5471	22	8.46	92.9	3.06	94.1	239	14.7	BDL	0.23	5.88
HG51	23.112	88.5296	14	20.1	86.6	4.78	92.9	550	28.5	0.22	0.42	7.60
HG52	23.1126	88.5293	22	40.8	90.4	2.23	89.7	511	23.1	BDL	0.33	8.23
HG53	23.0908	88.5233	22	71.9	97.8	11.3	98.2	383	28.1	0.79	1.57	9.59
HG54	23.0909	88.5242	30	85.8	96.6	9.63	98.8	256	14.5	0.34	2.74	10.4
HG55	23.0782	88.5134	27	308	99.7	10.9	94.5	152	25.6	0.70	4.96	9.86
HG56	23.0786	88.5137	30	293	98.0	10.6	97.2	193	27.8	1.33	2.97	9.72
Min				4.40	75.0	0.82	84.1	90.8	12.3	BDL	BDL	5.88
Median				54.3	95.6	5.31	94.5	177	23.1	1.32	2.22	10.0
Max				308	100	11.3	100	550	38.6	7.10	6.26	14.9
Brown sand aquifers (GSA)												
HG01	23.0446	88.50058	75	BDL	-	1.19	82.4	985	38.6	4.71	BDL	13.4
HG02	23.0453	88.49925	82	BDL	-	1.12	89.3	1030	22.2	1.53	0.90	13.7
HG03	23.0368	88.51119	72	BDL	-	1.07	97.2	830	17.6	2.56	0.43	14.7
HG04	23.0336	88.53647	50	BDL	-	0.24	83.3	1504	13.3	1.79	0.75	11.6
HG05	23.0338	88.53614	37	BDL	-	0.24	91.7	754	13.9	2.22	0.81	11.2
HG08	23.0328	88.57067	40	BDL	-	0.28	53.6	691	13.6	2.02	BDL	11.5
HG09	23.0332	88.56933	46	BDL	-	0.30	76.7	593	13.7	1.83	BDL	11.7
HG15	23.0472	88.56939	46	BDL	-	0.41	82.9	183	19.7	0.61	BDL	10.5
HG16	23.0567	88.52044	46	BDL	-	0.72	73.6	1073	26.8	1.06	0.60	11.7
HG17	23.0569	88.51964	46	7.40	0.0	0.53	77.4	1782	23.2	0.79	0.53	11.9
HG23	23.0761	88.54689	52	BDL	-	0.49	57.1	2082	14.8	1.86	0.48	9.39
HG24	23.0654	88.56206	49	BDL	-	0.50	76.0	351	26.0	0.66	0.40	10.5
HG25	23.0659	88.56225	40	BDL	-	0.49	59.2	323	32.9	0.58	0.36	10.4
HG26	23.0585	88.57661	55	8.69	94.6	0.32	68.8	1960	28.4	1.59	0.82	11.9
HG27	23.0586	88.57719	50	3.68	0.0	0.40	55.0	2337	26.4	1.97	0.77	11.1
HG31	23.0736	88.57206	46	2.24	0.0	0.42	61.9	870	25.9	BDL	BDL	10.5
HG41	23.0876	88.57431	46	BDL	-	0.62	67.7	886	18.8	0.12	BDL	10.4
HG42	23.0886	88.57381	37	BDL	-	0.45	44.4	541	19.5	3.78	BDL	10.7
HG43	23.0877	88.56419	46	BDL	-	0.41	36.6	1050	21.9	0.15	BDL	10.1
HG45	23.0911	88.54631	46	BDL	-	0.39	66.7	402	16.6	0.46	BDL	10.9
HG47	23.1058	88.56269	52	0.35	0.0	0.31	51.6	769	22.6	0.08	0.23	10.5
HG57	23.0681	88.53100	34	15.1	87.4	2.87	93.4	346	22.9	0.27	BDL	9.94
Min				BDL	BDL	0.24	36.6	183	13.3	BDL	BDL	9.39
Median				BDL	BDL	0.44	71.2	850	22.1	1.30	0.30	11.0
Max				15.1	94.6	2.87	97.2	2337	38.6	4.71	0.90	14.7

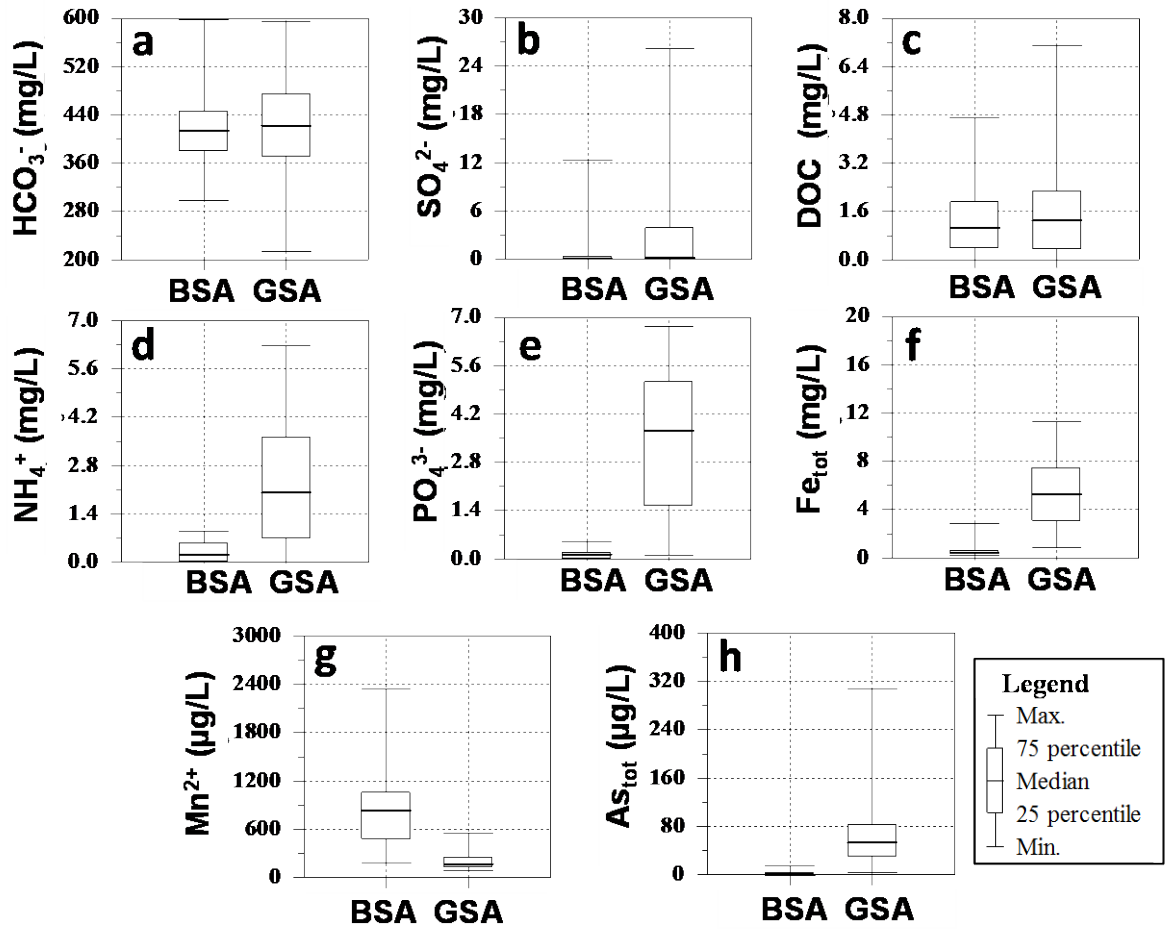

Figure 56. Box and Wiskers plot showing the distribution of major anion, DOC and redox species in groundwater of BSA and GSA.

out of 22 samples of BSA, in 18 (82%) and 21 (95%) samples dissolved Mn concentration exceeds 400 µg/L and 300 µg/L respectively (**Figure 56g**).

8.5.3.2. Ammonium (NH_4^+), phosphate (PO_4^{3-}) and nitrate (NO_3)

Ammonium (NH_4^+) concentrations in groundwater show considerable variability in the GSA aquifers from below detection level to about 6.3 mg/L (median: 2.2 mg/L, Table 22). In the groundwaters of the BSA wells the levels of NH_4^+ are consistently low and seldom exceed 1 mg/L (median: 0.3 mg/L). Similarly, the concentration of PO_4^{3-} in the GSA wells reach up to 6.75 mg/L with a median value of 3.7 mg/L (Table 22). This implies that GSA groundwater being more reduced show significant enrichment with species such as NH_4^+ and PO_4^{3-} compared to groundwater in BSA (**Figure 56d,e**).

8.6. Speciation modelling

Speciation modeling was performed by using the geochemical software package of PHREEQC (version 2.8) with Wateq4f database (Parkhurst and Appelo 1999) to calculate the value of P_{CO2} and saturation indices (SI = log [IAP/KT], where IAP and KT are ion activity product and equilibrium solubility constant at ambient temperature respectively) of major mineral phases that may control the chemistry of groundwater in two groups of aquifers. Using the PHREEQC code, the values of pe were further computed from measured Eh, using the relation:

pe = 16.9 × Eh at 25°C……(eqn. 8)

corresponding to Eh, Fe(II)/Fe(III) and As(III)/As(V) redox couples were calculated from the measured concentration of the

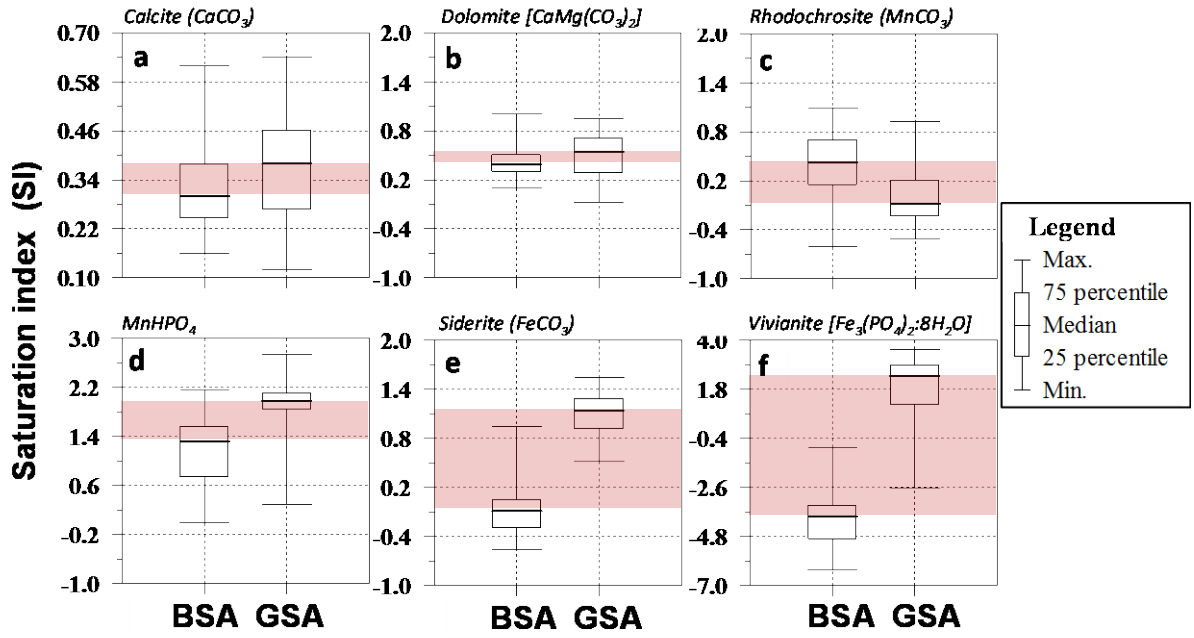

Figure 57. Box and Wiskers plot showing the calculated mineral saturation indices (SI) for groundwater samples from BSA and GSA in the Chakdaha study area in West Bengal, India The highlighted differences in the median SI values indicate that the solubility of Fe is the principal indicator of the redox status and strongly controlled by siderite and vivianite in the GSA groundwater.

Fe(II)/Fe(III) and As(III)/As(V) redox pairs respectively to assess the key redox processes regulating the prevailing redox potential in the aquifers.

The calculated P_{CO2} ranged between $10^{-3.42}$ to $10^{-2.9}$ atm, (median: $10^{-3.01}$ atm) and $10^{-3.63}$ to $10^{-2.61}$ atm (median: $10^{-3.05}$ atm) in the groundwater samples from BSA and GSA respectively. The SI calculation indicated that mosts groundwaters were nearly at equilibrium with calcite and dolomite (**Figure 57a,b**).

The distribution of SI for the major mineral phases, which may regulate the concentration of Fe(II) and Mn(II) in groundwater reveals that groundwater in BSA are mostly at equilibrium with respect to rhodochrosite ($MnCO_3$), whereas equilibriums with respect to siderite (FeCO3) and vivianite [$Fe_3(PO_4)_2$:$8H_2O$] are prevailing in groundwater of GSA (**Figure 57c,e,f**). Saturation Indices values further indicate that $MnHPO_4$ and Fe(III) mineral phases such as ferric hydroxide [$Fe(OH)_3$], goethite (FeOOH), hematite (Fe_2O_3) and magnetite (Fe_3O_4) are stable in both aquifers of the study area.

The differences in the median SI values between the BSA and GSA highlighted in **Figure 56a-f,** demonstrates that among the redox sensitive species, Mn and Fe, there is a wide difference in the SI values of Fe minerals, siderite and vivianite in the BSA and GSA and the solubility of Fe is strongly controlled by siderite and vivianite in the GSA groundwater (**Figure 57e,f**). On the other hand, although rhodochrosite exerts control on the solubility of Mn both in the BSA and GSA, the bandwidth is a narrow which perhaps could be explained through a narrow range of variability in the SI values of $MnHPO_4$ and exerts a greater control on the solubility of Mn in the GSA as compared to the BSA. (**Figure 57 c,d**).

8.7. Aquifer characterization

The BSA was distributed along central (north–south transect) and southwestern region, whereas the distribution of GSA was limited to northwest (beside Hooghly river) and eastern region (parallel to north–south transact of BSA) of the investigated area (**Figure 56**). In most of the boreholes, drilling revealed recovery of sand with a diverse range of sediment color and texture

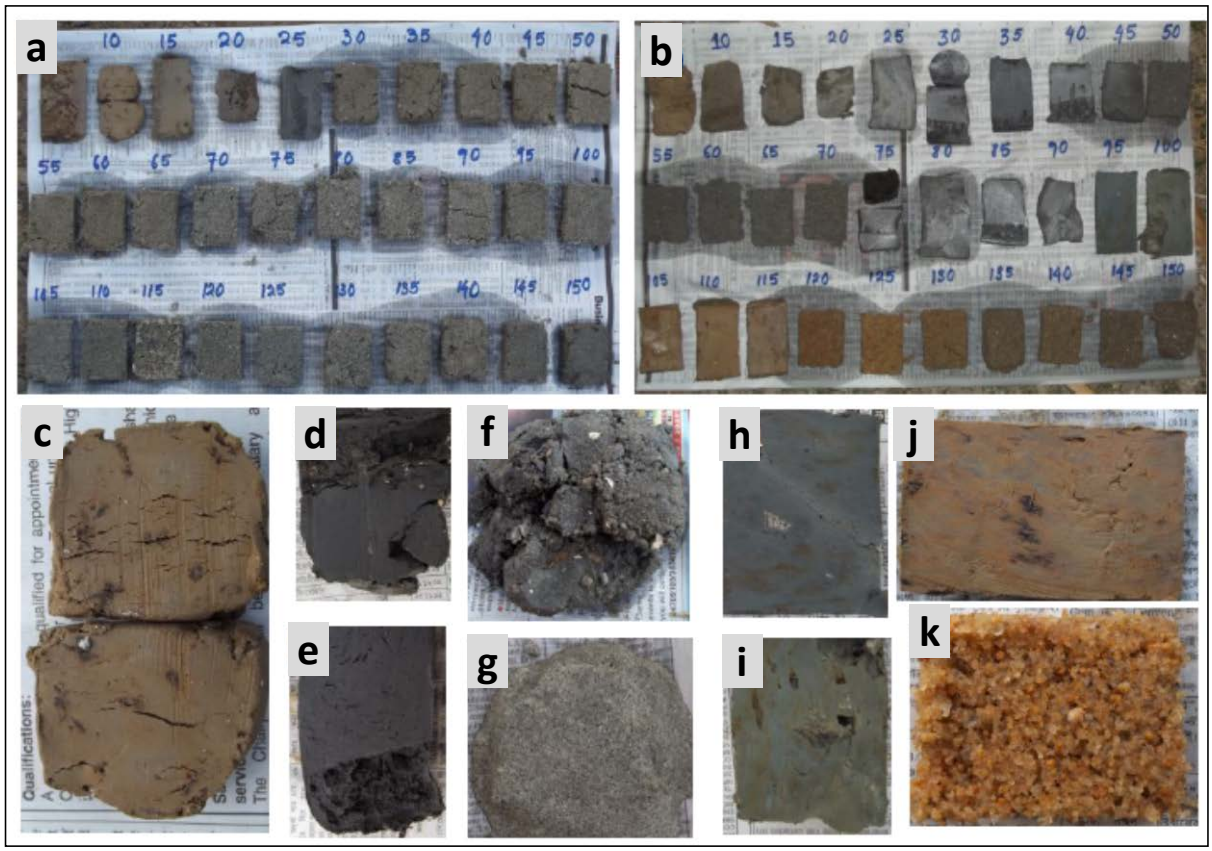

Figure 58. Photographs of few representative sediment samples collected during drilling over the study area. Hand written letters represent depth in feet from where samples were collected. a) BH-17: represents typical channel deposits, where a thick layer of sand extended from just below of surface sandy clay unit to the depth, where drilling was stopped (aquifer-1), b) BH-22: representing the interfluvial sequence between 50 – 70 ft, (aquifer-2), c) BH-17 (depth: light brown surface sandy clay layer with mottles of Fe and Mn oxyhydroxides at 3.03 m bgl, d) BH-2 black peaty materials at 10.6 m bgl, e) BH-13 black peaty sediments at 25.8 m bgl, f) BH-4 black peaty clay with shell fragments at depth of 24.5 m bgl, g) BH-4 typical dark grey colored sand representing aquifer-1 and 2 at depth of 27.3 m bgl, h) BH-22 pale blue colored clay layer at 28.9 m depth bgl, i) BH-22 olive colored clay layer (30.3 m bgl), j) BH-13 brown colored clay layer with mottles of Fe and Mn oxyhydroxides (31.8 m bgl), and k) BH-13 (37.9 m bgl): brown colored coarse sand of representing aquifer-3 (see Biswas et al. 2014b for details).

(**Figure 58**) which were remarkably similar to the observed set of sediment color and textures from the borehole cuttings in the Matlab region.

Over the entire study area the thickness of surface aquitard, which caps the BSA, was higher than that caps the GSA. Only at central northern part of the study area the GSA was overlying the BSA In most of these boreholes, the BSA was separated from the GSA by a red clay layer (**Figure 59**).

The depth to the BSA was maximum in southwestern part. Drilling of two boreholes (BH-11 and 12) at the southwestern region was stopped at 50 m even before reaching any aquifer. However, the driller confirmed the presence of BSA at the base of red clay layer around the depth of 70–80 m.

Using the lithologs from 29 driling sites (**Figure 60**), a 3D lithologic model for the area was developed by the visualizing software RockWorks ver. 15 (RockWare, Golden, CO, USA). The lithological data

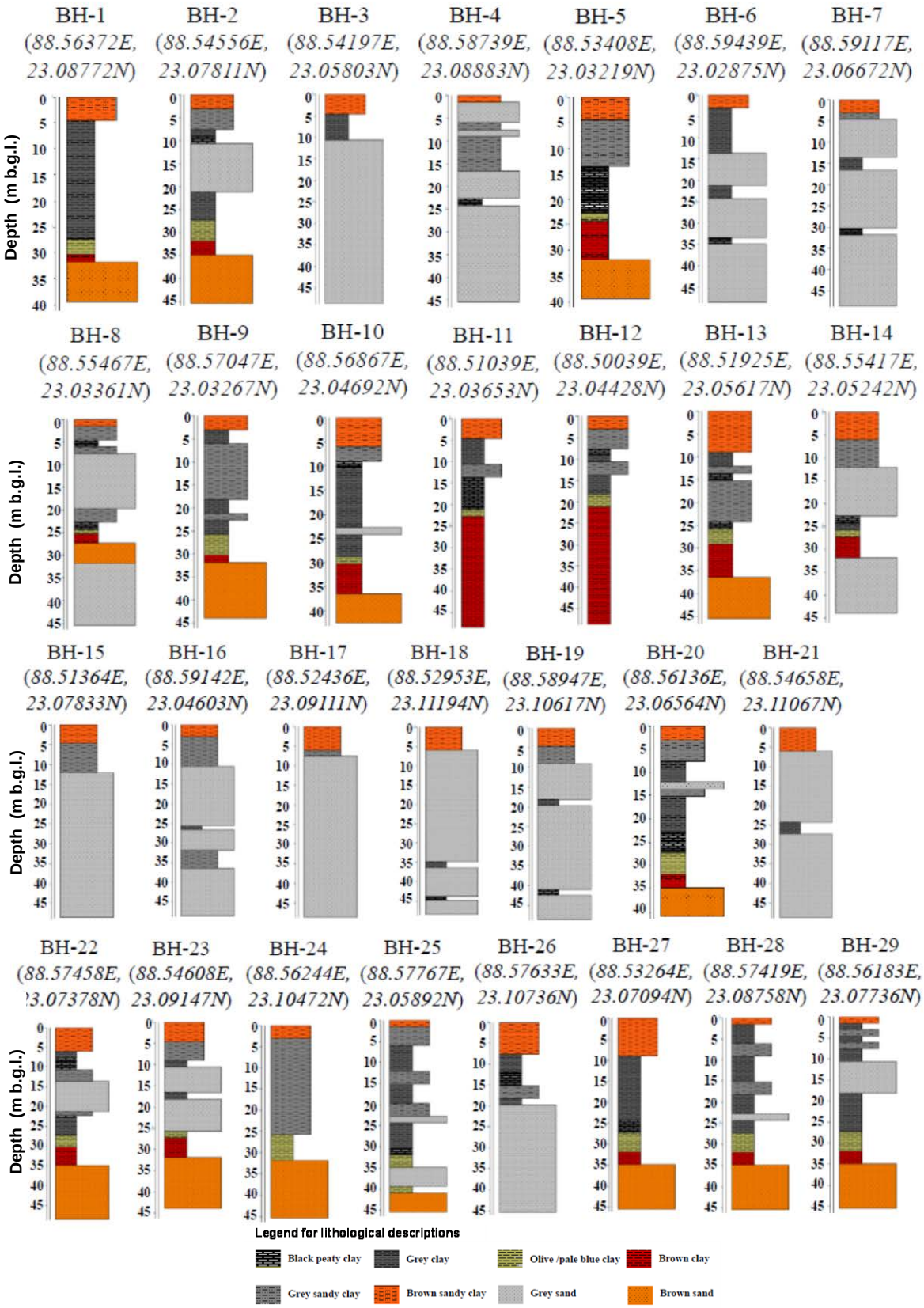

Figure 59. Litholog of individual boreholes from the 29 drilling sites showing the disposition of the grey sand aquifers (GSA) and brown sand aquifers (BSA).

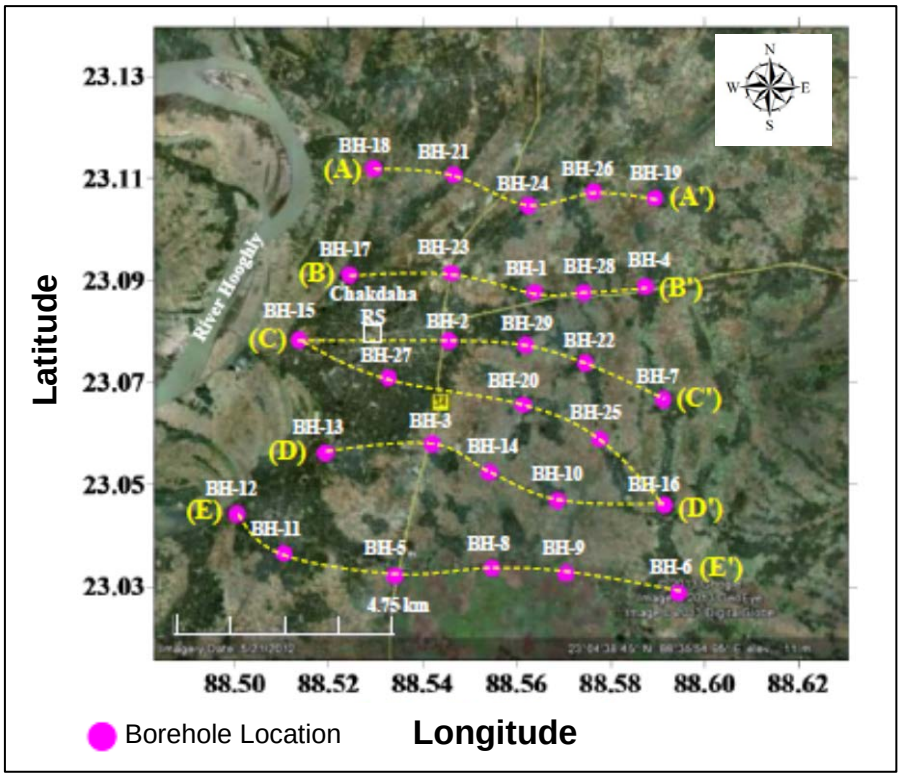

Figure 60. Location of 29 boreholes and 6 west – east traverses along which lithologic cross-section has been prepared (shown in Figure 53). The satellite image was acquired from Google Earth 6.0.2.

from each borehole were interpolated three dimensionally by the algorithm of lithoblending (detailed in Biswas et al. 2014b). Along 6 designated transects in the study area (**Figure 60**), 2D lithologic E-W cross-sections were prepared based on the borehole sediment information in the study area (**Figure 61**).

Additionally, plan-view maps were prepared to visualize the distribution of aquifers and aquitards at different specific depths over the study area (see Figure A2 in Biswas et al. 2014b, for details). These cross sections and plan view maps represent the distribution of a very complex aquifer aquitard framework within the drilling depth. The surface sandy clay layer is extended over the entire study area and the thickness varies spatially between 2 – 9 m, becoming thin along the east margin of the study area (BH-4, BH-7, BH-16) (**Figure 61**). In the upper portion of the surface sandy clay layer the presence of plant debris was common and the sediment was mostly light brown in color (**Figure 61**). The mottles of brown to black colored Fe and Mn oxyhydroxides were visible in the water table fluctuation zone (2 – 5 m bgl) (**Figure 57**). According to the type of formation, three types of aquifer can be distinguished within the drilling depth. Aquifer-1 is unconfined, extending continuously just underneath the surface sandy clay layer to the depth of 50 m bgl, where drilling was stopped. Aerially the aquifer-1 is distributed along the northwest and east margin of the study area, parallel to the River Hooghly and Ichamati respectively (**Figure 61**). Very fine to medium sized sand of dark grey color with a very little portion of silt are prevailing in the aquifer-1 (**Figure 61**), representing the palaeo-channel sequences (McArthur et al. 2008), deposited by River Hooghly and Ichamati. Occasionally, very thin films of organic carbon rich clay layers are inter-bedded within the aquifer-1, particularly along the east margin of the study area (BH-6, BH-7, BH-228 16) (**Figure 61**).

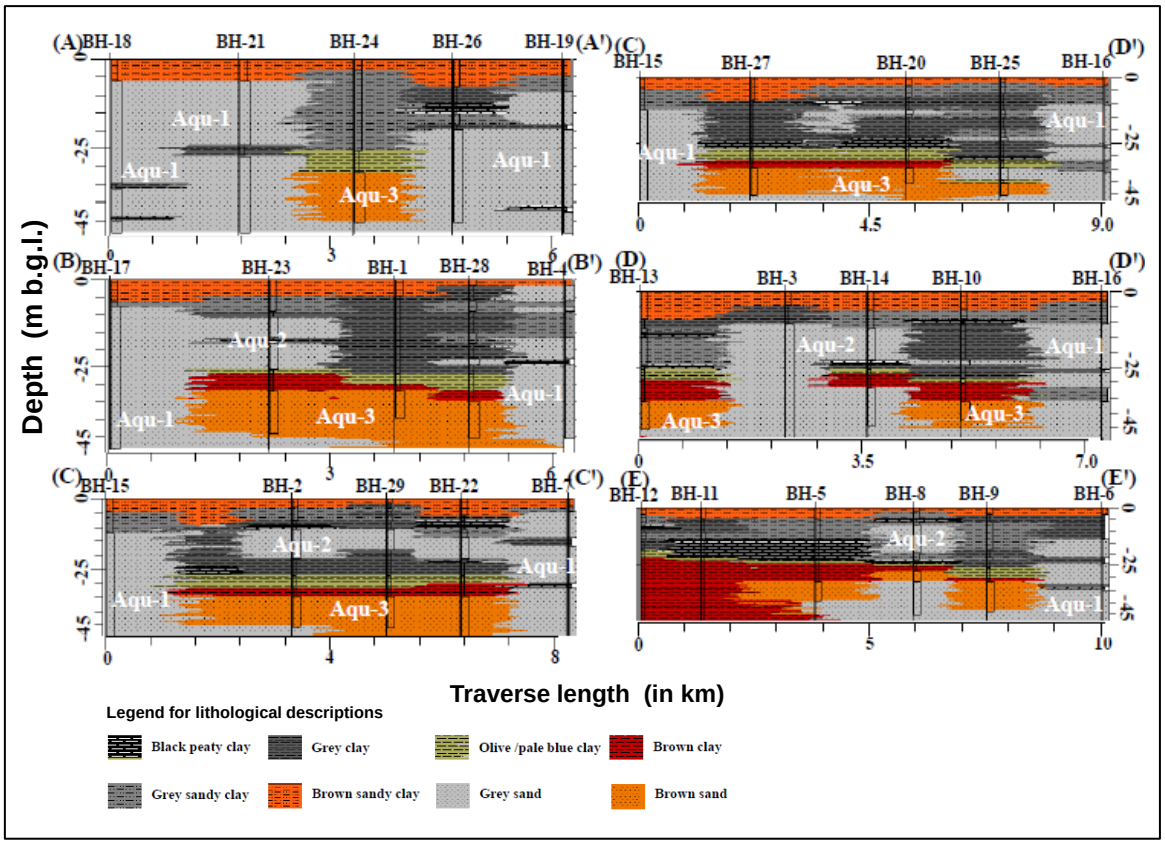

Figure 61. Six W - E lithological cross-sections along the traverses (Figure 59), showing the disposition of the GSA and the BSA based on the colour of the aquifer sediments. Note: Aqu-1, 2 and 3 represents Aquifer-1, 2 and 3 respectively.

8.8. Consequences of safe drinking water supply from BSA

The present study indicates that the concentration of dissolved As in groundwater of BSA is very low and can be considered for mass scale exploitation for safe drinking water supplies. The concentration of Mn is significantly higher in the BSA aquifers. than previous WHO drinking water guideline as well as Indian national drinking water standard. Recently, the elevated concentration of Mn in drinking water has also been identified as potential threat to human health worldwide (e.g. Buschmann et al. 2007, Ljung and Vahter 2007, Bundschuh et al. 2010, Nath et al. 2011). However, severity of Mn exposure is comparatively lower than As exposure (Hug et al. 2011), prolonged consumption of drinking water with elevated Mn may decrease the intellectuality (IQ) among children and also causes neurotoxic effect (Wasserman et al. 2006, Bouchard et al. 2011). The recent withdrawal of the drinking water guideline for Mn (WHO 2011) has been based on the argument that the commonly observed concentrations of Mn in drinking water sources worldwide are well below the health based guideline value of 400 µg/L. However, Mn levels in groundwaters from the sedimentary aquifers, are by and large exceed the former WHO drinking water standard for Mn. This also leads to the question for re-evaluation of drinking water guideline for Mn in near future.

The underlying health risk of Mn in drinking water needs to be addressed more rigorously before considering for mass scale exploitation of BSA as safe drinking water from the perspectives of the overall drinking water safety plan (WHO, 2004). Moreover, the sustainability of the BSA in terms of advective flow of groundwater in both natural and pumping conditions is highly suspected and deserves future study to

assess the risk of cross contamination (Mukherjee et al. 2011). However, considering the severity of As health risk in rural Bengal due to limited availability of As safe drinking water sources, the BSA can be targeted by the local drillers for drinking water supplies for As safe drinking water with the with regular monitoring program in rural areas of West Bengal. However, further exploration of safe aquifers must be initiated to identify aquifers with low As and Mn safe water and target them for the installation of safe drinking water wells to the affected population.

9. Concluding Remarks

Distinct relationship of sediment colour and corresponding As concentrations in water has been documented through a number of recent studies. Local drillers follow the practice of installing shallow tubewells in red sediments with low concentrations of As, with average and median values below the WHO drinking water guideline (10 µg/L). The levels of As in the off-white sediments are also similar, however, targeting off-white sands could be limited due to uncertainty of proper identification of colour, specifically when day-light is a factor. In most of the shallow wells (> 90%) installed in aquifers comprising black or grey sands, As concentration was high with an average of 239 µg/L and therefore installation of wells in shallow black sand aquifers must be avoided. Based on these findings a simple colour tool for targeting shallow aquifers for the installation of As safe community tubewells can be developed for the local drillers through more careful evaluation of the sensitivity of the hydrogeochemical results with respect to the color of the sediments (**Figure 62**). The low As wells installed in red coloured sediments comply with the drinking water standards for As, although elevated Mn concentration in both red and off-white sands above national drinking water standards, has emerged as a concern, although drinking water guideline for Mn has recently been withdrawn by WHO (WHO 2011). Installation of safe tubewells by the current approaches, and warrants a better understanding of the impacts of elevated Mn on human health. Given the proven toxic effects of As, this approach would prove to be a major relief in securing safe drinking water for reducing the exposure of As for the affected population.

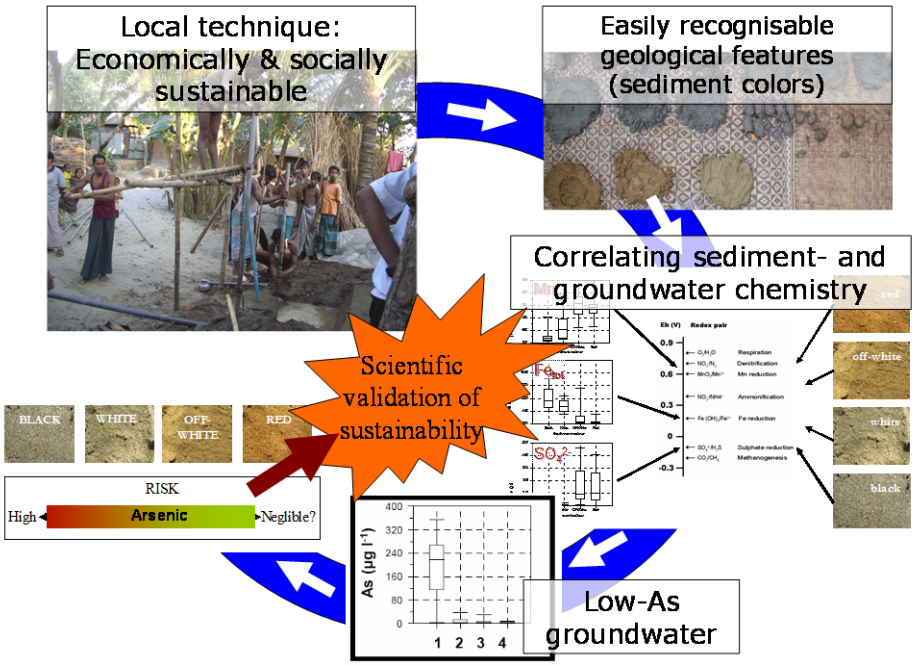

Figure 62. Conceptual framework for targeting safe aquifers by local drillers for tubewell installation.

Local driller target low-As aquifers as a viable option for providing people water for safe drinking. If low As aquifers can be delineated by features local drillers can use for installation of safe drinking water tubewells, this option should be promoted on national as well as local scale. Even so, this study has highlighted that risk for cross-contamination may occur locally. Installing irrigation or production wells for heavy abstraction at depth without proper management on the aquifers sustainability is strongly discouraged (Michael and Voss 2008, Burgess et al. 2010). Improved monitoring of tube wells is strongly encouraged (van Geen et al. 2007, Polya and Charlet 2009, Bhattacharya et al. 2011).

Targeting safe aquifers can thus be based on sediment colour and may prove to be a simple solution for delivering safe drinking water not only this region and but also in other regions with similar geological conditions. Understanding hydrogeological suitability of an area is of prime importance for tubewell installation. The assessment of targeting the safe aquifers may vary from a detailed investigation of subsurface hydrogeological system to a more simple installation of multi-level piezometer nests for monitoring of groundwater quality. For selecting the sites for monitoring wells it would be recommended to discuss with the local drillers to incorporate their knowledge about the local distribution of the target aquifers. In addition, mapping of large capacity water supply wells and clusters of irrigation wells is preferred to be done in order to identify the risks for cross contamination which could be induced due to multiple abstractions.

The results from this and similar studies can further contribute to develop a pragmatic management and mitigation policy with a holistic approach for the future use of the groundwater resources for drinking water supplies where sustainability of low As aquifers in regions with elevated concentrations remain a main concern.

10. REFERENCES

Abedin, M. J., Cresser, M. S., Meharg, A. A., Feldmann, J., Cotter-Howells, J., 2002. Arsenic accumulation and metabolism in rice (*Oryza Sativa L.*). Environmental Science and Technology 36: 962-968.

Aggarwal, P.K., Basu A.R., Poreda R.J., Kulkarni K.M., Froehlich K., Tarafdar S.A., Ali M., Ahmed N., Hussain A., Rahman M., Ahmed S.R., 2000. Isotope hydrology of groundwater in Bangladesh: implications for characterization and mitigation of arsenic in groundwater. IAEA-TC Project: BGD/8/016, IAEA, Vienna.

Ahmed, K.M., 2005. Management of the groundwater arsenic disaster in Bangladesh. In: Bundschuh, J., Bhattacharya, P. and Chandrashekharam, D. (Eds.) Natural Arsenic in Groundwater: Occurrence, Remediation and Management. Taylor and Francis Group, London, UK, pp. 283-296.

Ahmed, K.M., Bhattacharya, P., Hasan, M.A., Akhter, S.H., Alam, S.M.M., Bhuyian, M.A.H., Imam, M.B., Khan, A.A., Sracek, O., 2004. Arsenic contamination in groundwater of alluvial aquifers in Bangladesh: An overview. Applied Geochemistry 19(2): 181-200.

Akai, J., Izumi, K., Fukuhara, H., Masuda, H., Nakano, S., Yoshimura, T., Ohfuji, H., Anwar, H.M., Akai, K., 2004. Mineralogical and geomicrobiological investigations on groundwater arsenic enrichment in Bangladesh. Applied Geochemistry 19:215-230.

Allison, J.D.D., Brown, S., Novo-Gradac, K.J., 1991. MINTEQA2, a Geochemical Assessment Data Base and Test Cases for Environmental Systems. EPA, Athens, GA, U.S.

Anawar, H.M., Akai, J., Komaki, K., Terao, H., Yoshioka, T., Ishizuka, T., Safiullah, S., Kato, K., 2003. Geochemical occurrence of arsenic in groundwater of Bangladesh: sources and mobilization processes. Journal of Geochemical Exploration 77:109-131.

Appelo, C.A.J., Postma, D., 1999. Geochemistry, groundwater and pollution. AA Balkema Publishers, 536 p.

APSU, 2005. Arsenic Policy Support Unit, Interim report. Risk Assessment of Arsenic Mitigation Options, RAAMO II, Phase II Report, May 2005. International Training Network Centre, ITN, Bangladesh.

BGS and DPHE, 2001. Arsenic contamination of groundwater, vol 2, Final Report, BGS Tech. Rep. WC/00/19, British Geological Survey, Keyworth.

Bhattacharya, P., Chatterjee, D., Jacks, G., 1997. Occurrence of Arsenic-contaminated Groundwater in Alluvial Aquifers from Delta Plains, Eastern India: Options for Safe Drinking Water Supply. International Journal of Water Resources Development 13(1): 79-92.

Bhattacharya, P., Jacks G., Jana J., Sracek A., Gustafsson J.P., Chatterjee D., 2001. Geochemistry of the Holocene Alluvial sediments of Bengal Delta Plain from West Bengal, India: Implications on arsenic contamination in groundwater. In: Jacks G., Bhattacharya P. and Khan A.A. (Eds.) Groundwater Arsenic Contamination in the Bengal Delta Plain of Bangladesh, KTH Special Publication, TRITA-AMI Report 3084: 21-40.

Bhattacharya, P., Frisbie, S.H., Smith, E., Naidu, R., Jacks, G., Sarkar B., 2002a. Arsenic in the Environment: A Global Perspective. In: Sarkar, B. (Ed.) Handbook of Heavy Metals in the Environment,. Marcell Dekker Inc., New York, USA, pp. 147-215.

Bhattacharya, P., Jacks, G., Ahmed, K.M., Routh, J., Khan, A.A., 2002b. Arsenic in Groundwater of the Bengal Delta Plain Aquifers in Bangladesh. Bulletin of Environmental Contamination and Toxicology 69: 538-545.

Bhattacharya, P., Mukherjee, A.B., Jacks, G. and Nordqvist, S., 2002c. Metal contamination at a wood preservation site: characterisation and experimental studies on remediation. Science of the Total Environment 290(1-3): 165-180.

Bhattacharya, P., Ahmed, K.M., Hasan, M.A., Broms, S., Fogelström, J., Jacks, G., Sracek, O., von Brömssen, M., Routh, J., 2006a. Mobility of arsenic in groundwater in a part of Brahmanbaria district, NE Bangladesh. In: Naidu, R., Smith, E., Owens, G., Bhattacharya, P., Nadebaum, P. (Eds.), Managing Arsenic in the Environment: From Soil to Human Health. CSIRO Publishing, Melbourne, Australia, pp. 95-115.

Bhattacharya, P., Claesson, M., Bundschuh, J., Sracek, O., Fagerberg, J., Jacks, G., Martin, R.A., Storniolo, A.R., Thir, J.M., 2006b. Distribution and mobility of arsenic in the Río Dulce Alluvial aquifers in Santiago del Estero Province, Argentina. Science of the Total Environment 358: 97-120.

Bhattacharya, P., von Brömssen, M., Hasan, M.A., Ahmed, K M., Jacks, G., Sracek, O., Huq, S.M.I., Naidu, R., Smith, E., Owens, G., 2008. Arsenic mobilisation in the Holocene flood plains in Southcentral Bangladesh: Evidences from the hydrogeochemical trends and modeling results. In: Bhattacharya, P., Ramanathan, AL., Mukherjee A.B., Bundschuh, J., Chandrasekharam, D., Keshari, A.K. (Eds.) Groundwater for Sustainable Development: Problems, Perspectives and Challenges. Taylor and Francis/A. A. Balkema, The Netherlands, pp. 283-299.

Bhattacharya, P., Hossain, M., Rahman, S.N., Robinson, C., Nath, B., Rahman, M., Islam, M., von Brömssen, M., Ahmed, K.M., Jacks, G., Chowdhury, D., Rahman, M., Jakariya, M., Persson, L-Å., Vahter, M., 2011. Temporal and seasonal variability of arsenic in drinking water wells in Matlab, southeastern Bangladesh: A preliminary evaluation on the basis of a 4 year study. Journal of Environmental Science and Health, Part A 46: 1177-1184.

Berg, M., Stengel, C., Trang, P.T.K., Viet, P.H. Sampson, M.L., Leng, M., Samreth, S., Fredericks, D., 2007. Magnitude of arsenic pollution in the Mekong and Red River Deltas — Cambodia and Vietnam. Science of the Total Environment 372: 413-425.

Biswas, A., Nath, B., Bhattacharya, P., Halder, D., Kundu, A.K., Mandal, U., Mukherjee, A., Chatterjee, D., Mörth, C.-M., Jacks, G. 2012. Hydrogeochemical contrast between brown and grey sand aquifers in shallow depth of Bengal Basin: Consequences for sustainable drinking water supply. Science of the Total Environment 431: 402-412.

Biswas, A., Gustafsson, J.P., Neidhardt, H., Halder, D., Kundu, A.K., Chatterjee, D., Berner, Z., Bhattacharya, P., 2014a. Role of competing ions in the mobilization of arsenic in groundwater of Bengal Basin: Insight from surface complexation modelling. Water Research 55: 30-39.

Biswas, A., Bhattacharya, P., Mukherjee, A., Nath, B., Alexanderson, H., Kundu, A.K., Chatterjee, D., Jacks, G., 2014b. Shallow hydrostratigraphy in an arsenic affected region of Bengal Basin: Implication for targeting safe aquifers for drinking water supply. Science of the Total Environment 485-486: 12-22.

Bivén, A., Häller, S., 2007. Arsenic adsorption behaviour of oxidised aquifers in Matlab Upazila, Bangladesh. Master Thesis, Royal Institute of Technology, Stockholm, Sweden.

Bouchard, M.F., Sauvé, S., Barbeau, B., Legrand, M., Brodeur, M.E., Bouffard, T., Limoges, E., Bellinger, D.C., Mergler, D., 2011. Intellectual impairment in school-age children exposed to manganese from drinking water. Environmental Health Perspectives 119: 138-143

Brammer, H., 1996. The Geography of the Soils of Bangladesh. University Press Ltd.

Breit, G.N., Yount, J.C., Uddin, M.N., Muneem, A.A., Lowers, H.A., Driscoll, R.L., Whitney, J.W., 2006. Compositional data for Bengal delta sediment collected from boreholes at Srirampur, Kachua. Bangladesh. US Geological Survey Open-File Report 1222, 58 p.

Breit, G.N., Yount, J.C., Uddin, M.N., Muneem, A.A., Lowers, H.A., Berry, C.J., Whitney, J.W., 2007. Compositional data for Bengal delta sediment collected from a borehole at Rajoir, Bangladesh. US Geological Survey Open-File Report 1022, 46 p.

Bundschuh, J., Farias, B., Martin, R., Storniolo, A., Bhattacharya, P., Cortes, J., Bonorino, G., Alboury, R., 2004. Grounwater arsenic in the Chaco-Pampean Plain, Argentina: Case study from Robles County, Santiago del Estero Province. Applied Geochemistry 19(2): 231-243.

Bundschuh, J., Litter, M.I., Ciminelli, V.S.T., Margada, M.E., Cornejo, L., Hayas, S.F., Hoinkis, J., Alarcón-Herrera, M.T., Armienta, M.A., Bhattacharya, P., 2010. Emerging mitigation needs and sustainable options for solving the arsenic problems of rural and isolated urban areas in Latin America. Water Research 44: 5828-5845.

Burgess, W.G., Hoque, M.A., Michael, H.A., Voss, C.I., Breit, G.N., Ahmed, K.M., 2010. Vulnerability of deep groundwater in the Bengal Aquifer System to contamination by arsenic. Nature Geoscience 3: 83–87.

Buschmann, J., Berg, M., Stengel, C., Sampson, M.L., 2007. Arsenic and manganese contamination of drinking water resources in Cambodia: Coincidence of risk areas with low relief topography. Environmental Science and Technology41, 2146–2152.

Cai, L., Liu, G., Rensing, C., Wang, G., 2009. Genes involved in arsenic transformation and resistance associated with different levels of arsenic-contaminated soils BMC Microbiology 9:4.

Caldwell, B.K., Smith, W.T., Caldwell, J.C., Mitra, S.N., 2005. Trends in water usage and knowledge of arsenicosis in Bangladesh. Population, Space and Place 11(4): 211-223.

Chakraborti, D., Rahman, M.M., Paul, K., Chowdhury, U.K., Sengupta, M.K., Lodh, D., Chanda, C.R., Saha, K.C., Mukherjee, S.C., 2002. Arsenic calamity in the Indian Subcontinent: What lessons have been learned? Talanta 58: 3-22.

Chatterjee, D., Roy, R.K., Basu, B.B., 2005. Riddle of arsenic in groundwater of Bengal Delta Plain-role of non-inland source and redox traps. Environmental Geology 49: 188-206.

Claesson, M., Fagerberg, J., 2003. Arsenic in ground water of Santiago del Estero – Sources, mobility patterns and remediation with natural materials. Master Thesis, Dept. of Land and Water Resources Engineering, KTH, Stockholm, Sweden, TRITA-LWR-EX-03-05, 59 p.

Cohen, D., Ward, C.R., 1991. Sednorm-a program to calculate a normative mineralogy for sedimentary rocks based on chemical analyses. Computers and Geosciences 17(9):1235-1253.

Correll, R., Huq, S.M.I., Smith, E., Owens, G., Naidu, R., 2006. Dietary intake of arsenic from crops. In: Naidu, R., Smith, E., Owens, G., Bhattacharya, P., Nadebaum, P. (Eds.) Managing arsenic in the environment: from soil to human health. CSIRO Publishing; Melbourne, Australia, pp. 251-268.

Datta, S., Neal, A.W., Mohajerin, T.J., Ocheltree, T., Rosenheim, B.E., White, C.D., Johannesson, K.H., 2011. Perennial ponds are not an important source of water or dissolved organic matter to groundwaters with high arsenic concentrations in West Bengal, India. Geophysical Research Letters 38, L20404.

Dixit, S., Hering, J.G., 2003. Comparison of arsenic(V) and arsenic(III) sorption onto iron oxide minerals: Implications for arsenic mobility. Environmental Science and Technology 37: 4182-4189.

Dixit, S., Hering, J.G., 2006. Sorption of Fe(II) and As(III) on goethite in single- and dual-sorbate system. Chemical Geology 228: 6-15.

Dodd, J., Large, D.J., Fortey, N.J., Milodowski, A.E., Kemi, S., 2000. A petrographic investigation of two sequential extraction techniques applied to anaerobic canal bed mud. Environmental Geochemistry and Health 22: 281–296.

DPHE/DFID/JICA, 2006. Development of Deep Aquifer Database and Preliminary Deep Aquifer Map. Department of Public Health Engineering (DPHE), Government of Bangladesh, and Arsenic Policy Support Unit (APSU), Japan International Cooperation Agency (JICA), Bangladesh, Dhaka.

Dzombak, D.A., Morel, F.M.M., 1990. Surface Complexation Modelling-Hydrous Ferric Oxide. John Wiley, New York, USA, 393 p.

EPC/MMP, 1991. Dhaka Region Groundwater and Subsidence Study, Final Report. Engineering and Planning Consultants, Dhaka and Sir M. Macdonalds and Partners, UL. Report for Dhaka Water Supply and Sewerage. Authority under assignment to the World Bank.

Filgueiras, A.V., Lavilla, I., Bendicho, C., 2002. Chemical sequential extraction for metal partioning in environmental solid samples. Journal of Environmental Monitoring 4: 823-857.

Goldberg, S., 2002. Competitive adsorption of arsenate and arsenite on oxides and clay minerals. Soil Sci. Soc. Am. J. 66:413–421.

Goldberg, S., Johnston C.T., 2001. Mechanisms of arsenic adsorption on amorphous oxides evaluated using macroscopic measurements, vibrational spectroscopy and surface complexation modeling. Journal of Colloid and Interface Science 234: 204-216.

Goodbred S.L., Kuehl S.A., Steckler M.S., Sarker M.H., 2003. Controls on facies distribution and stratigraphic preservation in the Ganges–Brahmaputra delta sequence. Sedimentary Geology 155: 301–16.

Gunaratna, K.R., Shokri, A., Bhattacharya, P., Jacks, G., Bundschuh, J., von Brömssen, M., 2010. Microbial characterization of Holocene alluvial sediments in the Meghna Flood Plain of Matlab Upazila, Bangladesh In: J.-S. Jean, J. Bundschuh & P. Bhattacharya (Eds.) "Arsenic in Geosphere and Human Diseases, As 2010". Interdisciplinary Book Series: "Arsenic in the Environment—Proceedings". Series Editors: Jochen Bundschuh and Prosun Bhattacharya, CRC Press/Taylor and Francis, UK, pp. 140-142.

Gustafsson, J.P., 2011. Visual MINTEQ 3.0 Program, Website http://www.lwr.kth.se/english/OurSoftWare/Vminteq/index.html.

Gustafsson, J.P., Bhattacharya, P., 2007. Geochemical modelling of arsenic adsorption to oxide surfaces. In: Bhattacharya, P., Mukherjee, A.B., Bundschuh, J., Zevenhoven, R., Loeppert, R.H. (Eds.), Arsenic in Soil and Groundwater Environment: Biogeochemical Interactions, Health Effects and Remediation, Trace Metals and other Contaminants in the Environment, vol. 9. Elsevier B.V., Amsterdam, The Netherlands, pp. 153-200.

Halder, D., Bhowmick, S., Biswas, A., Mandal, U., Nriagu, J., Guha Mazumdar, D.N., Chatterjee, D., Bhattacharya, P., 2012. Consumption of Brown Rice: a potential pathway for arsenic exposure in rural Bengal. Environmental Science and Technology 46: 4142-4148.

Harvey, C.F., Swartz, C.H., Badruzzaman, A.B.M., Keon-Blute, N., Yu, W., Ali, M.A., Jay, J., Beckie, R., Niedan, V., Brabander, D., Oates, P.M., Ashaque, K.N., Islam, S., Hemond, H.F., Ahmed, M.F., 2002. Arsenic mobility and groundwater extraction in Bangladesh. Science 298: 1602-1606.

Harvey, C. F., Keon, N., W., Y., Ali, A., Jay, J., Beckie, R., Niedan, V., Brabander, D, Oates, P., Ahsfaque, K., Islam, S., Hemond, H.F., Ahmed, F., 2005. Groundwater arsenic contamination on the Ganges Delta: Biogeochemistry, hydrology, human perturbations, and human suffering on a large scale. Comptes-Rendus: Geoscience 337(1-2): 285-296.

Hasan, M.A., Ahmed, K.M., Sracek, O., Bhattacharya, P., von Brömssen, M., Broms, S., Fogelström, J., Mazumder, M. L., Jacks, G., 2007. Arsenic in shallow groundwater of Bangladesh: investigations from three different physiographic settings. Hydrogeology Journal 15: 1507-1522

Hasan, M.A., von Brömssen, M., Bhattacharya, P., Ahmed, K.M., Sikder, A.M., Jacks, G., Sracek, O., 2009. Geochemistry and mineralogy of shallow alluvial aquifers in Daudkandi upazila in the Meghna flood plain, Bangladesh. Environmental Geology 57: 499–511.

Hem, J.D., 1985. Study and Interpretation of the Chemical Characteristics of Natural Water. US Geological Survey Water Supply Paper 2254.

Hoque, B.A., Hoque, M.M., Ahmed, T., Islam, S., Azad, A.K., Ali, N., Hossaina, M., Hossain, M.S., 2004. Demand-based water options for arsenic mitigation: an experience from rural Bangladesh. Public Health 118(1):70-77.

Hoque, M.A., 2010. Models for Managing Deep Aquifer in Bangladesh, Ph.D. Thesis. Univ. College London, UK.

Hoque, M.A., Burgess, W.G., Shamsudduha, M., Ahmed, K.M., 2011. Delineating low-arsenic groundwater environments in the Bengal Aquifer. Applied Geochemistry 26: 614-623.

Horneman, A., van Geen, A., Kent, D. V., Mathe, P. E., Zheng, Y., Dhar, R. K., O'Connel, S. O., Hoque, M. A., Aziz, Z., Shamsudduha, M., Seddique, A A., Ahmed, K. M., 2004. Decoupling of As and Fe release to Bangladesh groundwater under reducing conditions. Part I: Evidence from sediment profiles. Geochimica et Cosmochimica Acta 68(17): 3459-3473.

Hug, S.J., Gaertner, D., Roberts, L.C., Schrimmer, M., Ruettimann, T., Rosenberg, T.M., Badruzzaman, A.B.M., Ali, M.A., 2011. Avoiding high concentrations of arsenic, manganese and salinity in deep tubewells in Munshiganj District, Bangladesh. Applied Geochemistry 26: 1077-1085.

Huq, S.M.I., Correll, R., Naidu, R., 2006. Arsenic accumulation in food sources in Bangladesh. In: Naidu, R., Smith, E., Owens, G., Bhattacharya, P. & Nadebaum, P. (Eds.) Managing Arsenic in the Environment: from soil to human health. CSIRO Publishing, Melbourne, pp. 279-290.

Jacks, G., Šlejkovec, Z., Mörth, M., Bhattacharya, P., 2013. Redox-cycling of arsenic along the water pathways in sulfidic metasediment areas in northern Sweden. Applied Geochemistry 35: 35-43 (DOI:10.1016/j.apgeochem.2013.05.002).

Jakariya, M., 2007. Arsenic in Tubewell Water: of Bangladesh. and Approaches for Sustainable Mitigation. TRITA-LWR PhD Thesis 1033, 28p.

Jakariya, M., Rahman, M., Chowdhury, A.M.R., Rahman, M., Yunus, M., Bhiuya, A., Wahed, M.A., Bhattacharya, P., Jacks, G., Vahter M., Persson, L.-Å., 2005. Sustainable safe water options in Bangladesh: experiences from the Arsenic Project at Matlab (AsMat). In: Bundschuh, J., Bhattacharya, P., Chandrashekharam, D. (Eds.) Natural Arsenic in Groundwater: Occurrence, Remediation and Management. A.A. Balkema, Taylor and Francis Group, London, pp. 319-330.

Jakariya, M., von Brömssen, M., Jacks, G., Chowdhury, A.M.R., Ahmed, K.M., Bhattacharya, P., 2007. Searching for sustainable arsenic mitigation strategy in Bangladesh: experience from two upazilas. International Journal of Environment and Pollution 31(3/4): 415-430.

JICA-Japanese International Development Agency, 2002. The study on the groundwater development of deep aquifers for safe drinking water supply to arsenic affected areqs in western Bangladesh. Kokusai Kogyo Co. Ltd., and Mitsui Mineral Development Engineering Co. Ltd.

Johnston, R.B., Hanchett, S., Khan, M.H., 2010. The socio-economics of arsenic removal. Nature Geoscience 3: 2-3.

Jonsson, L., Lundell, L. 2004. Targeting safe aquifers in regions with arsenic-rich groundwater in Bangladesh. Case study in Matlab Upazila. Minor Field Studies No 277. Swedish University of Agricultural Sciences, SLU External Relations, Uppsala. ISSN 1402-3237.

Kapaj, S., Peterson, H., Liber, K., Bhattacharya, P., 2006. Human health effects from chronic arsenic poisoning - A Review. Journal of Environmental Science and Health Part A 41: 2399-2428.

Kar, S., Maity, J.P., Jean, J-S., Liu, C-C., Nath, B., Yang, H-J., Bundschuh, J., 2010. Arsenic-enriched aqufers: Occurences and mobilization of arsenic in groundwater of Ganges Delta Plain, Barasat, West-Bengal, India. Applied Geochemistry 25: 1805-1814.

Kendie, S.B., 1996. Some factors influencing effective utilisation of drinking water facilities: women, income and health in north Ghana. Environmental Management 20(1): 1-10.

Lindberg, A.-L., Goessler, W., Gurzau, E., Koppova, K., Rudnai, P., Kumar, R., Fletcher, T., Leonardi, G., Slotova, K., Gheorghiu, E., Vahter, M., 2006. Arsenic exposure in Hungary, Romania and Slovakia. Journal of Environmental Monitoring. 8: 203–208.

Ljung, K., Vahter, M., 2007. Time to re-evaluate the guideline value for manganese in drinking water? Environmental Health Perspectives 115: 1533-1538.

Lowers, H.A., Breit, G.N., Foster, A.L., Whitney, J., Yount, J., Uddin, M.N., Muneem, A.A., 2007. Arsenic incorporation into authigenic pyrite, Bengal Basin sediment, Bangladesh. Geochimica et Cosmochimica Acta 71: 2699-2717.

Mandal, B.K., Suzuki, K.T., 2002. Arsenic round the world: a review. Talanta 58: 201-235.

Manning, B.A., Goldberg, S., 1997. Adsorption and stability of arsenic(III) at the clay mineral–water interface. Environmental Science Technology 31: 2005-2011.

McArthur, J.M., Ravencroft, P., Safiullah, S., Thirlwall, M.F., 2001. Arsenic in groundwater: testing pollution mechanism for sedimentary aquifers in Bangladesh. Water Resources Research 37: 109-117.

McArthur, J., Banerjee, D., Hudson-Edwards, K., Mishrab, R., Purohit, R., Ravenscroft, P., P., Cronin, A., Howarth, R.J., Chatterjee, A., Talukder, T., Lowry, D., Houghton, S., Chadha, D.K., 2004. Natural organic matter in sedimentary basins and its relation to arsenic in anoxic ground water: the example of West Bengal and its worldwide implications. Applied Geochemistry 19: 1255-1293.

McArthur, J.M., Ravenscroft, P., Banerjee, D.M., Milsom, J., Hudson-Edwards, K.A., Sengupta, S., Bristow, C., Sarkar, A., Tonkin, S., Purohit, R., 2008. How paleosols influence groundwater flow and arsenic pollution: A model from the Bengal Basin and its worldwide implication. Water Resources Research 44: W11411.

McArthur, J.M., Nath, B., Banerjee, D.M., Purohit, R., Grassineau, N., 2011. Palaeosol control on groundwater flow and pollutant distribution: The example of arsenic. Environmental Science Technology 45: 1376-1383.

Meharg, A.A., Scrimgeour, C., Hossain, S.A., Fuller, K., Cruickshank, K., Williams, P.N., Kinniburgh, D.G., 2006. Codeposition of organic carbon and arsenic in Bengal Delta Aquifers. Environmental Science Technology 40: 4928-4935.

Meng, X., Korfiatis, G.P., Christodoulatos, C., Bang S., 2001. Treatment of arsenic in Bangladesh well water using a household co-precipitation and filtration system. Water Research 35(12): 2805-2810.

Michael, H.A., Voss, C.I., 2008. Evaluation of the sustainability of deep groundwater as an arsenic-safe resource in the Bengal Basin. Proceedings of the National Academy of Sciences of the United States of America 105: 8531–8536.

Michael, H., Voss, C., 2009a. Controls on groundwater flow in the Bengal Basin of India and Bangladesh: regional modeling analysis. Hydrogeology Journal 17: 1561–1577.

Michael, H., Voss, C., 2009b. Estimation of regional-scale groundwater flow properties in the Bengal Basin of India and Bangladesh. Hydrogeology Journal 17: 1329–1346.

Milton, A.H., Hasan, Z., Shahidullah, S.M., Sharmin, S., Jakariya, M.D., Rahman, M., Dear, K., Smith, W., 2004. Association between nutritional status and arsenicosis due to chronic arsenic exposure in Bangladesh. International Journal of Environmental Health Research 14(2): 99-108.

Mozumder, M.R.H., 2011. Aqueous Phase Geochemical Characterisation and Delineation of Low Arsenic Aquifers in Matlab Upazila, SE Bangladesh. M.Sc. Thesis, Royal Institute of Technology, LWR-EX-11:08, 38p.

Mozumder, M.R.H., Bhattacharya, P., Ahmed, K.M., Hossain, M., Hasan, M.A., Islam, M.M., Jacks, G., von Brömssen, M., 2011. Groundwater redox-facies and aquifer sediment color characteristics in Matlab Upazila, SE Bangladesh. Geological Soceity of America, Abstracts with Programs 43(5): 222.

Mukherjee, A., Fryar, A.E., 2008. Deeper groundwater chemistry and geochemical modelling of the arsenic affected western Bengal basin, West Bengal, India. Applied Geochemistry 23: 863-892.

Mukherjee, A., Fryar, A.E., Howell, P., 2007. Regional hydrostratigraphy and groundwater flow modeling of the arsenic affected western Bengal basin, West Bengal, India. Hydrogeology Journal 15: 1397–1418.

Mukherjee, A., von Brömssen, M., Scanlon, B.R., Bhattacharya, P., Fryar, A.E., Hasan, M.A., Ahmed, K.M., Chatterjee, D., Jacks, G., Sracek, O., 2008. Hydrogeochemical comparison between the Bhagirathi and Meghna sub-basins, Bengal basin, India and Bangladesh: effects of overlapped redox zones on dissolved arsenic. Journal of Contaminant Hydrology 99: 31-48.

Mukherjee, A., Fryar, A.E., Scanlon, B.R., Bhattacharya, P., Bhattacharya, A., 2011. Elevated arsenic in deeper groundwater of the western Bengal basin, India: extent and controls from regional to local scale. Applied Geochemistry 26(4): 600-613.

Mukherjee, A.B., Bhattacharya, P., 2001. Arsenic in groundwater in the Bengal Delta Plain: Slow Poisoning in Bangladesh. Environmental Reviews 9:189-220.

Naidu, R., Smith, E., Owens, G., Bhattacharya, P., Nadebaum, P., 2006. Managing Arsenic in the Environment: From Soil to Human Health. CSIRO Publishing, Melbourne, Australia, 656 p.

Nath, B., Chakraborty, S., Burnol, A., Stüben, D., Chatterjee, D., Charlet, L. 2009. Mobility of arsenic in the sub-surface environment: An integrated hydrogeochemical study and sorption model of the sandy aquifer materials. Journal of Hydrology 364: 236-248.

Nath, B., Maity, J.P., Jean, J.S., Birch, G., Kar, S., Yang, H.J., Lee, M.K., Hazra, R., Chatterjee, D., 2011. Geochemical characterization of arsenic-affected alluvial aquifers of the Bengal Delta (West Bengal and Bangladesh) and Chianan Plains (SW Taiwan): Implications for human health. Applied Geochemistry 26: 705–711.

Nickson, R, McArthur, J., Burgess, W.G., Ahmed, K.M., Ravencroft, P., Rahman, M., 1998. Arsenic poisoning of Bangladesh groundwater. Nature 1998: 395-338.

Nickson, R, McArthur, J., Ravenscroft, P., Burgess, W.G., Ahmed, K.M., 2000. Mechanism of arsenic release to groundwater, Bangladesh and West Bengal. Applied Geochemistry 15: 403-413

Nickson, R.T., McArthur, J.M., Shrestha, B., Kyaw-Myint, T.O., Lowry, D., 2005. Arsenic and other drinking water quality issues, Muzaffargarh District, Pakistan. Applied Geochemistry 20(1):55-68.

Nicolli, H.B., Bundschuh, J., García, J.W., Falcón, C.M., Jean, J.-S. 2010. Sources and controls for the mobility of arsenic in oxidizing groundwaters from loess-type sediments in arid/semi-arid dry climates — evidence from the Chaco–Pampean plain (Argentina). Water Research 44: 5589–604.

Nicolli, H.B., Bundschuh, J., Blanco, M. del C., Panarello, H.O., Dapeña. C., Jean, J.-S. 2012. Arsenic and associated trace elements in groundwater from the Chaco–Pampean plain: results from 100 years of research. Science of the Total Environment 429: 36-56.

Nriagu, J.O., Bhattacharya, P., Mukherjee, A.B., Bundschuh, J., Zevenhoven, R., Loeppert, R.H., 2007. Arsenic in soil and groundwater: an overview. In: Bhattacharya, P., Mukherjee, A.B., Bundschuh, J., Zevenhoven, R. & Loeppert, R.H. (Eds.) Arsenic in Soil and Groundwater Environment:

Biogeochemical Interactions, Health Effects and Remediation, Trace Metals and other Contaminants in the Environment, Volume 9, Elsevier B.V. Amsterdam, The Netherlands, pp. 3–60.

Pal, T., Mukherjee, P.K., 2008. 'Orange sand' – a geological solution for arsenic pollution in Bengal Delta. Current Science 94: 31-33.

Pal, T., Mukherjee, P.K., 2009. Study of subsurface geology in locating arsenic-free groundwater in Bengal Delta, West Bengal, India. Environmental Geology 56: 1211-1125.

Parkhurst, D.L., Appelo, C.A.J., 1999. Users's Guide to PHREEQC (Version 2)-A Computer Program for Speciation, Batch-reaction, One-dimensional Transport and Inverse Geochemical Calculations. U.S. GEOLOGICAL SURVEY, Denver, Colorado, USA. 99-4259.

Petrusivski, B., Sharma, S., Schippers, J.C., Shordt, K., 2007. Arsenic in drinking water. Thematic Overview Paper 17. IRC International Water and Sanitation Centre. 57p.

Polya, D., Charlet, L., 2009. Rising arsenic risk? Nature Geoscience 2: 383-384.

Polya, D.A., Mondal, D., Giri, A.K., 2009. Quantification of deaths and DALYs arising from chronic exposure to arsenic in groundwaters utilized for drinking, cooking and irrigation of food crops in Preedy, V.R. & Watson, R. (Eds.) Handbook of Disease Burdens and Quality of Life Measures, Springer Science+Business Media LLC, USA, pp. 701-728.

Postma, D., Jakobsen, R., 1996. Redox zonation: equilibrium constraints on the Fe(III)/SO4-reduction interface. Geochimica et Cosmochimca Acta 60(17): 3169-3175.

Quevauviller, P., Rauret, G., Griepink, B., 1993. Single and sequential extraction in sediment and soils. International Journal of Environmental Analytical Chemistry 51:231-235.

Radloff, K.A., Zheng, Y., Michael, H.M., Stute, M., Bostick, B.C., Milhajlov, I., Bounds, M., Huq, M.R.,m Chowdhury, I., Rahman, M.W., Schlosser, P., Ahmed, K.M., van Geen, A. 2011. Arsenic migration to deep groundwater in Bangladesh influenced by adsorption and water demand. Nature Geoscience, NGEO 12833.

Rahman, A.A., Ravenscroft, P., 2003. Groundwater Resources and Development in Bangladesh – Background to the Arsenic Crisis, Agricultural Potential and the Environment. Bangladesh Centre for Advanced Studies. Dhaka:University Press Ltd.

Ravenscroft, P., 2001. Distribution of groundwater arsenic in Bangladesh related to geology. In: Bhattacharya, P., Jacks, G. & Khan, A.A. (Eds.) Groundwater Arsenic Contamination in the Bengal Delta Plain of Bangladesh. Proceedings of the KTH-Dhaka University Seminar, KTH Special Publication, TRITA-AMI Report 3084, pp. 41–56.

Ravenscroft, P., McArthur, J.M., Hoque, B.A., 2001. Geochemical and palaeohydrological controls on pollution of groundwater by arsenic. In: Chappell, W.R., Abernathy, C.O. & Calderon, R.L. (Eds.) Arsenic Exposure and Health Effects IV. Elsevier, Oxford, pp. 53-57.

Ravenscroft, P., Burgess, W., Ahmed, K., Burren, M., Perrin, J., 2005. Arsenic in groundwater of the Bengal Basin, Bangladesh: Distribution, field relations, and hydrogeological setting. Hydrogeology Journal 13(5-6): 727-751.

Ravenscroft, P., Brammer, H., Richards, K.S., 2009. Arsenic Pollution: A Global Synthesis. Wiley-Blackwell, U.K., 588p.

Reza, S.A.H.M., Jean, J-S., Lee, M-K., Yang, H-J., Liu, C-C., 2010. Arsenic enrichment and mobilization in the Holocene alluvial aquifers of the Chapai-Nawabganj district, Bangladesh: A geochemical and statistical study. Applied Geochemistry 25: 1280-1289.

Reza, S.A.H.M., Jean, J-S., Lee, M-K., Luo, S-D., Bundschuh, J., Li, H-C-., Yang, H-J., Liu, C-C., 2011. Interrelationship of TOC, As, Fe, Mn, Al and Si in shallow alluvial aquifers in Chapai-Nawabganj district, Bangladesh: implication for potential source of organic carbon. Environmental Earth Science 63: 955-967.

Robinson, C., Hossain, M., von Brömssen, M., Bhattacharya, P., Häller, S., Bivén, A., Jacks, G., Ahmed, K.M., Hasan, M.A., Thunvik, R., 2011. Dynamics of arsenic adsorption in the targeted arsenic-safe aquifers in Matlab, South-eastern Bangladesh: insight from experimental studies. Applied Geochemistry 26: 624–635.

Roychowdhury, T., Uchino, T., Tokunaga, H., Ando, M., 2002. Survey of arsenic in food composites from an arsenic-affected area of West Bengal, India. Food and Chemical Toxicology 40(11): 1611-21.

Saha, D., Sinha, U.K., Dwivedi, S.N., 2011. Characterization of recharge processes in shallow nd deeper aquifers using isotopic signatures and geochemical behaviour of groundwater in an arsenic-enriched part of the Ganga Plain. Applied Geochemistry 26: 432-443.

Sarkar, B., 2002. Heavy Metals in the Environment. Marcel Dekker, Inc., New York, 725 p.

Sharif, M.U., Davis, R.K., Steele, K.F., Kim, B., Hays, P.D., Kresse, T.M., Fazio, J.A., 2008. Distribution and variability of redox zones controlling spatial variability of arsenic in the Mississippi River Valley alluvial aquifer, southeastern Arkansas. Journal of Contaminant Hydrology 99: 49-67.

Sikder, M.S., Maidul, Z.M., Ali, M., Rahman, M.H., 2005. Socio-economic status of chronic arsenicosis patients in Bangladesh. Mymensingh Medical Journal 14(1): 50-53.

Singh, N., Jacks, G., Bhattacharya, P., 2005. Women and community water supply programmes: An analysis from a socio-cultural perspective. Natural Resources Forum 29(3): 213-223.

Smedley, P.L., Kinniburgh, D.G., 2002. A review of the source, behaviour and distribution of arsenic in natural waters. Applied Geochemistry 17: 517-568.

Smedley, P., Kinniburgh, D.G., Macdonald D.M.J., Nicolli, H.B., Barros, A.J., Tullio, J.O., Pearce, J.M., Alonso, M.S., 2005. Arsenic associations in sediments from loess aquifer of La Pampa, Argentina. Applied Geochemistry 20: 989-1016.

Smith, A.H., Lingas, E.O., Rahman, M. 2000. Contamination of drinking-water by arsenic in Bangladesh: a public health emergency. Bulletin of the World Health Organization 78(9): 1093-1103.

Sracek, A., Bhattacharya, P., Jacks, G., Gustafsson, J.P., 2001. Mobility of arsenic and geochemical modeling in groundwater environment. In: G. Jacks, P. Bhattacharya and A.A. Khan (Editors), Groundwater Arsenic Contamination in the Bengal Delta Plains of Bangladesh: Proceedings of the KTH-Dhaka UniversitySeminar, University of Dhaka, Bangladesh. KTH Special Publication, TRITA-AMI REPORT 3084: 9-20.

Sracek, O., Bhattacharya, P., Jacks, G., Gustafsson, J.-P., von Brömssen, M., 2004a. Behavior of arsenic and geochemical modeling of arsenic enrichment in aqueous environments. Applied Geochemistry 19(2): 169-180.

Sracek, O., Bhattacharya, P., von Brömssen, M., Jacks, G., Ahmed, K. M., 2004b. Natural enrichment of arsenic in groundwaters of Brahmanbaria district, Bangladesh: geochemistry, speciation modelling and multivariate statistics. In: J. Bundschuh, P. Bhattacharya and D. Chandrasekharam (Eds.)Natural Arsenic in Groundwater: Occurrence, Remediation and Management. Balkema, London, pp. 133-144.

Stollenwerk, K.G., 2005. Arsenic Attenuation by Oxidized Aquifer Sediments, Bangladesh, Behavior of Arsenic in Aquifers, Soils and Plants: Implications for Management. International Maize and Wheat Improvement Centre (CYMMYT), Cornell University, Texas A&M University, United States Geological Survey, Geological Survey of Bangladesh, Dhaka, Bangladesh.

Stollenwerk, K.G., Breit, G.N., Welch, A.H., Yount, J.C., Whitney, J.W., Forster, A.L., Uddin, M.N., Majumder, R.K., Ahmed, N., 2007. Arsenic attenuation by oxidised sediments in Bangladesh. Science of the Total Environment 379: 133-150.

Stüben, D., Berner, Z., Chandrasekharam, D., Karmakar, J., 2003. Arsenic enrichment in groundwater of West Bengal, India: geochemical evidence for mobilization of As under reducing conditions. Applied Geochemistry 18(9): 1417-1434.

Stute, M., Zheng, Y., Schlosser, P., Horneman, A., Dhar, R.K., Hoque, M.A., Seddique, A.A., Shamsudduha, M., Ahmed, K.M., van Geen, A., 2007. Hydrological control of As concentrations in Bangladesh groundwater. Water Resources Research 43: W09417.

Swartz, C.H., Blute, N.K., Bodruzzaman, B., Ali, M.A., Brabander, D., Jay, J., Besabcon, J., Islam, S., Hemond, H.F., Harvey, C., 2004. Mobility of arsenic in a Bangladesh aquifer: inferences from geochemical profiles, leaching data, and mineralogical characterization. Geochimica et Cosmochimica Acta 68 (22): 4539-4557.

Swedlund, P.J., Webster, J.G., 1999. Adsorption and polymerisation of silicic acid on ferrihydrite, and its effect on arsenic adsorption. Water Research 33(16): 3413-3422.

Tessier, A., Campbell, P.G.C., Bisson, M., 1979. Sequential extraction procedure for the speciation of particulate trace metals. Analytical Chemistry 51: 844-851.

Tuccillo, M.E., Cozzarelli, I.M., Herman, J.S., 1999. Iron reduction in the sediments of a hydrocarbon-contaminated aquifer. Applied Geochemistry 14: 655-667.

Uddin, A., Shamsudduha, M., Saunders, J.A., Lee, M-K., Ahmed, K.M., Chowdhury, M.T., 2011. Mineralogical profiling of alluvial sediments from arsenic-affected Ganges-Brahmaputra floodplain in central Bangladesh. Applied Geochemistry 26: 470-483.

Umitsu M., 1987. Late Quaternary sedimentary environment and landform evolution in the Bengal lowland. Geographical Review of Japan 60: 164-78.

Umitsu M., 1993. Late Quaternary sedimentary environments and landforms in the Ganges Delta. Sedimentary Geology 83: 177–86.

UN, 2001. United Nations Synthesis Report on Arsenic in Drinking Water. Draft Report.

UNDP, 1982. Groundwater Survey: The Hydrogeological Conditions of Bangladesh. UNDP Technical Report DP/UN/BGD-74-009/1, 113 p.

Vahter, M.E., Li, L., Nermell, B., Rahman, A., Arifeen, A.E., Rahman, M., Persson, L-Å., Ekström, E-C., 2006. Arsenic Exposure in Pregnancy: A Population-based Study in Matlab, Bangladesh. Journal of Health, Population and Nutrition 24(2): 236-245.

van Geen, A., Zheng, Y., Versteeg, R., Stute, M., Horneman, A., Dhar, R., Steckler, M., Gelman, A., Small, C., Ahsan, H., Graziano, J.H., Hussain, I., Ahmed, K.M., 2003. Spatial variability of arsenic in 6000 tube wells in a 25 km^2 area of Bangladesh. Water Resources Research 39: 1140-1155.

van Geen, A., Rose, J., Thoral, S., Garnier, J.M., Zheng, Y., Bottero, J.Y., 2004. Decoupling of As and Fe release to Bangladesh groundwater under reducing conditions. Part II: evidence from sediment incubations. Geochimica et Cosmochimica Acta 68(17): 3475-86.

van Geen, A., Cheng, Z., Jia, Q., Seddique, A.A., Rahman, M.W., Rahman, M.M., Ahmed, K.M., 2007. Monitoring 51 community wells in Araihazar, Bangladesh, for up to 5 years: Implications for arsenic mitigation. Journal of Environmental Science and Health Part A 42: 1729-1740.

Varsányi, I., Fodré, Z.s., Bartha, A., 1991. Arsenic in drinking water and mortality in the Southern Great Plain, Hungary. Environmental Geochemistry and Health 13: 14–23.

Varsányi, I., Kovács, L.Ó., 2006. Arsenic, iron and organic matter in sediments and groundwater in the Pannonian Basin, Hungary. Applied Geochemistry 21: 949–963.

Vencelides, Z., Sracek, O., Prommer, H., 2007. Modelling of iron cycling and its impact on the electron balance at a petroleum hydrocarbon contaminated site in Hnevice, Czech Republic. Journal of Contaminant Hydrology 89: 270-294.

von Brömssen, M., 1999. Genesis of high arsenic groundwater in the Bengal delta plains, West-Bengal and Bangladesh, Stockholm. M.Sc. thesis, LWR, KTH.

von Brömssen, M., 2012. Hydrogeological and geochemical assessment of aquifer systems with geogenic arsenic in southeastern Bangladesh – Targeting low arsenic aquifers for safe drinking water supplies in Matlab. PhD Thesis, TRITA LWR PhD 1063, 46 p.

von Brömssen, M., Bhattacharya, P., Ahmed, K.M., Jakariya, M., Jonsson, L., Lundell, L., Jacks, G., 2005. Targeting safe aquifers in regions with elevated arsenic in groundwater of Matlab Upazila, Bangladesh. In: Lombi, E., Tyrell, S., Nolan, A., McLaughlin, M., Pierzynski, G., Gerzabek, M., Lepp, N., Leyval, C., Selim, M., Zhao, F., Grant, C., Parker, D. (eds.) ICOBTE 8-2005, Symposium 4, 8th International Conference on the Biogeochemistry of Trace Elements (April 3-7, 2005), Book of Abstracts, Adelaide, Australia: 190-191.

von Brömssen, M., Jakariya, M., Bhattacharya, P., Ahmed, K.M., Hasan, M.A., Sracek, O., Jonsson, L., Lundell, L., Jacks, G., 2007. Targeting low-arsenic in Matlab Upazila, Southeastern Bangladesh. Science of the Total Environment 379(2–3): 121-132.

von Brömssen, M., Larsson, S.H., Bhattacharya, P., Hasan, M.A., Ahmed, K.M., Jakariya, M., Sikder, A.M., Sracek, O., Bivén, A., Doušová, B., Patriarca, C., Thunvik, R., Jacks, G., 2008. Geochemical characterisation of shallow aquifer sediments of Matlab Upazila, Southeastern Bangladesh – implications for targeting low-As aquifers. Journal of Contaminant Hydrology 99(1-4): 137-149.

von Brömssen, M., Markussen, L., Bhattacharya, P., Ahmed, K.M., Hossain, M., Jacks, G., Sracek, O., Thunvik, R., Hasan, M.A., Islam, M.M., Rahman, M.M., 2014. Hydrogeological investigation for

assessment of the sustainability of low-arsenic aquifers as a safe drinking water source in regions with high-arsenic groundwater in Matlab, southeastern Bangladesh. Journal of Hydrology 518: 373-392.

Wasserman, G.A., Liu, X., Parvez, F., Factor-Litvak, P., Ahsan, H., Levy, D., Kline, J., van Geen, A., Mey, J., Slavkovich, V., Siddique, A.B., Islam, T., Graziano, J.H., 2011. Asenic and manganese exposure and children's intellectual function. NeuroToxicology 32: 450-457.

Welch, A.L., Stollenwerk, K.G., 2003. Arsenic in Ground Water, Geochemistry and Occurrence. Kluwer Academic Publishers, Boston, 475 p.

Wenzel, W.W., Kirchbaumer, N., Prohaska, T., Stingeder, G., Lombi, E., Adriano, D.C., 2001 Arsenic fractionation in soils using an improve sequential extraction procedure. Analytica Chimica Acta 436: 309-323.

WHO, 2004. Guidelines Drinking Water Quality, Third edition, Volume 1, Recommendations. Geneva 2004 515 p.

WHO, 2011. Guideline for Drinking Water Quality. Fourth edition. Geneva: World Health Organization: Singapore; 2011.

Williams, P. N., Price, A. H., Raab, A., Hossain, S. A., Feldmann, J., Meharg, A. A., 2005. Variation in arsenic speciation and concentration in paddy rice related to dietary exposure. Environmental Science and Technology 39: 5531-5540.

Williams, P.N., Islam, M.R., Adomako, E.E., Raab, A., Hossain, S.A., Zhu, Y.G., Felfmann, J., Meharg, A.A., 2006. Increase in rice grain arsenic for regions of Bangladesh irrigating paddies with elevated arsenic in groundwaters. Environmental Science and Technology 40: 4903-4908.

Yan, X-P., Kerrich, R., Hendry, M.J., 2000. Distribution of arsenic (III), arsenic (V) and total inorganic arsenic in porewaters from a thick till and clay rich aquitard sequence, Saskatchewan, Canada. Geochimica et Cosmochimca Acta 62: 2637-2648.

Zheng, Y., van Geen, A., Stute, M., Dhar, R., Mo, Z., Cheng, Z., Horneman, A., Gavrieli, I., Simpson, H.J., Versteeg, R., Steckler, M., Grazioli-Venier, A., Goodbred, S., Shahnewaz, M., Shamsudduha, M., Hoque, M.A., Ahmed, K.M., 2005. Geochemical and hydrogeological contrast between shallow and deeper aquifers in two villages of Araihazar, Bangladesh: implication for deeper aquifers as drinking water sources. Geochimica et Cosmochimica Acta 69(22): 5203-5218.

APPENDIX I. MISTRA PROJECT OUTCOMES

A1 PhD Theses

Md. Jakariya (2007) *Arsenic in Tubewell Water: of Bangladesh. and Approaches for Sustainable Mitigation.* (Awarded 24 May, 2007)

M. Aziz Hasan (2008) *Arsenic in Alluvial Aquifers in the Meghna Basin, Southeastern Bangladesh: Hydrogeological and Geochemical Characterisation.* (Awarded 5 November 2008)

Mattias von Brömssen (2012) *Hydrogeological and Geochemical Assessment of Aquifer Systems with Geogenic Arsenic in Southeastern Bangladesh: Targeting Low Arsenic Aquifers for Safe Drinking Water Supplies in Matlab.* (Awarded 20 January, 2012)

Ashis Biswas (2014) *Arsenic Geochemistry in the Alluvial Aquifers of West Bengal, India Implications for Targeting Safe Aquifers for Sustainable Drinking Water Supply.* (Awarded 23 September 2013)

A2 Selected Publications

Journal articles

1. **Bhattacharya, P**., Ahmed, K.M., Hasan, M.A., Broms, S., Fogelström, J., Jacks, G., Sracek, O., von Brömssen, M. & Routh, J. (2006) Mobility of arsenic in groundwater in a part of Brahmanbaria district, NE Bangladesh In: Naidu, R., Smith, E., Owens, G., **Bhattacharya, P.** & Nadebaum. P, (Eds.) *Managing Arsenic in the Environment: From soil to human health.* CSIRO Publishing, Melbourne, Australia, pp. 95-115. (ISBN: 0643068686)
2. Naidu, R. & **Bhattacharya, P.** (2006) Management and remediation of arsenic from contaminated water. In: Naidu, R., Smith, E., Owens, G., **Bhattacharya, P.** & Nadebaum. P, (Eds.) *Managing Arsenic in the Environment: From soil to human health.* CSIRO Publishing, Melbourne, Australia, pp. 331-354. (ISBN: 0643068686)
3. Mukherjee, A.B., **Bhattacharya, P.,** Jacks, G. Banerjee, D.M., Ramanathan, A.L., Mahanta, C. Chandrashekharam, D., Chatterjee, D. & Naidu, R. (2006) Groundwater Arsenic Contamination in India: Extent and severity. In: Naidu, R., Smith, E., Owens, G., **Bhattacharya, P.** & Nadebaum. P, (Eds.) *Managing Arsenic in the Environment: From soil to human health.* CSIRO Publishing, Melbourne, Australia, pp. 533-594. (ISBN: 0643068686)
4. **Bhattacharya, P.**, Welch, A.H., Stollenwerk, K.G., McLaughlin, M.J., Bundschuh, J. & Panaullah, G. (2007) Arsenic in the Environment: Biology and Chemistry. *Science of the Total Environment* 379: 109-120 (doi:10.1016/j.scitotenv.2007.02.037).
5. von Brömssen, M., Jakariya, Md., **Bhattacharya, P**., Ahmed, K. M., Hasan, M.A., Sracek, O., Jonsson, L., Lundell, L. & Jacks G. (2007) Targeting low-arsenic aquifers in groundwater of Matlab Upazila, Southeastern Bangladesh. *Science of the Total Environment* 379: 121-132 (doi:10.1016/j.scitotenv.2006.06.028).
6. Jakariya, M., Vahter, M., Rahman, M., Wahed, M.A., Hore, S.K., **Bhattacharya, P.**, Jacks, G., Persson, L.-Å. (2007) Screening of arsenic in tubewell water with field test kits: evaluation of the method from public health perspective. *Science of the Total Environment* 379: 167-175 (doi:10.1016/j.scitotenv.2006.11.053).
7. Jakariya, M., von Brömssen, M., Jacks, G., Chowdhury, A.M.R., Ahmed, K.M. & **Bhattacharya, P.** (2007) Searching for sustainable arsenic mitigation strategy in Bangladesh: experience from two upazilas. *Int. J. Environment and Pollution.* 31(3/4): 415-430.
8. Jakariya, M., **Bhattacharya, P.** (2007) Use of GIS in local level participatory planning for arsenic mitigation: A case study from Matlab upazila, Bangladesh. *J. Environ. Sci. Health, Part A.* 42(12): 1933-1944. (DOI: 10.1080/10934520701567221).
9. Nriagu, J.O., **Bhattacharya, P.,** Mukherjee, A.B., Bundschuh, J., Zevenhoven, R. & Loeppert, R.H. (2007) Arsenic in soil and groundwater: an overview. In: **Bhattacharya, P.**, Mukherjee, A.B., Bundschuh, J., Zevenhoven, R. & Loeppert, R.H. (Eds.) *Arsenic in Soil and Groundwater Environment: Biogeochemical Interactions, Health Effects and Remediation*, Trace Metals

and other Contaminants in the Environment, Volume 9, Elsevier B.V. Amsterdam, The Netherlands: 3–60 (doi 10.1016/S0927-5215(06)09001-1).

10. Gustafsson, J. P. & **Bhattacharya, P.** (2007) Geochemical Modelling of Arsenic Adsorption to Oxide Surfaces. In: **Bhattacharya, P.**, Mukherjee, A.B., Bundschuh, J., Zevenhoven, R. & Loeppert, R.H. (Eds.) *Arsenic in Soil and Groundwater Environment: Biogeochemical Interactions, Health Effects and Remediation,* Trace Metals and other Contaminants in the Environment, Volume 9, Elsevier B.V. Amsterdam, The Netherlands: 153-200 (doi 10.1016/S0927-5215(06)09006-1).
11. Hasan, M. A., Ahmed, K. M., Sracek, O., **Bhattacharya, P.,** von Brömssen, M., Broms, S., Fogelström, J., Mazumder, M. L., Jacks, G. (2007) Arsenic in shallow groundwater of Bangladesh: investigations from three different physiographic settings. *Hydrogeol. Jour.* 15: 1507-1522 (DOI 10.1007/s10040-007-0203-z)
12. **Bhattacharya, P.,** von Brömssen, M., Hasan, M.A., Jacks, G., Ahmed, K.M., Sracek, O., Jakariya, M., Huq, S.M.I. Naidu, R., Smith, E. & Owens, G. (2008) Arsenic mobilisation in the Holocene flood plains in South-central Bangladesh: Evidences from the hydrogeochemical trends and modeling results. In: **Bhattacharya, P.,** Ramanathan, AL., Mukherjee A.B., Bundschuh, J., Chandrasekharam, D. & Keshari, A.K. (eds.) *Groundwater for Sustainable Development: Problems, Perspectives and Challenges.* Taylor and Francis/A. A. Balkema, The Netherlands: 283-299.
13. Mukherjee, A., **Bhattacharya, P.,** Savage, K., Foster, A. & Bunschuh, J. (2008) Distribution of geogenic arsenic in hydrologic systems: controls and challenges. *J. Cont. Hydrol.* 99(1-4): 1-7 (doi: 10.1016/j.jconhyd.2008.04.002).
14. Mukherjee-Goswami, A., Nath, B., Jana, J., Sahu, S.J., Sarkar, M.J., Jacks, G., **Bhattacharya, P.**, Mukherjee, A., Polya, D.A., Jean, J.-S., Chatterjee, D. (2008) Hydrogeochemical behavior of arsenic-enriched groundwater in the deltaic environment: Comparison between two study sites in West Bengal, India. *J. Cont. Hydrol.*. 99(1-4): 22-30 (doi: 10.1016/j.jconhyd.2008.04.004).
15. Mukherjee, A., von Brömssen, M., Scanlon, B.R., **Bhattacharya, P.,** Fryar, A.E., Hasan, M.A., Ahmed, K.M., Chatterjee, D., Jacks, G. & Sracek, O. (2008) Hydrogeochemical comparison between the Bhagirathi and Meghna sub-basins, Bengal basin, India and Bangladesh: effects of overlapped redox zones on dissolved arsenic. *J. Cont. Hydrol.* 99(1-4): 31-48 (doi:10.1016/j.jconhyd.2007.10.005).
16. von Brömssen, M., Larsson, S.H., **Bhattacharya, P.,** Hasan, M.A., Ahmed, K.M., Jakariya, M., Sikder, A.M., Sracek, O., Bivén, A., Doušová, B., Patriarca, C., Thunvik, R. & Jacks, G. (2008) Geochemical characterisation of shallow aquifer sediments of Matlab Upazila, Southeastern Bangladesh – implications for targeting low-As aquifers. *J. Cont. Hydrol.*. 99(1-4): 137-149 (doi:10.1016/j.jconhyd.2008.05.005).
17. Bundschuh, J., García, M.E., Birkle, P., Cumbal, L.H. & **Bhattacharya, P.** (2009) Occurrence, health effects and remediation of arsenic in groundwaters of Latin America. In: J. Bundschuh, M.A. Armienta, P. Birkle, **P. Bhattacharya,** J. Matschullat & A.B. Mukherjee (eds.): *Natural Arsenic in Groundwater of Latin America — Occurrence, health impact and remediation.* Interdisciplinary Book Series: "Arsenic in the Environment" Volume 1, J. Bundschuh & **P. Bhattacharya** (Series Editors), CRC Press/Balkema, Leiden, The Netherlands, pp. 3-16. ISBN: 978-0-415-40771-7.
18. Sracek, O., Novák, M., Sulovský, P., Martin, R., Bundschuh J.& **Bhattacharya, P.** (2009) Mineralogical study of arsenic-enriched aquifer sediments at Santiago del Estero, Northwest Argentina. In: J. Bundschuh, M.A. Armienta, P. Birkle, **P. Bhattacharya,** J. Matschullat & A.B. Mukherjee (eds.): *Natural Arsenic in Groundwater of Latin America — Occurrence, health impact and remediation* Interdisciplinary Book Series: "Arsenic in the Environment" Volume 1, J. Bundschuh & **P. Bhattacharya** (Series Editors), CRC Press/Balkema, Leiden, The Netherlands, pp. 61-68. ISBN: 978-0-415-40771-7.

19. Jakariya, M., **Bhattacharya, P.,** Hassan, M.M., Ahmed, K.M., Hasan, M.A. & Nahar, S. (2009) Temporal variations of groundwater arsenic contrations in Southwest Bangladesh. In: J. Bundschuh, M.A. Armienta, P. Birkle, **P. Bhattacharya,** J. Matschullat & A.B. Mukherjee (eds.): *Natural Arsenic in Groundwater of Latin America — Occurrence, health impact and remediation*. Interdisciplinary Book Series: *Arsenic in the Environment* Volume 1, J. Bundschuh & **P. Bhattacharya** (Series Editors), CRC Press/Balkema, Leiden, The Netherlands, pp. 225-233. ISBN: 978-0-415-40771-7.
20. Bundschuh, J., **Bhattacharya, P.,** von Brömssen, M., Jakariya, M., Jacks, G., Thunvik, R., Litter, M.I. & García, M.E. (2009) Arsenic-safe aquifers as a socially acceptable source of safe drinking water —What can rural Latin America learn from Bangladesh experiences? In: J. Bundschuh, M.A. Armienta, P. Birkle, **P. Bhattacharya,** J. Matschullat & A.B. Mukherjee (eds.): *Natural Arsenic in Groundwater of Latin America — Occurrence, health impact and remediation*. Interdisciplinary Book Series: *Arsenic in the Environment* Volume 1, J. Bundschuh & **P. Bhattacharya** (Series Editors), CRC Press/Balkema, Leiden, The Netherlands, pp. 677-685. ISBN: 978-0-415-40771-7.
21. Kim, K.-W., Bang, S., Zhu, Y-G., Meharg, A.A. & **Bhattacharya, P.** (2009) Arsenic geochemistry, transport mechanism in the soil–plant system, human and animal health issues. *Envion. International* 31(3): 453-454. (doi 10.1016/j.envint.2009.01.001
22. Hasan, M.A., von Brömssen, M., **Bhattacharya, P.,** Ahmed, K. M., Sikder, A.M., Jacks, G. & Sracek, O. (2009) Geochemistry and mineralogy of shallow alluvial aquifers in Daudkandi upazila in the Meghna flood plain, Bangladesh. *Env. Geol.* 57: 499-511. (DOI 10.1007/s00254-008-1319-8).
23. Rahman, M.M., Naidu, R., **Bhattacharya, P.** (2009) Arsenic contamination in groundwater in the Southeast Asia region. *Environ. Geochem. & Health* 31: 9–21 (DOI 10.1007/s10653-008-9233-2)
24. **Bhattacharya, P.,** Hasan, M.A., Sracek, O., Smith, E., Ahmed, K.M., von Brömssen, M., Huq S.M.I, Naidu, R. (2009) Groundwater chemistry and arsenic mobilizationin the Holocene flood plains in south-central Bangladesh. *Environ. Geochem. & Health* 31: 23-44 (DOI 10.1007/s10653-008-9230-5)
25. Mukherjee, A., **Bhattacharya, P.,** Shi, F., Fryar, A.E., Mukherjee, A.B., Xie, Z.M., Sracek, O., Jacks, G. & Bundschuh, J. (2009) Trends of solute chemistry evolution in the groundwater of arsenic-affected Huhhot basin, Inner Mongolia, P.R. China: its similarity and dissimilarity with the western Bengal basin, India. *Applied Geochemistry* 24(12): 1835-1851 (doi.10.1016/j.apgeochem.2009.06.005)
26. Hasan, M.A., **Bhattacharya, P.**,. Sracek, O., Ahmed, K.M., von Brömssen, M. & Jacks, G. (2009) Geological controls on groundwater chemistry and arsenic mobilization: Hydrogeochemical study along an E-W transect in the Meghna basin, Bangladesh. *Jour. Hydrology* 378: 105-118. (DOI: 10.1016/j.jhydrol.2009.09.016)
27. Biswas, A., Nath, B., **Bhattacharya, P.**, Halder, D., Kundu, A.K., Mandal, U., Mukherjee, A., Chatterjee, D., Mörth, C.-M. & Jacks, G. (2012) Hydrogeochemical contrast between brown and grey sand aquifers in shallow depth of Bengal Basin: Consequences for sustainable drinking water supply. Science of the Total Environment 431: 402-412 (doi:10.1016/j.scitotenv.2012.05.031).
28. Biswas, A., **Bhattacharya, P.**, Mukherjee, A., Nath, B., Alexanderson, H., Kundu, A.K., Chatterjee, D. & Jacks, G. (2014) Shallow hydrostratigraphy in an arsenic affected region of Bengal Basin: Implication for targeting safe aquifers for drinking water supply. Science of the Total Environment 485-486: 12-22 (doi: 10.1016/j.scitotenv.2014.03.045).

Edited books

1. *"Managing Arsenic in the Environment: From soil to human health",* Editors: R Naidu (University of South Australia, Adelaide, SA, Australia), E Smith, G. Owens (University of South Australia,

Adelaide, SA, Australia), **P Bhattacharya** (Sweden) & P. Nadebaum (Australia) (eds.), © 2006, CSIRO Publishing, Australia ISBN: 0643068686, 664p.

2. *"Arsenic in Soil and Groundwater Environment: Biogeochemical Interactions, Health Impacts and Remediation"*. Elsevier Science, BV, Netherlands (**P Bhattacharya** (Sweden), A.B. Mukherjee (Finland), J. Bundschuh (Costa Rica), R. Zevenhoven (Finland) & R. Loeppert (USA) (eds.) In the Elsevier Series *"Trace Elemnts in the Environment"* Series, Volume 9 Series Editor: Jerome Nriagu May, 2007, © 2007 ElsevierBV, Amsterdam, The Netherlands, ISBN-13: 978-0-444-51820-0, 653p.
3. *"Groundwater and Sustainable Development: Problems, Perspectives and Challenges"* **P. Bhattacharya,** AL Ramanathan, A.B. Mukherjee, J. Bundschuh D. Chandrashekharam & AK Keshari (eds) © 2008, Taylor & Francis Group, London, ISBN 978-0-415-40776-2, 460p.
4. *"Natural arsenic in groundwaters of Latin America — Occurrence, health impact and remediation"*. Bundschuh, J. Armienta, M.A., P. Birkle, **Bhattacharya, P.,** Matschullat, J..& Mukherjee, A.B. (eds.) Interdisciplinary Book Series: *"Arsenic in the Environment"* Volume 1, Series Editors: Jochen Bundschuh and **Prosun Bhattacharya,** © 2009 CRC Press/Taylor and Francis (ISBN: 978-0-415-40771-7).
5. *"Assessment of Groundwater Resources and Management"*. AL Ramanathan, **P. Bhattacharya,** AK Keshari, J. Bundschuh, D. Chandrashekharam & SK Singh (eds) © 2009, I.K. International Publishing House Pvt. Ltd., New Delhi, Bangalore India, ISBN 978-81-906757-2-7, 486p.
6. *"The Global Arsenic Problem: Challenges for Safe Water Production"*. N. Kabay, J. Bundschuh, B. Hendry, M. Bryjak, K. Yoshizuka, **P. Bhattacharya** & S. Anac (eds.) Interdisciplinary Book Series: *"Arsenic in the Environment"* Volume 1, Series Editors: Jochen Bundschuh and **Prosun Bhattacharya** © 2010 CRC Press/Taylor and Francis (ISBN-13: 978-0-415-57521-8)
7. *"Arsenic in Geosphere and Human Diseases"*. J.-S. Jean, J. Bundschuh & **P. Bhattacharya** Interdisciplinary Book Series: *"Arsenic in the Environment—Proceedings As 2010"* Series Editors: Jochen Bundschuh and **Prosun Bhattacharya** © 2010 CRC Press/Taylor and Francis (ISBN-13: 978-0-415-57898-1)

Special Issues of Peer-reviewed journals

1. Guest Editor (The Science of the Total Environment) *"Arsenic in the Environment: Biology and Chemistry"* Editors: **Bhattacharya, P.,** Welch, A.H., Stollenwerk, K.G. McLaughlin, M., Bundschuh, J. & Panaullah., G, July 2007, *Sci. Tot. Environ.* v. 379 (2-3): 106-266.
2. Guest Editor (Journal of Contaminant Hydrology) *"Distribution of Geogenic Arsenic in Hydrologic Systems: Controls and Challenges"* Editors: Mukherjee, A., **Bhattacharya, P.,** Savage, K., Foster, A. & Bunschuh, J. July, 2008, *J. Cont. Hydrol.* v. 99 (1-4): 1-150.
3. Guest Editor (Environment International) "*Arsenic Geochemistry, Transport Mechanism in the Soil-Plant System, Human and Animal Health Issues*" Editors: Kim, K.-W., Bang, S., Zhu, Y. G., Meharg, A. A. & **Bhattacharya, P.**, April, 2009. *Environmental International.* v. 35(3): 453-515.
4. Guest Editor (Environmental Geochemistry and Health) "*Arsenic in the Environment—Risks and Management Strategies*" Editors: Naidu, R. & **Bhattacharya, P.**, April, 2009 *Environmental Geochemistry and Health* v. 31 (Supplement 1): 1-113.
5. Guest Editor (Applied Geochemistry) *"Arsenic and Other Toxic Elements in Global Groundwater Systems"* Eds. Mukherjee, A., **Bhattacharya, P.,** Fryar, A.E., April, **2011** *Applied Geochemistry* v. 26(4): 415-654.
6. Guest Editor (The Science of the Total Environment) *"Arsenic in Latin America, an unrevealed continent: Occurrence, health effects and mitigation"* Eds. Bundschuh, J., Litter, M. & **Bhattacharya, P.**, July **2012** v. 429 (Special Section): 1-122.

A3 MISTRA POPULAR SCIENTIFIC DISSEMINATIONS

1. Mistra (2011) "Han letar efter arsenikfritt grundvatten". *Mistra Nyhetsbrev* 9: 10-11.
2. Mistra (2013) "Röd sand har blivit symbol för säkert dricksvatten". In: Henrik Lundström (Ed.) *Djärva Projekt med Stor Potential, Mistras Idéstöd 2001–2011*:33.

MISTRA
STIFTELSEN FÖR MILJÖSTRATEGISK FORSKNING

MISTRAS IDÉSTÖD 2001–2009

Han letar efter arsenikfritt grundvatten

Arsenik av naturligt ursprung förekommer i grundvatten i bland annat Bangladesh och Argentina. Ett av Mistras idéstödsprojekt går ut på att utpröva metoder för att hitta arsenikfritt grundvatten.

Arsenikförorenat grundvatten är ett utbrett problem i flera delar av världen, bland annat i Bangladesh, Indien, Sydostasien, Centralamerika och Argentina. Samtidigt växer behovet av rent dricksvatten i takt med att befolkningarna växer. Ett billigt sätt att få vatten har hittills varit att installera brunnar som ofta utförs av lokala brunnsborrare.

ARSENIK STÖRSTA RISKEN

Den största risken i nämnda områden är att jorden/sedimenten innehåller arsenik som sedan löses ut i vattnet som därmed utgör en hälsorisk.

I idéstödsprojektet ”Targering safe aquifers in regions with high arsenic groundwater and its worldwide implications” arbetar forskarna därför med att ta fram en vetenskaplig grund för att verifiera utprövade metoder för att avgöra var det är säkert att borra efter vatten i framförallt Bangladesh och Argentina.

– Ett problem är att grundvatten med låga arsenikhalter ofta förekommer i nära anslutning till grundvatten med hälsovådliga halter. Det gäller därför att hitta tillförlitliga och enkla metoder för att ta reda på var det är säkert att borra efter vatten, säger Prosun Bhattacharya, projektledare och docent på institutionen för mark- och vattenteknik vid KTH.

En kartläggning av brunnarna i Bangladesh visar att 25 procent av brunnarna har vatten som innehåller 50 mikrogram arsenik per liter vilket är mer än det tillåtna gränsvärdet och ungefär hälften av brunnarna har arsenikhalter på mindre än tio mikrogram per liter vilket är högsta tillåtna värde.

– Hittills har man prövat flera olika metoder för att filtrera bort arseniken men ute i byarna har man inte förtroende för metoderna utan vill hellre komma åt rent grundvatten, därför måste vi hitta metoder som gör det enkelt att hitta fram till arsenikfritt grundvatten, säger han.

Forskarna har undersökt bland annat om djupet på brunnarna spelar in eller om det är kvalitén på sedimenten som spelar in.

– Men vi har inte kunnat fastställa att djupet på brunnarna är avgörande, snarare handlar det om kvalitén på det omgivande sedimentet, säger han.

FÄRGEN PÅ SEDIMENTEN

I Bangladesh har det visat sig att sedimentens färg, som varierar i en vid skala från svart via rött till orange, återspeglar arsenikhalten i grundvattnet.

– Genom att jämföra färgen på sedimentet och halten av arsenik i grundvattnet har vi kunnat visa att det finns en korrelation mellan sedimentens färg och halten av arsenik, säger Prosun Bhattacharya.

Forskarna undersöker även de mekanismer som påverkar bindningen av arsenik i sedimenten.

– Vi undersöker nu de processer som eventuellt styrs av vissa mikroorganismer och i så fall vilka, eller om ▶

Prosun Bhattacharya

MISTRAS IDÉSTÖD

Under åren 2001 – 2008 har Mistra finansierat sammanlagt 30 så kallade idéstödsprojekt med cirka 160 miljoner kronor. Syftet med Mistras idéstöd har varit att bidra till att förverkliga nyskapande forskningsprojekt med stor potential för en bättre miljö. Ett idéstödsprojekt ska ha starka inslag av djärvhet, originalitet och kreativitet. Forskningen ska vara upptäckande, nytänkande och/eller omprövande. Forskningen kan också uttryckligen utmana eller ifrågasätta etablerade synsätt.

MISTRA
STIFTELSEN FÖR MILJÖSTRATEGISK FORSKNING

”Det gäller att hitta tillförlitliga och enkla metoder för att ta reda på var det är säkert att borra efter vatten.”

det är halten av järnoxid i sedimentet som är avgörande, säger han.

Projektet har inte bara undersökt hur man ska hitta arsenikfritt grundvatten utan även hur man uppnår ett hållbart vattensystem.

– Om man tar grundvatten till jordbruket så ökar vattenflödena i det hydrologiska systemet, om man däremot enbart använder det till dricksvatten ökar inte vattenflödena i samma takt.

Idéstödsprojektet har lett till ytterligare forskningsprojekt, bland annat i Indien där forskarna utvecklar metoder för hur man hittar säkra vattenområden.

– Genom projektet har vi också kunnat inleda ett omfattande samarbete med flera andra länder. Problemet med arsenikförorenat grundvatten finns på många håll i världen. Vår förhoppning är att den kunskap vi tar fram ska komma till användning i andra områden där sedimenten liknar dem i Bangladesh, säger Prosun Bhattacharya.

– Brunnar med arsenikförgiftat vatten kan ligga i samma område som brunnar med rent vatten, men det finns ännu inte några vetenskapligt utprövade metoder för att fastställa var eller på vilka djup man kan borra efter friskt vatten, säger Prosun Bhattacharya.

Targeting safe aquifers in regions with high arsenic groundwater and its worldwide implications

Röd sand har blivit symbol för säkert dricksvatten

Fakta

Projektledare: Prosun Bhattacharya

Organisation: Kungliga tekniska högskolan

Projekttid: 2006-2010

Anslag: 3,6 miljoner kronor

Utmaningen

I Bangladesh är förhållandena sådana att färgen på olika geologiska sediment kan knytas till halten arsenik i grundvattnet. Syftet med projektet var att ge brunnsborrare ett enkelt verktyg att avgöra när de nått ett grundvattenmagasin med acceptabla arsenikhalter.

Svart, vit, beige eller röd? En enkel färgskala har blivit ett viktigt redskap för brunnsborrare i Bangladesh att borra till rätt djup och hitta arsenikfritt vatten. Idéstödsprojektet har bidragit till att fler människor idag har tillgång till ett säkert dricksvatten.

Arsenikförgiftningarna i Bangladesh har kallats en av vår tids största miljökatastrofer. Miljontals människor på landsbygden riskerar att förgiftas av naturligt förekommande arsenik i grundvatten från sin egen brunn.

– Jag har själv mätt upp brunnar med 975 mikrogram arsenik per liter, det vill säga hundra gånger högre än WHO:s gränsvärde, säger Prosun Bhattacharya, professor vid Institutionen för mark- och vattenteknik vid KTH.

Olika insatser har gjorts, bland annat för att rena arsenik med filter. Sådana tekniska metoder fungerar sällan lika bra efter några år, konstaterar Prosun Bhattacharya, som med sina gedigna kunskaper inom grundvattenkemi, istället såg en annan, långsiktig lösning. Efter att ha jobbat många år i Indien, som har liknande geologiska förutsättningar som Bangladesh, visste han att grundvatten med höga arsenikhalter endast förekommer på vissa djup i marken. Omkring tre fjärdedelar av alla grundvattenreservoarer, akvifärer, hade dock betydligt lägre arsenikhalter.

– Då kom frågan upp om vi inte istället kunde ta vatten från de här säkra akvifärerna.

En dialog inleddes med lokala brunnsborrare i regionen Matlab i sydöstra Bangladesh. Det visade sig att när de ibland borrade djupare, förbi akvifärer med höga halter arsenik, stötte de på en annan typ av sand.

Genom att utnyttja borrarnas erfarenheter, och i samarbete med Sida även stärka deras kunskaper, har forskarna inom idéstödsprojektet etablerat en färgskala, där exempelvis röd, vit och svart sand signalerar en viss typ av grundvatten.

– Får man upp röd sand är det med 95 procents säkerhet ett säkert vatten att dricka, säger Prosun Bhattacharya.

Forskningen i projektet har handlat mycket om att klassificera de olika jordlagren och att karaktärisera grundvattnets sammansättning. En komplikation är att grundvatten från akvifärer med röd sand visat sig innehålla relativt höga manganhalter. Hälsofaran med mangan i dricksvatten är dock inte klarlagd, enligt Prosun Bhattacharya, och WHO har i dagsläget inget gränsvärde.

En viktig fråga har varit att öka kunskapen om hur grundvattnets nivåer varierar, eftersom det på sikt kan förändra arsenikhalten i olika akvifärer. Projektet har bidragit till att bygga ut ett nationellt system av mätstationer med så kallade piezometrar, som kontinuerligt mäter grundvattennivåer.

– Mätnätverket ska säkerställa långsiktigt säkert vatten. Det har gjorts med medel från både Mistra och Sida, säger Prosun Bhattacharya.

VID BORRNING efter dricksvatten följer sand med upp till ytan. Genom att studera färgen på sanden får brunnsborrare i Bangladesh ett snabbt besked om vattnet är säkert att dricka.

Viktigaste resultat

1. Utvecklat ett praktiskt verktyg för brunnsborrare, som utifrån en färgskala på sand kan avgöra om grundvatten har acceptabel arsenikhalt. Fler människor i Bangladesh får därmed tillgång till giftfritt dricksvatten.
2. Uppbyggnad av ett nätverk av mätstationer med så kallade piezometrar, som kontinuerligt mäter grundvattennivåer.
3. Resultaten har spridits på flera konferenser och projektets deltagare har diskuterat strategier med Bangladeshs regering för att hantera arsenikproblematiken.

REPORT, MISTRA IDEA SUPPORT GRANT
STOCKHOLM, SWEDEN 2015

TRITA-LWR.REPORT 2015:01
ISSN 1650-8610
ISBN 978-91-7595-461-5

Naturally occurring arsenic (As) in groundwater has undermined the success of supplying safe drinking water in Bangladesh. Arsenic is mobilized in groundwater through reductive dissolution of Fe(III)-oxyhydroxide especially in the younger (Holocene) sediments leading to severe public health consequences. Many of the mitigation options provided during the last two decades have not been well accepted by the people and instead, local well drillers target aquifers for abstraction of arsenic-safe groundwater on the basis of the colour of the sediments. This MISTRA Idea Support Grant project report incorporates the results of the studies carried out to validate the local drillers´ strategy in Bangladesh to low arsenic groundwater by assessing the colour of the sediments through systematic groundwater and sediment sampling, detailed chemical analysis of water, sediment extractions, mineralogical investigations and hydrogeochemical- and groundwater flow modelling.

The studies carried out in Matlab in Chandpur District of Bangladesh indicate that the idea on targeting low-arsenic groundwater is facilitated through identification of the colour of the sediments with decreasing levels of As concentrations in black, off-white, white and red as perceived by the local drillers. Each of the sediment colour category is characterized by a set of unique hydrochemical characteristics that can be used to conceptualize a “sediment colour strategy” that would enable the local drillers to identify arsenic-safe aquifers. Thus, linking the colour of the sediments with groundwater chemistry would be useful to develop a simple sediment colour-based tool for targeting shallow aquifers for the installation of As safe community tubewells for the local drillers through more careful evaluation of the sensitivity of the hydrogeochemical results with respect to the colour of the sediments. The results based on the studies in Matlab, was also replicated in Chakdaha Block in West Bengal, India, where identical set of grey sand and brown sand aquifers were identified with similar sediment and hydrochemical characteristics of aquifers and the approach for finding arsenic-safe drinking water sources through the initiatives of the local drillers in a sustainable manner.